

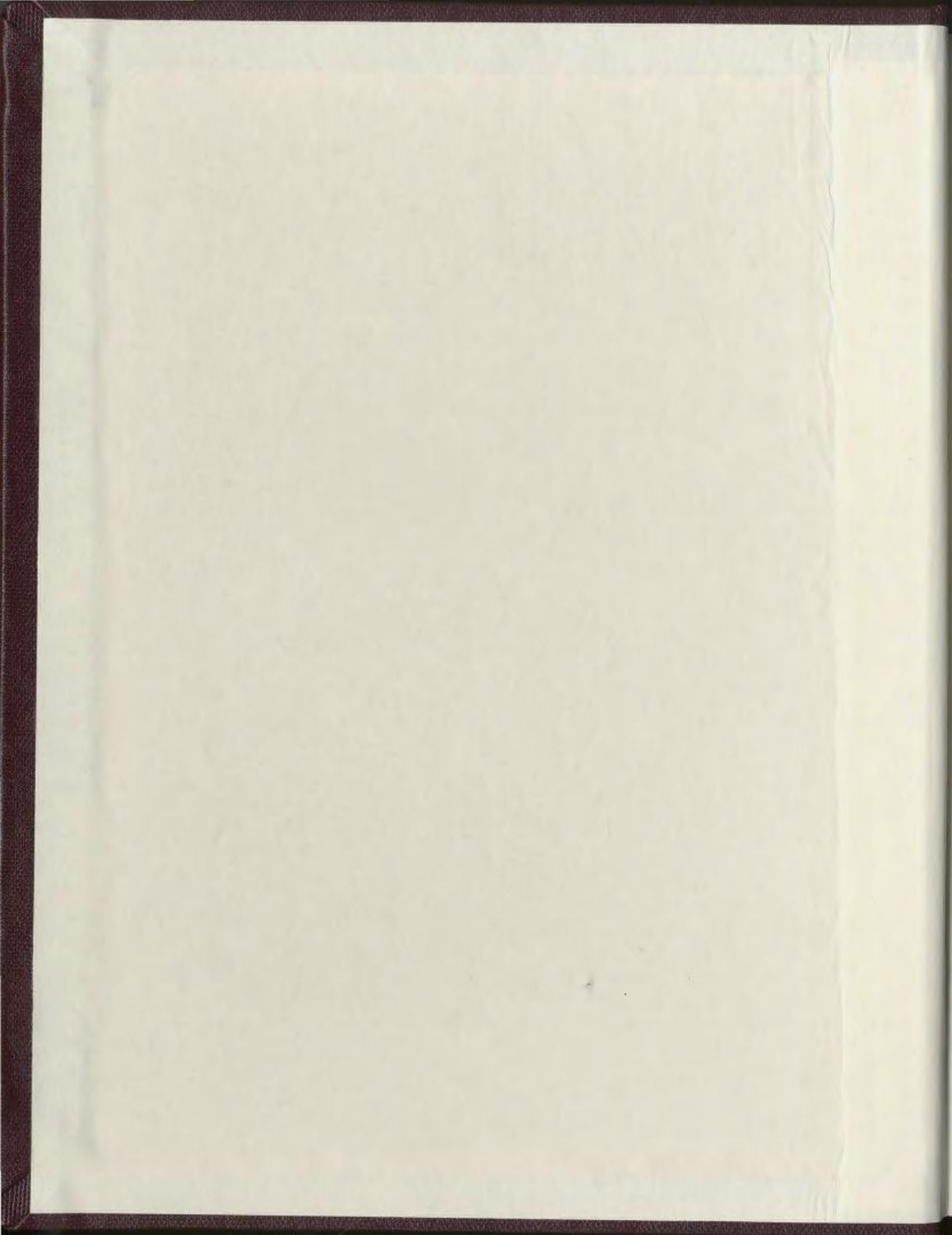
GEOLOGY, U-Pb GEOCHRONOLOGY, AND STABLE
ISOTOPE GEOCHEMISTRY OF THE HAMMER DOWN
GOLD PROSPECT, GREEN BAY DISTRICT,
NEWFOUNDLAND

CENTRE FOR NEWFOUNDLAND STUDIES

**TOTAL OF 10 PAGES ONLY
MAY BE XEROXED**

(Without Author's Permission)

DAVID HENRY RITCEY





National Library
of Canada

Acquisitions and
Bibliographic Services Branch

395 Wellington Street
Ottawa, Ontario
K1A 0N4

Bibliothèque nationale
du Canada

Direction des acquisitions et
des services bibliographiques

395, rue Wellington
Ottawa (Ontario)
K1A 0N4

Votre lieu - *Votre référence*

Our lie - *Notre référence*

NOTICE

The quality of this microform is heavily dependent upon the quality of the original thesis submitted for microfilming. Every effort has been made to ensure the highest quality of reproduction possible.

If pages are missing, contact the university which granted the degree.

Some pages may have indistinct print especially if the original pages were typed with a poor typewriter ribbon or if the university sent us an inferior photocopy.

Reproduction in full or in part of this microform is governed by the Canadian Copyright Act, R.S.C. 1970, c. C-30, and subsequent amendments.

AVIS

La qualité de cette microforme dépend grandement de la qualité de la thèse soumise au microfilmage. Nous avons tout fait pour assurer une qualité supérieure de reproduction.

S'il manque des pages, veuillez communiquer avec l'université qui a conféré le grade.

La qualité d'impression de certaines pages peut laisser à désirer, surtout si les pages originales ont été dactylographiées à l'aide d'un ruban usé ou si l'université nous a fait parvenir une photocopie de qualité inférieure.

La reproduction, même partielle, de cette microforme est soumise à la Loi canadienne sur le droit d'auteur, SRC 1970, c. C-30, et ses amendements subséquents.

Canada



National Library
of Canada

Acquisitions and
Bibliographic Services Branch

395 Wellington Street
Ottawa, Ontario
K1A 0N4

Bibliothèque nationale
du Canada

Direction des acquisitions et
des services bibliographiques

395, rue Wellington
Ottawa (Ontario)
K1A 0N4

Your file *Votre référence*

Our file *Notre référence*

The author has granted an irrevocable non-exclusive licence allowing the National Library of Canada to reproduce, loan, distribute or sell copies of his/her thesis by any means and in any form or format, making this thesis available to interested persons.

L'auteur a accordé une licence irrévocable et non exclusive permettant à la Bibliothèque nationale du Canada de reproduire, prêter, distribuer ou vendre des copies de sa thèse de quelque manière et sous quelque forme que ce soit pour mettre des exemplaires de cette thèse à la disposition des personnes intéressées.

The author retains ownership of the copyright in his/her thesis. Neither the thesis nor substantial extracts from it may be printed or otherwise reproduced without his/her permission.

L'auteur conserve la propriété du droit d'auteur qui protège sa thèse. Ni la thèse ni des extraits substantiels de celle-ci ne doivent être imprimés ou autrement reproduits sans son autorisation.

ISBN 0-612-01911-X

Canada

**Geology, U-Pb Geochronology, and Stable Isotope Geochemistry
of the Hammer Down Gold Prospect,
Green Bay District, Newfoundland**

by

© David Henry Ritcey, B.Sc., B.A.

**A thesis submitted to the School of Graduate Studies
in partial fulfillment of the requirements for the degree of
Master of Science**

**Department of Earth Sciences
Memorial University of Newfoundland**

June, 1993

St. John's

Newfoundland

ABSTRACT

The Hammer Down gold prospect is an important example of the numerous mesothermal gold occurrences associated with structural zones of regional extent in the Newfoundland Dunnage Zone.

The main mineralized zones in the Hammer Down prospect consist of structurally controlled quartz veins with abundant pyrite, chalcopyrite, and sphalerite, hosted by volcanic and sedimentary rocks of the Ordovician (Arenig) Catchers Pond Group, and by Early Silurian felsic porphyry dykes. Gold-bearing veins postdate sub-greenschist metamorphism and an early phase of deformation, and were produced synchronously with a locally intense S_2 fabric related to folding. Veins were preferentially emplaced in narrow brittle-ductile high strain zones within and adjacent to felsic dykes. The gold-bearing veins and S_2 fabric are locally folded, and mineralized zones are truncated by a late brittle fault. Barren, paragenetically late veins, characterized by fluorite and low contents of sulphide minerals, are abundant in and near the gold-bearing zones.

Gold is present within pyrite and along sulphide grain boundaries in veins and in locally sericitized, carbonatized, and pyritized wall rock. Hydrothermal alteration adjacent to veins is restricted to narrow zones, or is absent. Alteration of mafic rocks is characterized by muscovite, calcite, pyrite, quartz, and rutile, and is marked by enrichment in the lithophile elements K and Rb, and by sporadically elevated levels of

Cu, Zn, and S.

Felsic tuff from the Hammer Down prospect has an igneous U-Pb zircon age of $480 \pm 4/-3$ Ma, and records arc volcanism in the Dunnage Zone. Felsic dykes from the prospect, which have a strong spatial association with gold, are petrographically and chemically distinct from the nearby King's Point volcanic-plutonic complex, but they are correlative with the Burlington Granodiorite, a regional plutonic unit of the eastern Baie Verte Peninsula. Zircon from a felsic dyke cut by a gold-bearing vein has a high degree of Proterozoic inheritance. Acicular zircon grains from this dyke have a $^{207}\text{Pb}/^{206}\text{Pb}$ age of 437 ± 3 Ma, which is considered the age of intrusion, and is a maximum age limit for gold deposition.

Isotopic compositions of quartz ($\delta^{18}\text{O} = 11.4 \pm 0.7$) and calcite and ferroan dolomite from gold-bearing veins ($\delta^{13}\text{C} = -6.2 \pm 0.7$) are typical of mesothermal vein systems elsewhere. Oxygen isotope thermometry using quartz, chlorite, and muscovite indicates mineralization temperatures between 240 and 320°C. The ore-forming solutions had calculated $\delta^{18}\text{O}$ values between 2.2 and 5.2 ‰ and δD values between -27 and -42 ‰, which are compatible with a predominantly metamorphic source having some meteoric contribution. Age constraints and regional considerations place the gold mineralizing event within a period of crustal extension and widespread magmatism that were part of an important Silurian orogenic phase in central Newfoundland. A meteoric component in the vein fluid system is attributed to the extensional setting, which promoted influx of surface water to deeper reservoirs.

ACKNOWLEDGEMENTS

From beginning to end, this project required the initiative and assistance of many persons and organizations. I thank my supervisors at Memorial University, Dr. Mark Wilson and Dr. Greg Dunning, for their enthusiastic support and thoughtful guidance. Noranda Exploration Company provided logistic support in the field, access to their property, drill core, and maps, and funding for analytical work. These benefits were made available largely through the efforts of Dan McInnis, who is thanked personally. Financial support was received from a Natural Sciences and Engineering Research Council (NSERC) postgraduate scholarship and NSERC grants to G. Dunning and M. Wilson. I received helpful observations, comments, and advice in the field and in the laboratory from many sources, and gratefully thank Benoit Dubé, Damien Gaboury (acknowledged for his questions and his answers), Peter Andrews, Mike Basha, Alan Huard, Peter Cawood, and Jim Connelley. Peter Cawood and Brian Fryer allowed me to use their data to add to the regional picture. The students of "Knob Alley" and other corners of the Department of Earth Sciences at M.U.N., particularly Jahan Ramezani, Rod Churchill, and Adrian Timbal, are thanked immensely for sharing their computing skills, their geological knowledge and curiosity, and their humour. My friends and family provided a special kind of support. Thanks are also owing to the friendly people of King's Point, who welcomed me into their community and their homes during two field seasons.

TABLE OF CONTENTS

Abstract	ii
Acknowledgements	iv
Table of Contents	v
List of Tables	viii
List of Figures	ix
List of Photographic Plates	xii
Chapter 1 INTRODUCTION	1
1.1 General statement	1
1.2 Mesothermal gold deposits	3
1.3 Approach and scope of thesis	7
1.4 Location and access of the study area	11
Chapter 2 GEOLOGIC SETTING OF THE HAMMER DOWN GOLD PROSPECT	13
2.1 Introduction: The Appalachian Orogen in Newfoundland	13
2.2 Geology of Central Newfoundland and the King's Point area	19
2.3 Metallogeny of gold in Newfoundland	28
2.4 Summary	32
Chapter 3 GEOLOGY OF THE HAMMER DOWN PROSPECT AND HOST ROCKS	33
3.1 Introduction	33
3.2 General geology and structural setting of gold mineralization	33
3.2.1 Orientation and distribution of veins	33
3.2.2 Late brittle faulting	43

3.3 Volcanic, sedimentary, and related rocks	44
3.3.1 Field relations	44
3.3.2 Petrography	47
3.3.3 Chemistry	53
3.4 Felsic intrusive rocks	64
3.4.1 Field relations	64
3.4.2 Petrography	67
3.4.3 Chemistry	71
3.5 Summary	77
Chapter 4 ALTERATION AND GOLD MINERALIZATION	79
4.1 Introduction	79
4.2 Vein morphology and mineralogy	80
4.3 Wall rock alteration	93
4.3.1 Mineralogy	93
4.3.2 Chemistry	97
4.4 Mineral paragenesis	105
4.5 Summary	110
Chapter 5 GEOCHRONOLOGY	112
5.1 Introduction	112
5.2 Description of samples	113
5.2.1 Volcanic rocks	113
5.2.2 Felsic intrusive rocks	113
5.2.3 Hydrothermal assemblages	114
5.3 Techniques	116
5.3.1 Preparation of mineral fractions	116
5.3.2 Analytical procedures	119
5.4 Results	120
5.4.1 Presentation of data	120
5.4.2 Age and correlation of volcanic rocks	122
5.4.3 Age and correlation of felsic intrusive rocks	124
5.4.4 U-Pb analysis of hydrothermal assemblages	129
5.5 Summary	130

Chapter 6 STABLE ISOTOPE GEOCHEMISTRY	131
6.1 Introduction	131
6.2 Techniques	132
6.2.1 Sample preparation	132
6.2.1.1 Carbonate minerals	132
6.2.1.2 Silicate minerals	132
6.2.1.2 Whole rock samples	133
6.2.2 Mass spectrometry	134
6.3 Results	134
6.3.1 Multiple vein types	134
6.3.2 Oxygen isotope thermometry	139
6.3.3 Isotopic source tracers	149
6.3.4 Mineral composition and fluid evolution	153
6.3.5 Whole rock oxygen isotope variations	154
6.4 Summary	159
Chapter 7 DISCUSSION AND MODEL FOR GOLD MINERALIZATION	160
7.1 Synthesis of geological and geochemical data	160
7.1.1 Geologic and tectonic environment of gold deposition	160
7.1.2 Origin of hydrothermal fluids	165
7.1.3 Mechanism of gold transport and deposition	172
7.2 Comparison to other mesothermal gold deposits	176
7.2.1 General characteristics and fluid regimes	176
7.2.2 Polymetallic mineral assemblages	183
7.3 Outstanding problems	187
7.4 Conclusions	188
References Cited	192
Appendix A - Sample locations	212
Appendix B - Whole rock chemistry	218

List of Tables

Table 5.1	U-Pb Isotopic Data
Table 5.2	U-Pb Zircon Ages for Some Major Felsic Units of the Northwestern Notre Dame Subzone
Table 5.3	Th/U Ratios of Zircon From Sample D-1
Table 6.1	Isotopic Compositions of Vein Quartz and Carbonate Minerals
Table 6.2	Mean and Range for Quartz and Calcite Isotopic Compositions of Type II and Type III Veins
Table 6.3	Oxygen isotopic Fractionation Between Quartz and Carbonate Minerals in Type II and Type III Veins, and Calculated Equilibrium Temperatures
Table 6.4	Calculated Temperatures from $\delta^{18}\text{O}$ Values of Coexisting Quartz, Chlorite, and Muscovite
Table 6.5	O and H isotopic Compositions of Fluids in equilibrium with Hydrothermal Assemblages
Table 6.6	Oxygen Isotopic Composition of Whole Rock Samples
Table A-1	Outcrop Sample Locations
Table A-2	Drill Core Sample Locations
Table B-1	Whole Rock Chemistry

List of Figures

- Figure 1.1** Map of Newfoundland showing location of study area
- Figure 2.1** Tectonic - stratigraphic divisions of Newfoundland
- Figure 2.2** Geological map of the King's Point area
- Figure 3.1** Generalized geological map of the Hammer Down prospect and surrounding area
- Figure 3.2** Lower hemisphere stereographic projections of rock fabrics and quartz veins
- Figure 3.3** Geologic cross section of the Hammer Down prospect
- Figure 3.4** Detailed geology of the main Hammer Down trench exposure
- Figure 3.5** Alkali oxide - silica plot for chemical classification of volcanic and related rocks
- Figure 3.6** Alkali - total ferrous iron - magnesia (AFM) plot for volcanic and related rocks
- Figure 3.7** Bivariate variation diagrams of TiO_2 , Al_2O_3 , Fe_2O_3^* , and CaO against MgO
- Figure 3.8** TiO_2/Zr vs. Nb/Y plot for chemical classification of volcanic rocks
- Figure 3.9** Discrimination diagrams using ratios of Ti , Y , Zr , and Nb
- Figure 3.10** TiO_2 vs. Zr plot for separation of arc and within plate settings of intermediate to felsic volcanic rocks
- Figure 3.11** Chondrite-normalized extended rare-earth element plots for mafic volcanic, volcanic-sedimentary, and intrusive rocks
- Figure 3.12** Chondrite-normalized extended rare-earth element plots for felsic volcanic or volcanic-sedimentary rocks

- Figure 3.13 Chemical classification of granitic and related rocks by molecular alkali-lime-alumina relations
- Figure 3.14 Alkali - total ferrous iron - magnesia (AFM) plot for felsic porphyry dykes
- Figure 3.15 Niobium-Yttrium bivariate plot for chemical characterization of felsic intrusive rocks
- Figure 3.16 Chondrite-normalized extended rare-earth element plots for felsic porphyry dykes and units from the eastern Baie Verte Peninsula
- Figure 4.1 Alkali oxides / Al_2O_3 vs total iron oxides (Fe_2O_3) / Al_2O_3 and $\text{MgO} / \text{Al}_2\text{O}_3$
- Figure 4.2 K_2O vs. Ba and K_2O vs. Rb
- Figure 4.3 Geochemical profile of selected major element oxides DDH MS-89-16
- Figure 4.4 Geochemical profile of selected trace elements in DDH MS-89-16
- Figure 4.5 Paragenetic sequence of metamorphic and hydrothermal minerals
- Figure 5.1 U-Pb Concordia plot for SV-2 felsic tuff zircon samples
- Figure 5.2 U-Pb Concordia plot for D-1 felsic dyke zircon samples
- Figure 6.1 C and O isotopic compositions of carbonate minerals
- Figure 6.2 Histograms of $\delta^{18}\text{O}$ values of quartz
- Figure 6.3 $\delta^{18}\text{O}$ values of quartz and calcite mineral pairs
- Figure 6.4 Calculated δD and $\delta^{18}\text{O}$ values of hydrothermal fluids
- Figure 6.5 Recalculated C and O isotopic compositions of carbonate minerals
- Figure 7.1 Compilation of radiometric ages from the Baie Verte Peninsula and Hammer Down prospect

- Figure 7.2 Schematic cross section of a collisional orogen, showing possible fluid reservoirs and flow paths
- Figure 7.3 Schematic cross section of a metamorphic core complex, showing possible fluid reservoirs and flow paths
- Figure 7.4 Compilation of ^{18}O values of quartz from mesothermal gold deposits of various ages
- Figure 7.5 Calculated δD and $\delta^{18}\text{O}$ values of hydrothermal fluids in the Hammer Down prospect compared to compositional fields for other lode gold deposits

List of Photographic Plates

- | | |
|-------------------|---|
| Plate 3.1 | S₁ planar fabric developed in epidotized pillow lava |
| Plate 3.2 | Brittle-ductile S₂ fabric with dextral offset in felsic porphyry dyke |
| Plate 3.3 | Gold-bearing quartz veins along margins of felsic porphyry dykes |
| Plate 3.4 | Unfoliated breccia of lower brittle fault |
| Plate 3.5 | Porphyritic texture of felsic volcanic rock |
| Plate 3.6 | Clastic texture with abundant albite in epidotized basaltic rock |
| Plate 3.7 | Intense epidote, chlorite, and actinolite alteration in basaltic rock |
| Plate 3.8 | Fresh orthopyroxene phenocryst in basalt |
| Plate 3.9 | Quartz- and feldspar- porphyritic texture in felsic dyke |
| Plate 3.10 | Sericite and calcite alteration in felsic porphyry dyke |
| Plate 4.1 | Gold grains within pyrite and along grain boundaries |
| Plate 4.2 | Coarse gold within pyrite and along fractures |
| Plate 4.3 | Calcite, quartz, chalcopyrite, and sphalerite along fractures in gold-bearing pyrite |
| Plate 4.4 | Euhedral and skeletal pyrite grains in sphalerite |
| Plate 4.5 | Chalcopyrite inclusions or exsolution lamellae along crystallographic planes in sphalerite |
| Plate 4.6 | Chalcopyrite inclusions or exsolution lamellae along crystallographic planes of sphalerite |
| Plate 4.7 | Chlorite, quartz, and sphalerite in fracture within high grade gold-bearing vein |

- Plate 4.8** Chlorite, quartz, chalcopyrite, and sphalerite in veinlet cutting altered wallrock adjacent to high grade vein
- Plate 4.9** Pyrite with galena, magnetite, chalcopyrite, and lead telluride
- Plate 4.10** Gold or electrum, and gold-silver telluride with pyrite, lead telluride, galena, and magnetite
- Plate 4.11** Calcite, quartz, and fluorite in vein cutting S_2 fabric, but locally offset
- Plate 4.12** Interstitial fluorite in calcite-rich vein oblique to S_2 fabric
- Plate 4.13** Internally cleaved tensional quartz veins cutting S_2 in mafic volcanic rock, felsic porphyry dyke, and quartz vein
- Plate 4.14** Tensional quartz veins cutting felsic porphyry dyke and shear-parallel quartz vein
- Plate 5.1** Prismatic rutile oriented along crystallographic planes of calcite
- Plate 5.2** Unabraded prismatic zircon from felsic tuff sample SV-2
- Plate 5.3** Unabraded zircon prisms from felsic porphyry dyke sample D-1
- Plate 5.4** Unabraded zircon needles from felsic porphyry dyke sample D-1.

Chapter 1

INTRODUCTION

1.1 General statement

Deformed and metamorphosed Lower Paleozoic rocks host mesothermal lode gold mineralization at the Hammer Down prospect near King's Point, in the Green Bay district of Newfoundland (Figure 1.1). The Hammer Down prospect was discovered by Noranda Exploration Limited in 1987, and is among Newfoundland's most significant areas of gold mineralization. The nature of the host rocks and ore zones, particularly their chemical and isotopic characteristics and age, form the subject of this thesis.

Mesothermal gold mineralization is likely linked to tectonic events that were active over an area much larger than that of any individual prospect or deposit, and the mineralization must therefore be described and studied within a broad and complete geological context. Description and study of the Hammer Down prospect and its geologic and tectonic setting will produce a better understanding of the ore forming processes, will contribute to an increased knowledge of metallogeny in the Appalachians, and will also help to identify new areas for potential mineral deposits.

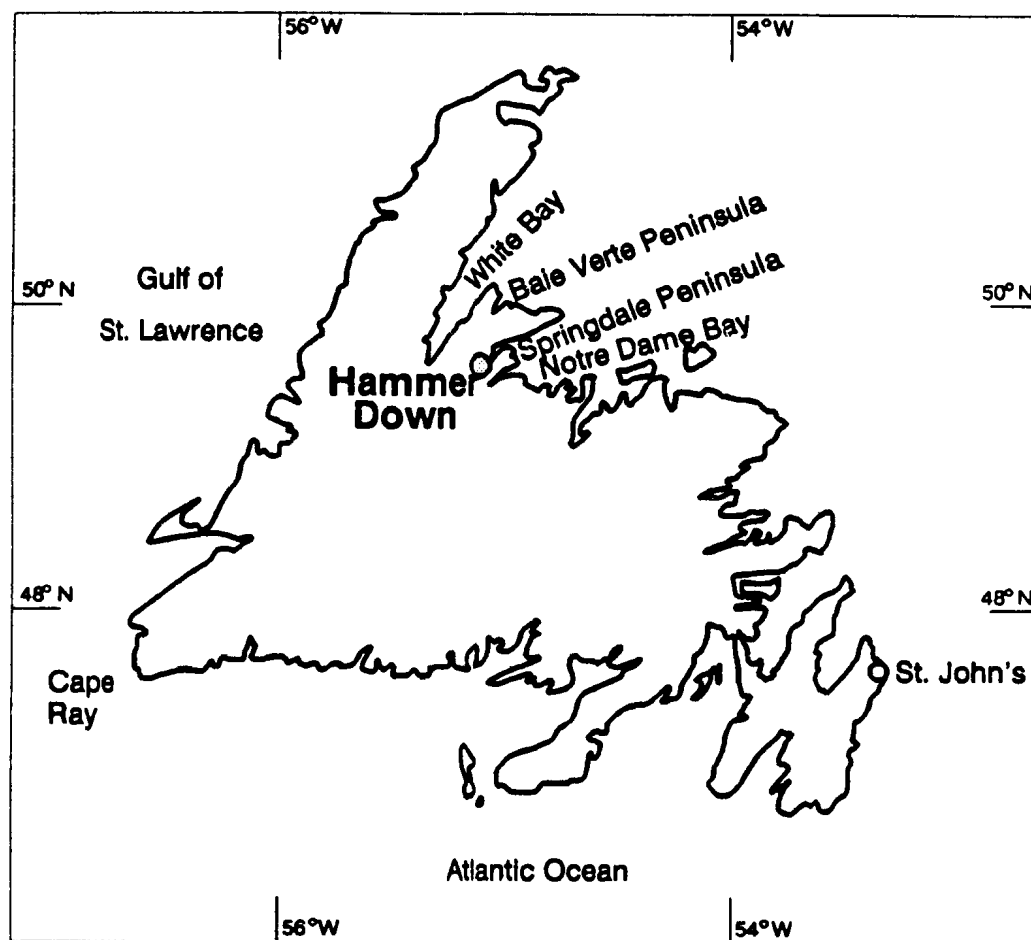


Figure 1.1 Map of Newfoundland showing location of study area and other geographic locations mentioned in text.

1.2 Mesothermal gold deposits

Mesothermal gold deposits constitute an important class of mineral resource that has been the subject of much scientific interest in recent years. The complexities of individual gold occurrences do not permit the development of any single, universally applicable genetic model, but the important geological and geochemical features that are shared by many mesothermal lode gold deposits do suggest a common mode of origin, and allow comparison of different deposits that are widely distributed in space and time. The term mesothermal was applied by Lindgren (1937) to mineral deposits formed near or adjacent to deep seated intrusive bodies, but it is generally applicable to those deposits formed under intermediate crustal conditions of pressure and temperature, not necessarily linked to any igneous process.

Precambrian greenstone belts, particularly those of the Australian Yilgarn Block, shield areas of southern Africa, and the Superior Province in the Canadian Shield, contain many of the largest, best known, and most completely studied mesothermal gold deposits. Important Phanerozoic examples include deposits in the Ural Mountains and Central Asia (Boradaevskaya and Rozhkov, 1977; Boyle, 1979;), the Ballarat slate belt of Australia (Sandiford and Keays, 1986; Cox *et al.*, 1987), the Meguma terrane of Nova Scotia (Kontak *et al.*, 1990), the Mother Lode and other districts of California (Bohlke and Kistler, 1986; Weir and Kerrick, 1987), the Cordillerran districts of Alaska and western Canada (Goldfarb *et al.*, 1988; 1991a;

Nesbitt *et al.*, 1986), the Southern Alps of New Zealand (Koons and Craw, 1991; Craw, 1992), and the Italian Alps (Curti, 1987). Mesothermal gold deposits of all ages have a geodynamic setting of tectonic accretion, crustal thickening, regional deformation, prograde metamorphism, and magmatism related to orogenesis (Barley *et al.*, 1989; Kerrich and Wyman, 1990; Barley and Groves, 1992). The deposits are generally present in sub-greenschist to amphibolite facies metamorphic rocks, with a wide variety of host lithologies. Within belts or terranes that host mesothermal gold districts, deposits are spatially associated with faults or shear zones of regional extent, but most are located in second or higher order structures (Colvine, 1989; Eisenlohr *et al.*, 1989; review in Kerrich, 1989a). The orebodies consist of structurally controlled veins and zones of altered rock, typically containing a hydrothermal assemblage dominated by quartz, muscovite, albite, pyrite, and carbonate minerals that overprints the textures and mineralogy of regional metamorphism in the host rocks.

Mesothermal gold deposits in shear zones are clearly epigenetic, and the O, Sr, and Pb isotopic contrasts that exist between ore zones and host rocks imply the introduction of fluid from an external source (*e.g.* Bohlke and Kistler, 1986; Curti, 1987; Kerrich *et al.*, 1987; King and Kerrich, 1989; Mueller *et al.*, 1991). The provinciality of isotopic signatures indicates that there is no single or unique source of fluids or solutes in mesothermal gold systems (Kerrich, 1989b). Temperatures calculated from oxygen isotopic fractionation between coexisting minerals in mesothermal gold deposits and from fluid inclusion filling temperatures are generally

in the range from 200 to 400°C (compilation in Kerrich, 1989b). When the temperature of mineralization is known, the hydrogen and oxygen isotopic composition of hydrothermal fluids may be calculated from measured $\delta^{18}\text{O}$ and δD values of minerals using mineral-water isotope fractionation factors. Coupled with salinity data from fluid inclusion studies, isotopic characteristics distinguish mesothermal deposits from epithermal gold-silver deposits, gold-bearing porphyry systems and volcanogenic sulphide deposits.

Ore-forming solutions for major deposits of the Abitibi Greenstone Belt and the Mother Lode and Allegheny districts of California have O and H isotopic compositions that are most consistent with a metamorphic origin (Bohlke and Kistler, 1986; Weir and Kerrick, 1987; compilations in Kerrich, 1987; 1989b), although a magmatic contribution cannot always be ruled out (Kerrich, 1989b). A generalized model of metamorphic devolatilization (*e.g.*; Groves and Phillips, 1987; Kerrich, 1989a) and focussed fluid flow (*e.g.* Sibson *et al.*, 1988) accounts for many geological and geochemical features of mesothermal gold deposits. In a terrane of tectonically thickened crust experiencing prograde metamorphism, fluid is continuously evolved at depth (*e.g.* Fyfe *et al.*, 1978; Yardley, 1983), and unless fine scale permeability allows it to escape, fluid pressure builds until it exceeds the lithostatic load and can be released by seismogenic fault failure (Sibson *et al.*, 1988). These expelled fluids, with their solute loads acquired by interaction with various rock units, move upward into regions that may have already passed peak metamorphic

conditions. Veins and mesothermal gold deposits are emplaced in fault zones that served as fluid passageways, or in fluid traps that may promote the ponding of fluids and development of saddle reef veins in folded metaturbidite sequences (*e.g.* Cox *et al.*, 1987). Episodic fluid flow may be generated by cyclic pressure variations as outlined by Sibson *et al.* (1988), and produce the multiple phases of fluid influx and mineralization that are evident from vein textures and geometric relationships in some mesothermal deposits.

Circulating meteoric water contributed to the fluid reservoirs of some gold vein systems in high level felsic plutons within the Abitibi Greenstone Belt (Kennedy and Kerrich, 1987, cited in Kerrich, 1987), and has been suggested as a major contributor to mesothermal gold systems of the Canadian Cordillera and elsewhere (Nesbitt *et al.*, 1986; Nesbitt, 1988). From numerical models of heat flow, tectonic uplift, and fluid movement adjacent to major fault zones in accretionary belts, Koons and Craw (1991) proposed a mechanism for precipitation of gold-quartz veins by mixing of meteoric and metamorphic water.

Precise ages for host rocks or direct dating of gold mineralization allow the timing of ore formation to be compared to ages of other tectonic, metamorphic, or magmatic events in a region. Emplacement of mesothermal gold deposits is typically a late kinematic event in the development of greenstone belts and accretionary orogens (Barley *et al.*, 1989; Kerrich, 1989a; Kerrich and Wyman, 1990). The mineralization postdates regional metamorphism (*e.g.* Bohlke and Kistler, 1986; Jemielita *et al.*,

1990; Goldfarb *et al.*, 1991b; Wong *et al.*, 1991; Kontak *et al.*, 1993), but may be synchronous with or younger than certain types of magmatic activity. Mesothermal gold deposits have a strong spatial association with felsic plutonic bodies, but the link arises from the mechanical suitability of the intrusions as hosts to vein systems, and is not typically considered to be a direct genetic relationship (*e.g.* Colvine, 1989). Magmatic-hydrothermal models for mesothermal gold have been proposed by Cameron and Hattori (1987) and Burrows and Spooner (1987), on the bases of spatial and temporal associations with felsic plutonism, mineralogic and isotopic evidence for oxidizing conditions, and carbon isotope systematics. Arguments for and against these models have been reviewed by Kerrich (1989b). Prograde metamorphism, devolatilization and fluid movement, and partial melting are all among the consequences of thermal equilibration in thickened crust, such that magmatic activity and the formation of mesothermal gold deposits may share a common tectonic origin, but, in general, no direct genetic links need exist.

1.3 Approach and scope of thesis

The geology of western and central Newfoundland is characterized by allochthonous oceanic terranes that were accreted to the ancient North American continental margin during Ordovician and Silurian ocean closure and continental collision. Intrusive rocks related to various phases of orogenic activity are abundant,

and are the immediate hosts to the richest gold bearing zones in the Hammer Down prospect. The geologic setting of this gold prospect is generally one of tectonic accretion, orogenesis, metamorphism, and magmatism, similar to the tectonic regimes that generated large lode gold deposits ranging in age from Archean to Tertiary, (e.g., Barley *et al.* 1989, Kerrich and Wyman 1990).. The Appalachian orogenic belt in Newfoundland contains the major geologic elements of a mesothermal setting, such that gold mineralization can be studied in the context of a large pre-existing database, and accepted models of ore deposition can be applied and tested. The principal aims of this project are to characterize the style of gold mineralization in the Hammer Down prospect, integrate it into the regional geological development, and compare it to other gold deposits in Newfoundland and to larger, better known gold occurrences.

This study is based on field and petrographic observations, and on chemical and isotopic analyses of rocks and minerals. The project started with mapping of rock types, structure, and hydrothermal alteration in outcrops and trenches, and careful examination of selected drill cores from the Hammer Down prospect and the associated Muddy Shag and Rumbullion mineralized zones. Approximately 50 days were spent in the study area in August and September 1990, and August 1991. This time was apportioned as follows: 8 days reconnaissance of regional geology and gold deposits of the district; 7 days investigating local geology; 25 days examining drill core and collecting samples; 10 days mapping in outcrops and exploration trenches. Drill core from 15 holes was studied, and approximately 2200 m of core was logged.

Porphyritic felsic dykes that host gold-bearing veins are particularly abundant in the Hammer Down prospect, and their close spatial relationship with the widest and richest zones of gold mineralization was a major reason for selection of this particular area for detailed study. Diluted geological reserves in the main Hammer Down mineralized zone are 403,000 T at an average gold grade of 12.5 g/T, with all assays above 60 g/T cut to 60 g/T.

This thesis includes a descriptive account of rocks in the prospect area, and of the mineral assemblages associated with gold. The geometry of mineralized zones is described, but it is not the intent of this project to develop or present a detailed structural model. Petrographic study of thin sections and polished sections identified the minerals and textures in veins and variably altered host rocks. More detailed mineralogical studies using X-ray diffraction methods and scanning electron microscopy gave information on composition and distribution of mineral phases.

A suite of fresh and variably altered host rocks and samples of regionally important geologic units was analysed for major and trace element contents by standard methods of atomic absorption spectroscopy (AAS), inductively coupled plasma optical emission spectroscopy (ICP-OES), X-ray fluorescence spectroscopy (XRF), and inductively coupled plasma mass spectroscopy (ICP-MS). Data from chemical analyses were used to characterize the host rocks, to make potential correlations among regional geologic units, and to give some indication of elemental mobility during the metasomatic processes that accompanied gold deposition.

U-Pb dating and stable isotopic analyses were undertaken to better understand the mineralizing process and to relate these processes to the geologic development of the region. Outcrop samples of volcanic and intrusive host rocks were selected from the Hammer Down prospect for dating by U-Pb zircon geochronology. In an attempt to directly determine the age of mineralization, hydrothermal rutile from vein margins was also collected for U-Pb dating.

Based on field relations and petrography, suites of samples were selected for carbon, oxygen, and hydrogen isotopic analyses of vein constituents and variably altered host rocks. Stable isotopic compositions of vein and wallrock minerals reflect the conditions and source of hydrothermal fluids, and record the interaction of fluid with host rocks. To test whether fluid compositions evolved through time, the different vein types identified by field mapping and petrography were analyzed.

Specific goals of this thesis are:

- 1) to produce a descriptive account of host rocks from the Hammer Down gold prospect, the structures that control the distribution of gold bearing veins, and the style and degree of alteration that accompanied mineralization;
- 2) to use petrographic and mineralogical studies to distinguish different morphologies and generations of veins, and to characterize the mineral assemblages of veins and altered zones adjacent to them;
- 3) to obtain chemical analyses of fresh and altered rocks from the gold prospect in order to describe and classify the host rocks and compare them to

regional geologic units, and to identify the chemical changes arising from interaction with hydrothermal fluids;

4) to generate radiometric ages for volcanic and intrusive host rocks from the prospect;

5) to employ stable isotope analyses of rocks and minerals from the vein and alteration minerals as constraints on fluid sources and temperature of mineralization;

6) to apply stable isotope analyses of variably altered host lithologies as a monitor of interaction between vein-forming fluids and wall rocks, accompanied by the petrographic and chemical characterizations of alteration.

7) to develop a genetic model for fluid movement and gold deposition in the Hammer Down prospect that can be placed in the context of Newfoundland geology and of other mesothermal gold deposits found worldwide.

1.4 Location and access of the study area

The Hammer Down prospect and associated gold showings are within a block of mineral exploration claims known as the Rendell - Jackman property, under the present control of Major-General Resources Limited. The prospect is located at latitude 49° 32' north and longitude 56° 15' west, on NTS map sheet 12 H/9 (King's Point), 5 km south of the community of King's Point (population *ca.* 1000).

Newfoundland provincial highway 391 transects the Rendell - Jackman property and provides easy access within 2 km of the mineralized zones. A well maintained logging road and a network of forest trails leads to the outcrops and trench exposures of the immediate prospect area.

The dominant physiographic feature of the King's Point area is the 200 m high scarp of the Green Bay fault, along the coast of Southwest Arm and 1.5 km west of the Hammer Down prospect. Irregular, hilly topography typifies the study area and most of the Springdale Peninsula, with multiple fault controlled ridges, valleys, and ponds. Elevations are only locally greater than 150 m throughout the Springdale Peninsula, but reach 250 m near the Rendell - Jackman property, and exceed 350 m northwest of the Green Bay Fault. Bedrock exposure is generally moderate to poor in the Hammer Down area, with dense forest and a widespread till cover that includes localised thick glacial-deltaic deposits. Although the Hammer Down gold prospect is located on a hillside at 150 to 200 m elevation, the immediate area is poorly drained, probably owing to the irregular bedrock surface. Several areas of bog and swamp larger than 0.5 km² with no bedrock exposure exist near the mineralized zones on the Rendell - Jackman property.

Chapter 2

GEOLOGIC SETTING OF THE HAMMER DOWN GOLD PROSPECT

2.1 Introduction: The Appalachian Orogen in Newfoundland

This chapter includes an overview of the regional geologic setting of the Hammer Down prospect, summarized in large part from published sources. More detailed descriptions of rocks from the prospect area, based upon this study, are presented in Chapter 3 and Chapter 4.

The Newfoundland Appalachians record the development and demise of an early Paleozoic ocean basin (Iapetus Ocean of Harland and Gayer, 1972). The Island of Newfoundland provides a cross section through the Appalachian Orogen, and based upon contrasts in structure and stratigraphy of Ordovician and older rocks, has been divided from west to east into the Humber, Dunnage, Gander, and Avalon tectonic-stratigraphic zones (Figure 2.1; Williams, 1979). The Humber and Avalon zones contain the essential elements of the Western and Avalon Platforms (Williams, 1964), which were considered by Wilson (1966) to be continental blocks that had evolved on opposite sides of an Early Palaeozoic oceanic tract, and were brought into proximity by closure of the ocean. Tectonostratigraphic zones or subzones east of the Humber Zone of the northern Appalachians are regarded as terranes (e.g. Williams and Hatcher, 1982; Barr and Raeside, 1989) that were accreted to the North American continent.

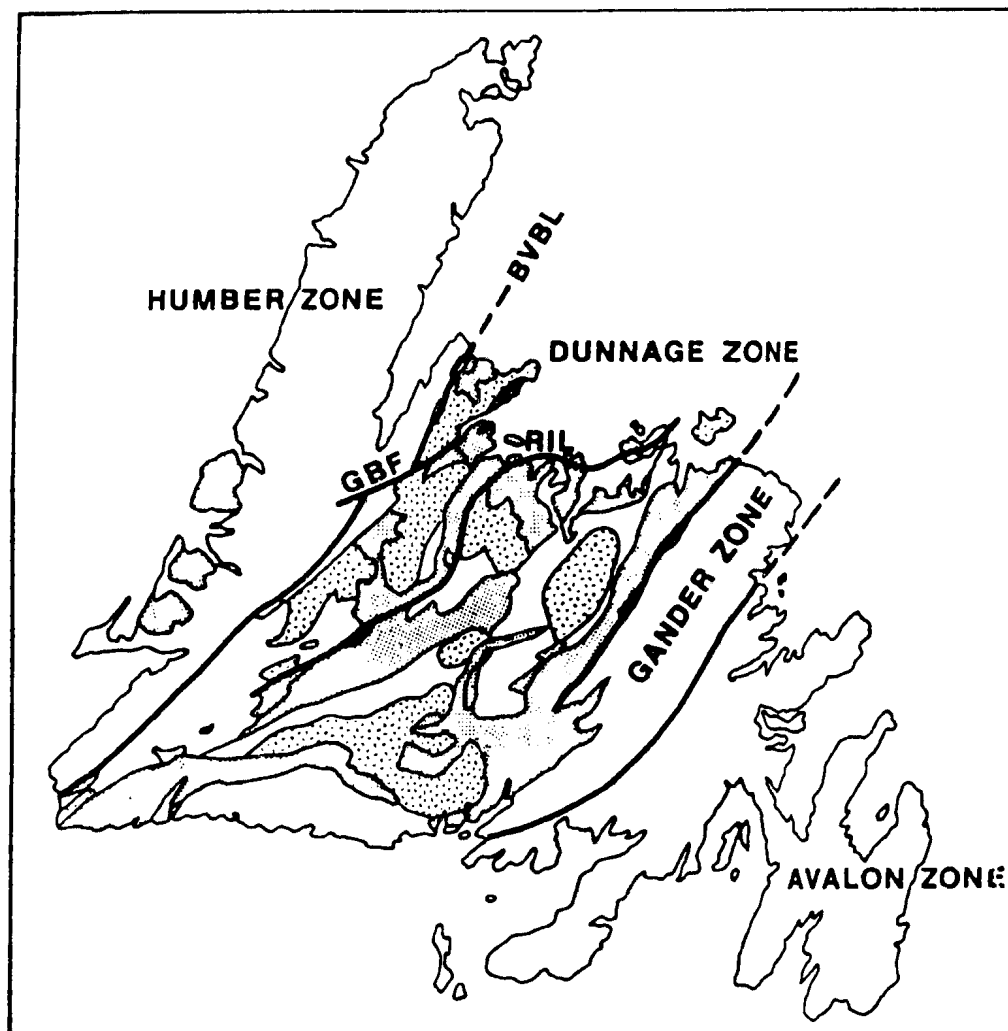


Figure 2.1 Tectonic - stratigraphic divisions of Newfoundland, and generalized geology of the Dunnage Zone, adapted from Swinden (1991). Stippled areas are underlain by Iapetan volcanic, epiclastic, and ophiolitic rocks; Hachured pattern identifies major areas of Silurian intrusive and volcanic rocks. BVBL = Baie Verte-Brompton Line; GBF = Green Bay Fault; RIL = Red Indian Line.

The Avalon Zone contains Hadrynian sedimentary and volcanic rocks unconformably overlain by Lower Cambrian to Lower Ordovician clastic sequences (Williams, 1979; King, 1988). On the Avalon Peninsula, these units are relatively undeformed and unmetamorphosed, but Avalonian rocks are intensely reworked by Paleozoic orogenesis along the south coast of Newfoundland (e.g. O'Brien *et al.*, 1989) and elsewhere in the Appalachians. Pre-Appalachian magmatic episodes at approximately 760 Ma, 680 - 670 Ma, 620 Ma and 580 - 550 Ma are characteristic of the Avalon Zone (O'Brien *et al.*, 1992).

The Gander Zone is made up dominantly of Cambrian and Ordovician metaclastic rocks, including gneiss and migmatite. The high degree of deformation and metamorphism hinders interpretation of the original sedimentary nature of these units, although they are generally considered to be marine deposits from the eastern margin of Iapetus (Williams, 1979; Colmann-Sadd, 1980). Major deformation of Gander Zone rocks took place during the Ordovician Penobscot Orogeny, and was accompanied by ophiolite emplacement along the zone boundary (Dec and Colman-Sadd, 1990; Colman-Sadd *et al.*, 1992). Gander Zone units are exposed as tectonic windows through the allochthonous eastern Dunnage Zone (Colman-Sadd and Swinden, 1984; Williams *et al.*, 1988). Depositional linkages were established between the Gander Zone and the Exploits Subzone of the Dunnage Zone after the Late Arenig (Colman-Sadd *et al.* 1992).

Of particular interest in this study are the Humber and Dunnage Zones of

Newfoundland, which represent the ancient North American (Laurentian) continental margin and the Iapetus Ocean, respectively. Rocks of the Humber Zone include crystalline Grenvillian basement unconformably overlain by dominantly marine Upper Precambrian and Lower Paleozoic sedimentary sequences (Williams, 1979; Williams and Hiscott, 1987), that were subsequently affected by Appalachian deformation. North and west of the Appalachian structural front, undeformed equivalents of these strata are a cover sequence upon the Canadian Shield. The middle Ordovician Taconic Orogeny is recorded in the Humber Zone by the emplacement of allochthonous oceanic rocks, including the well known ophiolites of western Newfoundland. During transport and emplacement, these ophiolitic units shed debris to form Early and Middle Ordovician (Arenigian and Llanvirnian) easterly-derived flysch (Stevens, 1970).

Together with Humber Zone allochthons, the Dunnage Zone contains "vestiges of Iapetus" (Williams, 1979), and records the geologic history of ocean closure. The Humber-Dunnage boundary is marked by the Baie Verte-Brompton Line (BVBL) (Williams and St. Julien, 1982), a narrow, steep structural zone characterized by mafic volcanic rocks, marine sediments, and discontinuous ophiolitic complexes. Metaclastic rocks or the extensive carbonate sequences of the Humber Zone are the main units present to the northwest, and marine volcanic and sedimentary sequences lie to the east and south of the boundary (Williams, 1979). Although the BVBL is locally covered by post-Ordovician rocks or disrupted and overprinted by younger

structures, it is generally traceable throughout the Canadian Appalachians (Williams and St. Julien, 1982). Grenville basement rocks are not exposed east of the BVBL, but they are interpreted from seismic data to extend eastward at depth for at least 70 km beneath north-central Newfoundland (Keen *et al.*, 1986), approximately to the central part of Notre Dame Bay. Ophiolite emplacement in western Newfoundland is dated stratigraphically as an Ordovician event, and by inference, movement on the BVBL is of a similar age. Hornblende and biotite $^{40}\text{Ar}/^{39}\text{Ar}$ cooling ages reported by Dallmeyer (1977), and Dallmeyer and Hibbard (1984) from the Fleur de Lys Supergroup west of the BVBL range from 420 Ma to 345 Ma (Middle Silurian to Early Carboniferous) however, and there is no documented metamorphic or plutonic event of Ordovician age in the Baie Verte or western Notre Dame Bay region that might have accompanied terrane emplacement or ophiolite obduction along the BVBL (G.R. Dunning and P.A. Cawood, unpublished U-Pb age data).

The Dunnage Zone is heterogeneous, but it is characterized throughout by early Palaeozoic mafic volcanic rocks, ophiolite suites, mélanges, and marine sedimentary rocks (Williams, 1979). Based on Ordovician and Silurian features, the Dunnage Zone has been divided into a northwestern Notre Dame Subzone and a southeastern Exploits subzone (Williams *et al.*, 1988). Most of the Ordovician marine volcanic sequences within the Dunnage Zone have the petrologic, geochemical, and isotopic characteristics of volcanic arcs, back-arc environments, or supra-subduction zone spreading centres (e.g. Swinden *et al.*, 1988; Swinden, 1991).

Volcanic arcs were developed by subduction of Iapetan oceanic crust over a span of more than 50 Ma, from the Late Cambrian to Middle Ordovician (Dunning *et al.*, 1991). During the early part of this subduction history, passive margin sedimentation continued in the Humber Zone. Plutonic rocks of magmatic arc character in parts of western and central Newfoundland, such as those of the Rainy Lake Complex which have a U-Pb igneous zircon age of 438 ± 8 Ma, provide evidence that tectonic and magmatic activity related to, or influenced by, the subduction of oceanic crust may have continued into the Early Silurian (Whalen *et al.*, 1987). Marine sedimentary rocks of Silurian age in the Dunnage Zone imply the persistence of at least a minor seaway after the Ordovician Penobscot and Taconic orogenic phases.

Silurian volcanic and intrusive rocks are widespread throughout the Dunnage Zone, and their distribution is not related to the fourfold zonal division of Newfoundland. In the northwestern portion of the Dunnage Zone, including the King's Point, Springdale, and Baie Verte regions, the area of exposure of intrusive and extrusive Silurian felsic units exceeds that of the older marine units. Age constraints on deformation, metamorphism, and magmatism identify a discrete, important, and widespread pulse of Silurian orogenesis in Newfoundland (Dunning *et al.*, 1990).

Devonian (Acadian) and Carboniferous (Alleghenian) orogenic activity is evident from fault movements and the development and deformation of sedimentary basins (e.g. Knight, 1983). These disturbances may also have contributed to the

generation and movement of fluids in the crust and to the development, deformation, or remobilization of mineral deposits.

2.2 Geology of central Newfoundland and the King's Point area

The Notre Dame Subzone comprises the northwestern portion of the Dunnage Zone, and contains an Ordovician-Silurian stratigraphic sequence that is distinct from that of the southeastern part, or Exploits Subzone. The Red Indian Line is a rectilinear fault or fault system (Williams *et al.*, 1988) that forms a major boundary delineating the two broadly similar oceanic terranes (Figure 2.1). Volcanic arc sequences are widespread throughout the Dunnage Zone, but thick units of Upper Ordovician and Silurian greywackes and conglomerates are characteristic of the Exploits Subzone, and are absent in the Notre Dame Subzone (Williams *et al.*, 1988). Lower to Middle Ordovician brachiopods of the Exploits Subzone belong to the Celtic faunal realm (Williams *et al.*, 1988), in contrast to the North American affinities of an age-equivalent conodont fauna of the Notre Dame Subzone (Nowlan and Thurlow, 1984; Williams *et al.*, 1988). Swinden *et al.* (1988) and Williams *et al.* (1988) have noted isotopic contrasts of volcanogenic sulphide deposits on opposing sides of the Red Indian Line.

Stratigraphy and the history of geologic study in the Notre Dame Bay area are extensively reviewed by Dean (1978). Several, approximately coeval volcanic and

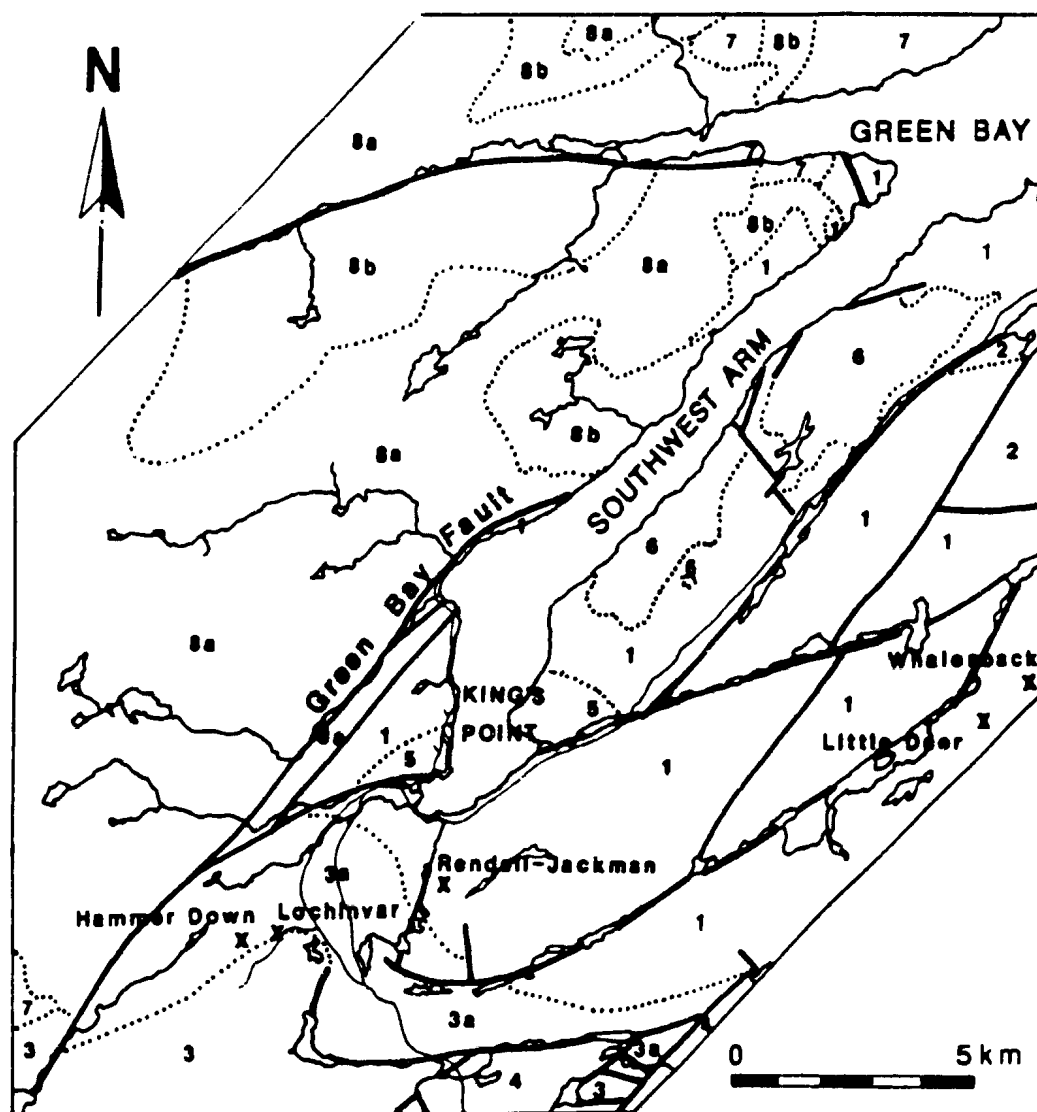


Figure 2.2 Geological map of the King's Point area, compiled from Neale *et al.* (1960), Hibbard (1983), Mercer *et al.* (1985), Kontak and Strong (1986), Kean and Evans (1987), and Andrews (1990a).

1	Lush's Bight Group
2	Western Arm Group
3, 3a	Catchers Pond Group
	3a. Argillite, mafic tuff, and chert-bearing unit
4	Springdale Group
5	Carboniferous rocks
6	Colchester and Coopers Cove plutons
7	Burlington Granodiorite
8a, 8b	King's Point complex
	8a. felsic porphyry (extrusive in part)
	and silicic volcanic rocks
	8b. Granitoid rocks
.....	Geological contact, approximate position
—	Fault
X	Mine or major mineral prospect

Figure 2.2 (continued) Legend for geological map of the King's Point area.

sedimentary sequences of Ordovician age are exposed along western Notre Dame Bay and on the Baie Verte Peninsula, where units of the Notre Dame Subzone are thrust over basement and Humber Zone rocks. Major lithologic units in the King's Point area are included in Figure 2.2, which includes parts of the Baie Verte and Springdale peninsulas.

The Hammer Down prospect is hosted by a sequence of volcanic and sedimentary rocks of the Catchers Pond Group, and by dykes that intrude these units. Neale *et al.* (1960) included the dominantly mafic rocks in the study area as part of the Lush's Bight Group [originally defined and described outside of the study area by Espenshade (1937), cited in Dean (1978)], to which they assigned an Ordovician age, and the dominantly felsic volcanic rocks to the south were placed within an unnamed Silurian unit, although they are now known to be Ordovician in age and broadly coeval with the mafic units. The Catchers Pond Group is a volcanic arc sequence, formally defined by Dean (1978), that is exposed over an area of approximately 150 km² and is dominated by pillow lava, agglomerate, tuff, and felsic lava. The sedimentary and mafic volcanic rocks underlying most of the area between King's Point and Catchers Pond (unit 3a on Figure 2.2) were mapped by Kean and Evans (1987) as bedded tuff, chert, argillite, and iron formation, although their map does not extend west to the Hammer Down prospect. This unit (3a) is part of the Catchers Pond Group or the uppermost portion of the Lush's Bight Group (Kean, 1988; Kean and Evans, 1990). Based on the presence of felsic tuff in the immediate prospect area,

the host rocks are considered to be part of the Catchers Pond Group rather than the Lush's Bight Group, which includes only mafic and ultramafic units (Kean, 1988). The present northwestern boundary of the Catchers Pond and Lush's Bight Groups is the Green Bay Fault, although this may be a feature that significantly postdates the original stratigraphic development and accretion of the oceanic terranes in central Newfoundland.

The Lush's Bight, Catchers Pond, Western Arm, and Cutwell Groups are generally considered as conformable sequences, although the contacts have been modified by faults (Dean, 1978; Kean, 1988). Along the eastern shore of Southwest Arm, the Middle Ordovician or older (Kean, 1988), dioritic to granitic Cooper's Cove and Colchester plutons intrude basaltic pillow lava of the Lush's Bight Group. Thirty-five km east of King's Point, the Lush's Bight Group is "apparently intruded by" (Kean, 1988) the Brighton Gabbro, which has an $^{40}\text{Ar}/^{39}\text{Ar}$ hornblende age of 495 \pm 5 Ma (Stukas and Reynolds 1975). Limestone beds within volcanic successions of the Catchers Pond Group 5 km south of the study area contain Arenig trilobites (Dean, 1970) and conodonts (O'Brien and Szybinski, 1989), indicative of an age older than 470 Ma using the Ordovician time scale of Tucker *et al.* (1991), and younger than approximately 488 Ma (Palmer, 1983). A maximum age for the base of the Arenig is provided by a U-Pb zircon age of 498 \pm 6/-4 Ma for Tremadocian strata of the Victoria Lake Group of central Newfoundland (Evans *et al.*, 1990). Felsic volcanic units of the Catchers Pond Group are lithologically similar to those of the

Cutwell and Western Arm Groups, which overlie the Lush's Bight Group 25 km east and northeast of King's Point (Kean, 1988; Kean and Evans, 1990). The Cutwell Group contains graptolites and conodonts indicative of a Llanvirnian or older age (Meyer *et al.*, 1988; O'Brien and Szybinski, 1988; Williams, 1988), and has a U-Pb zircon age of $469 \pm 5/-3$ Ma (Dunning and Krogh, 1991). MacLean (1947, cited in Kean, 1984), reported an Early Ordovician brachiopod from the Western Arm Group.

In the vicinity of King's Point, the Catchers Pond and Lush's Bight Groups are intruded by numerous felsic porphyritic dykes and plugs, of probable Devonian or Silurian age (Neale *et al.*, 1960). A series of these dykes is host to a large proportion of the gold ore in the Hammer Down prospect. Regionally extensive rock units of Silurian age near the study area include the Burlington Granodiorite and Cape Brulé Porphyry (G.R. Dunning and P.A. Cawood, personal communication, 1992), the Springdale Group (Whalen *et al.*, 1987; Coyle and Strong, 1987; Coyle, 1990), and the King's Point volcanic-plutonic Complex (Mercer *et al.*, 1985; Kontak and Strong, 1986; Coyle, 1990). All of these units except the Cape Brulé Porphyry are included in Figure 2.2.

The Burlington Granodiorite is exposed over a wide area of the eastern Baie Verte peninsula, where it intrudes Lower Ordovician ophiolite and volcanic arc sequences (Hibbard, 1983; Epstein, 1983), and is nonconformably overlain by Silurian sedimentary and volcanic rocks (Neale and Nash, 1963). As a regional unit, the body has been mapped only at a reconnaissance scale, and includes quartz diorite,

granodiorite, tonalite, quartz monzonite, and granite phases (Hibbard, 1983; Epstein, 1983; Mercer *et al*, 1985; Kontak and Strong, 1986). The Burlington Granodiorite may constitute a composite pluton or intrusive suite (Hibbard, 1983) and has recently yielded concordant U-Pb zircon ages of 440 ± 2 Ma and 432 ± 2 Ma from two geographically separate localities (G.R. Dunning and P.A. Cawood, unpublished data).

The Cape Brulé Porphyry is a high level intrusive or extrusive quartz- and feldspar-porphyrific body exposed over an area of 200 km² on the eastern Baie Verte Peninsula (Hibbard, 1983). Zircon from the porphyry has a U-Pb age of 436 ± 2 Ma (G.R. Dunning and P.A. Cawood, unpublished data), which overlaps with the measured ages of the two dated Burlington Granodiorite samples. The Cape Brulé Porphyry intrudes the Ordovician Pacquet Harbour Group and the Betts Cove ophiolitic complex, but its relationships and possible correlation to other Silurian units are unclear (Hibbard, 1983), and some of the reported field relations are contradicted by recent U-Pb dating.

The Springdale Group is a thick, extensive sequence of Silurian subaerial mafic and felsic volcanic rocks, and fluviatile sedimentary rocks that generally lies unconformably upon Lower Ordovician volcanic rocks of the Lush's Bight, Catchers Pond, and Roberts Arm Groups (Coyle and Strong, 1987). In the King's Point and Hammer Down area, conglomerate, sandstone, basalt and tuff of the Springdale Group are in fault contact with Ordovician units (Figure 2.2; Kean and Evans, 1987).

Silurian volcanic and sedimentary rocks of similar character are widespread southwest of King's Point and Springdale, in the eastern portion of the Baie Verte Peninsula, and along the west side of White Bay (*e.g.* Coyle and Strong, 1987). These units form part of an overlap assemblage that straddles the Baie Verte-Brompton Line. U-Pb zircon dating has yielded ages of $432 \pm 2/-1$ for crystal-lithic tuff of the lowest volcanic unit in the Springdale Group, and 425 ± 3 Ma for a stratigraphically higher tuff interbedded with sandstone (Coyle, 1990). Whalen *et al.* (1987) determined a U-Pb zircon age of 429 ± 2 Ma for a Springdale Group rhyolite.

Felsic volcanic and intrusive rocks of the King's Point Complex (Mercer *et al.*, 1985; Kontak and Strong, 1986), are exposed north of King's Point at Rattling Brook and Southwest Arm and 1.5 km west of the Hammer Down area (Figure 2.2). The Green Bay fault places these rocks in contact with the Ordovician marine units. U-Pb zircon dating (Coyle, 1990) indicates an age of 427 ± 2 Ma for a syenitic intrusive unit of the complex. Volcanic units within the King's Point Complex were included by Hibbard (1983) as part of the Cape St. John Group, which is exposed approximately 40 km northeast of the study area, on the Baie Verte Peninsula, and has a U-Pb zircon ages of 427 ± 2 Ma (Coyle, 1990). These felsic units are regionally correlative with the Silurian Springdale Group and its associated intrusive rocks (Coyle and Strong, 1987).

Paleogeographic reconstructions (*e.g.* Hibbard, 1983, and references therein; Coyle and Strong, 1987) that place the King's Point Complex adjacent to the main

body of the Springdale Group, and the Betts Cove ophiolite complex (with its sedimentary and volcanic cover sequence) adjacent to the Lush's Bight and Catchers Pond Groups, imply approximately 50 km of dextral movement on the Green Bay fault during or after the major Silurian magmatic episode.

The Green Bay fault is a major structure within the Dunnage Zone, and may have played an important role in the focusing of fluids related to the deposition of gold in the study area. Displacement along the fault zone possibly accompanied Ordovician development, disruption, or emplacement of Iapetan terranes. The latest established movement probably took place during the Carboniferous or younger periods (Hibbard, 1983). The surface trace of the Green Bay fault projects southwestward into that of the Cabot or Long Range Fault, which forms part of a major transcurrent fault system running from the southwest tip of Newfoundland through the Carboniferous Deer Lake Basin to White Bay. Along part of its course, this fault system overprints or is coincident with the Baie Verte-Brompton Line. The Green Bay fault is generally not well exposed (Z.A. Szybinski, personal communication, 1991, Dubé *et al.*, 1992), and the possible sense of movement is therefore poorly constrained.

Several exposures of Carboniferous sedimentary rocks unconformably overlie the Lush's Bight Group at King's Point but they are at least partly bounded by faults (Figure 2.2 ; Kean and Evans, 1987).

The Ordovician rocks of the King's Point area have undergone greenschist or

sub-greenschist facies metamorphism, with widespread development of carbonate, chlorite and epidote, and lesser actinolite and white mica. A similar style and degree of metamorphism is widely displayed throughout the Lush's Bight Group (Kean, 1988), which underlies most of the Springdale Peninsula. Widespread epidote-rich alteration is considered by Kean (1988) to have predated or accompanied regional deformation. Hydrothermal alteration associated with gold mineralization in the Hammer Down prospect overprints earlier metamorphic mineral assemblages.

2.3 Metallogeny of gold in Newfoundland

Ore deposits are the products of geologic processes that are operative on large temporal and spatial scales, leading to development of a metallogenic province where the prevailing tectonic regime may produce numerous deposits exhibiting a certain style of mineralization. In describing the known gold occurrences of Newfoundland, and outlining the potential for economic deposits, Snelgrove (1935) noted certain similarities with prospects and deposits throughout the "Appalachian Gold Belt" of eastern Canada and the United States, where similar geologic settings existed. Gold occurrences in Newfoundland include those with many features common to the large Archean lode deposits, but other styles of mineralization linked to different tectonic settings also exist. The largest historical producers of gold in Newfoundland were volcanogenic sulphide deposits that were mined primarily for copper, zinc, and lead

(Tuach *et al.*, 1988). In the past decade, gold has been a major exploration target in its own right.

Precambrian rocks in Newfoundland contain gold mineralization that predates the Appalachian orogenic cycle, although deposits may have been substantially remobilized or deformed by later events. Hadrynian volcanic rocks in the Avalon Zone contain up to 5 g/T Au with pyrophyllite, alunite, sericite, specular hematite, lazulite, and pyrite (Huard and O'Driscoll, 1986) at the Hickey's Pond prospect on the Burin Peninsula, and at several other occurrences in similar settings. The alteration assemblages indicate an epithermal or fumarolic environment related to volcanic or high level intrusive activity (Huard and O'Driscoll, 1986).

The Hope Brook gold mine, on the south coast of Newfoundland, is within Precambrian to Cambrian phyllite units with silica, sericite, and pyrophyllite alteration (O'Brien, 1989). Metallic mineralization consists of fine grained gold, pyrite, chalcopyrite, and minor tellurides, bismuthinite, cassiterite, and native silver (Tuach *et al.*, 1988). The orebody is highly deformed, and disruption or remobilization introduces considerable uncertainty into genetic models, as discussed by Tuach *et al.*, (1988) and Dubé, (1990), although the style of alteration and mineralization suggests an overprinted epithermal system, probably of Precambrian age (Yule, 1990).

On the western side of White Bay, gold bearing shears and stockwork are associated with alkali feldspar, silica, sericite, and pyrite alteration in Grenvillian

granitoid rocks (Tuach, 1987), with minor remobilized mineralization that extends into overlying Eocambrian quartzite. Late Precambrian rift-related magmatism in the area, described by Williams *et al.* (1985), may be linked to the deposition of gold (Tuach, 1987).

Rocks of Late Cambrian to Silurian age contain by far the largest number of gold deposits in Newfoundland. Based on contrasts in structural style, stratigraphy, and associated alteration, several styles or genetic types of gold mineralization have been recognized in the Dunnage Zone (Tuach *et al.*, 1988; Dubé, 1990; Evans, 1991, 1992). Stratabound gold mineralization at Nugget Pond on the Baie Verte Peninsula is developed in clastic sediments within the pillow lava sequence of the Betts Cove (ophiolitic) Complex (Dubé, 1990). The host rocks are undeformed, and mineralization is interpreted by McBride (1989, cited in Dubé, 1990) to be syngenetic with a volcanogenic exhalative process. Epigenetic gold deposits are vastly more numerous, and are widespread throughout the Dunnage Zone. A brittle-ductile style of deformation, alteration dominated by quartz, pyrite, muscovite (sericite), chlorite, and carbonate minerals, and the regional setting in metamorphic terranes indicate a mesothermal origin for the majority of occurrences. Gold occurrences in mafic to ultramafic units of the Ordovician accreted terranes, and in some Silurian mafic intrusive rocks, have many of the typical structural and mineralogical features of mesothermal deposits in Archean greenstone belts. Epigenetic vein deposits are also abundant in predominantly felsic Silurian to Devonian volcanic rocks. Major

mesothermal type deposits and prospects of Newfoundland include Cape Ray, Stog'er Tight, Pine Cove, and Hammer Down. The ore zones consist of single or multiple sulphide-rich quartz veins (*e.g.* Cape Ray and Hammer Down), extensive areas of hydrothermal replacement adjacent to vein systems (*e.g.* Stog'er Tight), or both (*e.g.* Pine Cove). The mesothermal type deposits are spatially associated with major geologic structures, but are localized in smaller faults or shear zones (Dubé, 1990). In these epigenetic deposits, it is the age of mineralization rather than of the host rock that links gold deposition to a specific tectonic setting. The development of mesothermal gold deposits in central Newfoundland is generally attributed to heat and fluid flow associated with Silurian or younger orogenic activity, although mineralization at Cape Ray has been genetically linked to fluids from Devonian granitic rocks on the basis of chemical and isotopic evidence (Wilton and Strong, 1986).

Certain prospects in central Newfoundland contain textural and mineralogical evidence of an epithermal origin. At Bobbys Pond near Victoria Lake, alteration minerals include native sulphur, alunite, and orpiment (Evans, 1992), in a large zone that contains anomalous gold values, but no gold assays greater than 0.1 g/T. Several prospects in the Gander Lake area contain hydrothermal breccias, or abundant chalcedony with cockade textures that distinguish these occurrences from the mesothermal deposits (Evans, 1991; 1992).

2.4 Summary

Terranes of central Newfoundland are dominated by Cambrian to Silurian marine volcanic and sedimentary sequences, and by Silurian terrestrial volcanic rocks and intrusive suites. Structure and stratigraphy, coupled with detailed, precise radiometric dating indicate major orogenic pulses in the Ordovician and Silurian Periods.

The Hammer Down gold prospect is hosted by felsic dykes that intrude volcanic and sedimentary rocks of the Lower Ordovician (Arenig) Catchers Pond Group, which is a volcanic arc sequence that forms part of an accreted oceanic terrane within the Dunnage Zone. Gold is present in a series of structurally controlled quartz veins. The prospect is spatially associated with the Green Bay fault, a major structure of regional extent, and the overall structural setting is similar to that of some other gold occurrences in Newfoundland and to mesothermal gold deposits in other orogenic belts.

Chapter 3:

GEOLOGY OF THE HAMMER DOWN PROSPECT AND HOST ROCKS

3.1 Introduction

This chapter contains descriptions of the structures and rock units that host gold mineralization in the Hammer Down prospect. The host rocks are described and characterized by their appearance and contact relations in outcrop and in drill core, and their mineralogy and texture as revealed by microscopic study. Whole-rock chemical compositions are used for classification of the host rocks, and for correlations with other igneous units of regional extent. All of the host rocks in the prospect area are metamorphosed, but in the following sections they are described by the igneous or sedimentary rock names of their protoliths.

3.1 General geology and structural setting of gold mineralization

3.2.1 Orientation and distribution of veins

The main mineralized quartz veins and hydrothermally altered areas in the Hammer Down prospect are contained within a series of steeply dipping zones of highly strained rocks. A detailed structural description of the Rendell - Jackman area and a more complete interpretation of the relationship between veins and structural elements are given by Dubé *et al.* (1992). A brief account of the empirical structural relationships is included here in order to describe the geometry of the ore zones and

their host rocks.

Volcanic and sedimentary rocks of the Catchers Pond Group and felsic porphyry dykes that intrude them are the hosts to gold mineralization at the Hammer Down gold prospect. Deformation that predates the intrusion of felsic porphyry dykes has produced a bedding-parallel S_1 planar fabric (Dubé *et al.*, 1992), which is the main fabric evident throughout exposures on the property (Figure 3.1; Plate 3.1). A second event of deformation locally folds S_1 (particularly at the Wistaria outcrops 110 m south of Hammer Down and in the Rumbullion zone; Dubé *et al.*, 1992), and has an associated axial planar fabric (S_2) that affects volcanic rocks and felsic dykes (Plate 3.2). Localized areas of strong S_2 development (D_2 high strain zones; Dubé *et al.*, 1992) are the principal sites of gold mineralization.

In the Hammer Down prospect, felsic dykes are cut or offset along steep 095° trending S_2 planes by both brittle and ductile shearing. Stereographic plots of several rock fabrics and mineralized vein orientations are presented in Figure 3.2. Many mineralized shears and veins trend close to 095° in the main Hammer Down trench exposure, although orientations are variable because veins were preferentially emplaced along dyke margins and within dykes that exhibit brittle as well as ductile D_2 deformation (Figures 3.3 and 3.4). Mineralized veins are generally within D_2 high strain zones, but are not necessarily parallel to S_2 , because of mechanical heterogeneity and anisotropy of the host. The lithological complexity of the Hammer Down prospect makes many structural relationships less clear than at other areas of

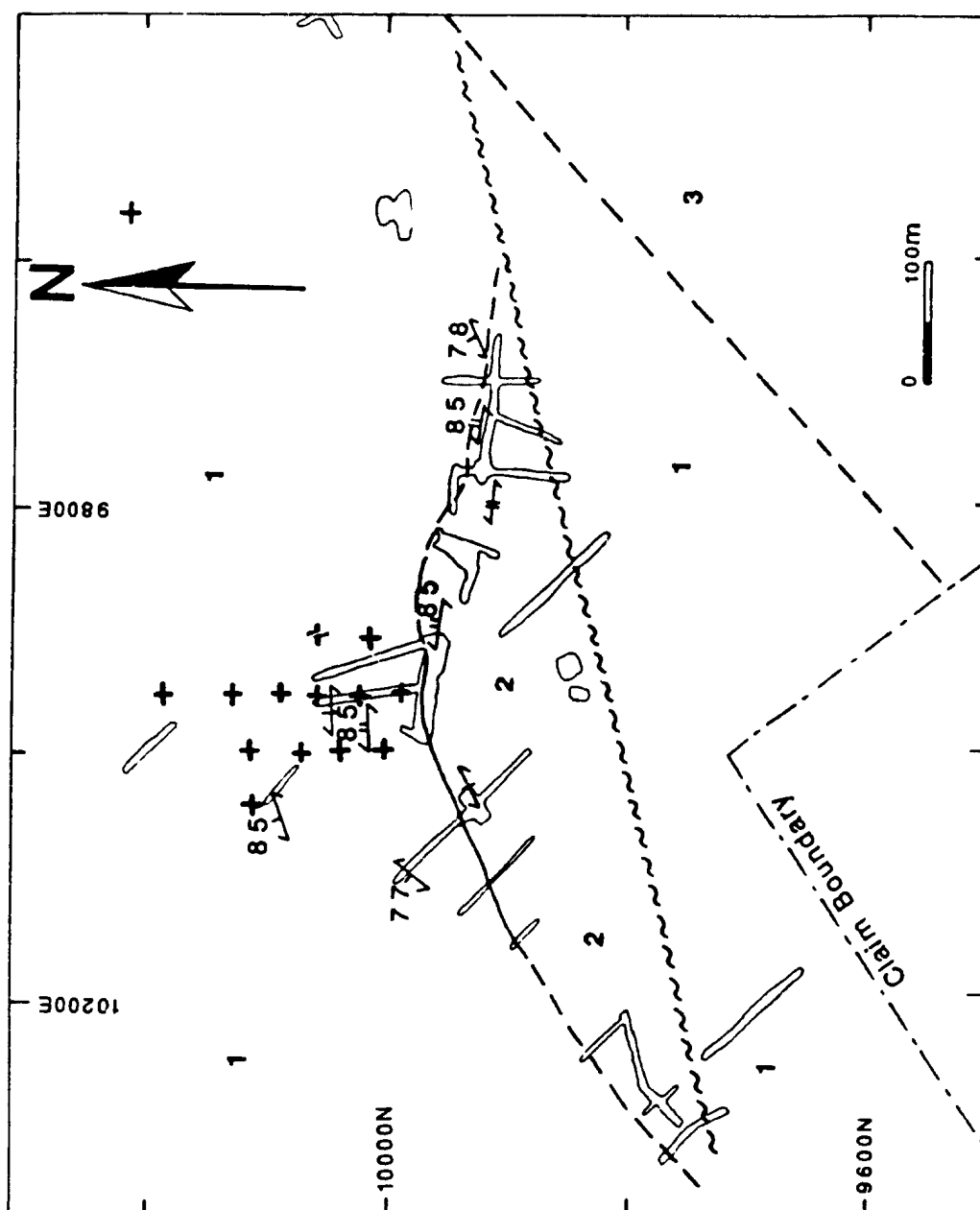




Figure 3.1 Generalized geological map of the Hammer Down prospect and surrounding area, showing selected structural elements. Adapted from Andrews (1990a; 1990b), with modifications from this study.

1 Predominantly epidotized pillow basalt, with pillow breccia, chert, and volcanogenic sedimentary rocks

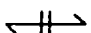
2 Mafic and felsic tuff and volcanogenic sedimentary rocks, locally calcite-rich

3 Predominantly felsic volcanic rocks, quartz-sericite schist

 Geological contact,
 approximate position

 Fault

  S1 foliation strike and dip, vertical

  S2 foliation strike and dip, vertical

 Diamond drill hole location

 Outline of trenches

Figure 3.1 (continued) Legend for geological map of the Hammer Down prospect.



Plate 3.1 S_1 planar fabric (subparallel to long axis of photograph) in epidotized pillow lava between Hammer Down prospect and Muddy Shag zone. Hammer handle for scale, approximately 30 cm long.



Plate 3.2 Brittle-ductile S_2 fabric (subparallel to long axis of photograph) within felsic porphyry dyke, immediate hangingwall of main mineralized zone in Hammer Down prospect. Metre stick for scale.

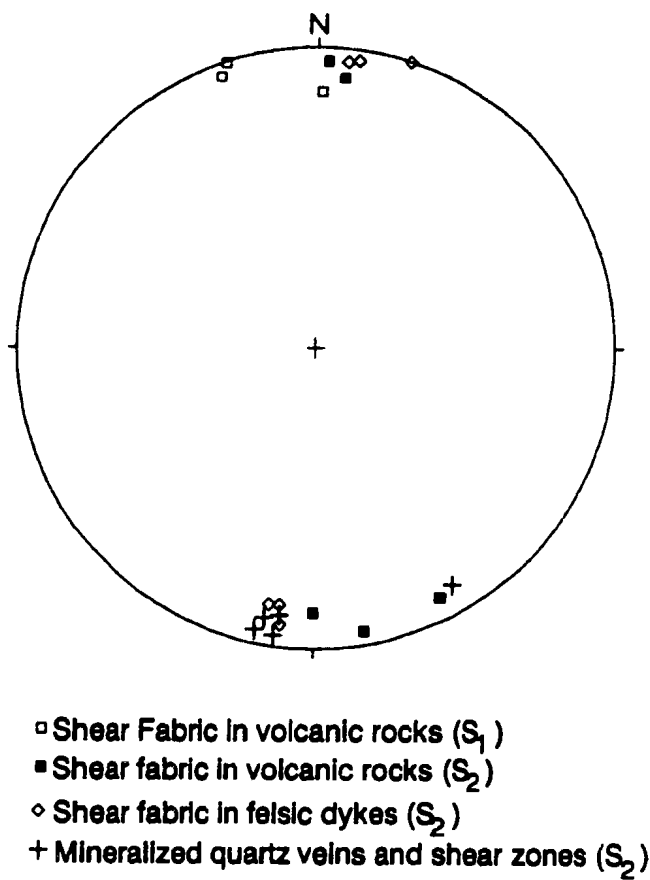


Figure 3.2 Lower hemisphere stereographic projections (poles to planes) of rock fabrics and quartz veins in the Hammer Down prospect.

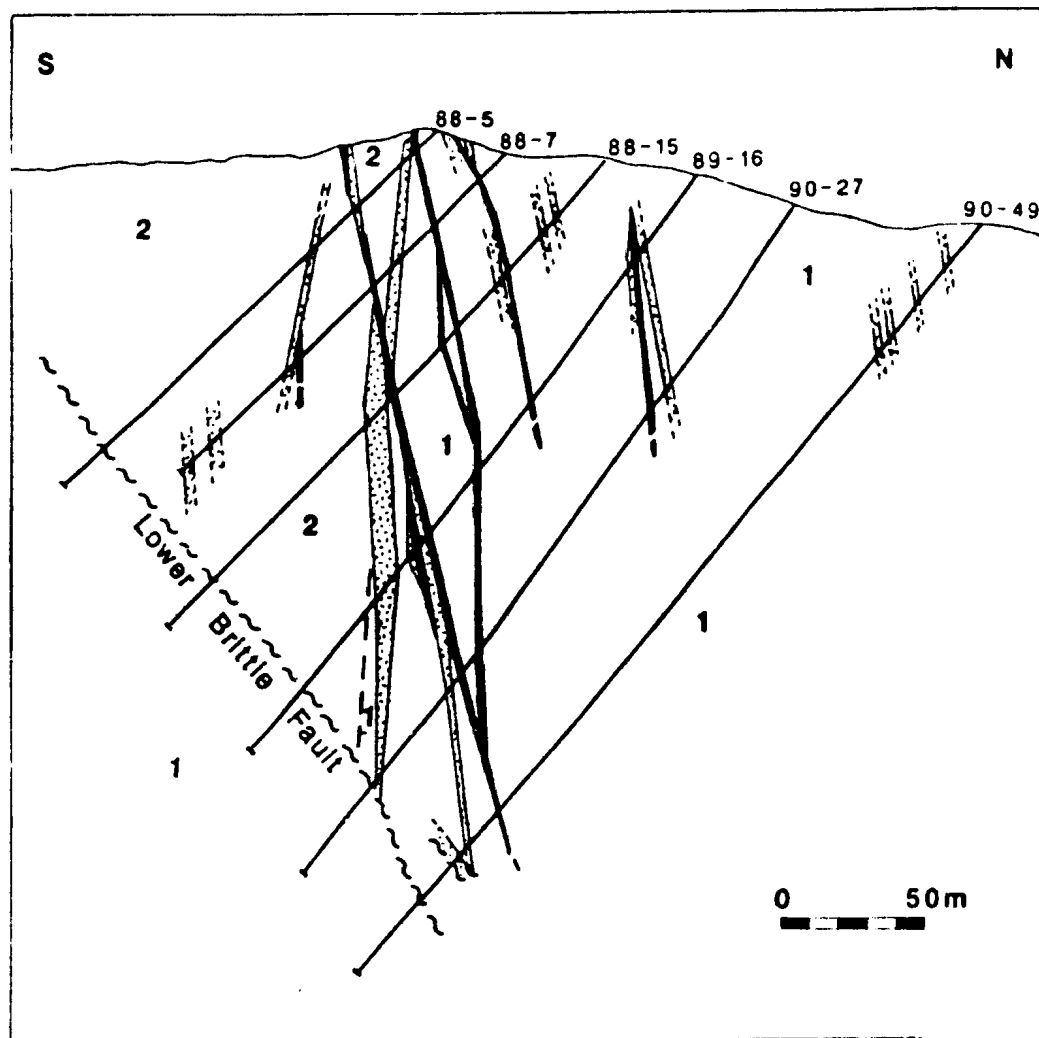


Figure 3.3 Geologic cross section along grid line 9950W of the Hammer Down prospect, based on surface mapping and drill core logging of labeled drill holes. Hachured pattern identifies felsic porphyry dykes; mineralized quartz veins are shown by solid dark pattern. Other symbols are as in Figure 3.1.

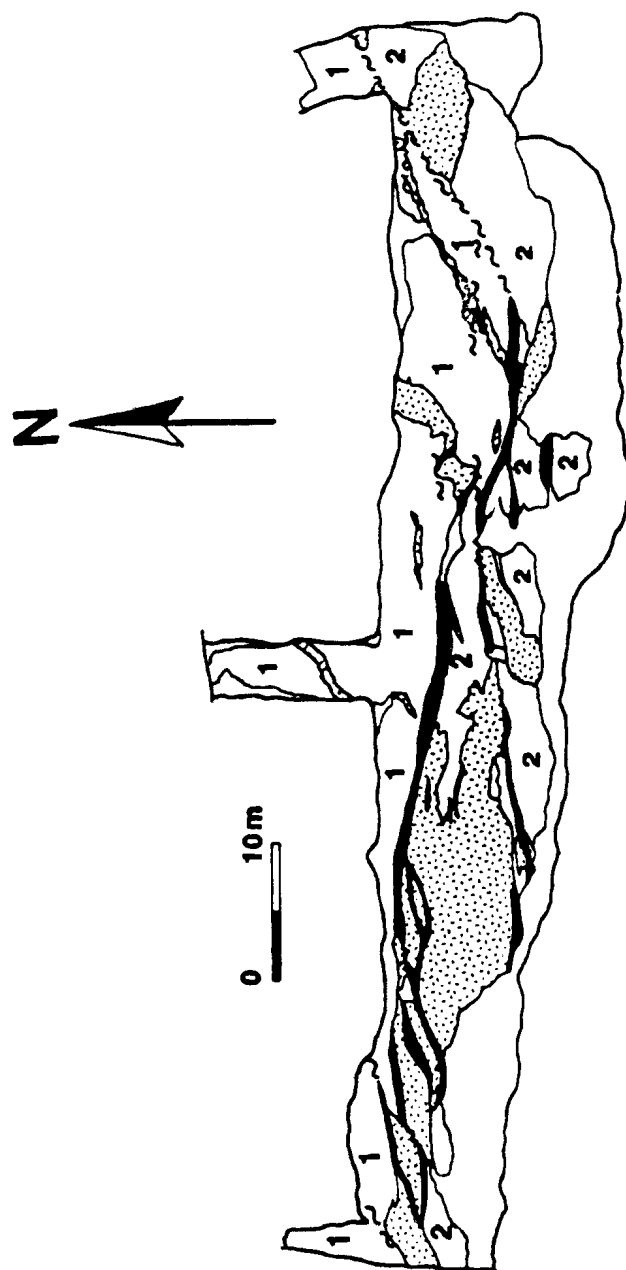


Figure 3.4 Detailed geology of the main Hammer Down trench exposure, showing close association of felsic porphyry dykes (hachured pattern) with mineralized quartz veins (solid dark pattern). Unit 1 is mafic and felsic volcanic and sedimentary rocks; unit 2 is predominantly epidotized pillow basalt; blank, unlabeled areas are covered by water or rubble. Other symbols are as in Figure 3.1

the property. At the western end of the trench, in an area termed the Hammer Down flexure (Andrews, 1990b), there is a series of weakly mineralized shears and faulted felsic porphyry bodies (Plate 2.3) oriented near $060^{\circ}/90^{\circ}$. This flexure projects southwestward into an area between the Hammer Down and Muddy Shag zones (Figure 3.1) that is strongly deformed but contains no gold mineralization. The strong fabric displayed there is interpreted as S_1 by Dubé *et al.* (1992), and therefore is not directly related to vein emplacement and the deposition of gold.

Deformation in the Rumbullion zone (200 m east of Hammer Down) more clearly demonstrates the geometrical relationships between certain structural elements. The zone is hosted by sedimentary and mafic volcanic rocks that are folded with axial planes generally parallel to the S_2 planar fabric, and fold hinges dipping steeply ($>65^{\circ}$) to the west. A subvertical east-west trending D_2 high strain zone contains a richly mineralized sheared vein within variably deformed mafic rocks. Abundant F_2 folds with wavelengths less than 20 cm wide are defined by discontinuous quartz-carbonate stringers or veinlets, typically 5 mm wide and 20 to 100 mm long, that are particularly common in the Rumbullion zone and the southern extremity of the main Hammer Down trench exposure.

Dubé *et al.* (1992) identified post-ore deformation (F_3) that affects the gold-bearing veins at the Muddy Shag zone, approximately 300 m southwest of Hammer Down. The orientations of strongly developed S_1 and S_2 fabrics in this zone are highly variable.



Plate 3.3 Rusty, gold-bearing quartz veins along margins of felsic porphyry dykes, and mineralized shears within dykes, located at west end of main Hammer Down trench. Metre stick for scale.

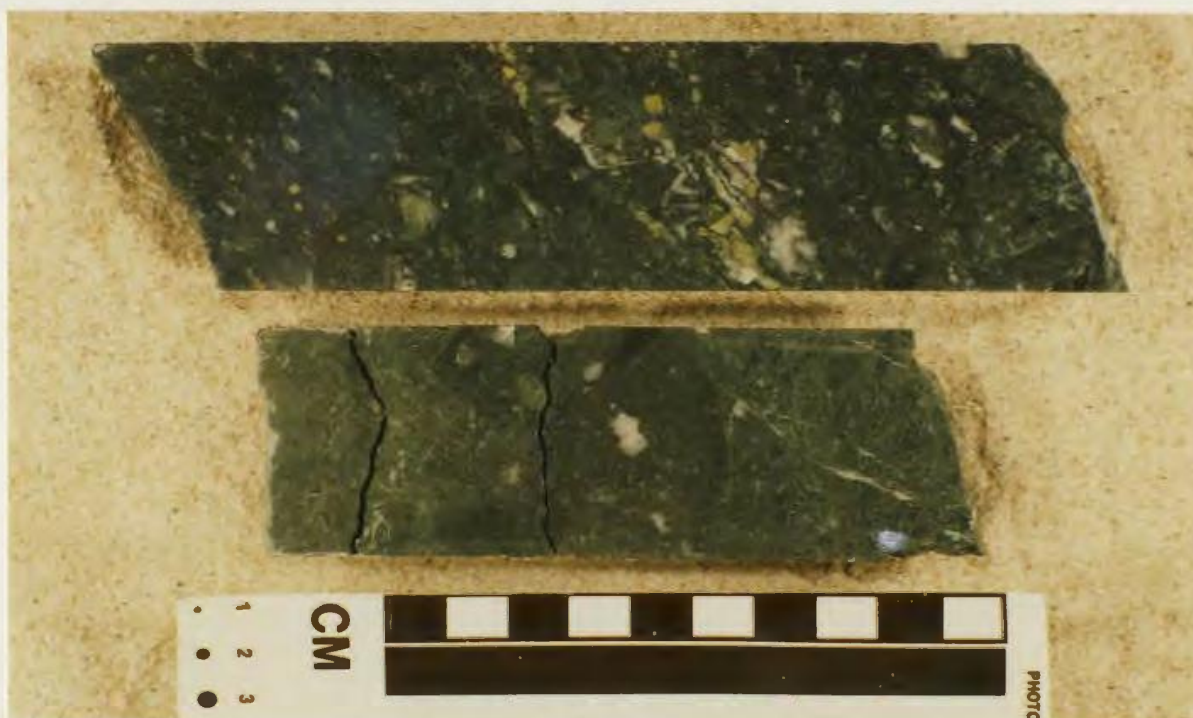


Plate 3.4 Unfoliated breccia of lower brittle fault in drill core DDH MS-89-27. Upper sample with abundant pale green epidote clasts is from 242 m depth, and lower sample with calcite veinlets and quartz fragments is from 243 m depth.

Where displacements on faults and narrow shear zones parallel to S_2 are observable in exposures of the main Hammer Down zone, offsets are typically less than 1 m. A dextral sense of displacement is most commonly displayed on surface, but shear along opposing limbs of F_2 folds has produced both dextral and sinistral offsets that are locally displayed and indicate the presence of an F_2 fold closure in the eastern portion of the trench (D. Gaboury and B. Dubé, personal communication, 1991; Dubé *et al.*, 1992).

The general structural model for gold mineralization on the Rendell - Jackman property is one of vein emplacement in dilational zones of accommodation that developed in the hinge zones of parasitic F_2 folds along the limbs of larger structures (Dubé *et al.*, 1992). In the Hammer Down prospect and Rumbullion showing, D_2 high strain zones and mineralized veins geometrically coincide with fold axes.

3.2.2 Late brittle faulting

A brittle fault that postdates gold mineralization dips moderately to the north, below the Hammer Down prospect. Gold-bearing veins were not observed in drill core below this lower brittle fault (LBF), or in outcrop south of its surface expression (Figure 3.3). In drill core, the LBF is marked by breccia with calcite veinlets 0.5 to 2 mm wide and massive to foliated fault gouge (Plate 3.4). Coherent to friable breccia in the fault zone is cemented by calcite to various degrees, and contains

abundant very fine grained pale green chlorite in the matrix. Fractured, calcite-cemented clasts 1 to 50 mm in maximum dimension are abundant and include hydrothermally altered felsic dyke material, sulphide-bearing milky quartz, and quartz-epidote clots similar to those that are widespread in outcrop and drill core. No kinematic indicators of the sense of movement on this fault were observed, and it is not exposed at surface, although it forms a prominent linear feature visible on aerial photographs.

3.3 Volcanic, sedimentary, and related rocks

3.3.1 Field relations

Host rocks in the Hammer Down gold prospect are lithologically diverse and heterogeneous. Principal rock types on the Rendell - Jackman property are basalt flows, along with mafic and felsic volcanic, volcanoclastic, and epiclastic rocks, and lesser volumes of clastic or chemical sedimentary rocks and diabase dykes. These units are intruded by felsic porphyry dykes that predate gold mineralization. Bedded sedimentary and volcanic rock units in the prospect area dip steeply to the north or northwest, but there are no indicators of the stratigraphic younging direction in outcrops or drill core.

Sedimentary rock types in the Hammer Down prospect include strongly magnetic maroon coloured chert and black pyrite-rich bands 1-5 cm thick that are

conformable with adjacent volcanic and tuffaceous rocks in the stratigraphic succession. These distinctive units are not laterally continuous, and they have not been correlated between drill holes. Dark grey or black sedimentary rocks are well exposed in an outcrop band 1 - 2 m wide along the southernmost margin of the main Hammer Down trench (Figure 3.4). This lithology contains abundant, narrow (less than 10 mm wide), tightly folded quartz-carbonate veinlets that are readily distinguished from the sulphide rich mineralized veins. The folded laminae or veins predate the D₂ phase of deformation and fluid influx that accompanied gold deposition. Intervals with abundant folded quartz and carbonate stringers were noted and collected from within the main mineralized zone and footwall zones of drill cores DDH MS-89-5, DDH MS-89-7, DDH MS-89-15, and DDH MS-89-16. Overall, sedimentary rocks are volumetrically minor, but they are predominant in some core intervals up to 50 cm in length. Massive to foliated, fine grained units are extensively exposed in the eastern portion of the main Hammer Down trench, and are weathered to a dark grey to blue-grey colour. In drill core, similar lithologies are grey to green-grey, and are not generally distinguishable macroscopically from basalt flows.

Felsic volcanic rocks are pale grey to dark grey-green coloured porphyritic tuff or resedimented tuff, with subhedral plagioclase and rare quartz phenocrysts in a fine grained sericitic and chloritic matrix. Individual bodies of silicic volcanic or epiclastic rocks in the main Hammer Down trench (Figure 3.1) are small, with less than 1 m² surface exposure, and the distinction between secondary silicification or

their original felsic nature is not always obvious in outcrop or hand sample. Lenses of silicic rocks are common in the immediate footwall of the Hammer Down prospect, where they are conformable with mafic volcanic and sedimentary units.

Approximately 120 m southwest of the main Hammer Down trench exposure, an outcrop of felsic tuff larger than 15 m² has a poorly exposed contact parallel to the main fabric in highly strained mafic rocks, and at the Wistaria outcrop, 100 m south of the main Hammer Down mineralized zone, mafic and felsic tuff are interbedded on a scale of 2 - 10 cm.

Mafic volcanic rocks are predominantly green to grey coloured leucoxene-bearing epidote altered tuff and pillow lava. Most basaltic units have a felty texture or exhibit a weak foliation defined by 0.1 - 2 mm plagioclase crystals or elongate aggregates of "leucoxene", which is an extremely fine grained or cryptocrystalline assemblage containing Fe- and Ti-oxides, rutile, and titanite. Development of the S₁ or S₂ fabric strongly accentuates this fabric. Most units described as basalt in drill core are dominantly dark green, medium to fine grained, with variable intensities of foliation. Within intervals dominated by mafic volcanic rocks, multiple flow contacts, chilled margins, and variations in grain size are visible in drill core. Where unit contacts are fine grained (possibly chilled), and less than 50 cm apart, the basaltic rocks are interpreted as pillow lavas. Other units appear to be massive flows. Away from highly strained zones, undeformed but pervasively altered and metamorphosed pillowed basaltic or andesitic rocks were observed in outcrop.

In outcrop and drill core, banded or bedded tuff and strongly flattened pillows impart a distinct layering to the rocks. Some tuffaceous units may be predominantly volcanic in origin, but others contain significant epiclastic or clastic components. Epidotized tuff and pillow lava are particularly abundant in the hangingwall above the strongly sheared and mineralized zones both in outcrop and in drill core.

Locally, crosscutting to semi-conformable basaltic dykes, 2 to 100 cm wide, are present on the Rendell-Jackman property and in drill core. Where tectonic fabrics are not well developed, as in the hangingwall of the main Hammer Down zone, some small dykes cut sharply across the S_0 fabric. In deformed intervals of drill core, mafic dykes are identifiable mainly on the basis of grain size, which exceeds 2 mm in some parts, in contrast to the fine grained basaltic units.

3.3.2 Petrography

Pyritic layers up to 5 cm thick are weakly or non magnetic, and consist of 55% fine granular quartz, 20% very fine grained chlorite and sericite, traces of white mica, and >20% pyrite as irregular blocky grains and 0.5 - 2 mm cubes. Some of these bands are folded in chaotic patterns on a scale of centimetres. There is no S_1 or S_2 fabric associated with these folds, and they are interpreted to have been produced by soft sediment deformation rather than the D_1 or D_2 deformational episodes.

Felsic volcanic rocks from the prospect contain partly sericitized plagioclase

phenocrysts in a matrix of fine grained chlorite, quartz, sericite, and carbonate (Plate 3.5). Quartz phenocrysts with variably developed subgrains and undulose extinction are common in an outcrop midway between the Hammer Down prospect and the Muddy Shag zone, and are absent in samples collected within the Hammer Down trench, where deformation, recrystallization, and alteration have significantly changed the original mineralogy and texture.

Moderately deformed mafic volcanic and tuffaceous intervals generally have a fabric defined by wispy chlorite with or without elongate aggregates of quartz and calcite. Actinolite is locally abundant as acicular or bladed crystals up to 3 mm long in bands 1 mm thick that are parallel to epidote + calcite + quartz (\pm titanite) layers and generally parallel to the pervasive rock fabric (Plate 3.6). Green pleochroic chlorite, dark brown or burgundy under crossed polars, is present in varying amounts (2 - 20%) as wisps or aggregates not larger than 0.2 mm. The most common forms of chlorite are interstitial flakes and grains, and fibrous masses. Adjacent to coarse calcite, pyrite, and quartz grains, rare aggregates or grains of chlorite up to 0.4 mm in maximum dimension are present. Clots of chlorite up to 2 mm long in some altered basalts may represent replaced primary ferromagnesian phenocrysts. Elongate chlorite grains and aggregates define a pervasive foliation in most basalt flows and volcanoclastic rocks, and contain abundant weakly aligned rutile (\pm titanite) inclusions 0.01 - 0.03 mm long, and rare magnetite. These inclusions are absent in chlorite from most very fine grained tuff or volcanogenic sedimentary rock samples. Finely

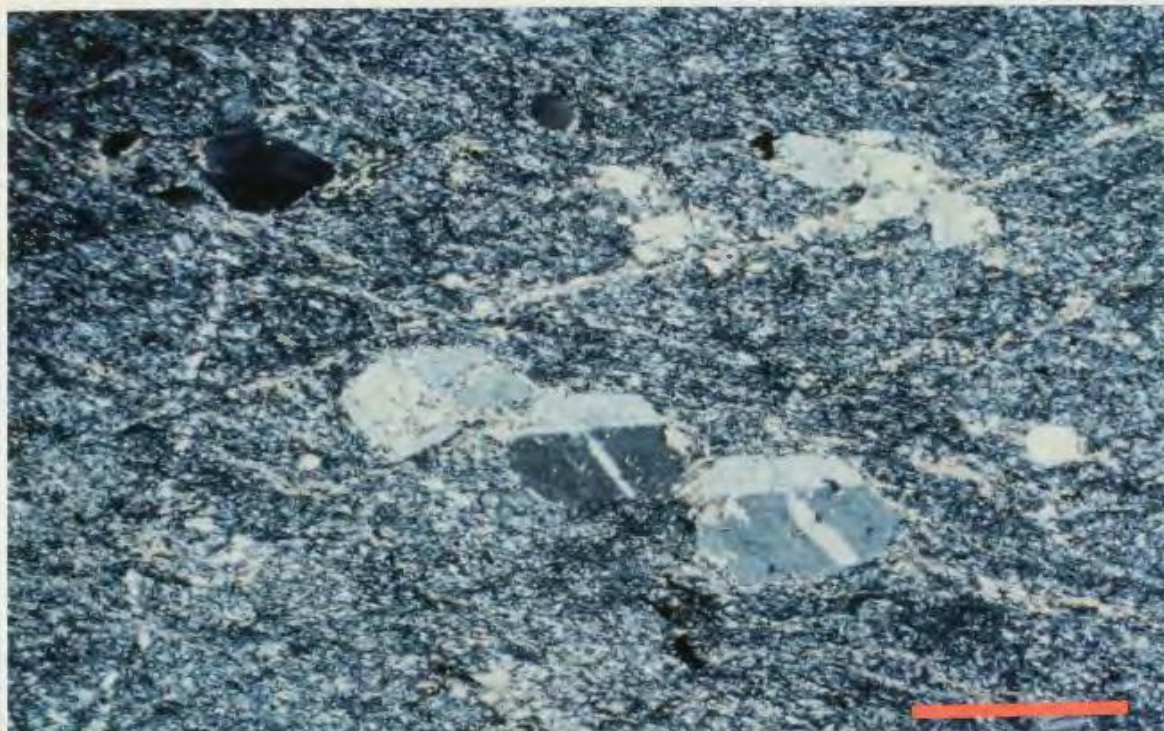


Plate 3.5 Porphyritic texture of felsic volcanic rock sample SV-2. View under crossed polars of quartz phenocryst (near extinction), and twinned plagioclase in sericite- and calcite-rich groundmass. Scale bar = 1 mm.



Plate 3.6 Epidote (high relief, yellow-brown), chlorite (green, patchy), and actinolite (bright green, acicular) in metamorphosed basaltic rock, sample DR-90-28. View under crossed polars. Scale bar = 0.1 mm.

laminated tuff samples typically contain variably sericitized and albitized feldspar microliths 0.01 - 0.05 mm long, extremely fine opaque grains (possibly including Fe-Ti-oxides, titanite, and rutile), abundant fine grained groundmass calcite, and 10 - 20 % fibrous and wispy chlorite (0.2 - 0.3 mm). These very fine ash tuffs or epiclastic rocks are locally interbedded with felsic volcanic rocks.

In most cases, the distinction between volcanic and clastic units is more evident in thin section than in outcrop and drill core. Banded mafic volcanoclastic rocks contain fresh anhedral plagioclase crystals, and abundant fine granular quartz and feldspar. Compositional layering and a clastic texture are evident in thin section (Plate 3.7). Calcite is widespread in the groundmass, and in 1 mm wide bands with fine granular titanite and very fine grained opaque iron-titanium oxides. Epidote is common in bands, lenses, and clots up to 5 cm diameter, along with carbonate and minor quartz. Basaltic flow samples have a weak pervasive foliation with elongate subhedral to anhedral fine grained interlocking laths of plagioclase, whereas semi-massive weakly to non-epidotized rocks from the Hammer Down trench have a fine grained clastic texture.

Two drill core samples of relatively fresh basalt from below the lower brittle fault contain 5 - 8 % orthopyroxene (Plate 3.8). The crystals are blocky subhedral phenocrysts with rare simple twins and weak, pale pink to green pleochroism. Anhedral granular clinopyroxene is a minor groundmass component of basalt samples with pyroxene phenocrysts, and comprises 5% of a basaltic dyke within the main

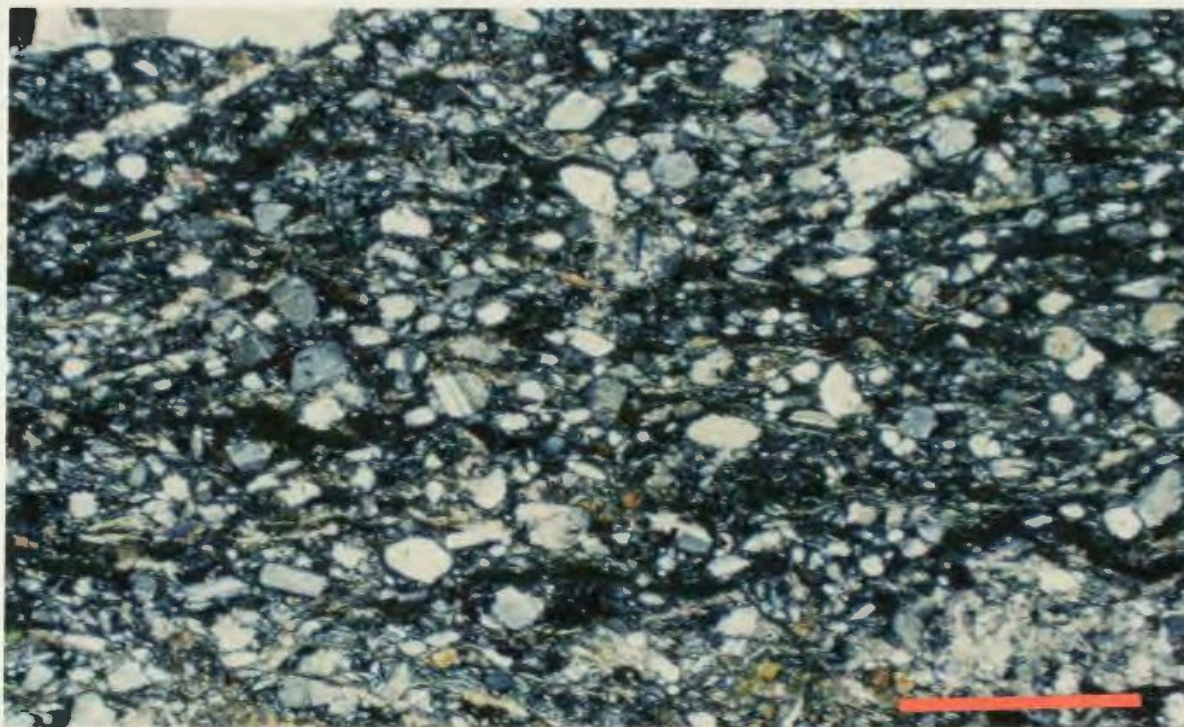


Plate 3.7 Clastic texture with abundant angular albite in calcite-rich epidotized and chloritized basaltic volcanoclastic rock, sample DR-90-31. View under crossed polars. Scale bar = 1 mm.

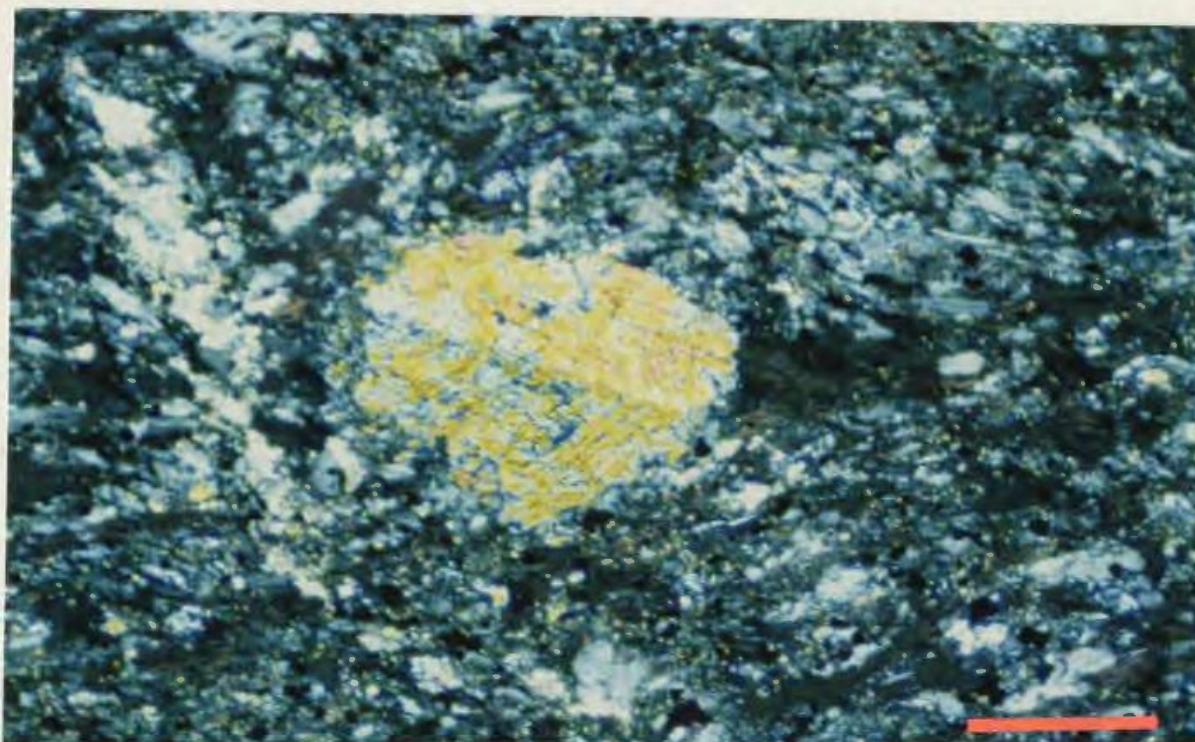


Plate 3.8 Fresh orthopyroxene phenocryst in weakly metamorphosed porphyritic basalt, sample DR-90-03. View under crossed polars. Scale bar = 0.2 mm.

mineralized zone of the Hammer Down prospect.

Mafic rocks near the main highly strained and mineralized zones are dominated by chlorite and granular calcite that overprint igneous or clastic textures. These schistose rocks cannot be designated as having originally been basalt flows or tuffaceous units. Intensely altered basalt contains up to 30% carbonate and 20% sericite, but it has locally been observed in thin section to contain patches less than 5 mm across that retain a 'felty' basaltic texture with weakly aligned albitized plagioclase laths.

Epidote- and chlorite-bearing assemblages are widely developed in rocks that do not display D_2 deformation, but their temporal relationship to deformational episodes is uncertain. Epidote-rich bands are parallel to S_0 or S_1 , and in drill core from the hangingwall of the main Hammer Down mineralized zone, aligned actinolite and chlorite define a rock fabric that is probably S_1 , since S_2 is only weakly developed outside of D_2 high strain zones. Locally, a weak foliation defined by stretched and flattened pale grey to cream-coloured leucoxene is parallel to epidote-rich bands, and is rarely wrapped around 2 - 25 mm epidote clots. The early chlorite + epidote \pm actinolite \pm leucoxene \pm carbonate metamorphic mineral assemblages appear to be broadly contemporaneous with development of the S_1 foliation, and are therefore interpreted to predate the emplacement of felsic porphyry dykes.

Assemblages containing chlorite, actinolite, white mica, and epidote are not uniquely indicative of greenschist facies metamorphism because these minerals are

also stable at very low metamorphic grades, including the prehnite-pumpelleyite or prehnite-actinolite facies (Miyashiro, 1973; Winkler, 1976; Liou *et al.*, 1985)). Low-grade, or greenschist facies metamorphism is typified by the presence of zoisite or clinozoisite (the iron-poor end-member of the epidote group) with chlorite (Winkler, 1976). The presence of relict igneous clinopyroxene is included by Mason (1978) as an indicator of metamorphism in the zeolite and prehnite-pumpelleyite facies with non-development of equilibrium assemblages. The overall abundance of epidote in contrast to zoisite or clinozoisite, coupled with the metamorphic and relict igneous mineralogy, is consistent with sub-greenschist facies metamorphism of the volcanic sequence that hosts the Hammer Down prospect.

3.3.3 Chemistry

Volcanic and epiclastic rocks that are believed to contain minimal sedimentary material are classified according to their alkali oxide and silica contents in Figure 3.5. Data for the majority of moderately altered and metamorphosed mafic rocks plot as a cluster in the compositional field for subalkaline basalt. Sample DR-90-21 is identified as alkali basalt, and is also chemically anomalous in terms of having the lowest silica content of any rock in the sample suite and by far the highest level of chromium (Table B-1 in Appendix B). Alkali enrichment related to metasomatism in samples DR-90-46 (plotted as "mugearite" in Figure 3.5) and DR-91-220

("trachyandesite") is expressed petrographically in these samples by intense sericite alteration and by pervasive albitization of plagioclase, respectively. The two felsic volcanic samples have an andesitic or dacitic composition based on overall appearance and mineralogy, but the addition of silica which is evident in thin section causes them to plot within the rhyolite field of Figure 3.5. Alkali addition in the sericite- and albite-rich rocks is also evident in the AFM diagram of Figure 3.6. The relatively unaltered mafic volcanic rocks form a cluster of data points near the boundary between tholeiitic and calc-alkaline rock types (Irvine and Baragar, 1971). Data from a medium grained, sheared mafic dyke is included in this plot for comparison to volcanic rocks. The limited degree of scatter observed in alkali, silica, iron, and magnesium contents of these rocks is attributable to metamorphism, hydrothermal activity, and the mineralogical and compositional heterogeneities that are indicated by field and petrographic observations. Contents of alkali elements, silica, iron, and magnesium are similar for the two analyzed felsic volcanic rocks, and a calc-alkaline character for these samples is indicated by Figure 3.6.

Four major element oxides are plotted against MgO content in Figure 3.7. If the mafic rocks are considered as a single cogenetic suite, considerable fractionation is required to produce the observed range of TiO_2 contents, which vary by a factor greater than three. Outliers from the main data trends include sample DR-90-21 which has the highest MgO content in the sample set, sample DR-90-46 which is an intensely altered sericite- and calcite-rich mafic rock with elevated Al_2O_3 and CaO

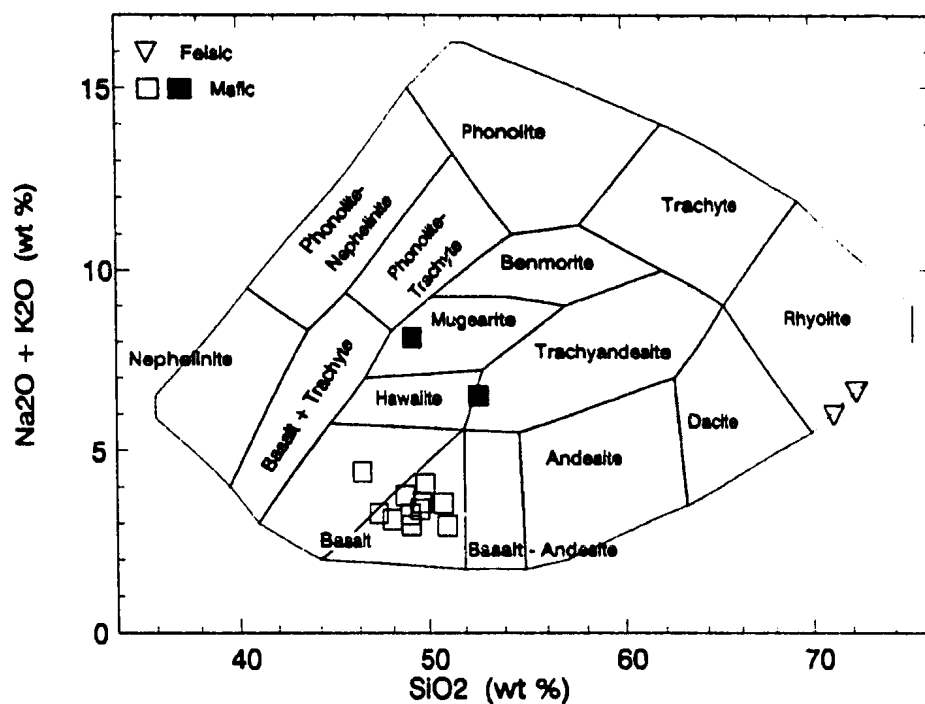


Figure 3.5 Alkali oxide - silica plot for chemical classification of volcanic and related rocks from the Hammer Down prospect. Triangles are data from felsic volcanic rocks; square symbols are for mafic rocks. Filled squares represent strongly albitized or sericitized mafic rocks (see text). Fields of rock types are from Cox *et al.* (1983).

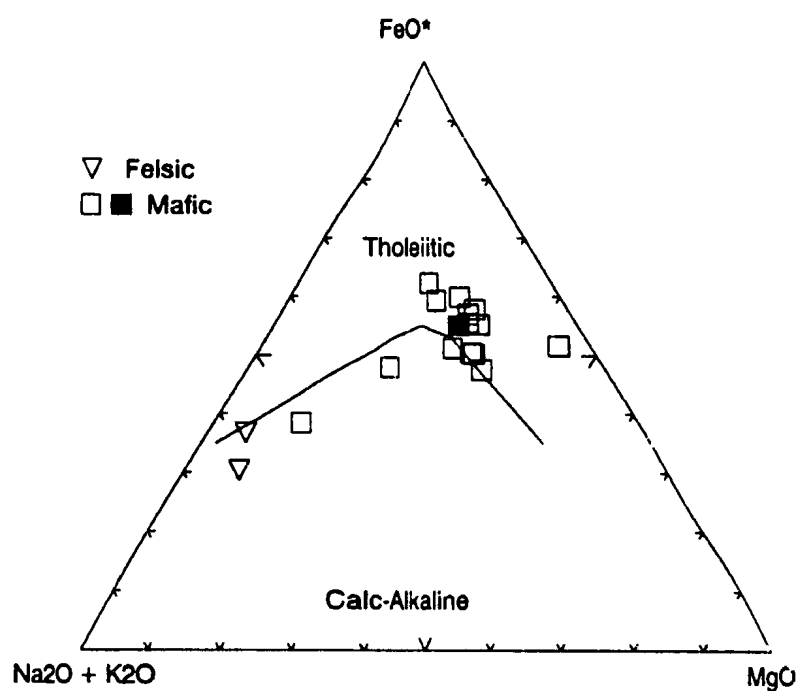


Figure 3.6 Alkali - total ferrous iron - magnesia (AFM) plot for volcanic and related rocks from the Hammer Down prospect, with division of calc-alkaline and tholeiitic suites from Irvine and Baragar (1971). Triangles are data from felsic volcanic rocks; square symbols are for mafic rocks. Filled square is data from a mafic dyke.

coupled with low MgO, sample DR-91-220 which is an undeformed pillow basalt with abundant albite and the lowest CaO content of any mafic rock in the sample suite, and calcite-rich tuff sample DR-91-125, which has the highest contents of Fe_2O_3 and CaO.

High field strength trace elements (HFSE) are generally immobile during metamorphism and metasomatism, and a characterization or classification of rocks based on contents or ratios of them is likely to be more reliable and internally consistent than one employing major elements that are essential components of metamorphic and hydrothermal minerals. All of the mafic rocks, except sample DR-90-21, are classified as basalt and andesite on a plot of TiO_2/Zr vs. Nb/Y (Figure 3.8).

Based on ratios of incompatible elements Nb, Y, Zr, and Ti (Figure 3.9), volcanic rocks from the Hammer Down prospect, again with the exception of sample DR-90-21, have an arc to mid-ocean ridge (MOR) geochemical signature, although the data cluster extends into the field for within-plate lavas on the discrimination diagram of Pearce and Cann (1973) in Figure 3.9a. Some of the characteristic geochemical features of basaltic lavas from arc settings are obscured by the effects of fractional crystallization in intermediate to felsic magmas (Pearce and Norry, 1979; Pearce, 1982). Because the plots in Figure 3.9 were designed primarily for rocks of basaltic composition, the absolute values of TiO_2 and Zr (information that is lost in the ratio plots of Figure 3.9) are plotted in Figure 3.10 to identify the volcanic arc geochemical nature of intermediate to felsic volcanic rocks from the prospect and of

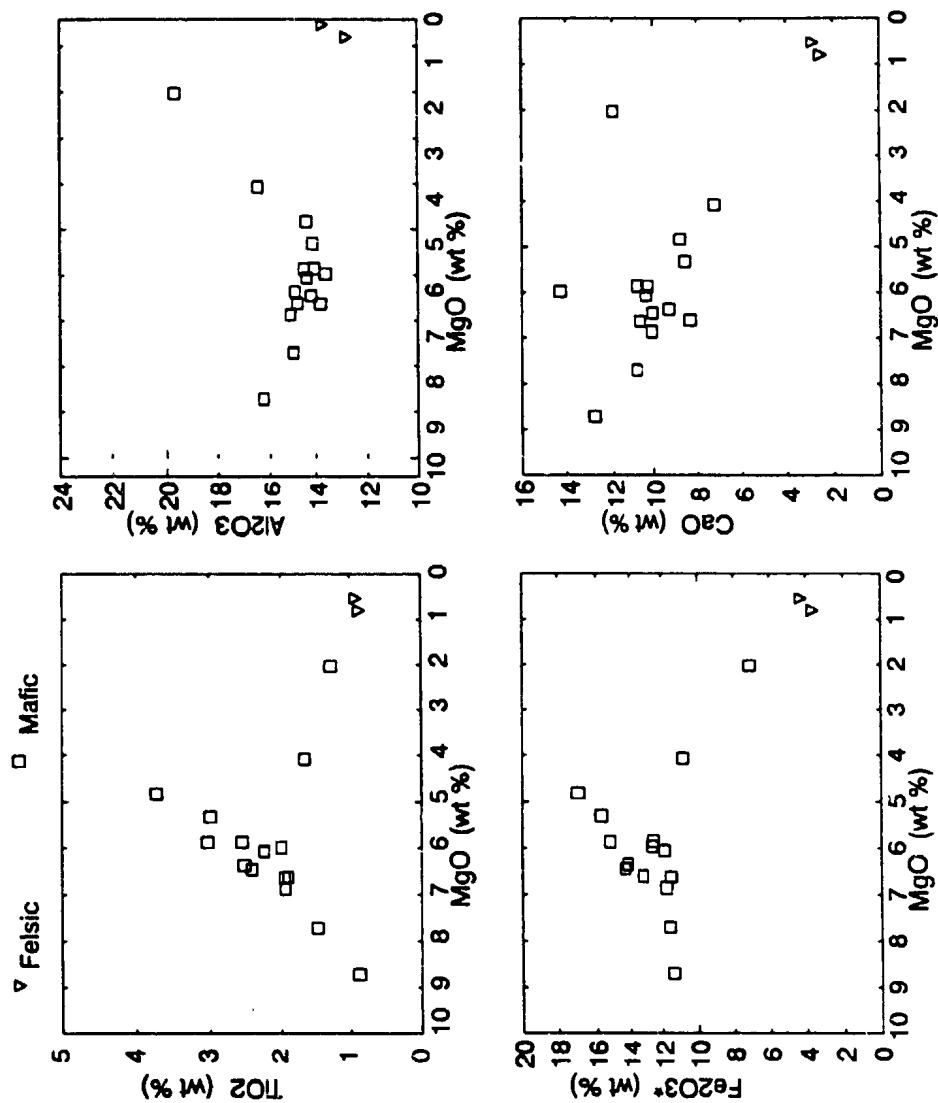


Figure 3.7 Bivariate variation diagrams of TiO_2 , Al_2O_3 , Fe_2O_3^* , and CaO against MgO . Triangles are data from felsic volcanic rocks; square symbols are for mafic rocks.

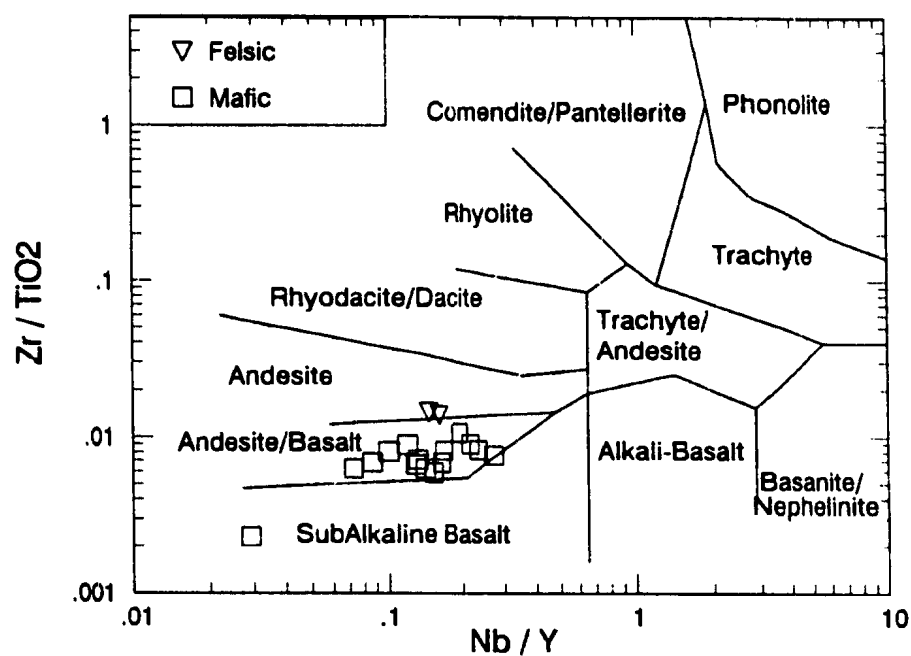


Figure 3.8 TiO_2/Zr vs. Nb/Y plot for chemical classification of volcanic rocks from the Hammer Down prospect. Triangles are data from felsic volcanic rocks; square symbols are for mafic rocks. Fields from Winchester and Floyd (1979).

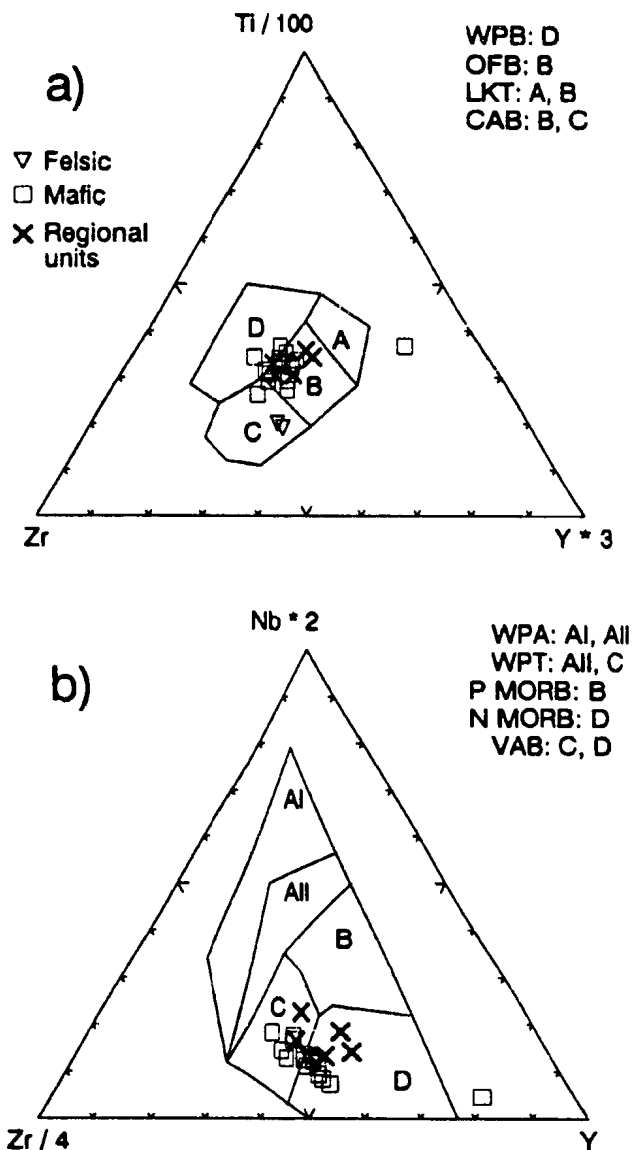


Figure 3.9 Samples of volcanic and related rocks from the Hammer Down prospect plotted on discrimination diagrams using ratios of Ti, Y, Zr, and Nb, with fields from (a) Pearce and Cann, (1973), and (b) Meschede, (1986). Triangles are data from felsic volcanic rocks; square symbols are for mafic rocks. Crosses signify Catchers Pond Group data from Jenner and Szybinski (1987). WPB = within-plate basalt; OFB = ocean floor basalt; LKT = low-K tholeiite; CAB = calc-alkaline basalt; WPA = within-plate alkaline; WPT = within-plate tholeiitic; P MORB = plume MORB; N MORB = normal MORB; VAB = volcanic arc basalt.

felsic rocks from the Catchers Pond Group and Western Arm Group (Jenner and Szybinski, 1987). A field for MOR rocks is not included in this diagram since rocks of these more felsic or evolved compositions are too rare in that tectonic setting (Pearce, 1982).

On chondrite-normalized extended trace element plots (Figure 3.11), data for most of the mafic rocks from above and below the main mineralized zone in the Hammer Down prospect have similar patterns, with small negative Nb anomalies. Except for a single sample of undeformed pillow lava collected more than 200 m from the gold prospect, they lack the negative Ta anomalies and high normalized Th values that are characteristic, along with relative depletion in Nb, of island arc rocks. The erratic behaviour of Ta is attributable in part to analytical problems, with lower accuracy and precision arising from memory effects in the ICP-MS technique. Sample DR-90-21 is highly anomalous in displaying a strong depletion of light rare earth elements, and a large positive Ta anomaly. Overall, the mafic volcanic rocks do not have a strong arc signature, and the trace element patterns in Figure 3.11 are similar to those of transitional calc-alkaline to tholeiitic mafic volcanic rocks and non-arc tholeiites from the Catcher's Pond and Lush's Bight Groups (Z.A. Szybinski, personal communication, 1992). The intermediate or mixed arc to non-arc geochemical signature of rocks from the King's Point area has been interpreted by Szybinski and Jenner (1989) to record the influence of volcanic arc and back-arc environments. One medium grained basaltic dyke that was analyzed is chemically

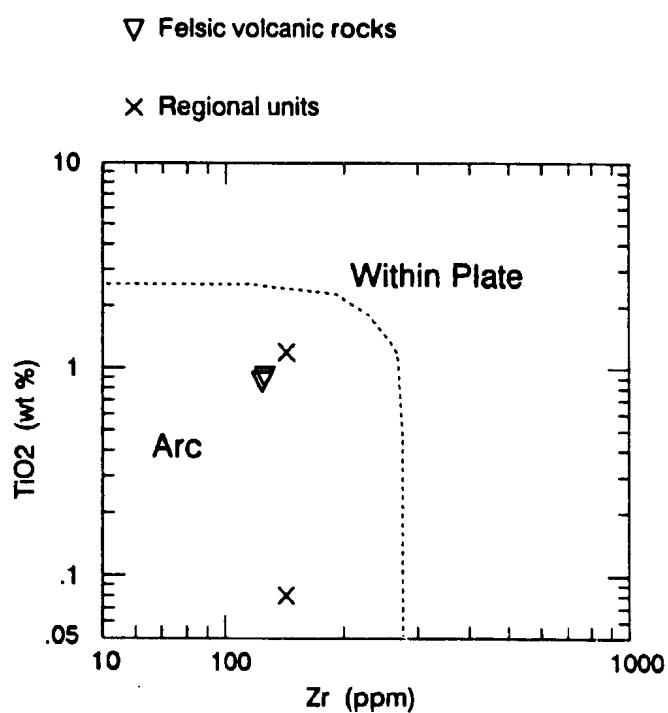


Figure 3.10 TiO₂ vs. Zr plot for separation of arc and within plate settings of intermediate to felsic volcanic rocks from the Hammer Down prospect (triangles), with field boundary from Pearce (1982). Crosses signify Catchers Pond Group and Western Arm Group data from Jenner and Szybinski (1987).

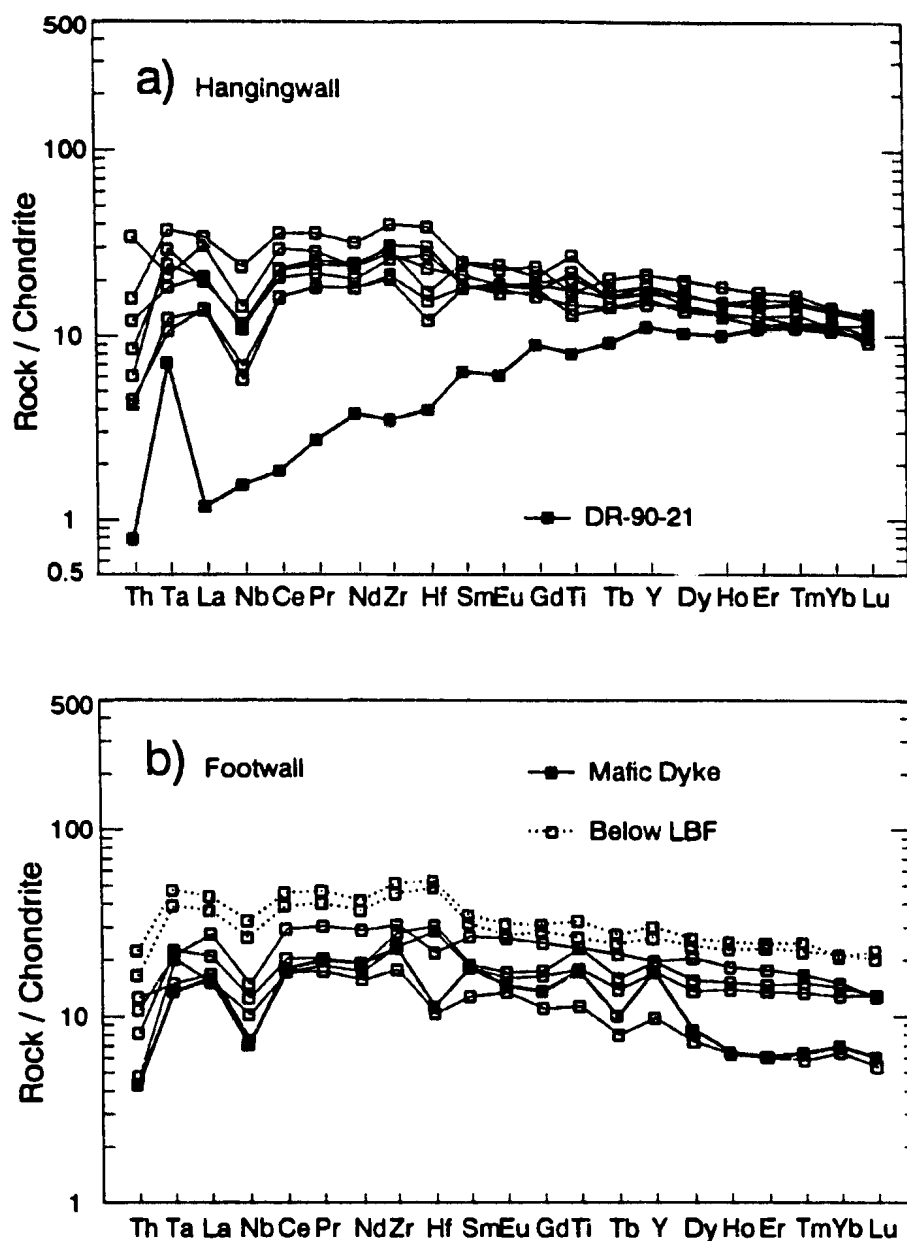


Figure 3.11 Chondrite-normalized extended rare-earth element plots for mafic volcanic, volcanic-sedimentary, and intrusive rocks from the hangingwall (a) and footwall (b) of the main mineralized zone in the Hammer Down prospect. Normalizing values are from Taylor and McLennan (1981), except for Ta, which is calculated from the chondritic ratio $Nb/Ta = 2.7$, given by Briqueau *et al.* (1984).

similar to the basaltic and mafic tuffaceous rocks. Mafic dykes and the volcanic rocks they intrude in the prospect area are metamorphosed to the same degree, exhibit the same structural styles, and probably formed during the same period of magmatic activity. Levels of the incompatible elements plotted in Figure 3.11b are slightly higher in basaltic rocks collected from drill core below the Lower Brittle Fault relative to those in rocks from the sequence above the fault.

Chondrite-normalized values of trace element contents in felsic (dacitic) volcanic rocks have approximately the same range as those in mafic rocks from the prospect area (*cf.* Figures 3.11 and 3.12). The felsic rocks are relatively depleted in Ti, which is probably a compatible element as a result of Fe- and Ti-oxide fractionation, and have more prominent negative Nb anomalies than mafic rocks associated with them.

3.4 Felsic intrusive rocks

3.4.1 Field relations

Deformed and altered felsic porphyry dykes, 30 cm to 7 m wide, are the immediate hosts to most of the largest mineralized quartz veins in the Hammer Down zone. They are interpreted to have played a mechanical role in the development of dilational space for vein emplacement (Dubé *et al.*, 1992). Medium grained buff coloured to pale grey dykes make up approximately 25% of the outcrop area in the

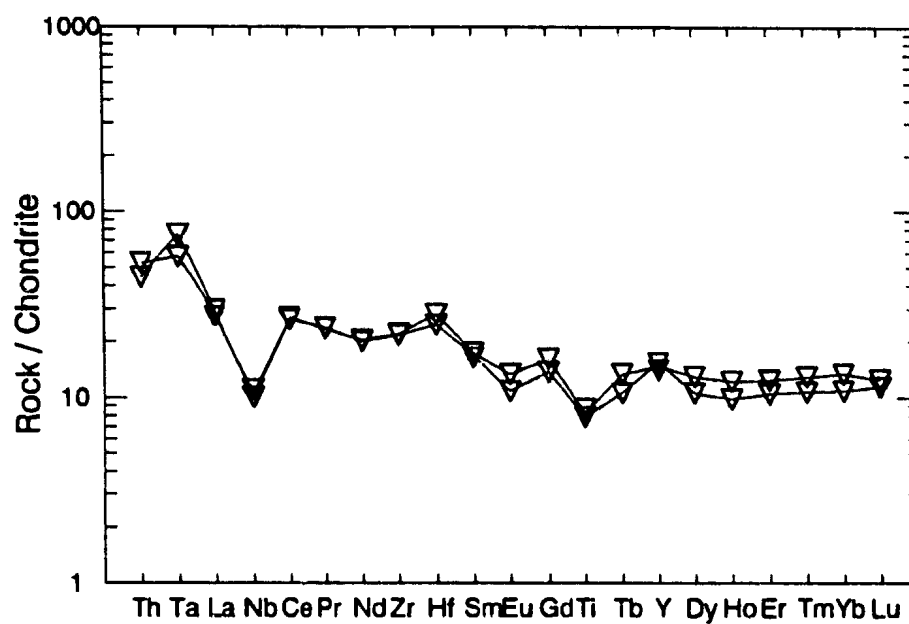


Figure 3.12 Chondrite-normalized extended rare-earth element plots for felsic volcanic or volcanic-sedimentary rocks from the Hammer Down prospect. Normalizing values are as in Figure 3.11.

main Hammer Down trench, where several sheared lenses or boudins of dyke material up to 8 x 15 m are surrounded or cut by gold-bearing veins (Figure 3.4). Many gold bearing veins were emplaced along sheared dyke margins, but away from high strain zones, the dykes have clear, sharp intrusive contacts with volcanic and sedimentary units. The S_2 fabric is developed in felsic dykes and in the host volcanic rocks (Dubé *et al.*, 1992). Felsic dykes in the prospect area have an overall medium grained granitoid or porphyritic appearance with feldspar and quartz phenocrysts, and contain 2 - 10% chlorite, as grains or aggregates of phenocrysts size and as smaller, dispersed flakes.

Felsic dykes or small plugs that may be correlative with those of the Hammer Down prospect have been mapped regionally by Neale *et al.* (1960). Similar dykes are also present in the Muddy Shag mineralized zone, in drill core from the Rumbullion zone, and were observed to intrude rocks of the Lush's Bight Group in roadside outcrops between King's Point and Rattling Brook 5 km northeast of the Rendell - Jackman property.

Fine grained silica and sericite alteration is locally developed in dykes, especially near and within the sheared and mineralized zones, where the porphyritic texture becomes obscured by recrystallization. Intensely strained and hydrothermally altered portions of dykes are composed largely of white clay-like material. In drill core DDH MS-90-27, the LBF cuts a felsic dyke and the resulting fault breccia contains fractured 1 - 15 cm clasts of hydrothermally altered dyke material.

3.4.2 Petrography

Relatively unaltered felsic porphyry dyke samples contain 25-35 % partly sericitized and albitized feldspar phenocrysts up to 2 x 7 mm, and 0-10% subhedral and anhedral quartz phenocrysts 1.5 - 2 mm (Plates 3.9 and 3.10). Multiply twinned grains are the most abundant phenocrysts, and represent albitized plagioclase. Simply twinned and untwinned feldspar grains may have been derived from potassium feldspar phases. All types of feldspar phenocrysts contain mica inclusions (up to 0.4 mm long) that may represent the restricted mobilization of sodium and potassium during metamorphism. The groundmass consists mainly of granular quartz, feldspar, sericite, and patches of calcite. Accessory igneous minerals include apatite, oxides, and zircon. Pyrite cubes 0.5 - 0.8 mm constitute less than 1% of the rocks, and may be of either igneous, metamorphic, or hydrothermal origin. Rare tabular pseudomorphs (0.4 x 4 mm) of chlorite and white mica after biotite contain randomly oriented rutile needles less than 0.025 mm long and minor opaque grains. Chlorite is also present as phenocryst to sub-phenocryst size bright green flakes and ragged aggregates that make up 7-10% of the rocks. These aggregates rarely contain granular epidote. Both types of chlorite are brown when viewed under crossed polars. Groundmass constituents are generally less than 0.1 mm in maximum dimension and are predominantly sericite and granular quartz, with minor opaque grains and rare epidote. All dyke samples, including those collected more than 100 m

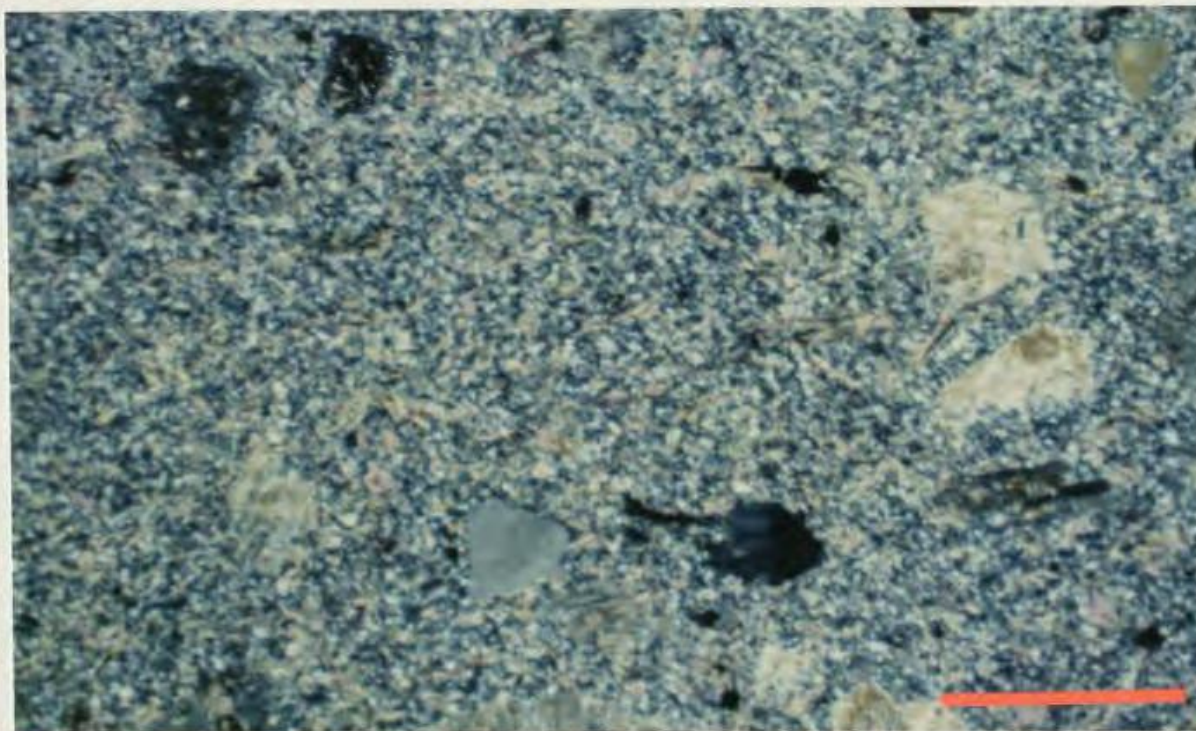


Plate 3.9 Quartz (grey, also dark grey near extinction) and feldspar (pale clouded yellow, also dark with birefringent muscovite inclusions) phenocrysts in moderately altered felsic dyke, sample DR-90-08. View under crossed polars. Scale bar = 1 mm.

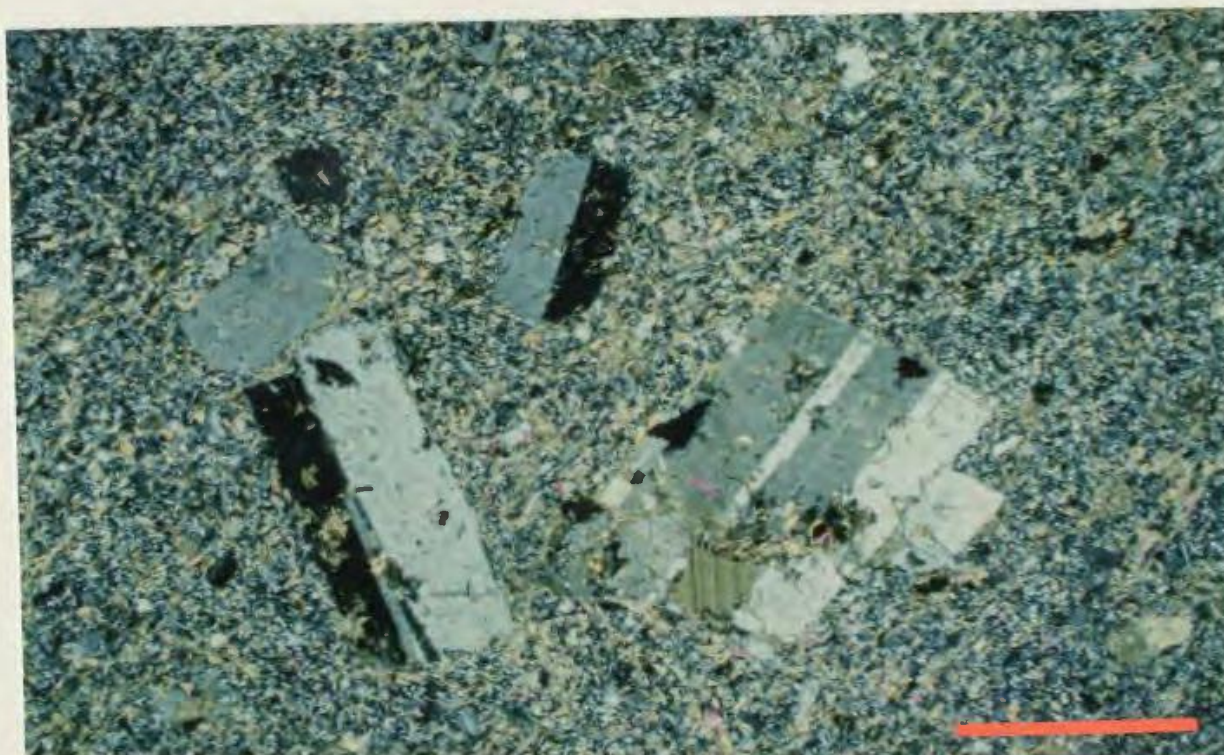


Plate 3.10 Highly birefringent sericite and calcite in groundmass and within feldspar phenocrysts of weakly altered (metamorphosed) felsic porphyry dyke sample D-3. View under crossed polars. Scale bar = 1 mm.

from mineralized zones, contain chlorite pseudomorphs and sericite.

If abundant albite in the felsic dykes was derived from more calcic plagioclase, the original dyke compositions were granodioritic or tonalitic by visual modal estimates of mineral abundances. The unmetamorphosed rocks may have contained considerably more potassium feldspar, with the potassium having been removed, or now present in the ubiquitous mica flakes within feldspar phenocrysts and throughout the groundmass.

Felsic dykes postdate the development of the S_1 fabric, and by the arguments presented earlier (Section 3.3.2), they therefore appear to have been emplaced after the growth of early metamorphic minerals in volcanic and sedimentary rocks. The dykes experienced a degree of metamorphism similar to that of the rocks they intrude. Pervasive and widespread metamorphism and alteration of dykes is characterized by albite, chlorite, white mica, and calcite, with rare epidote.

Eleven samples from the King's Point volcanic-plutonic complex were collected for comparison to felsic porphyry dykes from the Hammer Down prospect. Geographically, the King's Point complex is the nearest major felsic unit to the gold prospect, and has been proposed (*e.g.* Andrews and Huard, 1991) as a possible source or correlative for felsic porphyry dykes. Samples of intrusive porphyry from the complex have phenocryst assemblages made up of 25 - 50 % euhedral potassium feldspar, 5 - 10 % anhedral quartz, with or without bright blue amphibole grains tentatively identified here as riebeckite, although Nash (1962, cited in Hibbard, 1983)

notes arfvedsonite as an alternate possibility for peralkaline rocks from the same general area. Certain porphyritic extrusive or intrusive units of the King's Point complex are superficially similar in texture and appearance to felsic dykes of the Hammer Down prospect. The dykes are, however, far less quartz-rich and contain finer grained quartz and more sericite or chlorite in the groundmass. Pink medium grained inequigranular granite from the King's Point complex contains abundant tightly intergrown anhedral potassium feldspar and quartz, and rhyolite is composed of 65 % fine granular quartz with sutured boundaries. These latter two rock types are texturally and mineralogically distinct from any units in the immediate vicinity of the Hammer Down prospect.

3.4.3 Chemistry

The aluminum, calcium, sodium, and potassium oxide contents of relatively fresh igneous rocks form the basis of a common classification into peraluminous, metaluminous, and peralkaline types. In peraluminous rocks, molecular $\text{Al}_2\text{O}_3 > (\text{CaO} + \text{Na}_2\text{O} + \text{K}_2\text{O})$, metaluminous rocks contain $(\text{CaO} + \text{Na}_2\text{O} + \text{K}_2\text{O}) > \text{Al}_2\text{O}_3$, $> (\text{Na}_2\text{O} + \text{K}_2\text{O})$, and peralkaline rocks have $(\text{Na}_2\text{O} + \text{K}_2\text{O}) > \text{Al}_2\text{O}_3$. Molecular ratios are plotted in Figure 3.13 as a classification and as a discriminant of felsic units from the King's Point area. Felsic dykes from the Hammer Down prospect are metaluminous to weakly peraluminous, and are chemically distinct from samples of the King's Point Complex. Peralkalinity is a localized feature of the King's Point complex (Mercer *et al.*, 1985; Kontak and Strong, 1986) and has a mineralogical expression in the presence of alkali amphibole. Felsic intrusive and extrusive units from the eastern Baie Verte Peninsula exhibit a variety of chemical types, with samples from the Burlington Granodiorite (B.J. Fryer and P.A. Cawood, unpublished data; Epstein, 1983) generally being most similar to felsic dykes from the Hammer Down prospect.

No alkali enrichment trend is evident for fresh and altered felsic porphyry dykes in the AFM plot of Figure 3.14. Rock samples from the Burlington Granodiorite are similar to the Hammer Down dykes in terms of Na_2O , K_2O , FeO^* , and MgO contents. Data for the felsic dykes and Burlington Granodiorite do not

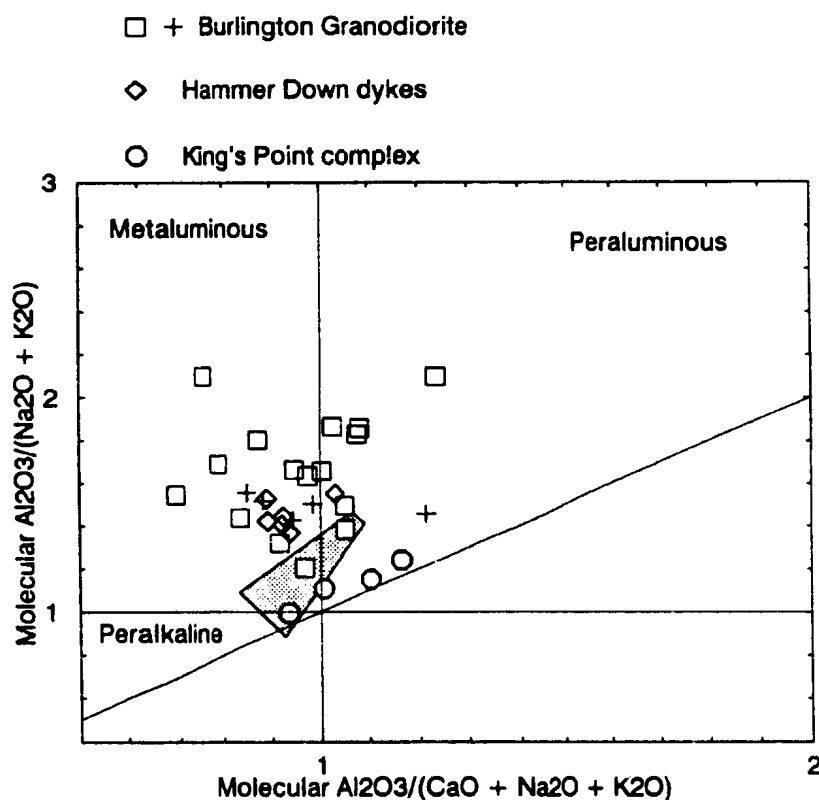


Figure 3.13 Chemical classification of granitic and related rocks by molecular alkali-lime-alumina relations. Diamonds are data for felsic porphyry dykes from the Hammer Down prospect; open circles are for the King's Point Complex; squares and crosses denote data for the Burlington Granodiorite compiled from Epstein, (1983), and unpublished data of B.J. Fryer and P.A. Cawood, respectively; shaded field contains data for the Cape St. John Group, Cape Brulé Porphyry, Dunamagon granite, and La Scie granite (B.J. Fryer and P.A. Cawood, unpublished data).

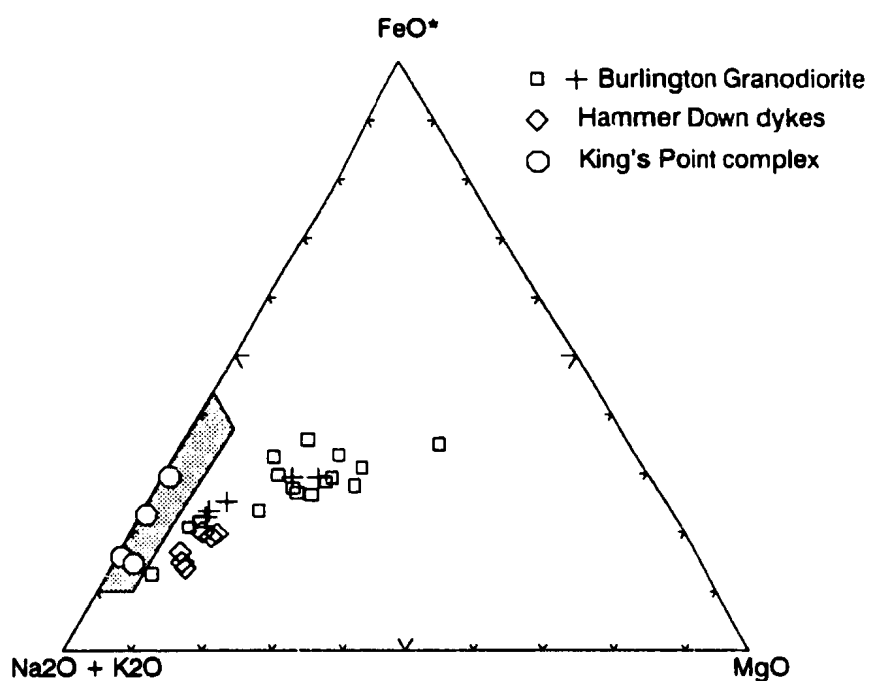


Figure 3.14 Alkali - total ferrous iron - magnesia (AFM) plot for felsic porphyry dykes from the Hammer Down prospect (diamonds), Burlington Granodiorite (crosses and small squares), King's Point complex (circles), and eastern Baie Verte felsic units (shaded field). Data sources are as in Figure 3.13.

overlap with the ranges for the King's Point complex and other Middle Silurian and younger felsic units from the eastern Baie Verte peninsula plotted on Figure 3.14. The Hammer Down dykes and King's Point rocks are also distinct from one another on a plot of Nb vs. Y (Figure 3.15) that indicates a volcanic arc or collisional plate boundary source for Hammer Down Dykes, in contrast to the within-plate signature of porphyry units from King's Point.

Trace element patterns of porphyry dykes and other felsic units are shown in Figure 3.16. The dykes are depleted in heavy rare earth elements relative to volcanic rocks from the Hammer Down prospect, and have relatively deep negative Nb anomalies (*cf.* Figure 3.16a, Figure 3.11, and Figure 3.12). The patterns for felsic dykes are generally similar to those of samples from the Burlington Granodiorite samples (B.J. Fryer and P.A. Cawood, unpublished data), although sample LG0219 from the Burlington Granodiorite has the best overlap with the range of Hammer Down dyke compositions. Extrusive and intrusive rocks from the King's Point complex have relatively elevated REE abundances and strong negative europium and titanium anomalies (Figure 3.16b) that set them apart from the Hammer Down dykes. Trace element patterns for felsic units from the eastern Baie Verte Peninsula other than the Burlington Granodiorite overlap to a great extent with those of samples from the King's Point complex.

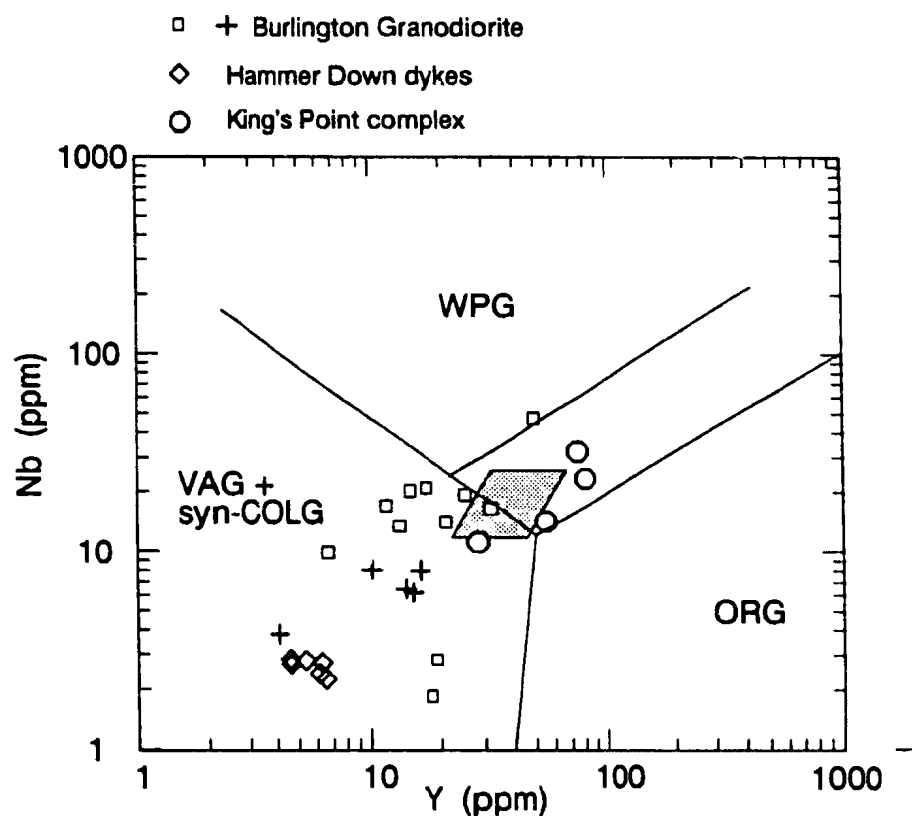


Figure 3.15 Niobium-Yttrium bivariate plot for characterization of felsic intrusive rocks: felsic porphyry dykes from the Hammer Down prospect (diamonds), Burlington Granodiorite (crosses and small squares), King's Point complex (circles), and eastern Baie Verte felsic units (shaded field). Fields of tectonic setting are from Pearce *et al.*, (1984). VAG + syn-COLG = volcanic arc and syn-collisional granitoids; WPG = within-plate granitoids; ORG = ocean-ridge granitoids. Symbols and data sources are as in Figure 3.13.

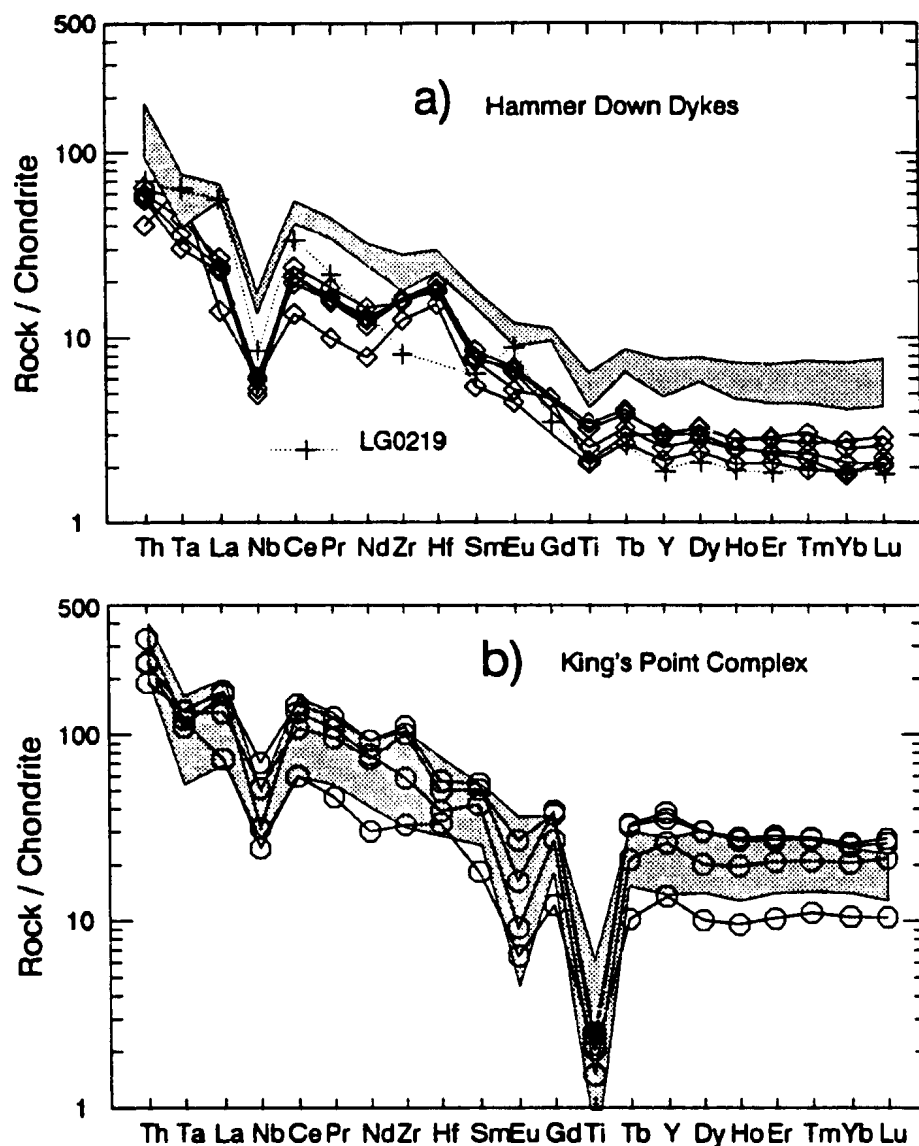


Figure 3.16 Chondrite-normalized extended rare-earth element plots for (a) felsic porphyry dykes from the Hammer Down prospect (diamond symbols), compared to units of the Burlington Granodiorite (shaded field and sample LG0219), and (b) intrusive and extrusive units of the King's Point Complex (circles), compared to regional felsic units from the eastern Baie Verte Peninsula (Dunamagon granite, La Scie granite, Cape St. John Group, and Cape Brulé Porphyry). Data sources are as in Figure 3.13. Normalizing values are as in Figure 3.11.

3.5 Summary

Field relations of veins and host rocks show that structure is the principal control on the distribution of gold-bearing zones. The main auriferous veins are generally within D_2 high strain zones that postdate greenschist or sub-greenschist metamorphism, the development of an early tectonic fabric in sedimentary and mafic volcanic rocks, and an intrusive episode that produced the characteristic felsic porphyry dykes of the Hammer Down prospect.

Formation of the main quartz veins contemporaneously with the development of the S_2 foliation, which is axial planar to F_2 folds, requires a mechanism for opening fluid passageways and physical space to be occupied by veins. Flexural slip on the limbs of folds can account for the component of apparent lateral offset observed in felsic dykes at the main Hammer Down trench without producing a laterally persistent shear zone that exhibits a uniform sense of displacement. The abundant felsic dykes in the Hammer Down area provided a mechanical heterogeneity that promoted dilational openings and allowed the influx of gold-bearing fluids (Dubé *et al.*, 1992).

The structural style of the lower brittle fault is distinct from that of the D_2 high strain zones that host gold mineralization. Late brittle faulting postdates the emplacement of felsic porphyry dykes and deposition of gold in the Hammer Down prospect.

Host volcanic rocks of the Hammer Down prospect are transitional or mixed arc to non-arc basalt or andesite, with minor dacitic tuff. The stratigraphic succession in the prospect area also includes chert, pyritic sedimentary rocks, and epiclastic or resedimented units.

Felsic porphyry dykes from the prospect are petrographically and chemically distinct from the Ordovician felsic volcanic host rocks and from nearby Silurian intrusive and extrusive units. These felsic dykes record a period of magmatic activity that is distinct from Ordovician arc volcanism and from the Silurian development of the nearby King's Point volcanic-plutonic complex. The Burlington Granodiorite is the best match to Hammer Down Dykes in terms of lithology, mineralogy, and chemistry.

Chapter 4

ALTERATION AND GOLD MINERALIZATION

4.1 Introduction

The mineralogy and structure of different vein sets in the Hammer Down gold prospect are described in this chapter. As an extension of the petrographic descriptions presented in Chapter 3, mineralogical and chemical changes that accompanied gold deposition and alteration in wall rocks are also documented.

Changes in mineralogy that correspond to varying degrees of hydrothermal alteration are best defined using petrography in combination with drill core and field descriptions. These mineralogical changes reflect the mobilization and redistribution of chemical components as well as the addition or removal of certain elements by hydrothermal solutions. Metamorphic minerals are present in all host rocks, and predate the hydrothermal assemblages associated with gold. Ore and gangue mineralogy and the style and extent of mineralogical or chemical changes that accompany gold deposition help characterize the fluid system and thereby contribute to the development of models for ore genesis.

4.2 Vein morphology and mineralogy

The Hammer Down prospect contains several types of veins and hydrothermal assemblages that are distinguished primarily by their mineralogy, but also by their internal structure and geometric relationship to other veins and to mapped rock fabrics. Deformed calcite-rich stringers in mafic volcanic and sedimentary rocks (section 3.2.1) predate D_2 deformation and deposition of gold, and are designated type I veins. Quartz-epidote clots and small folded quartz-carbonate veinlets (type I) probably represent seafloor alteration or early metamorphism of the volcanic and sedimentary succession of the host Catchers Pond Group, and are locally preserved within a few metres of the mineralized zones. Type II veins and the alteration assemblages associated with them are the main gold-bearing zones in the prospect, and developed contemporaneously with the S_2 fabric. Sulphide-poor veins that locally cut the S_2 foliation (section 3.2.1) are termed type III. Type IV veins and hydrothermal assemblages postdate gold mineralization and include calcite veinlets and breccia cement in the lower brittle fault.

Approximately six type II gold-bearing veins, up to 1 m wide, constitute the main Hammer Down mineralized zone, but the discontinuity of veins that is evident on a scale of 10 to 20 m in outcrop renders correlations in drill core difficult. The overall geometry of the orebody (Figure 3.3) is a system of steeply dipping veins. The main gold-bearing quartz veins have strongly sheared margins and are deformed

internally to varying degrees. They contain highly strained quartz, 5-70% pyrite, 2-20% sphalerite, 1-10% chalcopyrite, 0-10% calcite, 0-5% ferroan dolomite, and less than 2% each of galena, muscovite, chlorite, and scheelite. Hammarite, $\text{Pb}_2\text{Cu}_2\text{Bi}_4\text{S}_9$ (Mumme *et al.*, 1976), was reported by Andrews and Huard (1991) as a vein constituent, but was not observed during the course of this study. Several sulphide rich veins returned gold assays in excess of 200 g/tonne over drill core intervals 20 to 50 cm long. Weathered veins or gossanous zones in outcrop contain hematite, limonite, and residual gold grains that are the only occurrences of macroscopically visible gold in the Hammer Down prospect. The main gold-bearing vein in the Rumbullion zone contains abundant supergene covellite in association with sphalerite, chalcopyrite, and pyrite.

The largest type II gold-bearing veins in the Hammer Down prospect are composed principally of quartz and pyrite, and are strongly banded or laminated. Most gold in the Hammer Down zone is contained in these shear veins. The laminations within veins are discrete bands of highly strained quartz between spaced cleavage planes, or compositional bands dominated either by quartz or sulphide minerals. Subhedral pyrite grains up to 8 mm in size are extensively brecciated, with minor quartz and chlorite in pressure shadows and fractures. Most of the gold observed microscopically is rounded to irregular and angular inclusions in pyrite, smaller than 0.03 mm in maximum dimension, but ranging up to 0.1 mm (Plates 4.1 and 4.2). Gold is also present, but less abundant, at pyrite, sphalerite, chalcopyrite,

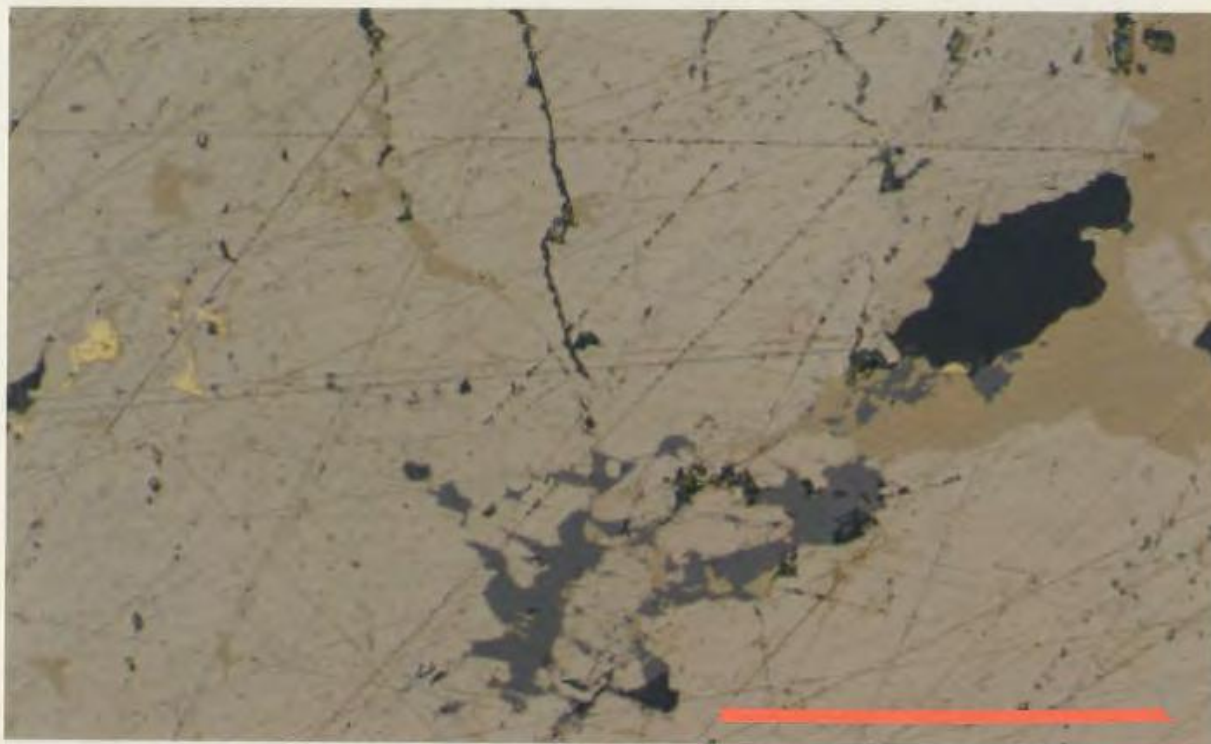


Plate 4.1 Gold grains (bright yellow) within pale yellow pyrite and along grain boundaries between chalcopyrite (yellow-brown), sphalerite (grey), and quartz (black). Sample DR-90-10, view in reflected light. Scale bar = 0.1 mm.

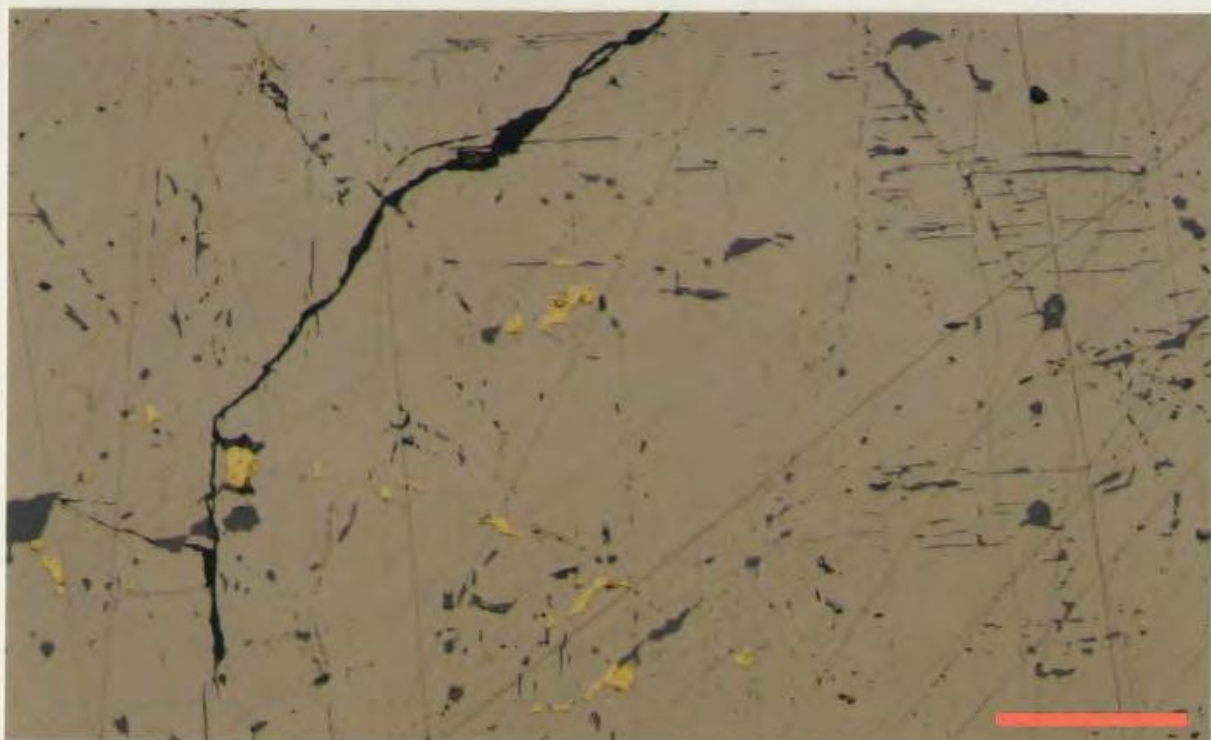


Plate 4.2 Coarse gold (bright yellow) within pyrite and along fractures. Sphalerite (grey) is also abundant in fractures and cleavage planes. Sample DR-90-11, view in reflected light. Scale bar = 0.1 mm.

and gangue grain boundaries, and is consistently in contact with at least one sulphide mineral. Several gold grains of various textural types in pyrite-rich highly strained type II veins were analyzed by semi-quantitative X-ray spectrometry coupled with scanning electron microscopy, and compositions were determined to be very uniform near $\text{Au}_{91}\text{Ag}_9$.

In certain type II veins or portions of veins, sphalerite and chalcopyrite are more abundant than pyrite. These base metal-rich veins are generally less deformed and have a lesser degree of compositional banding than those that are made up predominantly of quartz and pyrite. Sphalerite and chalcopyrite are present in type II veins as discrete anhedral grains or aggregates 0.1 - 10 mm across, and as blebs and stringers with fractured quartz and pyrite. Anhedral grains of galena, smaller than 2 mm, are much less common. Sphalerite in particular, and chalcopyrite less commonly, show textural evidence of late growth and remobilization (Plates 4.2 and 4.3). Gold is also locally recrystallized and coarsened along fractures. Anhedral and euhedral pyrite inclusions, 0.01 to 0.1 mm in maximum dimension, are common in sphalerite and rare in chalcopyrite where the host sulphide has flowed in a ductile manner. The growth of extremely elongate pyrite inclusions (Plate 4.4) represents either rapid growth of skeletal grains, or coprecipitation with crystallographic control by sphalerite prior to recrystallization and deformation of the host sulphide. Blebs and lamellae of chalcopyrite are locally distributed along crystallographic planes or growth zones in undeformed sphalerite (Plates 4.5 and 4.6). This ore texture

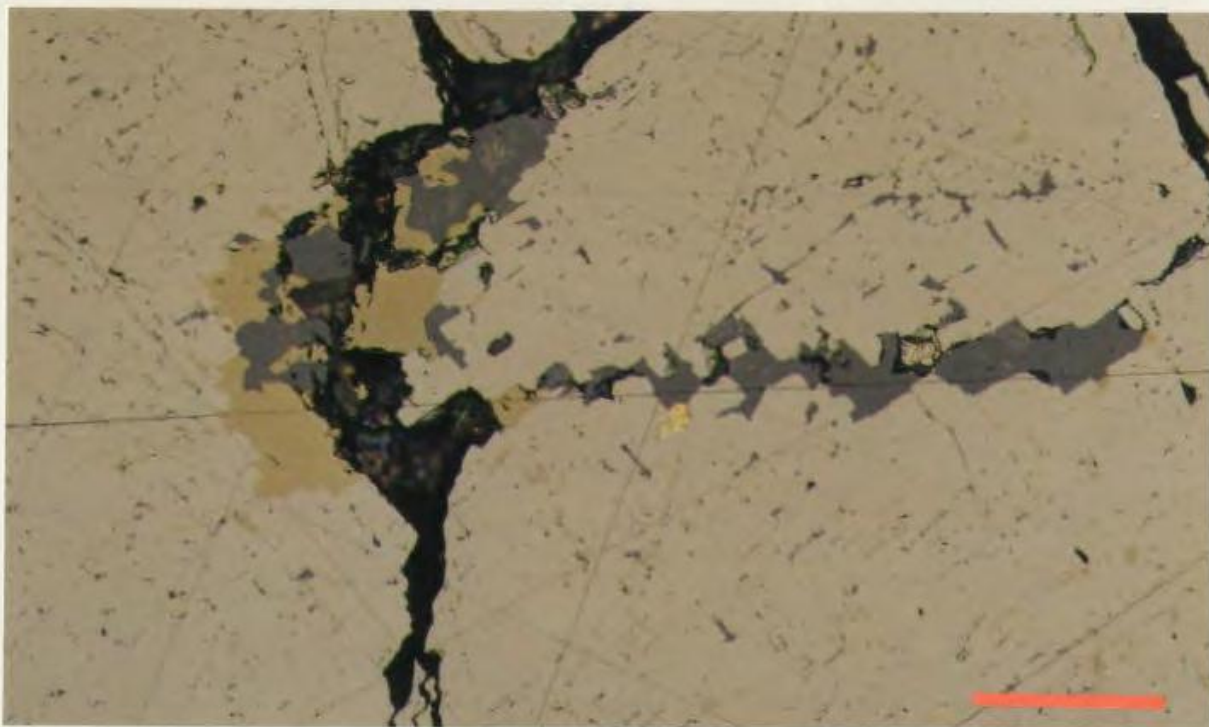


Plate 4.3 Calcite (dark, with internal reflections), quartz (black), chalcopyrite (yellow-brown), and sphalerite (grey) along fractures in gold-bearing pyrite. Sample DR-90-10, view in reflected light. Scale bar = 0.1 mm.

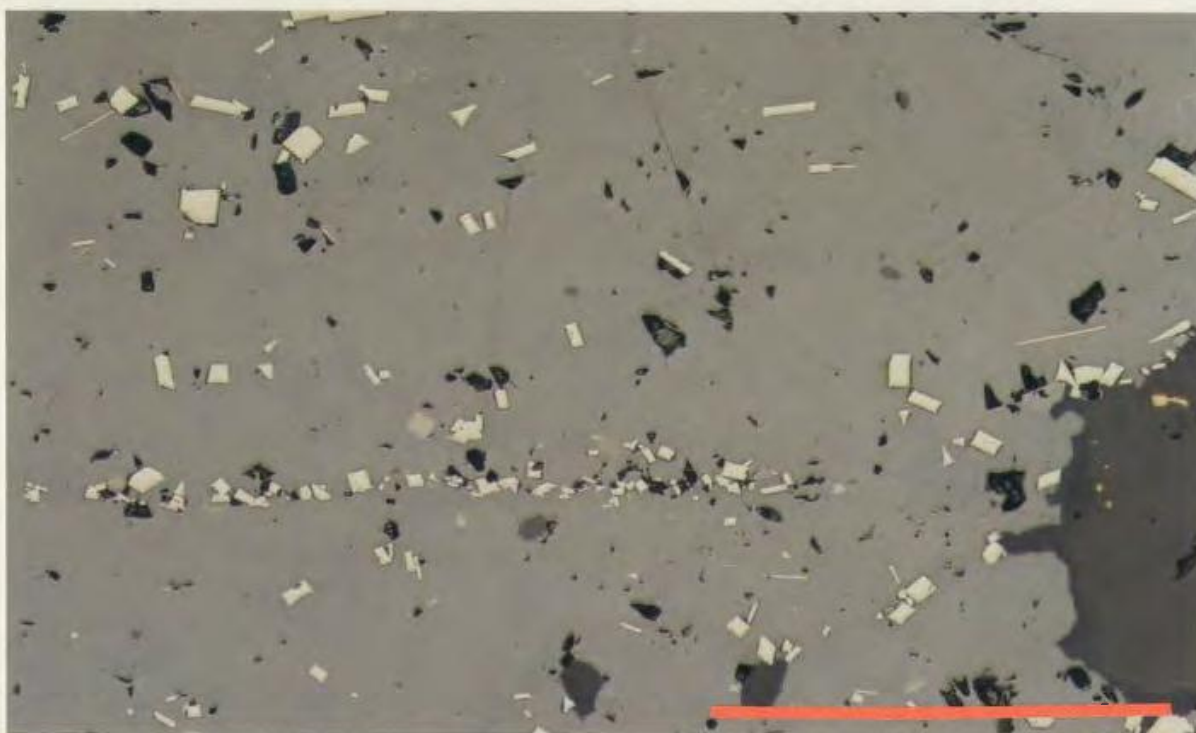


Plate 4.4 Euhedral and skeletal pyrite grains (pale yellow-white) in sphalerite within gold-bearing (type II) vein. Sample DR-91-100, view in reflected light. Scale bar = 0.1 mm.

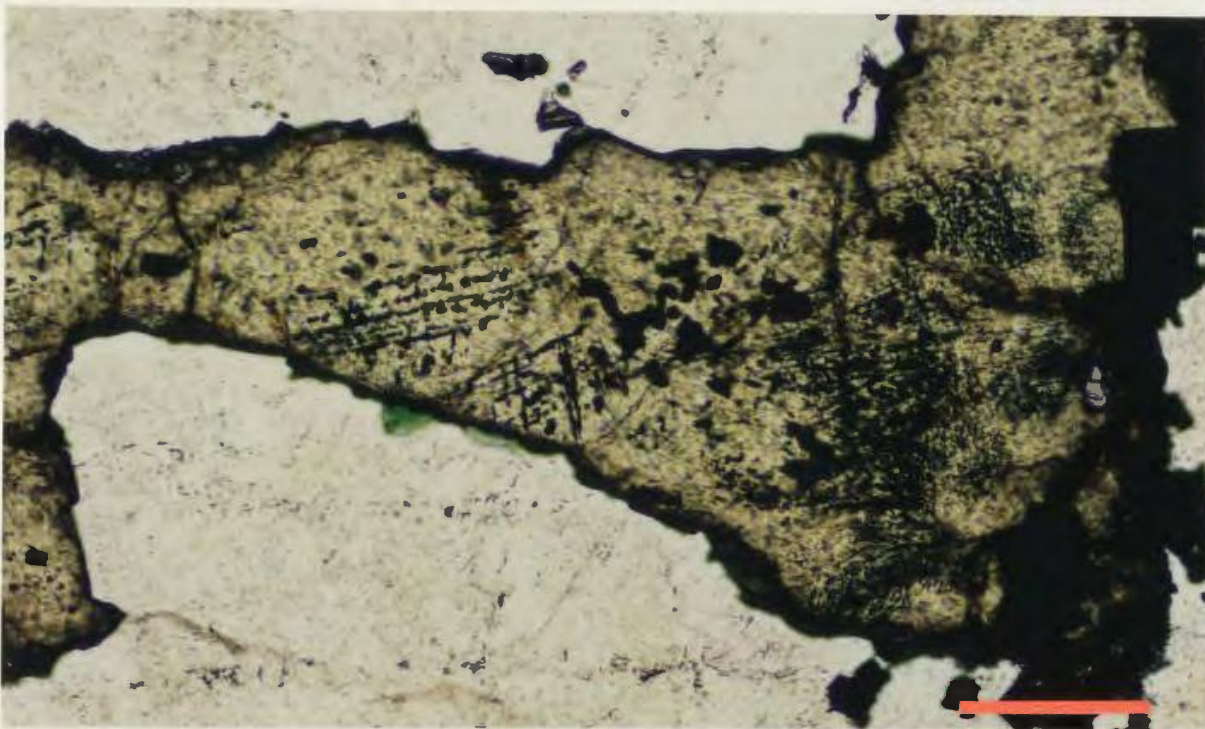


Plate 4.5 Chalcopyrite inclusions or exsolution lamellae (dark) along crystallographic planes in sphalerite (high relief, yellow) within gold-bearing (type II) vein. Sample DR-91-100, view in transmitted light. Scale bar = 0.2 mm.

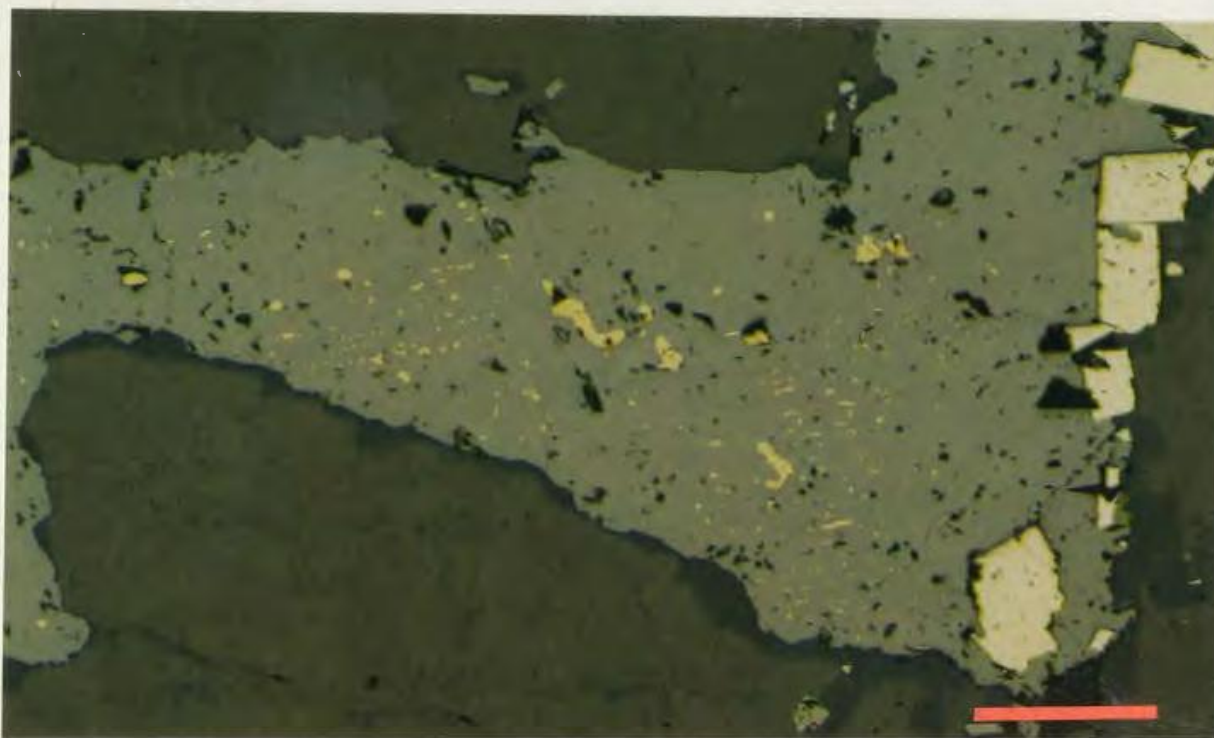


Plate 4.6 Chalcopyrite inclusions or exsolution lamellae (yellow) along crystallographic planes of sphalerite (grey). Sample DR-91-100, view in reflected light. Same field of view as in Plate 4.5, scale bar = 0.2 mm.

represents either co-precipitation of the two sulphide minerals or partial replacement of sphalerite by chalcopyrite ("chalcopyrite disease") (Barton and Bethke, 1987; Bortnikov *et al.*, 1991) along crystallographic planes. Blocky anhedral chalcopyrite inclusions that are distributed randomly within sphalerite are less common than other types of ore intergrowths. Quartz in all sulphide- and gold-rich type II veins has undulose extinction, and is locally brecciated. Pyrite exhibits no post-depositional textures except brittle fractures.

Bright green inclusion-free chlorite, brown or berlin blue under crossed polars, is widely distributed but not abundant in type II veins. It occurs as blocky grains or sheaf-like aggregates in some pressure shadows adjacent to pyrite, but is most commonly intergrown with pyrite or sphalerite along fractures subparallel to the main shear fabric within veins (Plate 4.7). In addition to the chlorite found in the main gold-bearing veins, intergrown chlorite, quartz, calcite, chalcopyrite, and sphalerite exist small veinlets that cut foliated pyritized wall rocks (Plate 4.8). Some portion of the chlorite in wall rocks and fractures, particularly that which is not intimately associated with sulphide minerals, may postdate the deposition of gold.

Iron-rich dolomite, or ankerite, is a minor constituent of some type II veins. It is present as blocky yellow-white grains up to 10 mm in maximum dimensions, closely intergrown with very fine grained calcite. Semi-quantitative SEM analysis of rhombohedral cleavage fragments picked from the most carbonate-rich vein yields the formula $\text{Ca}_{1.1}\text{Mg}_{0.4}\text{Fe}_{0.4}\text{Mn}_{0.1}(\text{CO}_3)_2$. This chemical composition represents ankerite

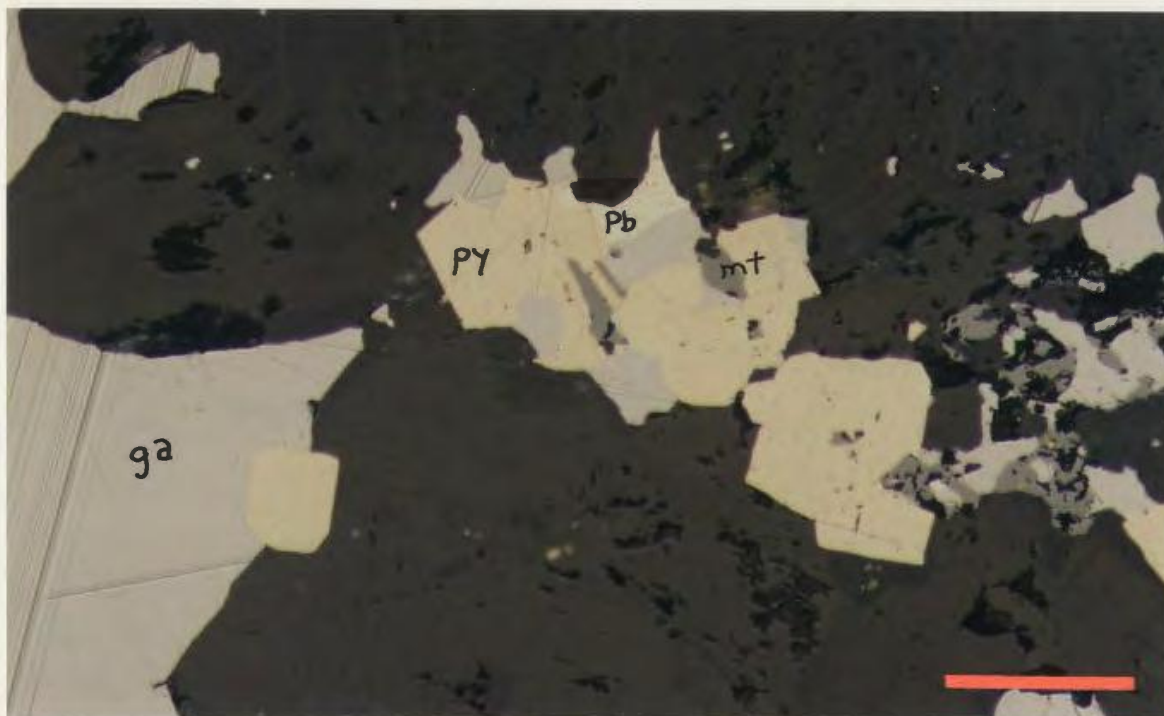


Plate 4.9 Equant pyrite (py, pale yellow), with anhedral galena (ga, grey-white), magnetite (mt, dark grey), and lead telluride (Pb, yellow-white), in type II vein. Sample DR-91-89, view in reflected light. Scale bar = 0.1 mm.

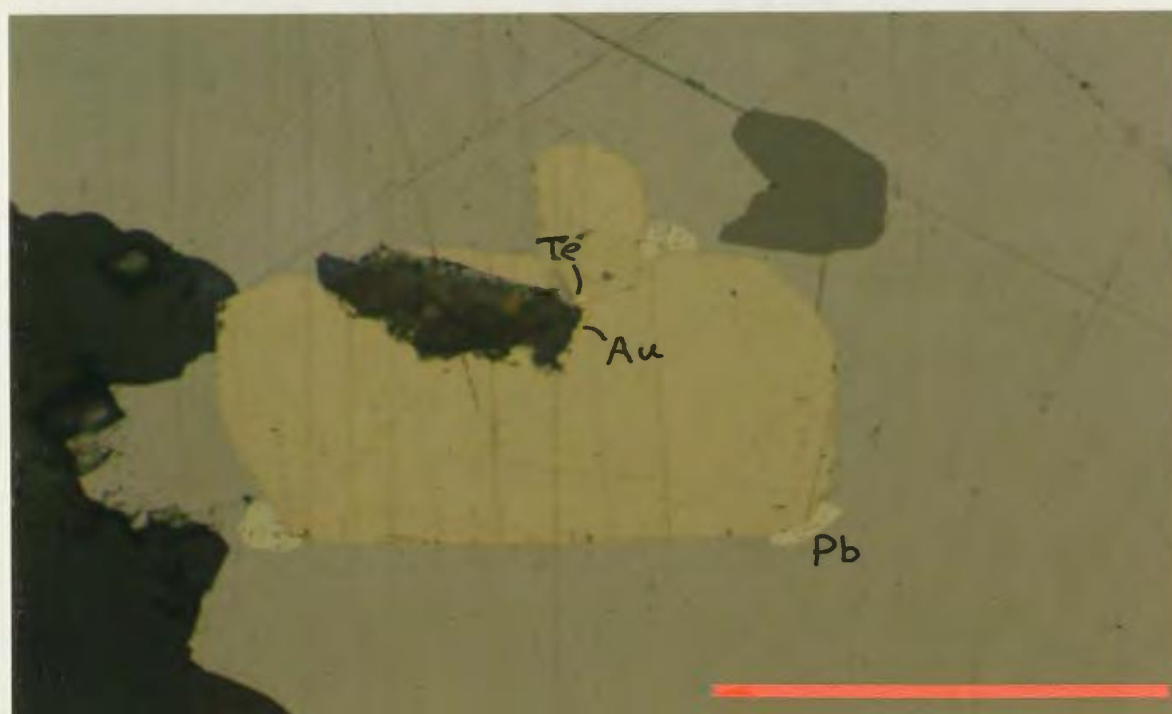


Plate 4.10 Gold or electrum (Au, yellow) and gold-silver telluride (Te) closely associated with pyrite (yellow), lead telluride (Pb), galena (pale grey), and magnetite (dark grey). Sample DR-91-89, view in reflected light. Scale bar = 0.1 mm.

by the criteria of Deer *et al.* (1966) (*i.e.* $\text{Mg:Fe} < 4:1$), but the mineral name ankerite is often reserved for material close to the end-member composition $\text{CaFe}(\text{CO}_3)_2$. Manganese substitution is common in dolomite and ankerite and a partial solid solution series extends to kutnahorite, $\text{CaMn}(\text{CO}_3)_2$ (Berry and Mason, 1959).

Sphalerite is common in some strongly deformed narrow (1-3 mm) calcite-rich type II veins. More rarely, galena and chalcopyrite exist in or adjacent to these veinlets, which are closely associated with type III vein sets containing fluorite, calcite, and pyrite. A single undeformed, carbonate-rich vein type, included in the type II population, contains coarse quartz and calcite, blocky and euhedral pyrite, anhedral galena, chalcopyrite, and minor blocky Pb telluride and magnetite grains (Plate 4.9), with flakes of gold and Ag-Au telluride (Plate 4.10). Semi-quantitative SEM analysis gave a composition of Ag_2AuTe for the gold-silver telluride. This analysis does not correspond to any reported mineral phase, but the bulk composition plots within a two-phase field on the experimental ternary Au-Ag-Te diagrams of Markham (1960), suggesting a mixture or intergrowth of hessite (Ag_2Te) and gold-silver alloy ($\text{Au}_{80}\text{Ag}_{20}$). This grain is closely associated with gold (Plate 4.10) of the approximate measured composition $\text{Au}_{80}\text{Ag}_{20}$.

Carbonate-rich and sulphide-poor veins (type III) commonly cut across shear fabrics and hydrothermally altered patches. Only rare examples of weakly deformed or undeformed veins contain abundant sulphide minerals, and they are predominantly

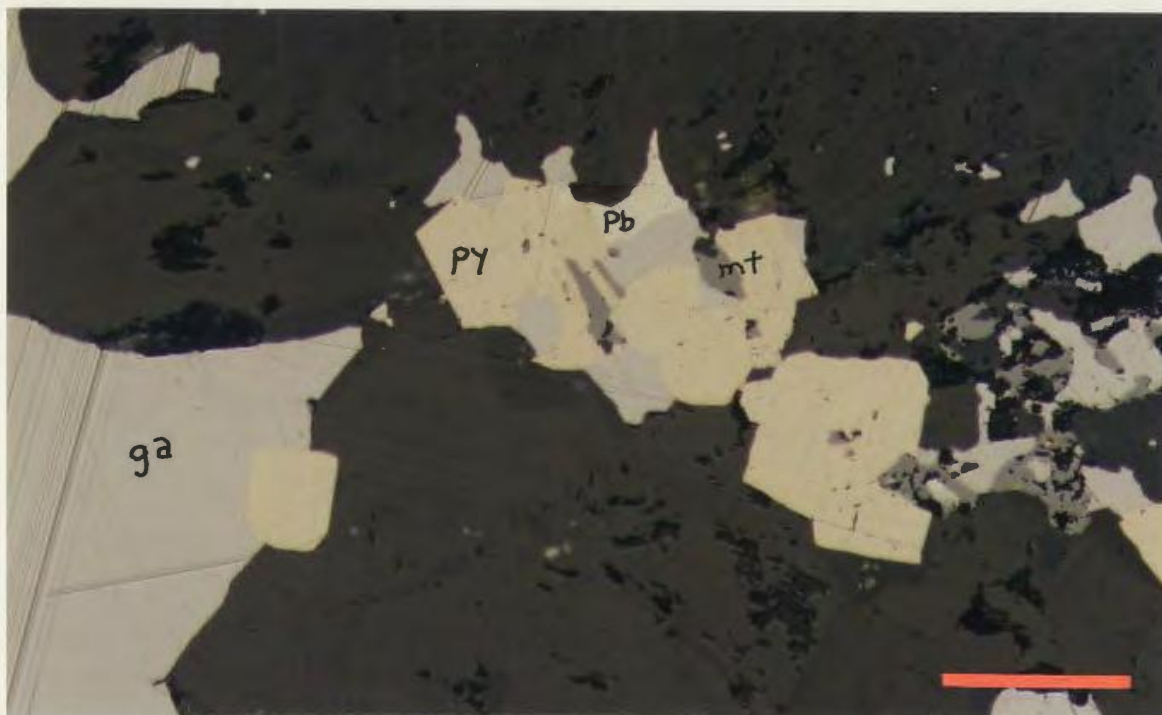


Plate 4.9 Equant pyrite (py, pale yellow), with anhedra galena (ga, grey-white), magnetite (mt, dark grey), and lead telluride (Pb, yellow-white), in type II vein. Sample DR-91-89, view in reflected light. Scale bar = 0.1 mm.

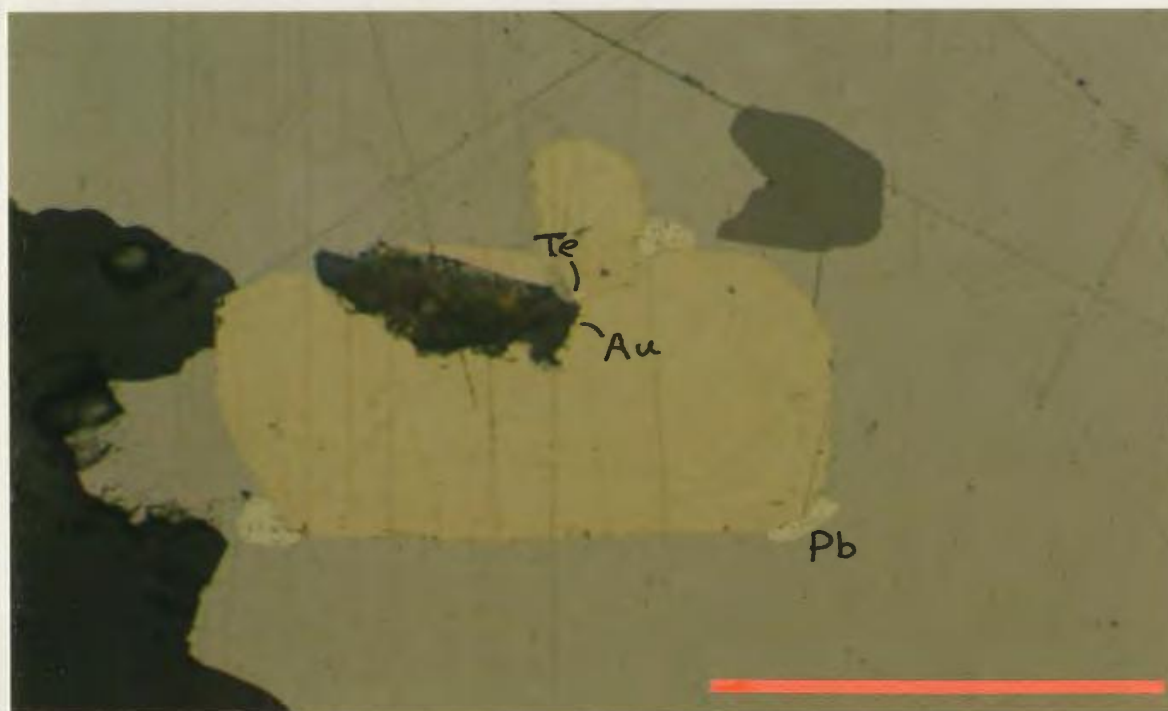


Plate 4.10 Gold or electrum (Au, yellow) and gold-silver telluride (Te) closely associated with pyrite (yellow), lead telluride (Pb), galena (pale grey), and magnetite (dark grey). Sample DR-91-89, view in reflected light. Scale bar = 0.1 mm.

composed of subhedral and euhedral grains of calcite and quartz up to 7 mm in size. In drill core, these type III veins are commonly seen to have small offsets (Plate 4.11), and they do not therefore entirely postdate deformational episodes. The main portions of calcite- and fluorite-bearing veins are not deformed internally (Plates 4.11 and 4.12). Some type III veins contain abundant fluorite as 1-5 mm cubes or as angular anhedral grains interstitial to calcite and quartz (Plates 4.11 and 4.12). In the west end of the main Hammer Down outcrop, vuggy, tensional quartz veins (type III) that cut dykes, sheared sulphide-rich veins, and foliated mafic rocks, are internally cleaved parallel to the S_2 fabric (Plate 4.13) and exhibit small offsets in the same dextral sense as felsic dykes (Plate 4.14) in the same outcrop area.

Numerous moderately deformed type III veins 1 - 4 mm wide are present within and near the main mineralized and highly deformed zones, and contain abundant quartz and calcite, uncommon purple fluorite (1-3 mm cubes or anhedral grains) and rare coarse white mica (> 2 mm). Microscopically, fluorite has not been observed in close textural association with gold or with any sulphide minerals other than pyrite, but it is common as deformed fine crystalline aggregates within a gold-bearing chloritized, pyritized, and sericitized interval of mafic rocks in drill core DDH MS-88-5, where its development appears to be closely linked with the main phase of deformation, alteration, and mineralization. On a scale of centimetres to metres, fluorite-bearing veins and assemblages are spatially related to the gold-bearing veins and their associated altered wall rocks, and type II and type III veins may share



Plate 4.11 Fluorite (F, purple) in type III vein cutting S_2 fabric, but locally offset. Sample DR-91-107.



Plate 4.12 Fluorite (black in XN), interstitial to calcite (highly birefringent) and euhedral quartz (quartz) in type III vein oblique to S_2 fabric in altered mafic host rock (left side of photograph). Sample DR-90-79, view under crossed polars. Scale bar = 1.0 mm.

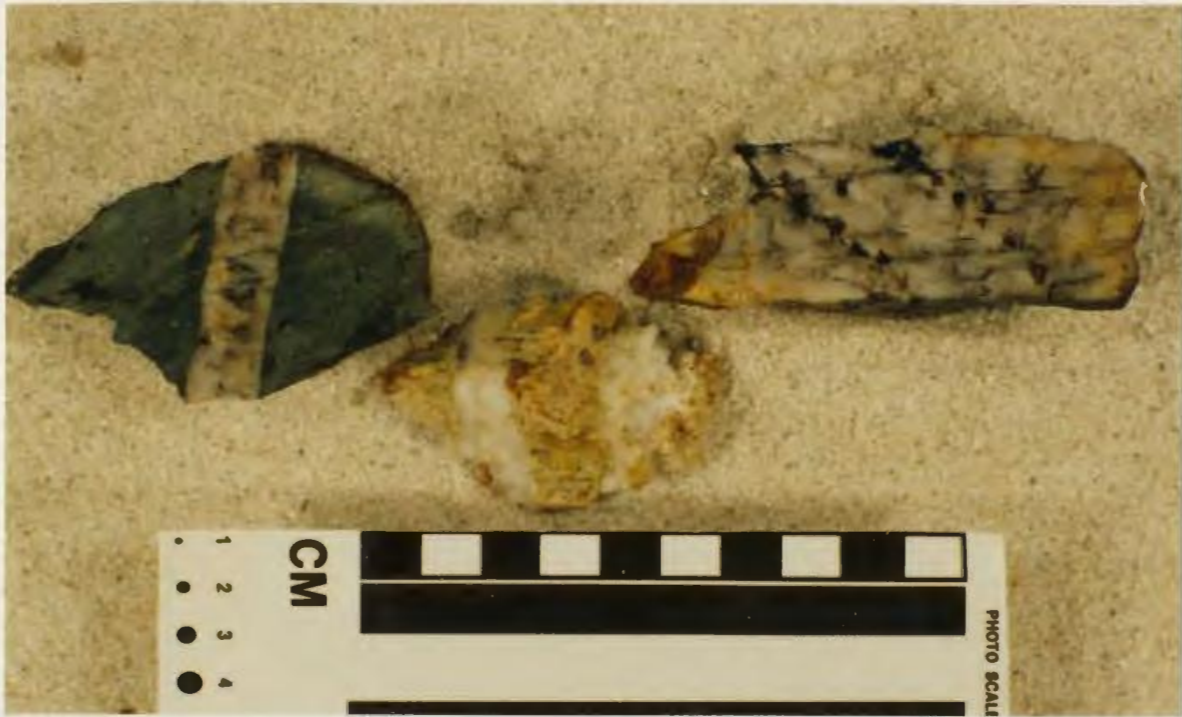


Plate 4.13 Tensional quartz veins (type III) cutting S_2 in (left to right) mafic volcanic rock, felsic porphyry dyke, and shear-parallel quartz vein. Samples V-5, V-3, V-4.



Plate 4.14 Tensional quartz veins (III), perpendicular to S_2 , cutting felsic porphyry dyke and shear-parallel rusty quartz vein (type II) at west end of main Hammer Down trench exposure. Hammer for scale, handle 30 cm long.

a common origin. Structural relationships suggest that type III veins are the same age or younger than type II veins and hydrothermal assemblages.

4.3 Wall rock alteration

4.3.1 Mineralogy

A very small proportion of the gold within the Hammer Down prospect is present in altered rocks adjacent to veins. Where observed petrographically, it is disseminated within pyrite, with the same textural features as gold in type II veins. No ore textures indicating deposition of gold-bearing assemblages by direct replacement of pre-existing minerals were observed. Strongly chloritized and variably sericitized volcanic and sedimentary rocks with 1 to 5 per cent disseminated pyrite contain up to 3 ppm Au (assay records of Noranda Exploration Co.), and a 3 m section of schistose felsic dyke in drill core DDH-MS-88-13 contains dispersed pyrite and numerous quartz-pyrite-calcite veinlets (type II or type III) along the S_2 foliation, and gave assay returns up to 0.5 ppm Au.

Alteration associated with the deposition of gold is superimposed upon the regional metamorphic assemblage characterized by epidote, calcite, and chlorite. The onset of strong shear deformation coincides with increasing chloritization such that chlorite (brown or berlin blue in crossed polars) exceeds 30 modal per cent in some fine grained schists within a few (0-3) metres of the main veins and alteration zones.

Chlorite is the most common metamorphic or hydrothermal mineral within D₂ high strain zones, but its relationship to gold is unclear, because some highly strained chlorite-rich zones without gold mineralization exist in the prospect area

Immediately adjacent to most type II veins, sericite is far more abundant than chlorite. In basalt flows and mafic dykes, leucoxene is present as abundant ragged, deformed grains or aggregates 0.5 - 2 mm in maximum dimensions, and Fe- and Ti-oxides may comprise a substantial portion of very fine-grained "dusty" opaque grains in moderately altered tuffaceous or epiclastic rocks. The distribution pattern of leucoxene is irregular, perhaps because of original lithological and mineralogical heterogeneities, but it occupies approximately the same range of distribution in altered mafic rocks as chlorite. Highly strained and altered rocks with sericite present in greater than trace amounts do not contain macroscopically visible leucoxene in drill core.

Magnetite has an irregular distribution, and is not definitively linked to the main auriferous hydrothermal fluid event associated with gold deposition. The sporadic magnetic character of many host rocks is attributed to processes of igneous crystallization, early sedimentary chemical precipitation, or regional metamorphism.

Secondary hydrothermal silica is common but it is not extensively or systematically developed outside of veins. In the margins of some type II veins, quartz in pressure shadows adjacent to pyrite has a comb texture, with elongate crystals parallel to S₂ and the vein boundary.

Hydrothermally altered mafic rocks are mottled dark green and grey in chloritic zones, and mustard yellow in extremely sericite-rich portions. Within a few centimetres of most type II veins, in wall rock inclusions within veins, the hydrothermal assemblage is composed of weakly aligned sericite (muscovite) flakes 0.05 to 1 mm long, fine granular quartz, pyrite, carbonate minerals, and granular red rutile. Very fine grained calcite and sericite constitute up to 50% of some altered vein margins and wall rock inclusions. Adjacent to some type II veins, however, sericitic alteration is conspicuously absent, and the more widespread chlorite-rich assemblages extend completely to the vein boundary. In vein margins, minor chlorite is present in pressure shadows adjacent to blocky pyrite grains, and is also intergrown with sericite, where it might be either a residual phase from regional metamorphism, coeval with sericite and other minerals of type II assemblages, or retrograde after the main mineralizing event.

Dark red rutile is a common accessory mineral in chloritized mafic units near type II veins and in more widespread regionally metamorphosed rocks. It is not substantially more abundant in the intensely sericitized vein margins. Orange and yellow rutile is locally abundant in altered felsic dyke sample D-1, which is cut by abundant calcite + quartz \pm fluorite \pm pyrite \pm sphalerite type II and type III veinlets at spacings between 5 and 100 mm.

The strongest sericite alteration is usually found adjacent to the largest quartz veins with the highest ore grades, but narrow type II quartz + carbonate + pyrite \pm

sphalerite veins in felsic dykes (*e.g.* D-1, DR-90-08) and in mafic rocks (*e.g.* DR-90-04) also have sericitic alteration halos. Up to 10% pyrite is present in some strongly sericitized rocks, and rare chalcopyrite was also observed in thin section.

The presence of numerous fault contacts between units, and the heterogeneity of the host rocks is likely to obscure any zonation of hydrothermal mineral assemblages that might ordinarily be developed during progressive deformation and alteration. In general, the main mineralized D₂ high strain zones are marked by an absence of epidote, and by variable amounts of chlorite, sericite (muscovite), carbonate (predominantly calcite), quartz, rutile, and pyrite. Calcite exists in all types of veins and assemblages in the Hammer Down prospect, and is sufficiently widespread that it is not useful in identifying ore zones. Calcite is locally abundant more than 10 metres beyond the main gold-bearing veins, particularly between the main ore zones and lower brittle fault, where it is a principal component of type I groundmass and vein assemblages not genetically related to gold.

Small lenses or bands of felsic volcanic rocks within deformed, altered, and mineralized zones (*e.g.* DR-90-18; SV-1) are characterized by finely intergrown quartz and sericite, with or without pyrite and calcite, and are cut by numerous narrow (0.5 - 2 mm) veinlets of fine granular quartz. This style of silicification occupies zones up to 50 cm wide in drill core or outcrop exposures that have evidently been the sites of a high degree of hydrothermal alteration and replacement, but they have only rare sulphide minerals and do not contain ore grade gold

mineralization.

Altered felsic dykes contain notably less carbonate and chlorite than mafic rocks from similar proximity to high strain zones and type II veins, but all felsic dykes from the prospect area contain some sericite. Alteration and deformation in dykes is accompanied by recrystallization and replacement of plagioclase that obscures the original igneous texture. In general, sericite is far more widespread in dykes, but it is nowhere developed to the same intensity as in some strongly altered mafic rocks immediately adjacent to type II veins.

4.3.2 Chemistry

Chemical constituents of the major hydrothermal minerals are those most likely to have been added, removed, or remobilized by fluids introduced during vein emplacement and wallrock alteration. The alkali elements K and Na are likely to be particularly mobile in hydrothermal systems, and are essential components of the metamorphic and hydrothermal minerals muscovite and albite. Chlorite is the most abundant and widespread Mg- and Fe-bearing alteration mineral involved in hydrothermal reactions, so its presence or absence should have some control on the concentrations of those major elements. In sericite-rich altered mafic rocks, chlorite is rare or absent, and pyrite is the most common iron-bearing mineral. Magnesium- and iron-bearing carbonate minerals are confined to certain type II veins, and were

not found in any wall rocks. In Figure 4.1, alkali elements (normalized to the alumina content in order to represent the silicate portion of the rock and thereby avoid spurious variations in absolute concentrations that might arise from the addition of carbonate) are plotted against magnesium oxide and total iron oxide. For felsic dykes, there is little or no variation in ratios of Al_2O_3 to K_2O , Na_2O , MgO , or Fe_2O_3^* that corresponds to the petrographically recognized range of alteration intensity. For mafic rocks, both $\text{MgO}/\text{Al}_2\text{O}_3$ and $\text{Fe}_2\text{O}_3^*/\text{Al}_2\text{O}_3$ vary by factors of two or more, but there is no systematic pattern of Fe or Mg enrichment or depletion. The mafic rock sample that yielded the lowest $\text{MgO}/\text{Al}_2\text{O}_3$ and $\text{Fe}_2\text{O}_3^*/\text{Al}_2\text{O}_3$ ratios is a sericite schist that contains only minor chlorite and pyrite. Three samples with abundant sericite have the highest $\text{K}_2\text{O}/\text{Al}_2\text{O}_3$ ratios of the mafic rocks, suggesting addition of potassium. Two weakly mineralized samples with abundant chlorite in addition to sericite have elevated $\text{K}_2\text{O}/\text{Al}_2\text{O}_3$ ratios, but values of $\text{MgO}/\text{Al}_2\text{O}_3$ and $\text{Fe}_2\text{O}_3^*/\text{Al}_2\text{O}_3$ that are similar to other mafic rocks that are not hydrothermally altered (*i.e.* metamorphosed, but without type II mineral assemblages). No consistent pattern exists for sodium in sericite-rich rocks, but the two samples that contain partially developed type II hydrothermal assemblages (sericite in margins of gold-bearing veins) do have relatively low $\text{Na}_2\text{O}/\text{Al}_2\text{O}_3$ ratios.

Potassium metasomatism is a feature of most Archean and younger mesothermal gold deposits (Kerrick, 1989b). K_2O concentrations in variably altered rocks from the Hammer Down prospect exhibit a positive correlation with Rb over

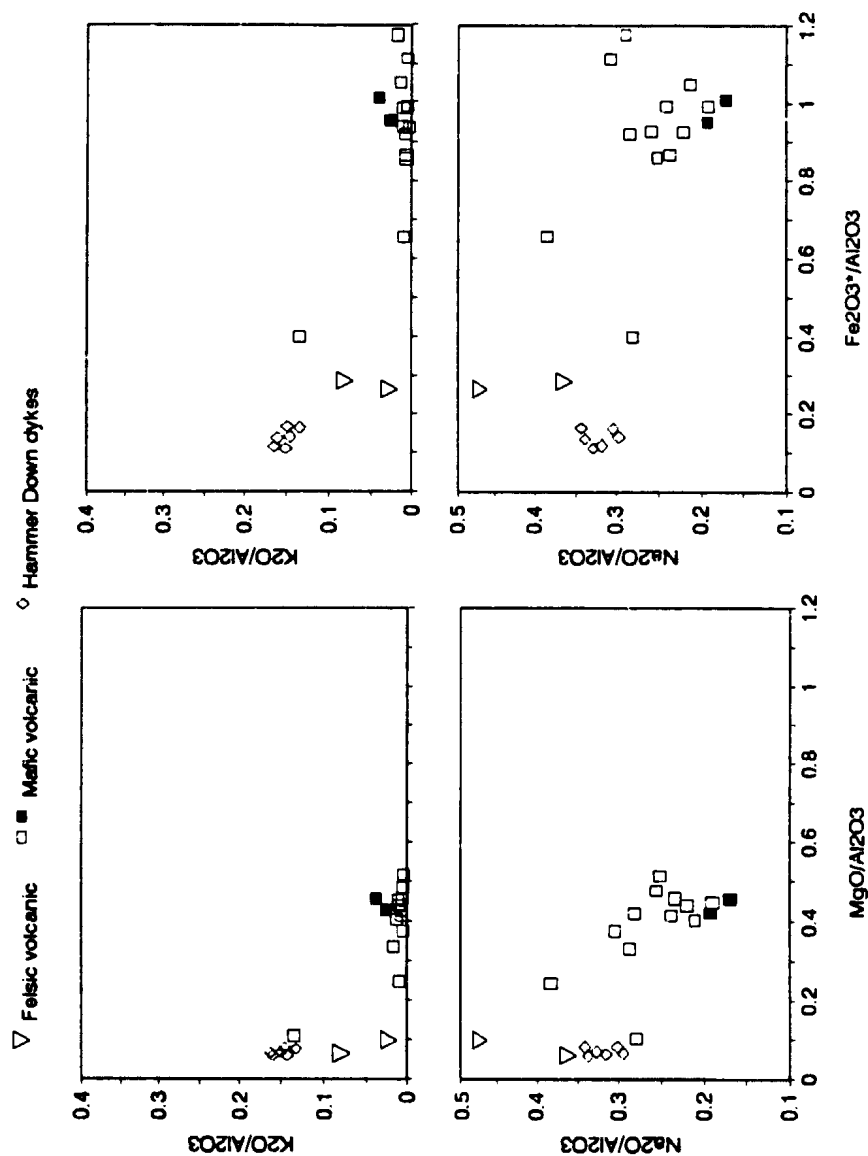


Figure 4.1 Alkali oxides / Al_2O_3 vs total iron oxides (Fe_2O_3) / Al_2O_3 and MgO / Al_2O_3 in whole-rock samples from the Hammer Down prospect. Triangles are data from felsic volcanic rocks; square symbols are for mafic rocks, and small diamond symbols are for felsic dykes. Filled symbols are for sericite altered and mineralized rocks.

several orders of magnitude, and have a less regular relationship with Ba (Figure 4.2). The lithophile elements K and Rb are consistently elevated in mafic rocks that contain pyrite and sericite associated with gold, relative to unaltered (metamorphosed) or strongly chloritized samples. Rb readily substitutes for K in many minerals, including muscovite, and Ba can also replace K in some potassic minerals. Notably, the two weakly mineralized mafic rock samples were collected approximately 50 cm from gold bearing veins, and are outside of the narrow mica- and sulphide-rich alteration zones that are restricted to the immediate margins of type II veins. Based on their mineralogy, these narrow zones, which locally contain gold, are likely to be far more enriched in alkali elements. Even at low or moderate intensities of sericitic alteration, K_2O , and Rb contents are very sensitive to hydrothermal replacement of the chlorite-rich assemblages. The five lowest K_2O and Rb values are from chlorite-rich samples collected near the main mineralized and highly strained zone in DDH MS-89-16. Their strong degree of separation from sericite-bearing samples is consistent with chloritization not being genetically associated with gold mineralization.

Where alteration haloes surrounding mesothermal gold deposits are extensive, K and Rb co-enrichments are generally developed in all host rock types (Kerrick, 1989b), but felsic porphyry dykes from the Hammer Down prospect, including those that are seen petrographically to be altered, do not display linear trends of lithophile element abundances in Figures 4.1 and 4.2. These altered felsic dykes are an example of host rock control on alkali content, in contrast to fluid control.

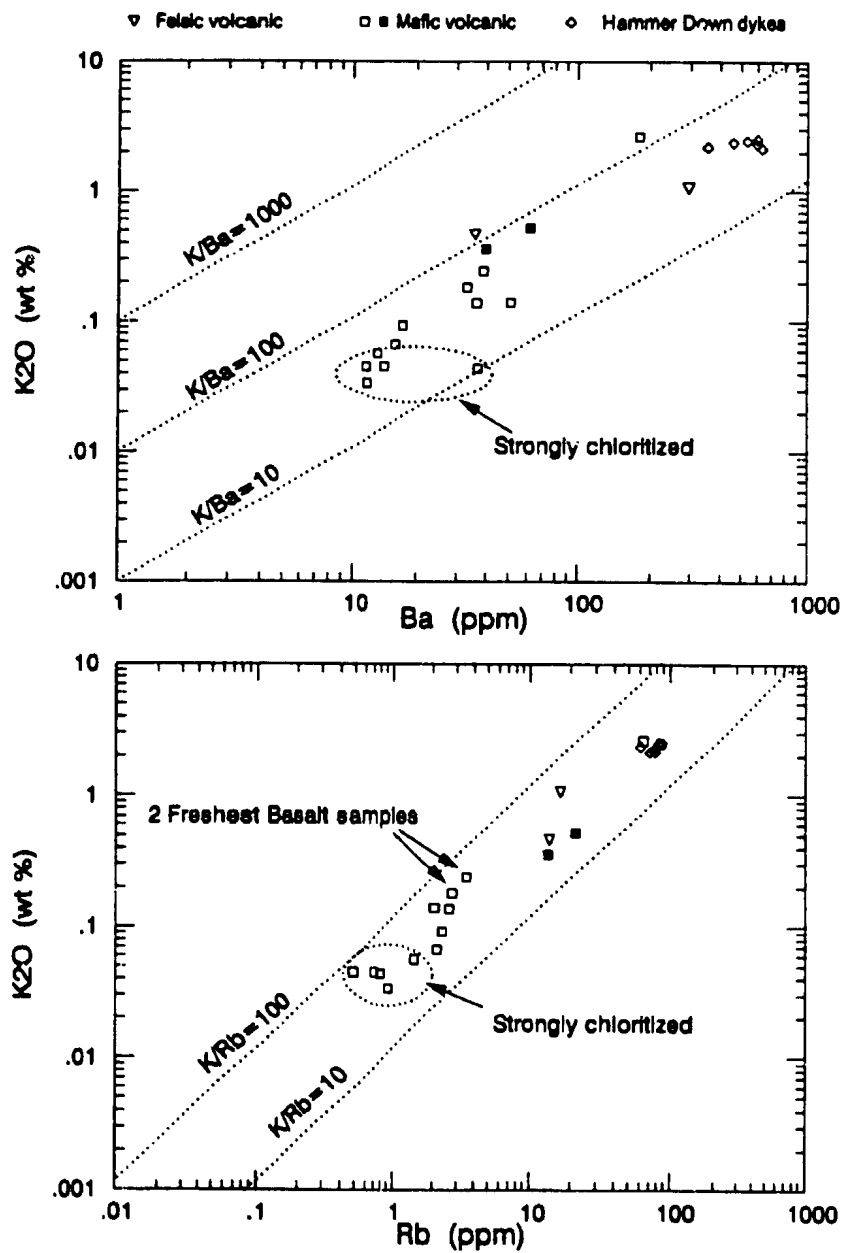


Figure 4.2 K₂O vs. Ba and Rb in whole-rock samples from the Hammer Down prospect. Triangles are data from felsic volcanic rocks; square symbols are for mafic rocks, and small diamond symbols are for felsic dykes. Filled symbols are for sericite altered and mineralized rocks.

Many of the petrographic observations are substantiated by geochemical profiles of selected elements in mafic rocks from drill core DDH MS-89-16 (Figures 4.3 and 4.4). Several gold-bearing type II veins are present within the drill core interval marked by shading in Figures 4.3 and 4.4, and constitute the main mineralized zone. The two samples with the lowest Na_2O contents, and two of the three most K_2O -rich samples are from this zone. The rock with the highest level of K_2O is not in close proximity to gold mineralization, and also has a high sodium content that makes it chemically distinct from samples that contain sericite and pyrite and are spatially associated with gold (*cf.* Figures 4.1 and 4.3). Although a high degree of chloritic alteration extends several metres away from veins, Figure 4.3 shows no large systematic change in either Fe or Mg content in or near the ore zone, but the profile does not include any chemical analyses for the most sericite-rich rocks immediately adjacent to veins, because they are too narrow for efficient or representative sampling. These narrow intervals with well-developed type II hydrothermal assemblages contain only rare magnesium-bearing minerals.

One high sulphur value in Figure 4.4 is from the mineralized zone near type II veins, but another from pyrite-rich mafic tuff or sediment at 205 m depth is not associated with gold. Enhanced sulphur content alone is not indicative of the style of alteration that accompanies gold because sulphide minerals are sporadically abundant in unmineralized host rocks. One copper value and two zinc values from the main mineralized zone are above background levels by factors of 5 or more. The

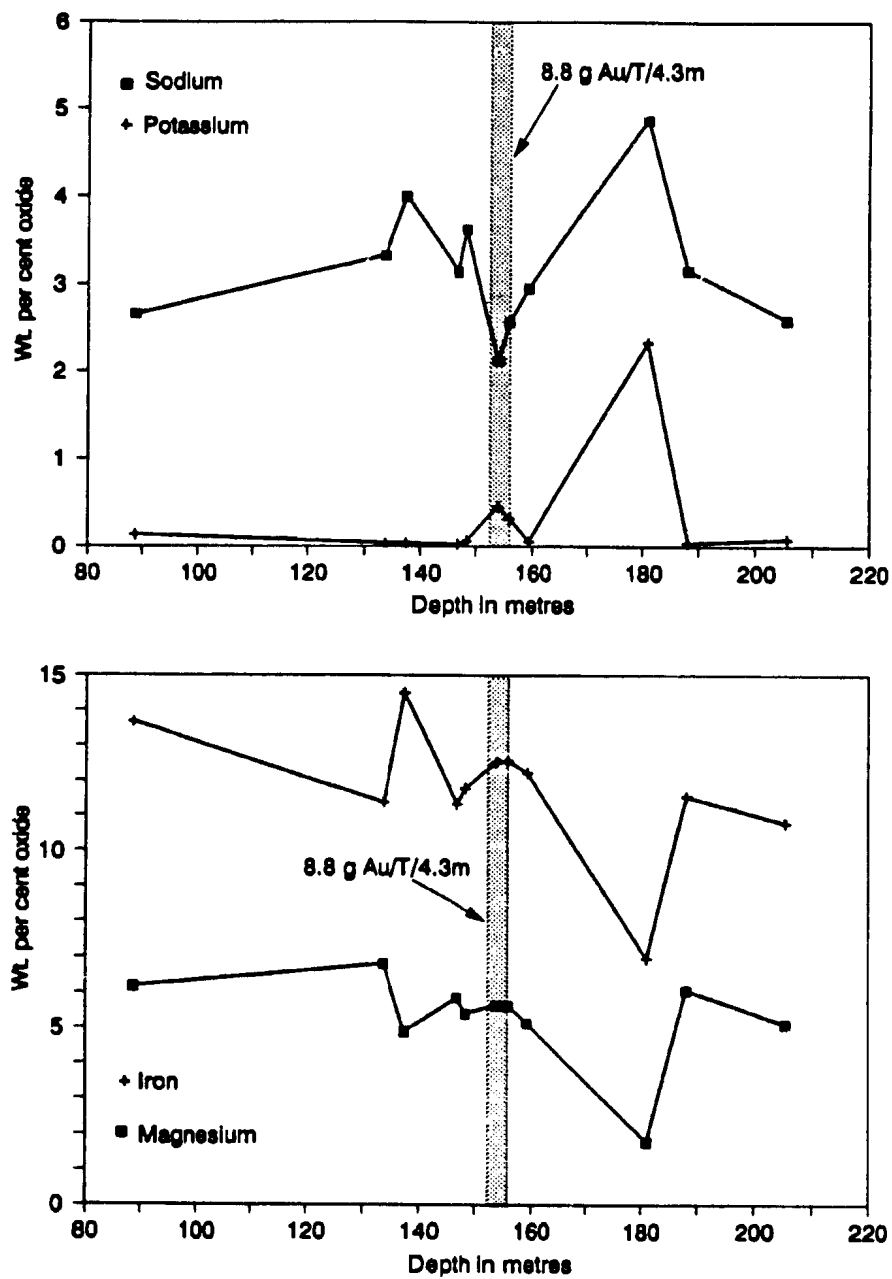


Figure 4.3 Geochemical profiles of Na_2O , K_2O , Fe_2O_3^* , and MgO (weight per cent) in drill core DDH MS-89-16.

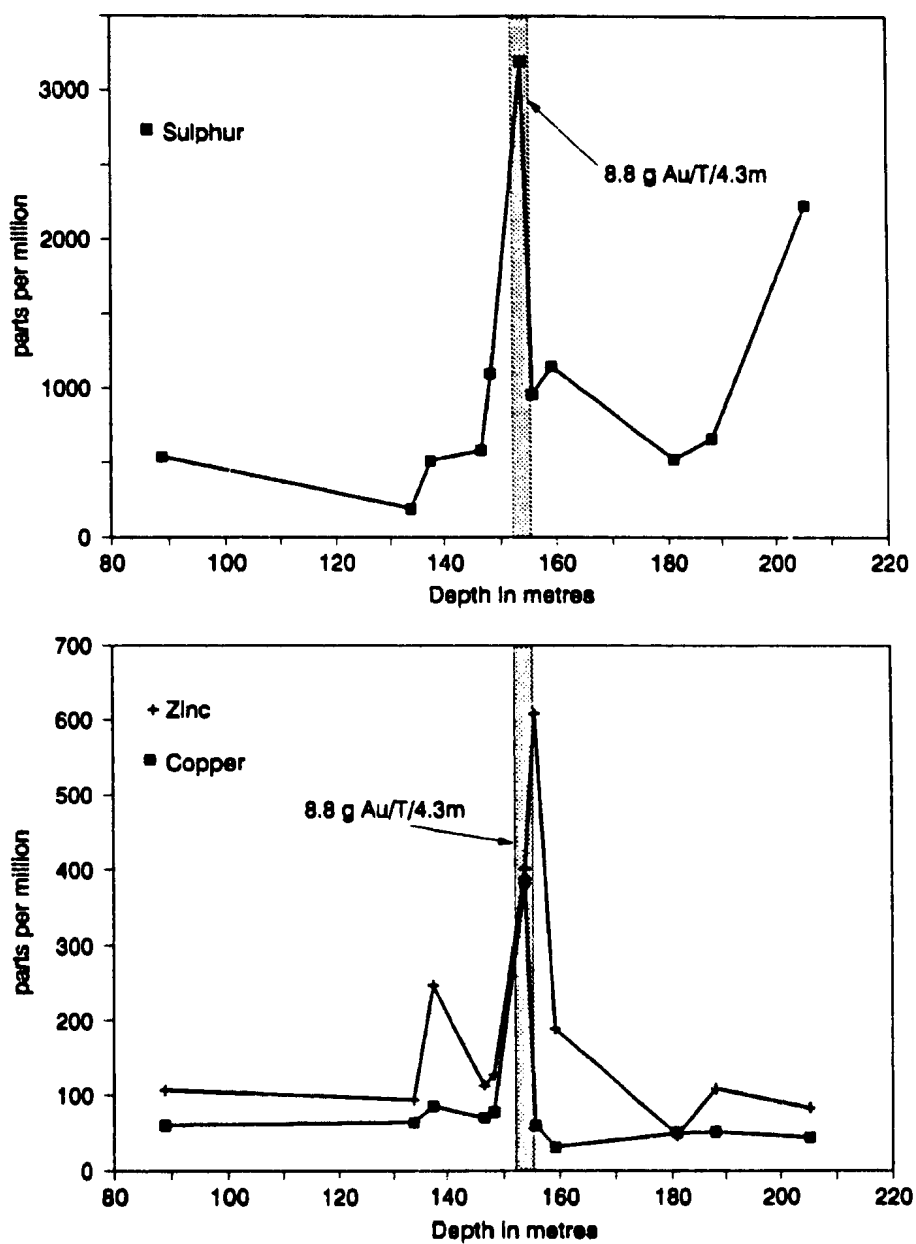


Figure 4.4 Geochemical profiles of S, Zn, and Cu (parts per million) in drill core DDH MS-89-16.

measurements reported in Figures 4.2, 4.3, and 4.4 indicate the deposition of metals, along with certain lithophile elements, in narrow, restricted zones outside of the gold-bearing veins in the Hammer Down prospect.

4.4 Mineral Paragenesis

The paragenetic sequence of metamorphic minerals and type I veinlets, of hydrothermal minerals in type II and type III veins and vein margins, and of fault breccia that postdates gold mineralization is summarized in Figure 4.5. The different phases of chlorite growth during regional metamorphism and hydrothermal alteration are not fully separable. Recrystallization, particularly of gold, sphalerite, and chalcopyrite, is recognized as an event that postdates the main phase of vein emplacement and ore mineral deposition.

Regional metamorphism and seafloor alteration of basaltic rocks produces epidote- and chlorite-rich assemblages by a variety of mineralogical and fluid reactions, including the following:



plagioclase

fluid



calcite

epidote

albite

fluid

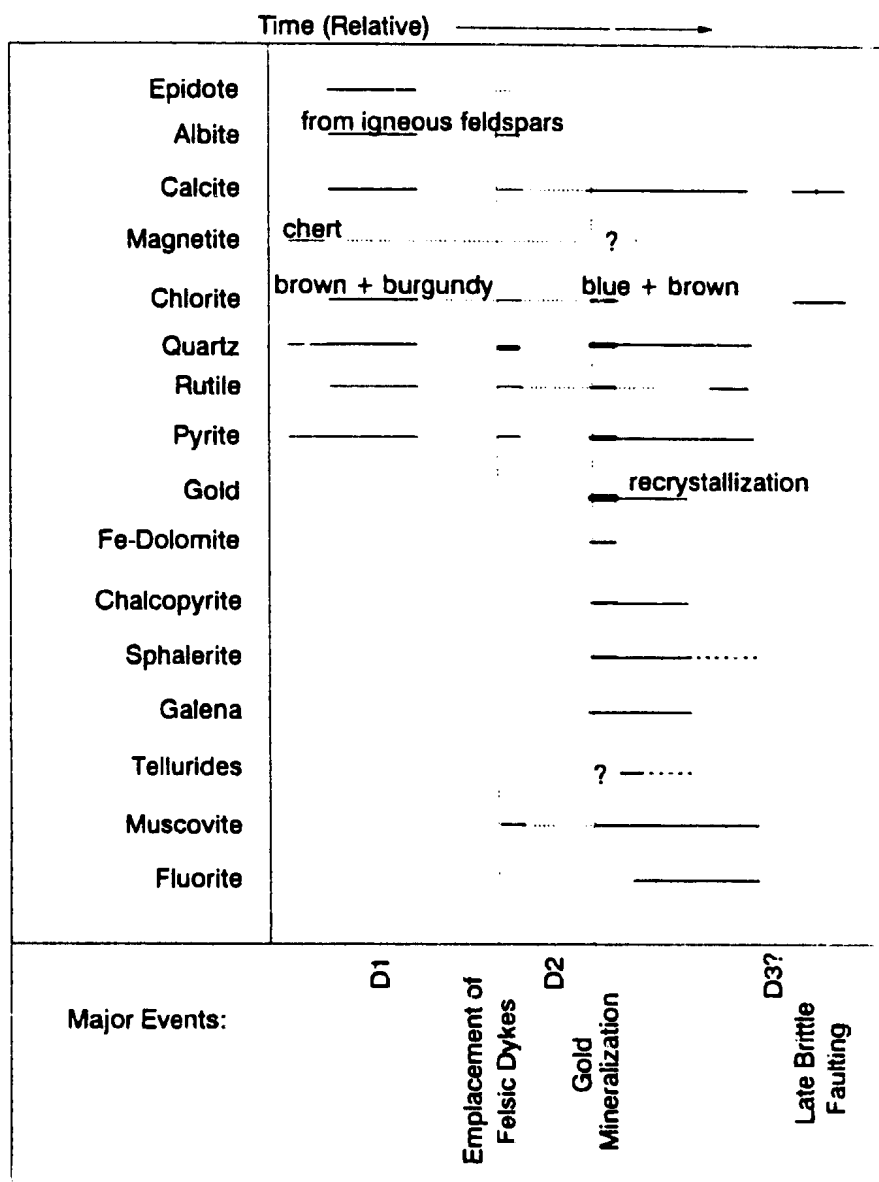
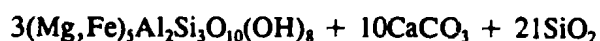


Figure 4.5 Paragenetic sequence of major metamorphic and hydrothermal minerals in the Hammer Down prospect. Thickness of lines is not directly proportional to modal volume, but indicates the relative importance of phases at various stages of mineral deposition. Dashed lines denote uncertain distribution of minerals in time.

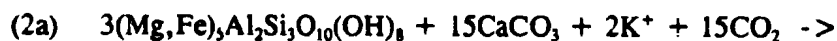


actinolite epidote fluid



chlorite calcite fluid?

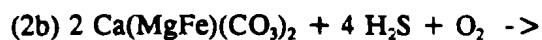
Chlorite is abundant in zones peripheral to type II veins, and also in strongly deformed mafic rocks not close to mineralized veins, whereas sericite becomes the predominant hydrothermal mineral immediately adjacent to most gold-bearing veins. The breakdown of chlorite during progressive hydrothermal alteration related to gold mineralization is required by petrographic observations, and the paucity of magnesian minerals in veins or sericitic margins suggests that a large proportion of magnesium was carried away from the vein system. If chloritic rocks outside the sericitic haloes were distal alteration zones associated with gold mineralization, they would constitute a sink for Mg. Albite is ubiquitous in regionally metamorphosed host rocks, and persists in most altered vein margins. Mineral reactions that are consistent with the observed trends in association with gold mineralization include:



chlorite calcite fluid



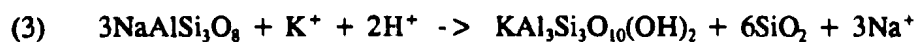
sericite ferroan dolomite fluid



ferroan dolomite fluid



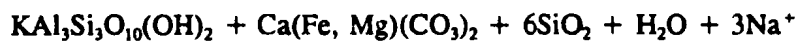
pyrite calcite fluid



albite fluid sericite fluid



albite chlorite calcite fluid

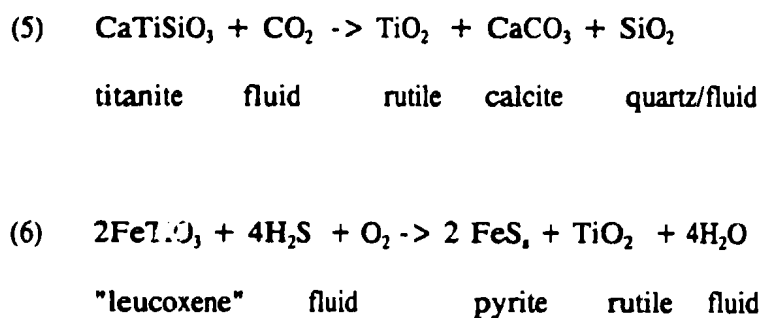


sericite ferroan dolomite quartz fluid

The very restricted and minor presence of iron and magnesium carbonate minerals in altered zones and veins of the Hammer Down prospect is a strong argument against the extensive operation of reactions (2a) and (4). If ferroan dolomite was produced in large quantities, the iron component must have reacted to a large extent with fluid to produce pyrite, which is the characteristic iron-bearing mineral in type II veins. Reaction (2b) removes Mg into solution, and (3) and (4) indicate mechanisms for production of a muscovite- and quartz-rich alteration assemblage that includes K enrichment and Na depletion, as observed in altered rocks

associated with gold (sections 4.3.1 and 4.3.2). Production of pyrite (with sulphur in the -1 oxidation state) from hydrogen sulphide in solution (S^{2-}) by reactions such as (2b) requires the net oxidation of sulphur. Changes in oxidation state may be achieved by reaction of free oxygen, as written in reaction (2b), or by reactions involving ferrous and ferric iron, which, for simplicity, are not incorporated into the chemical equations above.

Rutile is a conspicuous accessory mineral in hydrothermal assemblages, and can be formed from metamorphic or igneous minerals by several reactions:



The iron component of leucoxene and chlorite is presumably incorporated into pyrite by sulphidation reactions (6) or (2a) + (2b). Substitution of $\text{Au}(\text{HS})_2^-$ or other bisulphide complexes of gold into (2a) or (6) gives direct precipitation of gold by sulphidation of wall rock, which is a feasible mechanism for gold mineralization in the sericite- and pyrite-rich alteration zones.

4.5 Summary

Deposition of gold, during or prior to a deformational episode is demonstrated by the strong fabric in the main gold bearing (type II) veins and the pervasive deformation of quartz, pyrite, sphalerite, and chalcopyrite on a microscopic scale. Field relations and structural studies indicate type II vein emplacement to be synchronous with development of the S_2 foliation in localized zones of high strain. A small number of tensional quartz veins that cut shear veins and the S_2 fabric in mafic volcanic rocks and in felsic dykes are themselves cleaved and offset in the same dextral sense as mineralized shear zones in the Hammer Down trench, suggesting that some amount of movement along S_2 continued after the development of the main gold bearing veins.

In mafic rocks, strong chlorite and calcite alteration may extend for more than one metre adjacent to veins, but the scale of interaction between fluids and rocks around the type II veins generally seems to have been small. Progressive alteration of mafic volcanic rocks in mineralized high strain zones are marked by a decrease in chlorite abundance, by an increase in sericite and pyrite, and by the disappearance of epidote and macroscopic leucoxene aggregates. These indicators of gold mineralization may be very poorly developed, or present only on a scale of several centimetres. Strong hydrothermal alteration in narrow haloes around type II gold-bearing veins is petrographically identifiable on a scale of 1 metre or less, and is

marked by an increase in K, Rb, S, Cu, and Zn in mafic rocks. Na and Ba contents are irregular, but Na is generally depleted in and adjacent to mineralized zones, and Ba is somewhat coenriched with K_2O .

Chapter 5

GEOCHRONOLOGY

5.1 Introduction

The results of U-Pb isotopic dating of zircon from major host units at the Hammer Down prospect are presented and discussed in this chapter. Also included are the results of U and Pb isotopic analyses of hydrothermal rutile that were undertaken in an attempt to directly determine the absolute age of gold deposition. Age constraints are a vital part of a complete genetic model that can properly place gold mineralization within the regional geological context of orogenesis, metamorphism, and magmatism. The generation of precise radiometric ages for host rocks allows comparison or correlation to other rock units, and provides a characterization of the units that is more complete than, but complimentary to, that derived by field mapping, petrography, and geochemistry.

Field relations and structural studies indicate that gold mineralization in the Hammer Down prospect is a younger event than the emplacement of felsic porphyry dykes, which intrude volcanic and sedimentary rocks. The deposition of gold was synchronous with D₂ deformation and hydrothermal alteration.

5.2 Description of samples

5.2.1 Volcanic rocks

Approximately 25 kg of quartz and feldspar porphyritic dacite tuff was collected from a 2.5 m thick bed 100 m southwest of the main surface exposure of the Hammer Down prospect (sample SV-2) for U-Pb dating of the host volcanic sequence. Projection along strike of the S_1 or S_2 foliation places this unit in the footwall of the main ore zone (see Figure 3. 1). The sample is petrographically and chemically similar (Sections 3.2.2 and 3.2.3) to felsic volcanic or epiclastic rocks in the southern portion of the Hammer Down trench, in the immediate footwall of the main mineralized zone.

5.2.2 Felsic intrusive rocks

In the central part of the main Hammer Down trench exposure, a felsic porphyry dyke (sample D-1; Figure 3.3) with a clear intrusive relationship to volcanic rocks, and cut by a mineralized shear zone was sampled for zircon geochronology. Two 25 kg portions of rock were collected from the same outcrop area.

5.2.3 Hydrothermal assemblages

Rutile is an abundant and potentially U-bearing hydrothermal mineral that can be used to directly date the event of ore formation, provided that its paragenesis is directly related to that of gold.

Samples from strongly altered zones near the margins of high-grade gold-bearing type II veins in drill cores DDH MS-88-15 and MS-89-16 (Figure 3.3) contain abundant dark red rutile prisms and clusters of grains 0.005 to 0.02 mm in length. By visual inspection, these grains were deemed to be of inferior quality for isotopic analysis. Furthermore, similar grains are equally abundant in moderately altered rock exterior to the main mineralized zones, so that the time of their growth is not necessarily closely linked to that of gold.

Part of sample D-1 is a pervasively sheared and moderately altered felsic dyke that contains abundant type II and type III quartz + calcite + pyrite \pm fluorite \pm sphalerite veinlets that are subparallel to the S_2 foliation and have calcite- and sericite-rich haloes. Patches of calcite in the groundmass locally overgrow the S_2 fabric, but are themselves deformed. In the altered rock adjacent to veins, many of these patches contain prismatic to acicular striated orange and yellow rutile inclusions ranging from 0.03 to 0.08 mm in length that are oriented along crystallographic planes of the host calcite (Plate 5.1). Rare, smooth, elongate rutile crystals of similar dimensions and colour are also present in the pervasively altered portions of the rock, intergrown with

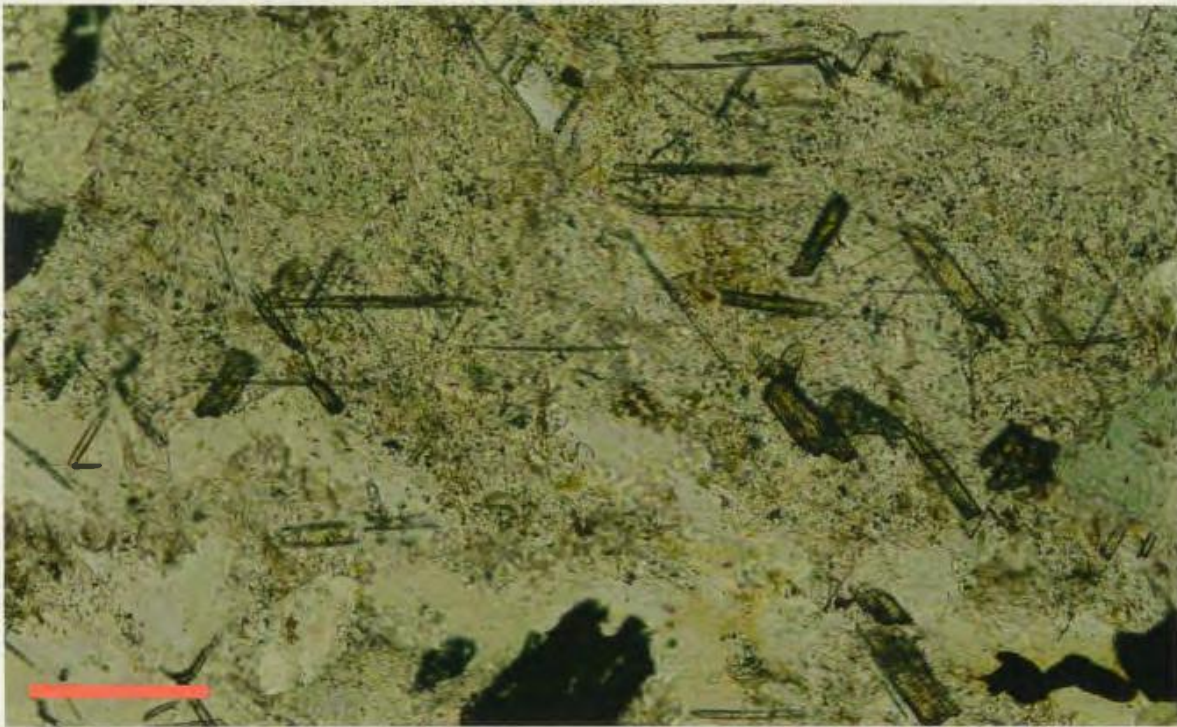


Plate 5.1 Prismatic rutile in thin section, oriented along crystallographic planes of calcite in pervasively altered groundmass of felsic porphyry dyke sample D-1. View in plane polarized light. Scale bar = 0.1 mm

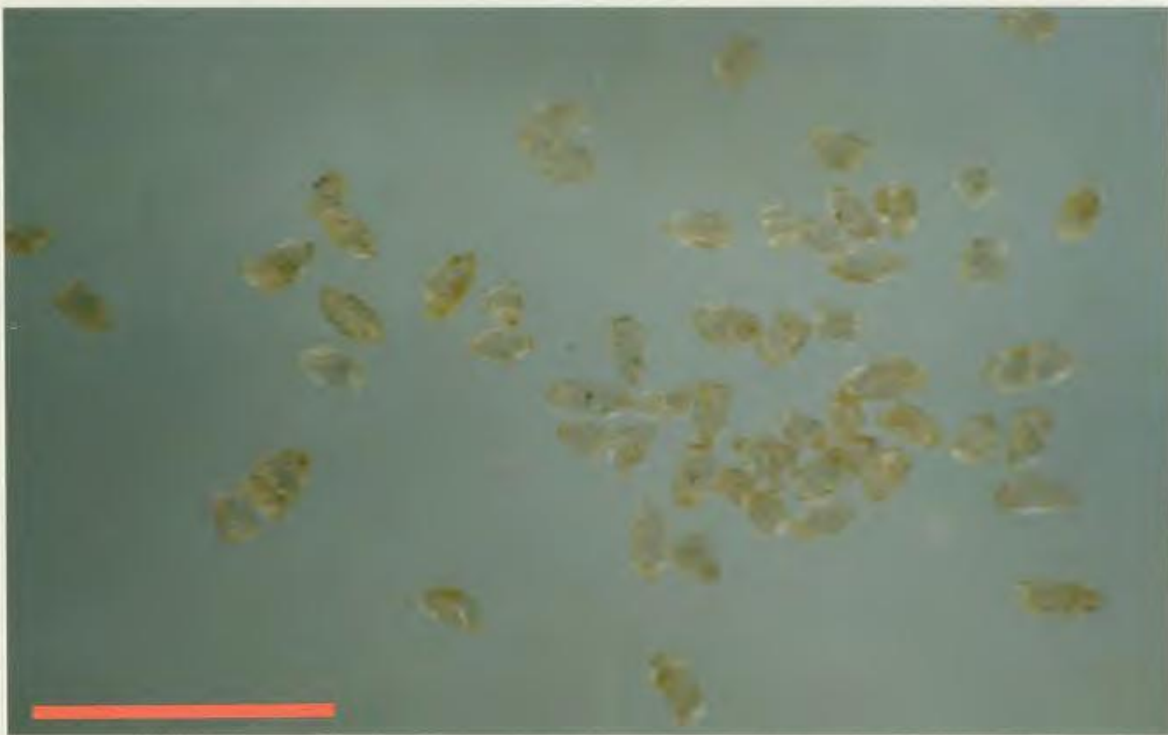


Plate 5.2 Unabraded prismatic zircon from felsic tuff sample SV-2. Scale bar = 0.5 mm.

sericite, quartz, and chlorite. The presence of striated rutile in calcite-rich altered patches is restricted to portions of dykes with abundant veinlets containing calcite \pm quartz \pm pyrite \pm fluorite or calcite \pm quartz \pm pyrite \pm sphalerite \pm galena.

Since some calcite rich veins are locally undeformed and cut the S_2 foliation that accompanied the main phase of mineralization, the crystallization of rutile in a calcite-rich assemblage is synchronous with or younger than the deposition of gold.

5.3 Techniques

5.3.1 Preparation of mineral fractions

25 kg of carefully selected and washed rock was passed twice through a jaw crusher, and pulverized in a steel disk mill. A 500 - 1000 g heavy mineral concentrate was obtained by washing on a Wilfley™ table. Material larger than 0.2 mm was separated with 70 mesh nylon seive cloth and not processed further, and the most magnetic particles (including abundant metallic fragments from the disk mill) from the finer grained portion were removed with a hand magnet. A heavy mineral fraction was collected with bromoform ($\rho \approx 2.9$ g/mL) in a separatory funnel. An initial Frantz™ (IF) magnetic separation was performed on the bromoform sink portion at side tilt of 10 degrees and 0.5, 1.2, and 1.6 ampere settings. The non-magnetic fraction collected at 1.6 A was processed with methylene iodide ($\rho \approx 3.1$ g/mL), and the sink portion was collected for further processing in a final Frantz™ (FF)

separation. The IF non-magnetic fraction of SV-2 was sufficiently small to be passed directly to the FF separation without employing methylene iodide. Zircon grains were obtained from non-magnetic fractions collected at a current of 1.6 A, and side tilts of 3, 1, and 0 degrees. Rutile from the second processed portion of sample D-1 was collected in a similar fashion at 5, 3, and 1 degree tilt.

Final fractions of SV-2 collected from the magnetic separator consisted largely of pyrite, apatite, and zircon. The sample yielded abundant stubby zircon prisms 0.02 - 0.05 mm in length (Plate 5.2), including many cracked, discoloured, and weakly magnetic grains or fragments. All the zircon grains were similar in size and shape, and appear to constitute a single population.

Final mineral fractions collected by magnetic separation from sample D-1 consisted predominantly of pyrite, apatite, rutile, fluorite, and various sizes and morphologies of zircon. The most abundant zircon grains were square doubly terminated prisms 0.03 - 0.2 mm long, some of which contained visible cores and inclusions (Plate 5.3). A few clear, gem-quality, equant to elongate (0.04 - 0.1 mm) multifaceted zircon grains were obtained. The dyke sample yielded approximately 60 acicular zircon crystals up to 0.25 mm long with length : width ratios greater than 6 : 1 (Plate 5.4). Magnetic FF fractions contained abundant red, orange, and yellow rutile prisms and fragments 0.04 - 0.08 mm in length, with rare elbow twins.

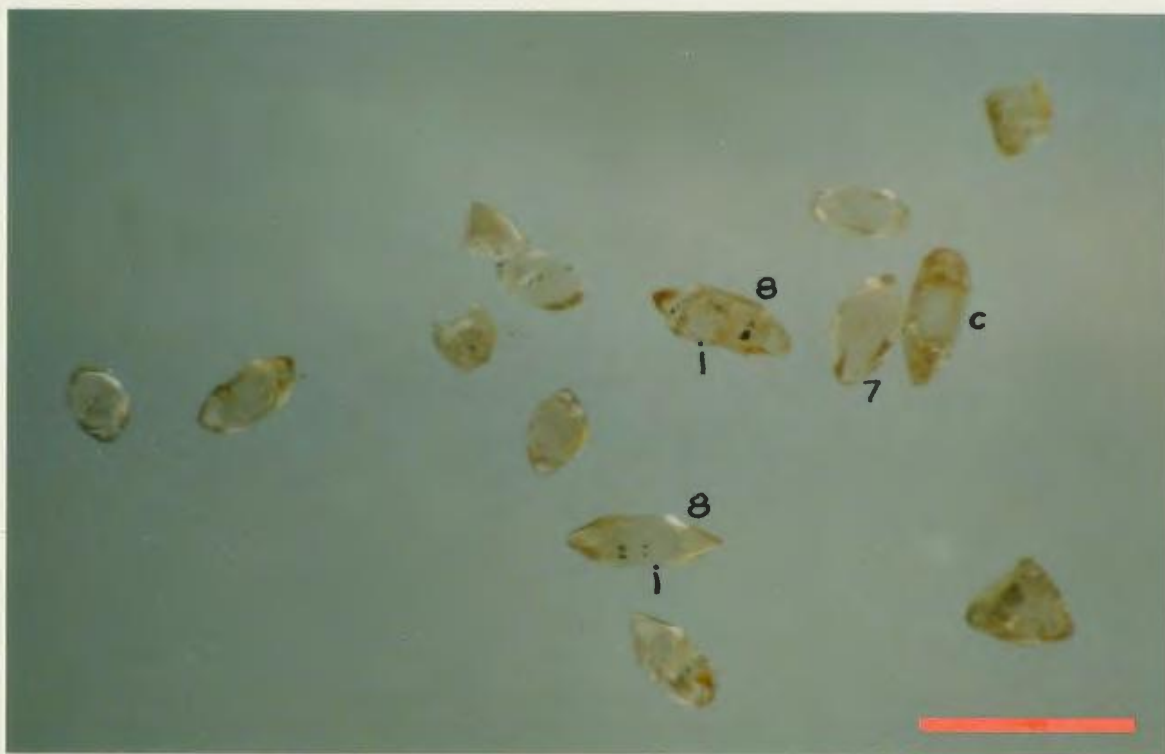


Plate 5.3 Unabraded zircon prisms from felsic porphyry dyke sample D-1, some with visible cores (c) and inclusions (i). Analyzed fractions 7 and 8 are labelled. Scale bar = 0.5 mm.



Plate 5.4 Unabraded zircon needles from felsic porphyry dyke sample D-1 (analyzed fraction 12). Scale bar = 0.5 mm.

5.3.2 Analytical procedures

Final picked fractions of zircon and rutile were selected on the basis of colour, clarity, and surface morphology of grains by hand picking under a binocular microscope. Table 5.1 includes the magnetic properties and abbreviated descriptions of the selected zircon grains. Two samples of striated rutile prisms were prepared. Certain fractions were processed by air abrasion with pyrite by the method of Krogh (1982), and the excess pyrite was dissolved in 4 N HNO_3 . After washing with distilled low-Pb HNO_3 , distilled water, and acetone, zircon grains were weighed and loaded into Teflon[®] (polytetrafluoroethene) capsules ("bombs") with distilled HF and HNO_3 for dissolution and an aliquot of mixed ^{205}Pb - ^{235}U spike. Rutile was dissolved in screw-top teflon bottles. After dissolution in sealed capsules at 210° C for 100 hours or more, U and Pb were converted to aqueous chloride complexes by drying followed by dissolution in 3.1 N HCl. U and Pb were successively isolated by small-volume ion-exchange chromatography with HCl, generally following the procedures developed by Krogh (1973). A similar process for rutile required separation of Fe, Ti, and P with HBr based chemistry. For each sample, eluants of U and Pb were collected in a single polymethylpentane beaker, slowly evaporated to a small droplet or solid crust, collected with a single drop of H_3PO_4 , and loaded with silica gel onto rhenium filaments in preparation for mass spectrometric measurements.

Isotopic measurements were carried out on a Finnigan MAT 262 thermal ionization mass spectrometer at Memorial University of Newfoundland. Data were collected between 1300 and 1600° C by ion-counter peak jumping for small samples, or by static Faraday multicollector mode with the ^{204}Pb peak measured in the ion counter.

5.4 Results

5.4.1 Presentation of data

Table 5.1 reports the U and Pb isotopic data for 14 mineral fractions. The data are corrected for laboratory procedure and loading blanks (5-10 pg total common Pb), isotopic composition of the spike, and mass fractionation within the mass spectrometer. Uncertainties and error limits on calculated isotopic ratios and ages were calculated by an error propagation procedure written by L. Heaman (Royal Ontario Museum, unpublished). Corrections for initial common Pb were based on isotopic compositions at the time of crystallization calculated from the two-stage growth model of Stacey and Kramers (1975).

Table 5.1 U-Pb Isotopic Data

FRACTIONS		CONCENTRATIONS			MEASURED		ATOMIC RATIOS						AGES (Ma)		
No.	Properties	Wt.	U	Pb rad.	total comm.	²⁰⁶ Pb ----- ²⁰⁴ Pb	²⁰⁸ Pb ----- ²⁰⁶ Pb	²⁰⁶ Pb ----- ²³⁸ U	²⁰⁷ Pb ----- ²³⁵ U	²⁰⁷ Pb ----- ²⁰⁶ Pb	²⁰⁶ Pb ----- ²³⁸ U	²⁰⁷ Pb ----- ²⁰⁶ Pb			
		(mg)	(ppm)	(ppm)	Pb(pg)										
								+/-	+/-			+/-			
SV-2 Catchers Pond Group Tuff:															
1	N2 -200 cracked prisms, abr	0.045	333	27.5	92	795	0.2049	0.07602	50	0.5949	42	0.05675	20	472	482
2	N3 -200 prisms + frags, abr	0.098	194	15.7	14	6486	0.1840	0.07562	30	0.5905	24	0.05664	10	470	477
3	N2 -200 prisms + frags, abr	0.038	180	14.2	19	1696	0.1627	0.07549	102	0.5900	72	0.05668	36	469	479
4	N2 -100 clear subhedral, abr	0.029	200	16.1	7	3665	0.1893	0.07515	58	0.5885	31	0.05680	36	467	484
5	M3 -200 prism frags	0.074	307	25.2	12	8978	0.2292	0.07422	36	0.5800	28	0.05668	10	462	479
6	N3 -200 prism frags	0.120	234	18.6	52	2508	0.2042	0.07356	34	0.5750	27	0.05669	14	458	480
D-1 Hammer Down Dyke:															
7	+100 1 clear prism, sl abr	0.017	185	22.0	11	1807	0.2865	0.10223	74	0.9097	68	0.06454	20	628	759
8	+100 prisms, abr	0.034	219	20.8	8	4576	0.1026	0.09408	70	0.9222	68	0.07110	20	580	960
9	N2 -100 prism tips, abr	0.014	322	29.0	37	689	0.1312	0.08705	72	0.8513	74	0.07093	20	538	955
10	N2 -200 prisms, abr	0.010	435	37.9	23	973	0.1589	0.08227	86	0.8063	86	0.07108	22	510	960
11	N2 -200 clear sharp grains	0.027	223	17.6	23	1302	0.1074	0.07837	70	0.6500	53	0.06016	16	486	609
12	N2 -200 euhedral needles	0.008	870	67.4	12	2373	0.2999	0.06637	82	0.5089	64	0.05562	12	414	437
D-1 Altered, Mineralized Zone:															
13	Clear yellow rutile, abr	0.020	9.0	0.9	274	21.3	0.4166	0.07854	162	0.7334	1714	0.06772	1472	487	
14	Yellow and orange rutile	0.039	10.3	1.0	289	24.7	0.4681	0.07315	98	0.5364	1074	0.05318	1000	455	

Notes: rad. = radiogenic; comm. = common; N2, M2, M3 = non-magnetic and magnetic fractions at 2 or 3 degree tilt on a Frantz™ isodynamic separator; +/-100, -200 = grain size greater than or less than 100 or 200 mesh; frags = fragments, abr = abraded (cf. Krogh, 1982); sl abr = slightly abraded. Atomic ratios are corrected for fractionation and spike, laboratory Pb blank of 5-10 picograms, and initial common Pb at the age of the sample calculated from the model of Stacey and Kramers (1975), and 1 picogram U blank. 2σ uncertainties are reported after the ratios and refer to the final digits.

5.4.2 Age and correlation of volcanic rocks

Zircon grains from the felsic volcanic host exhibit small variations in colour, structural integrity, magnetic susceptibility, and uranium content. Fractions of different grain sizes and physical properties (identified by the same data labels as in Table 5.1) yield six colinear points on the concordia diagram of Figure 5.1, and several ages marginally overlap concordia at the 2σ level of uncertainty. The measured U and Pb isotopic ratios yield a discordia line with an upper intercept of $479 \pm 10/-5$ Ma, and a lower intercept at -19 Ma. The large uncertainty in the upper intercept age reflects the limited range of $^{206}\text{Pb}/^{238}\text{U}$ ages. Fitting a line through a loosely constrained artificial point on concordia at 30 ± 30 Ma yields an upper intercept of $480 \pm 4/-3$ Ma, which is interpreted as the age of eruption. The unadjusted lower intercept naturally regresses near 0 Ma, indicating that there is no significant event of metamorphism or resetting, and the chosen limit of 30 ± 30 Ma covers the common observed range of lower intercepts of Dunnage Zone zircon data sets (*e.g.*, Dunning and Krogh, 1985). The six calculated $^{207}\text{Pb}/^{206}\text{Pb}$ ages are equivalent at the 2σ level of uncertainty, and have a mean of 480 Ma.

Eruption at $480 \pm 4/-3$ Ma corresponds to an Middle Arenigian age (Tucker *et al.*, 1991) for the volcanic host rocks in the Hammer Down prospect. This age is consistent with fossil evidence from the Catchers Pond Group and with palaeontologic and radiometric ages of other volcanic arc sequences in the Notre Dame Subzone

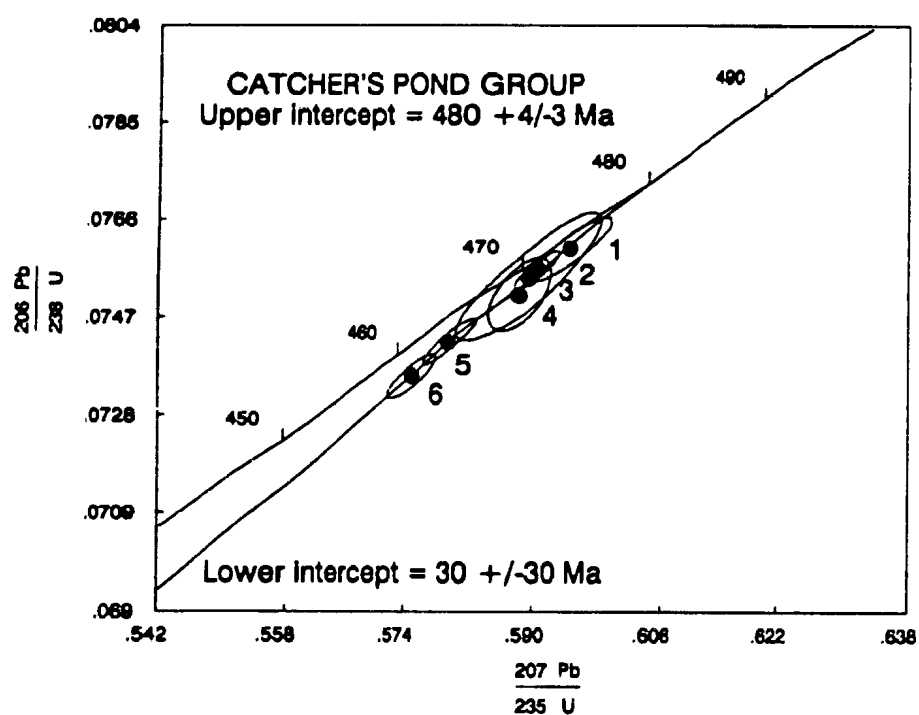


Figure 5.1 U-Pb Concordia plot for SV-2 felsic tuff zircon samples.

(Section 2.3; Dunning *et al.*, 1986; Dunning *et al.*, 1987). Within stated levels of uncertainty, the $480 \pm 4/-3$ Ma age for the Catchers Pond Group does not overlap the $469 \pm 5/-3$ Ma zircon age obtained from Cutwell Group rhyolite (Dunning and Krogh, 1991), and correlation of these two groups is not supported unless deposition of one or both units covers a sufficient time span to account for the age difference. If the Catchers Pond Group is an intact stratigraphic package overlying units of the Lush's Bight Group, then the Hammer Down prospect and the dated felsic tuff are near the base of the Catchers Pond Group.

5.4.3 Age and correlation of felsic intrusive rocks

Euhedral prismatic zircon fractions from dyke sample D-1 yield an array of discordant U-Pb ages (analyses 7-11 in Table 5.1; Figure 5.2). None of the analyzed grains contained visible cores, but isotopic analyses indicate substantial lead loss, zircon overgrowths, or both. $^{207}\text{Pb}/^{206}\text{Pb}$ ages up to 960 Ma suggest a large degree of zircon inheritance from middle Proterozoic or older rocks. The oldest $^{207}\text{Pb}/^{206}\text{Pb}$ ages are from small square euhedral prisms, pyrimadial prism tips, and large grains with scattered dark inclusions. Data from a single large grain (no. 7) and the unabraded clearest sharp grains and fragments (no. 11) plot nearer concordia, and are interpreted to contain the largest proportion of Paleozoic material.

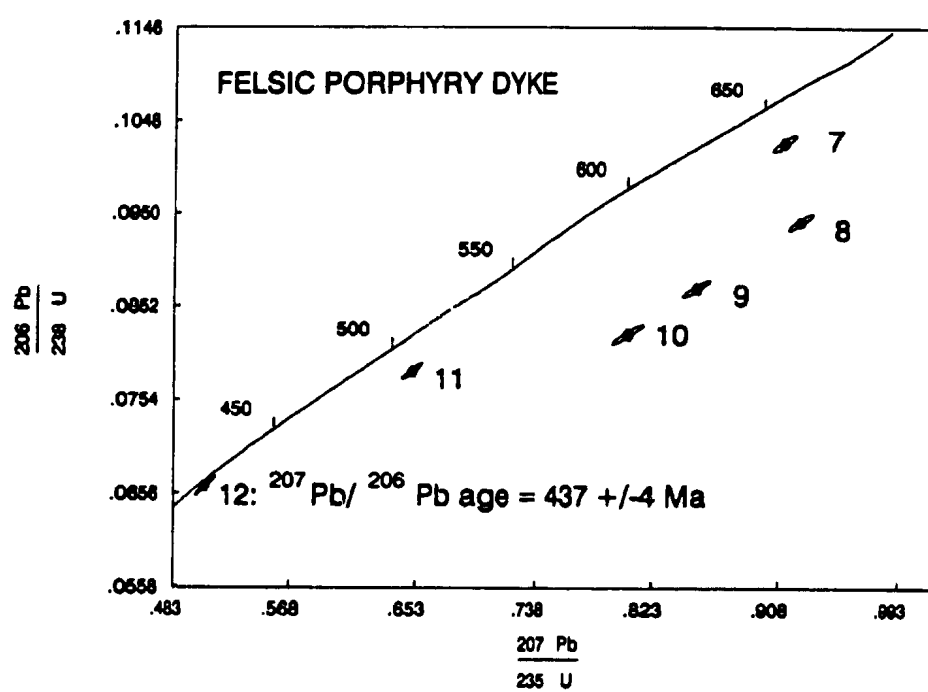


Figure 5.2 U-Pb Concordia plot for D-1 felsic dyke zircon samples.

Near concordant data were obtained from a small fraction of unabraded acicular zircon (analysis 12). The fragility of the acicular crystals precluded abrasion, and discordance is attributed to lead loss from the outermost parts of the grains. These grains are considered to be igneous in origin, and their $^{207}\text{Pb}/^{206}\text{Pb}$ age of 437 ± 4 Ma is interpreted as the age of dyke emplacement and crystallization. 437 Ma is an Early Silurian age, and with the level of uncertainty stated above, the calculated age range does not extend into the Late Ordovician by application of the time scale given by Tucker *et al.* (1991). Field relations, mineralogy, texture, and major and trace element chemistry of dykes observed or collected throughout the Hammer Down prospect match very well, indicating that they are the products of one magma batch and were emplaced during a single intrusive episode.

The interpreted 437 ± 4 Ma age of intrusion for the Hammer Down dykes overlaps with U-Pb zircon crystallization ages of the Burlington Granodiorite, Cape Brulé Porphyry, and the Rainy Lake Complex (Table 5.2). Early to Middle Silurian units of the King's Point complex, Springdale Group, Cape St. John Group, and Topsails batholith are resolvably younger than the interpreted intrusive age at Hammer Down. Of the Early Silurian units in the King's Point and Baie Verte region, the Burlington Granodiorite is the closest match in chemistry (Section 3.4.3) and age to the Hammer Down felsic porphyry dykes.

Acicular zircon from D-1 (fraction 12) contained the highest concentration of U for any fraction listed in Table 5.1, and also has a model Th/U ratio (Table 5.3),

Table 5.2

U-Pb Zircon Ages for Some Major Felsic Units of the Northwestern Notre Dame

Subzone

Unit	Age (Ma)	Reference
Rainy Lake Complex	438 +/- 4	1
Cape Brulé Porphyry	436 +/- 2	2
Burlington Granodiorite	440 +/- 2, 432 +/- 2	2
Cape St. John Group	427 +/- 2	3
Topsails Batholith	429 +/- 3 427 +/- 3	1
Springdale Group	429 +/- 4 422 - 434*	1 3
King's Point Complex	427 +/- 2	3

*Total maximum range of 3 U-Pb ages.

References for Table 5.3:

- (1) Whalen *et al.* (1987)
- (2) G.R. Dunning and P.A. Cawood, unpublished data, 1992
- (3) Coyle (1990).

Table 5.3

Model Th/U Ratios of Zircon From Sample D-1

Fraction (Table 5.1)	Description	$\frac{^{208}\text{Pb}}{^{206}\text{Pb}}$	Model Th/U
7	single euhedral prism	0.2865	0.583
8	grains with inclusions	0.1026	0.373
9	prism tips	0.1312	0.514
10	small prisms	0.1589	0.588
11	clear sharp grains	0.1074	0.346
12	Needles	0.2999	0.875

calculated from $^{208}\text{Pb}/^{206}\text{Pb}$ and sample weights of zircon samples, that is considerably higher than ratios for other fractions from the same rock. The criteria of morphology, U content, and Th/U ratio all indicate an origin for acicular zircon grains that is distinct from the sources of the highly discordant fractions of short, prismatic zircon. Th/U in igneous zircon will reflect the elemental ratio in the melt from which the grains crystallized, although the mineral-melt distribution coefficients are also influenced by physical conditions and bulk composition of the magma (Deer *et al.*, 1962, and references therein). The higher Th/U ratio in igneous zircon from the felsic porphyry dyke is interpreted to record a source component for the parent magma that has been relatively depleted in U, probably by the previous production and removal of hydrous melt fractions. Rocks of the mantle and lower continental crust are characterized by high Th/U ratios, in contrast to upper crustal reservoirs that have greatly enhanced U contents.

5.4.4 U-Pb analysis of hydrothermal assemblages

Yellow and orange rutile from felsic dyke sample D-1 (analyses 13 and 14 in Table 5.1) contain sufficient U for isotopic analyses, but the large corrections for non-radiogenic (common) Pb do not allow any meaningful age to be calculated for crystallization of the hydrothermal assemblages associated with gold. A large uncertainty in the isotopic composition of common Pb to be applied as a correction to

measured ratios leads to 2σ uncertainties of several tens of millions of years for $^{206}\text{Pb}/^{238}\text{U}$ ages. Without consideration of this uncertainty, the reported $^{206}\text{Pb}/^{238}\text{U}$ age of fraction no. 13 is 50 Ma older than the $^{207}\text{Pb}/^{206}\text{Pb}$ age of igneous zircon from the same rock. Ratios involving ^{207}Pb have uncertainties of 18 - 25% even with assumption of a known model common Pb isotopic composition, and $^{207}\text{Pb}/^{206}\text{Pb}$ ages are not reported for rutile in Table 5.1.

5.5 Summary

Felsic tuff from the Catchers Pond Group at the Hammer Down prospect has a U-Pb zircon age $480 \pm 4/-3$ Ma. A felsic dyke that hosts gold has a Pb-Pb zircon crystallization age of 437 ± 4 Ma, but contains abundant zircon of much greater age, probably inherited from underlying Grenvillian crust. Based on chemical composition and age similarities, the felsic porphyritic dykes in the prospect area are correlated with the Burlington Granodiorite, an early Silurian or latest Ordovician plutonic unit of the eastern Baie Verte Peninsula. D_1 deformation that affects the Catchers Pond Group volcanic and sedimentary rocks in the prospect predates Early Silurian intrusion of the felsic porphyry dykes. The timing of D_2 deformation and gold mineralization is constrained by the 437 ± 4 Ma age of intrusion for the host felsic dyke, which provides a maximum age limit for the event of gold deposition.

Chapter 6

STABLE ISOTOPE GEOCHEMISTRY

6.1 Introduction

In combination with geologic and geochemical data from hydrothermal deposits, stable isotope measurements may identify the source of ore-forming fluids, the temperature of mineral precipitation, and the physical and chemical mechanisms of ore deposition (*e.g.* Taylor, 1987). Hydrogen, carbon, and oxygen isotopic ratios in hydrothermal minerals are controlled by the temperature and isotopic composition of the fluid from which they were precipitated, or with which they reacted. In turn, the isotopic compositions of hydrothermal fluids reflect their origin, and thereby offer potential insight into the fluid source region, the mechanism of fluid transport, and the deposition of ore.

In this chapter, the results of stable isotope analyses of minerals and rocks from the Hammer Down prospect are presented and interpreted in terms of fluid events that form part of the geologic history of the prospect area. Minerals for isotopic analysis were obtained from petrographically characterized assemblages of known paragenesis.

6.2 Techniques

6.2.1 Sample preparation

6.2.1.1 Carbonate minerals

Most vein carbonate samples were sufficiently coarse grained that pure mineral separates could be obtained by direct picking of material crushed to 0.25 - 2 mm. Otherwise, carbonate-rich mineral concentrates or whole-rock samples were used. X-Ray diffraction patterns were used to identify the carbonate minerals present in samples to be analysed, and to give a semi-quantitative measure of the carbonate content of impure samples. Carbon dioxide for isotopic analysis was collected from the samples by reaction with anhydrous phosphoric acid under vacuum at a constant temperature of 25° C (McCrea, 1950).

6.2.1.2 Silicate minerals

Quartz, chlorite, and sericite (muscovite) were separated from veins and from variably altered host rocks and wallrock inclusions in veins. Quartz was obtained by hand picking of vein samples crushed to 0.1 -2 mm, and was washed with 20% HCl to remove calcite. For chlorite and mica samples, sieved fractions, with grains ranging from 0.06 to 0.5 mm, were washed in distilled water and alcohol, dried, and processed on a Frantz™ magnetic separator to yield mineral concentrates, which were

further purified by hand picking or by heavy liquid separation with bromoform. Mineral identity and purity were confirmed by X-Ray diffraction. Oxygen isotopic analysis requires mineral samples of greater than 95 % purity, so that oxygen from minor phases cannot contribute to the gas produced by sample reaction. Mineral samples were ground and reacted overnight with BrF_3 at 590 - 620°C (Clayton and Mayeda, 1963).

For hydrogen isotopic analysis, hydrous silicates were dried at 100°C for at least 20 hours in a vacuum oven, and their water extracted by heating at 1350° C using a radiofrequency generator (Suzouki and Epstein, 1976). Water was reduced to hydrogen gas for isotopic measurement by reaction with zinc metal at 460°C for 30 minutes.

6.2.1.3 Whole rock samples

A suite of variably altered felsic porphyry dyke and mafic volcanic rock samples was analyzed for oxygen isotopic composition to monitor the interaction between host rocks and ore-forming fluids. All the rock samples contained groundmass calcite that was removed with dilute HCl prior to final grinding. XRD patterns of acid washed samples and untreated whole-rock powders indicate that acid washing had no detectable effect on minerals such as chlorite; Chlorite XRD peaks for acid treated and untreated rocks were the same width and relative height.

6.2.2 Mass spectrometry

The isotopic compositions of CO_2 and H_2 gas were measured on a Finnigan Mat 252 mass spectrometer at Memorial University of Newfoundland. The isotopic results are reported in the standard δ notation in per mil (‰), relative to PDB (Pee Dee Belemnite) for carbon and V-SMOW (Vienna Standard Mean Ocean Water) for oxygen and hydrogen. NBS-28 quartz standard has a $\delta^{18}\text{O}$ value of +9.69, and NBS-19 carbonate standard has a $\delta^{13}\text{C}$ value of +1.99 and $\delta^{18}\text{O}$ value of +28.65 measured in the laboratories at Memorial University.

6.3 Results

6.3.1 Multiple vein types

Field mapping, core logging, and petrographic studies (Chapter 3 and Chapter 4) identify distinct types of veins or hydrothermal assemblages, based on their mineralogy and structure. The general classes of veins and hydrothermal assemblages described in section 4.2 are:

- I. Calcite veinlets and stringers folded by D_1 .
- II. Quartz- and sulphide-rich veins, most strongly sheared.
- III. Sulphide-poor veins that locally cut S_2 , most weakly sheared.
- IV. Calcite cement in breccia of the Lower Brittle Fault.

Carbon and oxygen isotopic compositions of carbonate minerals, and oxygen isotopic compositions of quartz from these four assemblages are recorded in Table 6.1. All carbonate samples analyzed were calcite, except ferroan dolomite from type II vein sample DR-91-103d. Carbonate isotopic compositions of the four vein types are compared in figure 6.2. The early, folded, type I veinlets exhibit a wider range of $\delta^{13}\text{C}$ values (-3.3 to -7) than other carbonate types displayed in Figure 6.1, possibly because they formed early in the geological evolution of the area and have interacted with many different fluid types since their original formation. These veinlets contain fine grained calcite and quartz with a granular texture that is similar to that of the groundmass in adjacent rocks. One sample (DR-90-57) that has the granular appearance of other early type I veinlets, but is transposed into the S_2 fabric, has the highest $\delta^{18}\text{O}$ value for veins of this group, and isotopically resembles calcite from type III veins that have a similar relationship to the S_2 foliation. The petrographic and structural character of one early, deformed calcite veinlet (sample DR-90-37) is preserved within 30 cm of a major mineralized type II vein, and this calcite sample is isotopically distinct from those of gold-bearing veins in that it has a $\delta^{18}\text{O}$ value of +10, which is lower than any measured value for calcite in type II veins.

Vein types II and III are most abundant within the main gold-bearing zones, and are of primary interest in understanding the fluid history of the Hammer Down prospect. Carbonate minerals from these two important vein types have little overlap in $\delta^{13}\text{C}$ and $\delta^{18}\text{O}$ values (Figure 6.1, Table 6.2), and the mean $\delta^{13}\text{C}$ values of calcite

Table 6.1
Isotopic Compositions of Quartz and Carbonate Minerals

Type	Sample	Description	Carbonate		Quartz
			$\delta^{13}\text{C}$	$\delta^{18}\text{O}$	$\delta^{18}\text{O}$
I	DR-90-37	Early deformed calcite vein	-5.22	9.98	
	DR-90-57	Early deformed calcite vein	-5.41	12.47	
	DR-91-126	Early deformed calcite vein	-6.95	8.16	
	DR-91-128	Groundmass calcite	-3.48	9.18	
	MV-1	Early deformed calcite vein	-3.96	9.01	
	MV-1	Early deformed calcite vein	-3.83	9.09	
	MV-3	Groundmass calcite	-5.73	9.67	
II	DR-90-07	Calcite with galena	-6.85	15.59	
	DR-90-07	Calcite with sphalerite	-6.52	14.36	
	DR-90-10	Sphalerite-rich vein with Au		11.88	12.13
	DR-90-11	Pyrite-rich vein with Au			10.96
	DR-90-53	Quartz-rich vein with Au			11.24
	DR-90-55	Sheared vein with pyrite	-6.48	13.08	
	DR-90-59	Ore-stage quartz-rich vein			11.56
	DR-91-84	Sphalerite-rich vein with Au			11.12
	DR-91-89	Telluride-bearing vein	-5.54	12.80	11.50
	DR-91-99	Quartz + pyrite in S2 fabric			10.92
	DR-91-100	Sphalerite-rich vein with Au			11.73
	DR-91-103c	Calcite-rich vein with Au	-5.68	12.57	11.62
	DR-91-103d	Fe-Dolomite with Au	-6.83	8.47	11.47
	DR-91-105	Sheared vein with pyrite	-6.43	13.42	11.66
	DR-91-107S	Sheared vein with pyrite	-6.74	12.02	

Table 6.1
(Continued)

Type	Sample	Description	Carbonate		Quartz
			$\delta^{13}\text{C}$	$\delta^{18}\text{O}$	$\delta^{18}\text{O}$
II	DR-91-108BB	Ore-stage calcite-rich vein	-6.49	14.11	11.64
	DR-91-188BL	Ore-stage calcite-rich vein	-6.32	13.40	11.23
	DR-91-133-1	Ore-stage quartz-rich vein			11.32
	DR-91-133-2	Ore-stage quartz-rich vein			10.71
	DR-91-133-3	Ore-stage quartz-rich vein			11.44
	V-4S	Quartz-pyrite vein with Au			11.09
	V-11	Rumbullion zone			11.24
III	DR-90-09	Calcite-rich with coarse mica	-6.40	13.73	11.26
	DR-90-43	Undeformed vein	-5.61	11.13	10.81
	DR-90-45	Moderate shear with fluorite	-5.22	9.51	11.29
	DR-90-78	Weakly sheared with fluorite	-4.97	11.00	
	DR-90-79	Undeformed vein with fluorite	-5.18	10.14	11.78
	DR-91-99	Calcite vein with minor pyrite	-5.15	10.47	
	DR-91-102	Undeformed vein	-5.42	9.45	11.49
	DR-91-107W	Weakly sheared with fluorite	-5.84	9.02	11.62
	V-3	Tensional quartz vein cuts S2			11.33
	V-4T	Tensional quartz vein cuts S2			12.74
	V-5	Tensional quartz vein cuts S2			11.79
IV	DR-91-117	Breccia fault veinlet	-5.07	9.05	
	DR-91-118	Fault breccia veinlet	-5.23	8.19	
	DR-90-62	White fault breccia cement	-4.19	11.79	
	DR-90-62	Pink fault breccia veinlet	-4.26	11.80	
	DR-90-64-2	Fault breccia cement	-4.53	9.69	

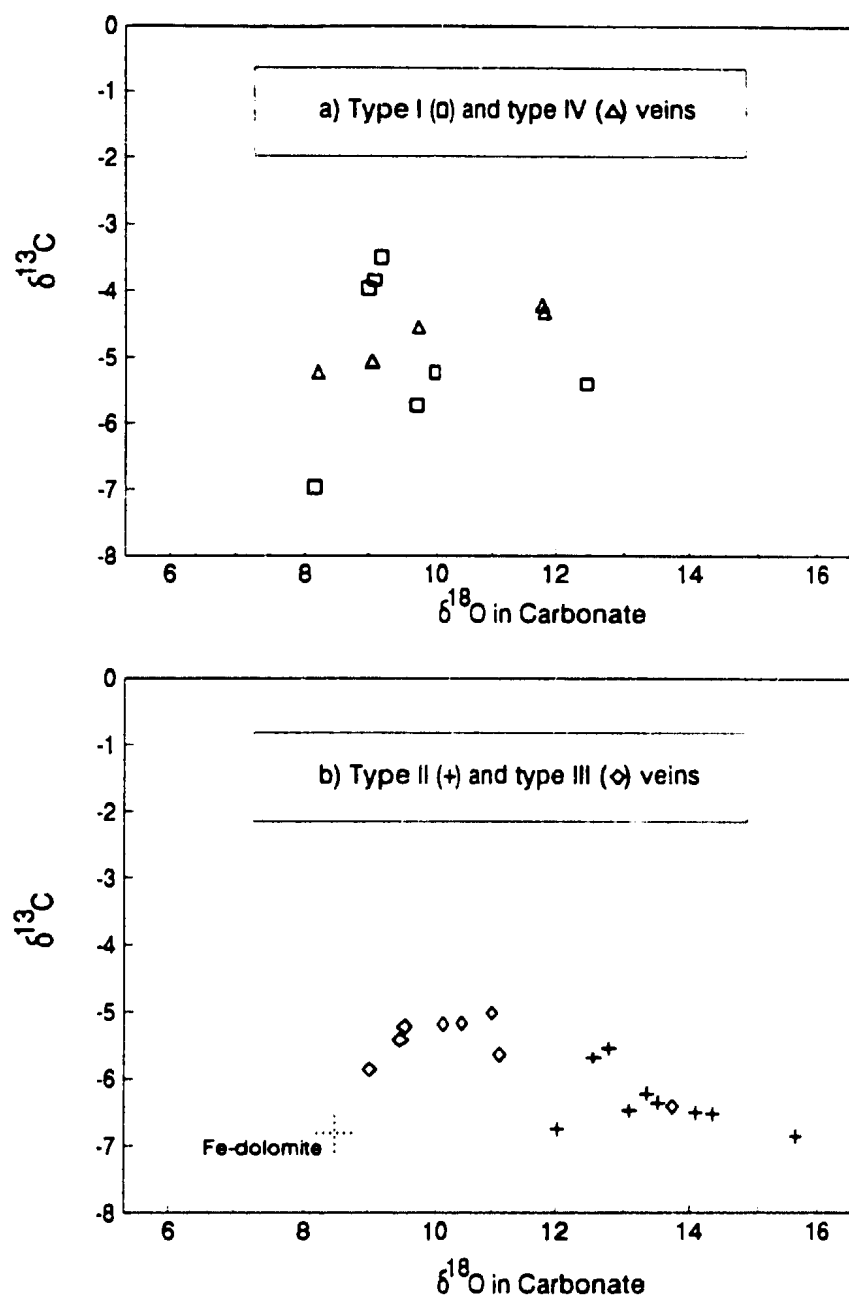


Figure 6.1 a) and b) C and O isotopic compositions of carbonate minerals from vein types I, II, III, and IV. Squares indicate calcite from type I early folded veinlets, triangles indicate calcite cement in LBF breccia (type IV), diamonds indicate type III vein calcite, small crosses indicate calcite from type II veins, and the large broken cross marks data for ferroan dolomite from type II vein sample DR-91-103.

from type II veins is significantly lower (t-test at 95% confidence level) than that of type III veins. Although O and C isotopic compositions of calcite generally discriminate type II and type III veins, quartz from the two vein groups has nearly the same range of oxygen isotopic compositions, with $\delta^{18}\text{O}$ between 10.7 to 12.7, as indicated in Table 6.2 and the histograms of Figure 6.2. Carbon isotope fractionation factors between dolomite and calcite are smaller than 1 ‰ at temperatures above 200°C (Sheppard and Schwartz, 1970), and ferroan dolomite from type II vein sample DR-91-103 has a $\delta^{13}\text{C}$ value of -6.9, which is similar to values for calcite in the same vein type, but its oxygen isotopic composition ($\delta^{18}\text{O} = 8.4$) is lighter than any other analyzed type II or type III carbonate mineral sample.

Five calcite samples from the late brittle fault breccia have $\delta^{13}\text{C}$ values consistently between -4.2 and -5.2, and have $\delta^{18}\text{O}$ values that range from 8.2 to 11.8. The carbon and oxygen isotopic compositions of calcite from the breccia samples do not overlap those from vein types II and III in Figure 6.1.

6.3.2 Oxygen isotope thermometry

The isotope fractionation factor, α , between two substances is an equilibrium constant, and as such, it varies with temperature (*e.g.* Faure, 1986). For oxygen isotope exchange between minerals A and B,

Table 6.2
Mean and Range for Quartz and Calcite Isotopic Compositions of
Type II and Type III Veins

		Calcite		Quartz
		$\delta^{13}\text{C}$	$\delta^{18}\text{O}$	$\delta^{18}\text{O}$
Type II	mean	-6.3	13.5	11.4
	range	-5.5 - -6.8	11.9 - 15.6	10.7 - 12.1
Type III	mean	-5.5	10.6	11.6
	range	-5.0 - -6.4	9.0 - 13.7	10.8 - 12.7

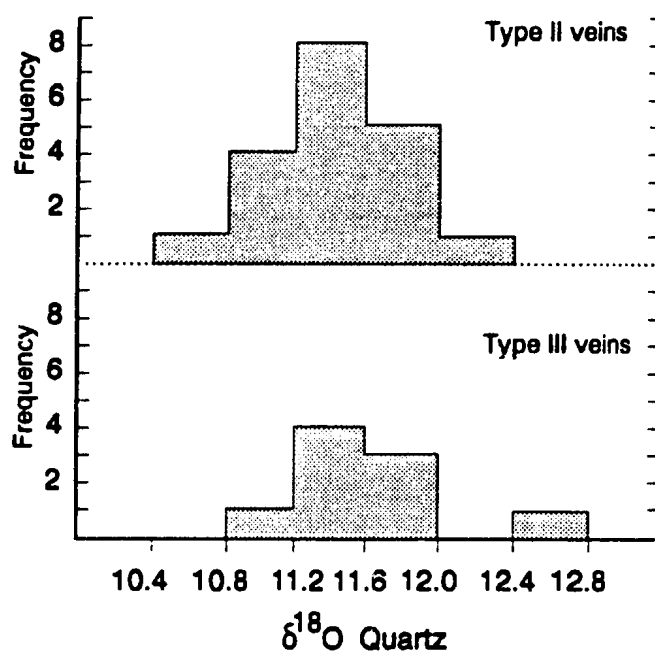


Figure 6.2 Histograms of $\delta^{18}\text{O}$ values of quartz from type II and type III veins.

$$\alpha_{A-B} = (^{18}\text{O}/^{16}\text{O})_A / (^{18}\text{O}/^{16}\text{O})_B ,$$

which can be related to the standard δ notation as

$$\alpha_{A-B} = (1000 + \delta^{18}\text{O}_A) / (1000 + \delta^{18}\text{O}_B) ,$$

or for the general case of an unspecified isotope system,

$$\alpha_{A-B} = (1000 + \delta_A) / (1000 + \delta_B) .$$

For values of α near unity, the general expression can be rewritten as

$$1000 \ln \alpha_{A-B} \approx \delta_A - \delta_B = \Delta_{A-B} .$$

Based on theoretical considerations, experimental measurement, or both, $1000 \ln \alpha$ or Δ can be calculated for mineral pairs or for mineral - water equilibria, and applied as isotopic thermometers (review in Kyser, 1987). For the majority of systems, $1000 \ln \alpha$ is an approximately linear function of T^{-2} , with T in Kelvin.

If equilibrium isotopic compositions are preserved in mineral assemblages, they can be applied to determine the temperature of mineral deposition or of re-equilibration. Isotopic fractionation ($\Delta_{\text{quartz-carbonate}}$) for quartz-calcite and quartz-ferroan

dolomite mineral pairs in type II and type III veins are listed in Table 6.3 and displayed graphically in Figure 6.3. Lines of equal temperature in Figure 6.3 are calculated from the calcite-water fractionation of O'Neill *et al.* (1969) and quartz-water fractionation of Clayton *et al.* (1972). Data points that plot to the right of the line with $\delta^{18}\text{O}_{\text{quartz}} = \delta^{18}\text{O}_{\text{calcite}}$ indicate disequilibrium in quartz-calcite mineral pairs. Strongly deformed type II veins are characterized by calcite that has isotopically heavier oxygen than the coexisting quartz, and this negative fractionation indicates that the vein minerals were not deposited in equilibrium, or did not retain equilibrium after emplacement. No type II or III calcite sample with a $\delta^{18}\text{O}$ value greater than 10.5 ‰ is in isotopic equilibrium with coexisting quartz. The majority of vein samples with negative quartz-calcite ^{18}O fractionations are deformed, and calcite in them is variably strained, recrystallized, and fractured. The enrichment of ^{18}O in calcite is interpreted to be the result of retrograde exchange of oxygen with the same fluid at lower temperatures, or with a different fluid that has a higher $\delta^{18}\text{O}$ value. Coarse undeformed calcite and quartz from the gold- and telluride-bearing type II vein (DR-91-89) and type III vein sample DR-90-43 have negative oxygen isotope fractionations, indicating that isotopic disequilibrium need not be accompanied by strong deformation. Quartz-calcite oxygen isotope thermometry yields temperatures between 206 and 330° C for four weakly deformed or unstrained type III veins (Table 6.3). Ferroan dolomite from type II vein sample DR-91-103 gives an unrealistic temperature of less than 100°C coupled with quartz, using the dolomite-water

Table 6.3
Oxygen Isotopic Fractionation Between Quartz and Carbonate Minerals
in Type II and Type III Veins, and Calculated Equilibrium Temperatures

SAMPLE	$\Delta_{\text{Quartz} - \text{Calcite}}$	Temperature, °C
Type II Veins:		
DR-91-108BL	-2.17	-
DR-91-108BB	-2.47	-
DR-91-103c	-0.95	-
DR-91-103c	-1.10	-
DR-91-103d	3.00	45
DR-91-105	-1.76	-
DR-91-89	-1.30	-
Type III Veins:		
DR-90-09	-2.47	-
DR-90-43	-0.32	-
DR-91-107w	2.60	206
DR-90-79	1.64	330
DR-90-45	1.78	306
DR-91-102	2.04	268

Temperatures are calculated with quartz-water fractionation of Clayton *et al.* (1972), calcite-water fractionation of O'Neil *et al.* (1969), and dolomite-water fractionation of Matthews and Katz (1977).

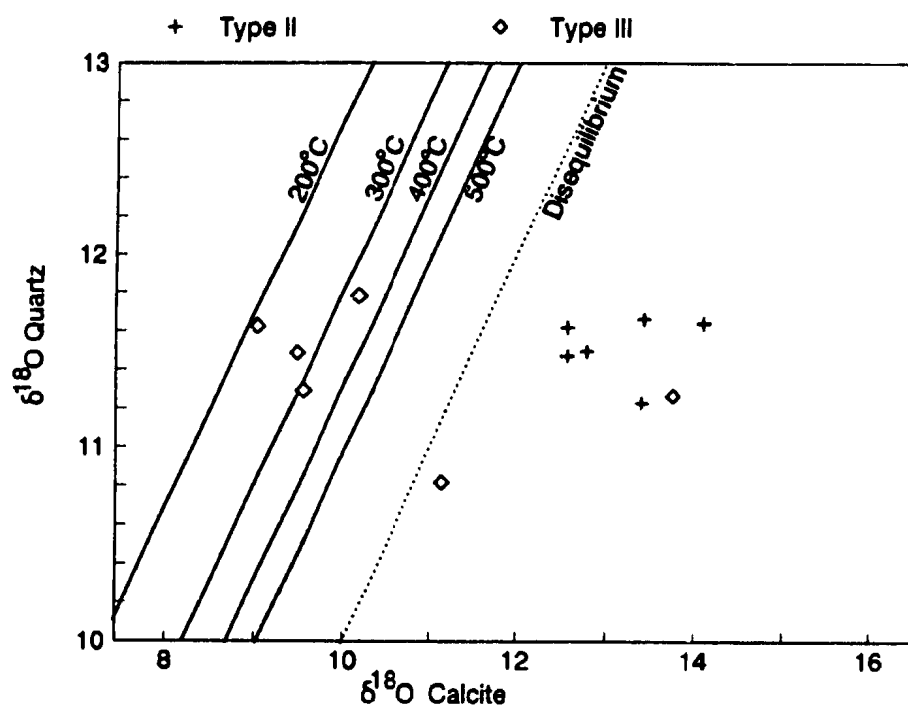


Figure 6.3 $\delta^{18}\text{O}$ values of quartz and calcite mineral pairs. Small crosses indicate data from type II veins, and diamonds are for type III veins. Oblique lines are labelled with equilibrium temperatures calculated with the fractionation factors of O'Neil *et al.* (1969) and Clayton *et al.* (1972).

fractionation of Matthews and Katz (1977), and the two carbonate minerals in this vein are not in isotopic equilibrium. This isotopic feature of dolomite is common in mesothermal gold deposits from the Abitibi Belt (Kerrick, 1987). The ^{18}O depletion in ferroan dolomite and enrichment in calcite implies isotopic perturbation by the multiple processes of isotopic exchange with fluids having low $\delta^{18}\text{O}$ values, and exchange at low temperatures or with fluids enriched in ^{18}O .

Quartz and other silicate minerals are far more resistant than carbonates to isotopic resetting, and are likely therefore to retain their original isotopic ratios. The isotopic compositions of quartz-chlorite and quartz-muscovite mineral pairs from the Hammer Down gold prospect and their calculated equilibrium temperatures are listed in Table 6.4. Several of the samples that contain quartz with chlorite or quartz with muscovite also have calcite or ferroan dolomite temperatures reported in Table 6.3. In general, the measured ^{18}O fractionations between quartz and chlorite in type II samples listed in Table 6.5 should yield more reliable temperatures than the quartz-muscovite fractionations, because the fine grained muscovite (sericite) in these two samples is contaminated with several to 20 per cent albite, as revealed by XRD patterns. The equilibrium quartz-albite ^{18}O fractionation between 250 and 300°C is approximately 2 ‰ (Clayton *et al.*, 1972; Matsuhisa *et al.*, 1979), so albite in these samples will have $\delta^{18}\text{O}$ values approximately between 9 and 9.5 ‰, and the $\delta^{18}\text{O}$ values, Δ values, and equilibrium temperatures for these two samples are recalculated for 15% contamination by albite with a $\delta^{18}\text{O}$ value of 9.0 for DR-91-99, and 9.5 for

Table 6.4
Calculated Temperatures from $\delta^{18}\text{O}$ Values of Coexisting Quartz, Chlorite, and Muscovite

SAMPLE		$\delta^{18}\text{O}$	$\Delta_{\text{Quartz-mineral}}$	Temperature, °C
Type II veins and assemblages:				
DR-91-99	Quartz	10.92		
	Chlorite	4.5	6.42	323
	Muscovite	5.81 (6.29)	5.11 (4.64)	193 (218)
DR-91-103	Quartz	11.54*		
	Chlorite ¹	3.78	7.76	257
	Chlorite ²	4.21	7.33	276
	Muscovite ³	7.18 (7.53)	4.36 (4.01)	236 (261)
	Muscovite ⁴	8.17 (8.37)	3.37 (3.17)	317 (339)
Type III veins:				
DR-90-09	Quartz	11.26		
	Muscovite	7.08	4.25	243
DR-90-45	Quartz	11.29		
	Muscovite	7.53	3.76	281

Notes: Temperatures are calculated with quartz-water fractionation of Clayton *et al.* (1972), chlorite-water fractionation of Wenner and Taylor (1971), and muscovite-water fractionation of O'Neil and Taylor (1969). For muscovite in type II veins and assemblages, $\delta^{18}\text{O}$ values, Δ values, and temperatures are corrected for 15% by weight albite content in the analyzed samples, as discussed in the text, and uncorrected values are given in parentheses.

* = mean of two analyses

¹ +80 mesh grains, mostly +60

² -60 +100 mesh grains

³ -80 +100 mesh grains

⁴ -100 +120 mesh grains

DR-91-103. Type II samples DR-91-99 (schistose felsic porphyry dyke) and DR-91-103 (gold-rich quartz vein) yield quartz-chlorite temperatures between 257°C and 323°C, whereas quartz-muscovite temperatures for type III vein samples DR-90-09 and DR-90-45 range from 237 to 281°C. Given the uncertainties in extrapolating the muscovite-water ^{18}O fractionation of O'Neil *et al.* (1969) below 400°C, there is no strong evidence for a substantial difference in the temperature of formation of type II and type III veins. The uncorrected quartz-muscovite temperatures calculated for samples DR-91-99 and DR-91-103 are best regarded as maximum temperatures, because the reported $\delta^{18}\text{O}$ values for sericite may be excessively high owing to the presence of isotopically heavy impurities. Muscovite in sample DR-91-99 yields a temperature in combination with quartz that is anomalously low compared to the rest of the thermometry dataset, and the quartz-chlorite mineral pair in this sample gives a temperature of 323°C, which is 50 to 70° higher than quartz-chlorite temperatures calculated for type II vein DR-91-103. Isotopic disequilibrium in DR-91-99 can be partly explained if muscovite has exchanged oxygen to attain a lower value of $\delta^{18}\text{O}$. An alternative interpretation to reconcile the isotopic decoupling of chlorite and sericite is that chlorite has undergone retrograde exchange at a low temperature, leading to a higher value of $\delta^{18}\text{O}$ and a higher calculated temperature of equilibrium with quartz, whereas sericite has retained its isotopic composition. Sample DR-91-99 contains veinlets with quartz, calcite, and pyrite, but the main hydrothermal minerals in the rock are abundant sericite and chlorite aligned with pyrite in a strongly

developed planar S_2 fabric in a high strain zone 3 metres from any large type II vein. At the time of fluid influx and emplacement of type II veins, temperature gradients away from veins may have been sufficient to precipitate hydrothermal minerals in the schistose dyke at temperatures substantially below the 243 to 323°C range calculated for vein minerals.

6.3.3 Isotopic source tracers

A fundamental part of any genetic model for ore deposition is an understanding of fluid origins in hydrothermal mineral deposits (*e.g.* Taylor, 1974; Taylor, 1987). Some reservoirs that contribute O, H, and C to an ore-forming system may have diagnostic isotopic signatures that uniquely identify specific sources, but overlapping reservoirs, mixing, unmixing, disequilibrium, and retrograde processes are among the effects that can produce complex isotopic records with non-unique interpretations in ore deposits.

If CO_2 was the only carbon-bearing species in the ore-forming fluid, equilibrium values of $\delta^{13}C$ calculated for the fluid at temperatures between 200°C and 350°C would be about 1 ‰ different than those measured in calcite or ferroan dolomite (Kyser, 1987; Kerrich, 1989b). The carbon isotopic composition of precipitated carbonate is affected by Eh, pH, and the concentration of total dissolved carbon in solution, so that isotopic compositions of total carbon in solution are not

directly determined from $\delta^{13}\text{C}$ values of carbonate minerals alone (Colvine *et al.*, 1988; Kerrich, 1989b). Carbon and oxygen isotopic compositions from all type I, II, III, and IV carbonate samples fall within the range of data from mesothermal gold deposits of the Abitibi Greenstone Belt, for which $\delta^{18}\text{O}$ values of calcite and ferroan dolomite are between 8 to 16 ‰ and $\delta^{13}\text{C}$ values vary from -1.5 to -9 (Kerrich, 1987; 1990). Carbonate minerals in veins and hydrothermally altered rocks of the Hammer Down prospect are inferred to have formed from fluids with $\delta^{13}\text{C}$ values between -4 and -8 ‰, which is not diagnostic of fluids uniquely derived from either metamorphic or igneous sources, and is close to the $\delta^{13}\text{C}$ value of -5.5 ‰ reported by Ohmoto and Rye (1979) for the isotopic composition of average crustal carbon. The $\delta^{13}\text{C}$ values of fluids for type II and III veins are consistent with derivation from large-scale "average" crustal reservoirs (Kerrich, 1989b). Based in part on the presence of carbonate minerals with $\delta^{13}\text{C}$ values near igneous values of -6 ‰, various workers have developed genetic models for Archean mesothermal lode gold deposits that involve CO_2 influx from the mantle, or orthomagmatic derivation of CO_2 -bearing fluids, as reviewed by Kerrich (1989a; 1989b).

Marine carbonate is an isotopically uniform reservoir of carbon, with $\delta^{13}\text{C}$ values between -2 and 0, and carbonate minerals of marine origin developed by seafloor alteration have values of $\delta^{13}\text{C}$ in a narrow range near 0‰ (Muehlenbachs, 1987). Carbonates of this type have $\delta^{18}\text{O}$ values above +20, reflecting their low temperature of formation (Muehlenbachs, 1987), and are isotopically distinct from

calcite and ferroan dolomite in the Hammer Down prospect. Atmospheric CO_2 has a $\delta^{13}\text{C}$ value near -7 (Taylor, 1987), and aqueous carbonate can be calculated to have $\delta^{13}\text{C}$ values 4 to 10 ‰ higher than the gaseous CO_2 with which it is in equilibrium at surficial temperatures (Kyser, 1987, and references therein). Dissolved carbonate of atmospheric origin would therefore have $\delta^{13}\text{C}$ values of -3 ‰ or higher, generally similar to the composition of marine carbonate. Carbon derived from meteoric or marine reservoirs is expected to be isotopically heavier than the carbon in calcite or ferroan dolomite from the Hammer Down prospect.

A variety of metamorphic processes can produce CO_2 -bearing fluids with isotopically light or heavy carbon (*e.g.* Ohmoto, 1986). Decarbonation reactions during prograde metamorphism produce CO_2 that has $\delta^{13}\text{C}$ and $\delta^{18}\text{O}$ values that are higher than the starting carbonate material, so that metamorphism of marine carbonate rocks ($\delta^{13}\text{C} \approx 0$) would yield positive $\delta^{13}\text{C}$ values in fluids derived from them. Isotopically light fluids, with values of $\delta^{13}\text{C}$ below -10 can be produced by hydrolysis and oxidation of organic carbon (Ohmoto, 1986; Colvine *et al.*, 1988; Kerrich, 1989b).

Table 6.5 lists the O and H isotopic compositions of aqueous fluids in equilibrium with quartz, chlorite, and muscovite at temperatures selected from Table 6.4. Fluid δD values were calculated from the fractionations for chlorite and muscovite empirically derived by Taylor (1974). For hydrothermal assemblages in altered wall-rock samples DR-90-54, DR-90-65, and DR-91-94, there is no direct

Table 6.5
O and H Isotopic Composition of Fluids in Equilibrium with Hydrothermal
Assemblages

SAMPLE	Hydrous Mineral	$\delta D_{\text{Mineral}}$	$\delta^{18}O_{\text{Quartz}}$	Temperature, °C	$\delta^{18}O_{\text{fluid}}$	δD_{fluid}
Type II veins and assemblages:						
DR-90-54	muscovite	-72.2	10.7-12.1	260 - 300	2.20-5.20	-36.8 - -39.9
DR-90-65	muscovite	-74.0	10.7-12.1	260 - 300	2.20-5.20	-38.6 - -41.7
DR-90-94	muscovite	-63.8	10.7-12.1	260 - 300	2.20-5.20	-28.4 - -31.5
DR-91-99	chlorite	-71.0	10.92	300	4.03	-27.0
DR-91-99	muscovite	-64.1	10.92	300	4.03	-31.8
DR-91-103	chlorite	-79.5	11.54	265	2.99	-33.1
Type III veins:						
DR-90-09	muscovite	-64.8	11.26	245	1.82	-27.6
DR-90-45	muscovite	-68.6	11.29	278	3.56	-34.7

Notes: Fluid compositions calculated with quartz-water ^{18}O fractionation factors of Clayton *et al.* (1972) and H isotope fractionation curves of Taylor (1974) for muscovite-water and chlorite-water.

evidence for the temperature of formation, and a possible range of fluid compositions in equilibrium with these samples has been calculated for the temperatures and $\delta^{18}\text{O}_{\text{quartz}}$ values of type II assemblages. The calculated water compositions are compared to major fluid reservoirs in Figure 6.4. There is a close similarity in the H and O isotopic compositions of hydrothermal fluids in type II and type III veins. Compositions of hydrothermal fluids for the Hammer Down prospect show incomplete overlap with the field for metamorphic water, and imply a component with lower values of $\delta^{18}\text{O}$, possibly meteoric water or seawater. Mixed fluids from the four principal reservoirs identified in Figure 6.4 could produce the calculated compositions for veins and hydrothermal assemblages in the Hammer Down prospect.

6.3.4 Process of mineral deposition and fluid evolution

Quartz isotopic compositions in type II and type III veins are very similar, and the two vein sets formed at similar temperatures. The average $\delta^{13}\text{C}$ value of carbonate minerals in type II veins is, however, nearly 1 ‰ lower than that of type III veins (Table 6.1; Figure 6.1). If calcite and ferroan dolomite have retained their original carbon isotopic ratios, vein carbonates became, on average, enriched in ^{13}C in progression from the gold-bearing type II veins to the paragenetically later type III veins. At different temperatures, carbon-bearing fluids of the same isotopic composition will be in equilibrium with carbonate minerals that are distinct principally

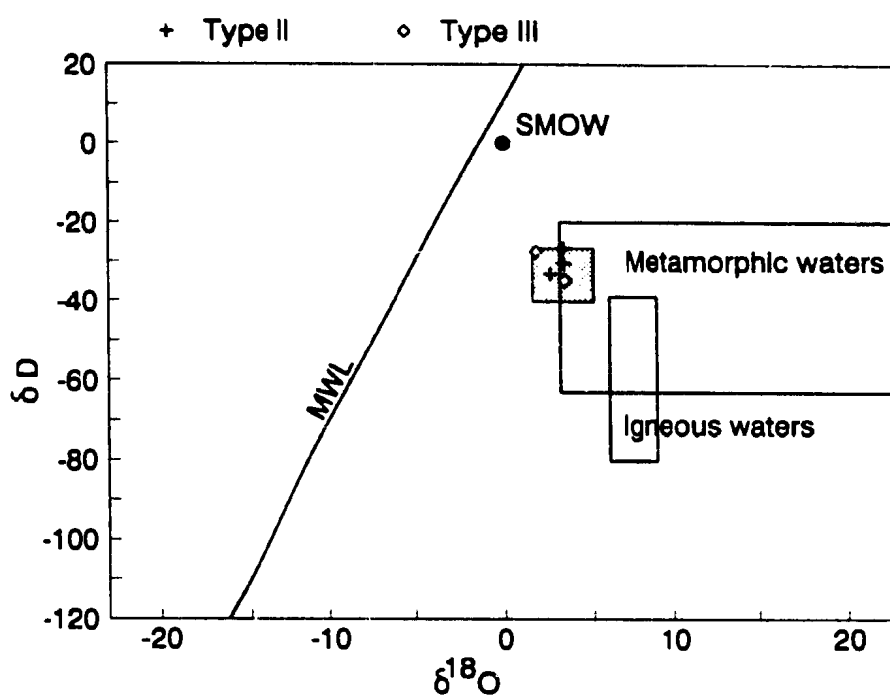


Figure 6.4 Calculated δD and $\delta^{18}O$ values of hydrothermal fluids in type II (crosses) and type III (diamonds) veins, with data from Table 6.4. For reference, compositional fields of metamorphic and primary igneous waters (Taylor, 1974), standard mean ocean water (SMOW), and the meteoric water line (MWL) are shown.

in their ^{18}O content, whereas different $\delta^{13}\text{C}$ values, as noted for type II and type III veins, arise mainly from isotopic characteristics of hydrothermal fluids. In Figure 6.5, the calculated oxygen isotopic compositions of carbonate minerals in equilibrium with their coexisting quartz at 250°C are presented, in order to display a possible evolutionary trend. For samples without quartz, $\delta^{18}\text{O}$ values of calcite in equilibrium with the full range of quartz isotopic compositions for the appropriate vein type listed in Table 6.1, with a temperature range from 200 to 300°C , were employed to construct labelled compositional fields. Fields for type II and type III veins have similar $\delta^{18}\text{O}$ values, and show considerable overlap, but an evolutionary trend is evident from type II to type III, and can be projected toward the compositions for calcite from late type IV veinlets and breccia cement (values not recalculated), which are the youngest hydrothermal assemblages in the prospect.

6.3.5 Whole rock oxygen isotopic variations

Whole rock $\delta^{18}\text{O}$ values of mafic rocks from the prospect area $+6.8$ and $+8.3$, for strongly epidote altered pillow basalt (sample DR-90-28) and weakly altered pillow basalt or andesite with abundant albite and chlorite (sample DR-91-220), respectively (Table 6.6). $\delta^{18}\text{O}$ values for fresh basalt from mid-ocean ridges occupy a narrow range between 5.5 and 5.9 ‰ (Taylor, 1968; Muchlenbachs, 1986), and most mafic volcanic arc rocks that were erupted without major influence of

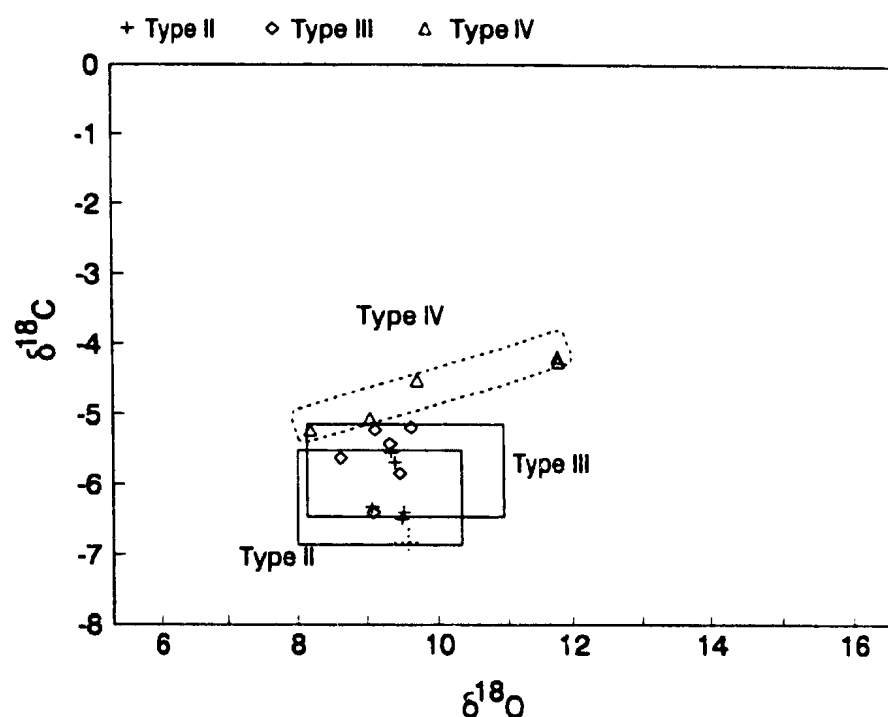


Figure 6.5 C and O isotopic compositions of carbonate minerals from vein types I and II, recalculated to isotopic equilibrium with coexisting quartz, and for calcite in type IV veins. Diamonds indicate type III vein calcite, small crosses indicate calcite from type II veins, triangles indicate calcite cement in LBF breccia (type IV), and the large broken cross marks data for ferroan dolomite. Rectangular compositional fields for type II and type III calcite were determined as outlined in the text.

continental crust have $\delta^{18}\text{O}$ values between 5.5 and 6.5 ‰ (Stern and Ito, 1983; Taylor 1986; Taylor and Sheppard, 1986). The ^{18}O enrichment of mafic volcanic rocks from the Hammer Down prospect is similar in degree to that in hydrothermally altered seafloor basalt that has exchanged oxygen extensively with ocean water at temperatures below 150°C (Muehlenbachs, 1986; 1987).

Five variably altered felsic porphyry dykes from the prospect area listed in Table 6.6 have $\delta^{18}\text{O}$ values between +8.1 and +9.4‰, with a mean of +8.9‰. There is no strong correlation between isotopic composition and the degree of deformation or hydrothermal alteration and recrystallization, but the highest $\delta^{18}\text{O}$ value is for the freshest dyke (sample D-3), collected more than 20 m from any major mineralized zone, and the lowest value is from a strongly altered and recrystallized dyke (sample DR-90-14). Intermediate values were obtained for some altered and sheared dykes and for relatively fresh samples. The lack of a continuous trend in ^{18}O content with progressive alteration and deformation is attributed to the generally small but variable degree of interaction between type II vein fluids and host rocks, and to the competing alteration trends of silicification, which adds isotopically heavier quartz to the rocks, and of sericite alteration, which adds isotopically lighter material. The normal range of $\delta^{18}\text{O}$ values for granitic magmas extends from 6 to near 15, depending largely on source characteristics (Taylor, 1980; Taylor and Sheppard, 1986), but the observed isotopic characteristics of felsic dykes from the Hammer

Table 6.6
Oxygen Isotopic Composition of Whole Rock Samples

Sample	Description	$\delta^{18}\text{O}$
DR-90-28	Epidote altered pillow basalt	6.79
DR-91-220	Albite altered pillow basalt	8.31
D-3	Fresh felsic dyke	9.44
DR-90-48	Slightly altered felsic dyke	8.97
D-1	Moderately altered felsic dyke	9.74
DR-90-17	Moderately altered felsic dyke	8.58
DR-90-14	Strongly altered felsic dyke	8.06
DR-90-38	Strongly altered felsic dyke	9.05

Down prospect could also be produced by extensive exchange of oxygen with aqueous fluids under conditions of low-grade metamorphism

6.4 Summary

Calcite and ferroan dolomite from type I, II, III, and IV veins and hydrothermal assemblages have carbon and oxygen isotopic compositions that are compatible with deposition from hydrothermal fluids of crustal origin, without any major addition from marine or other sources. With a single exception, vein types II and III are separable on the basis of oxygen isotopic composition of calcite, but quartz and calcite in all analyzed mineral pairs from the type II veins are not in equilibrium, and the $\delta^{18}\text{O}$ values of calcite in these veins (and some type II samples) probably do not reflect their original hydrothermal compositions.

Gold-bearing type II veins, and type III veins that were emplaced during or after the main stage of gold deposition in the Hammer Down prospect formed at temperatures between 240°C and 320°C, which are consistent with temperatures in the general class of mesothermal gold deposits as compiled by Kerich (1989b). The calculated oxygen and hydrogen isotopic compositions of vein-forming fluids are similar for the two vein sets, and have $\delta^{18}\text{O}$ values between 2.2 and 4.0, and δD values between -27 and -42. The isotopic composition of fluids allow possible contributions from metamorphic, meteoric, magmatic, or marine water sources.

Chapter 7

DISCUSSION AND MODEL FOR GOLD MINERALIZATION

7.1 Synthesis of geological and geochemical data

7.1.1 Geologic and tectonic setting of gold deposition

Mineralized zones within the Hammer Down gold prospect and associated showings are hosted by a predominantly mafic volcanic and sedimentary sequence of the Ordovician Catchers Pond Group. Volcanic activity in the Catcher's Pond Group and other arc sequences within the Dunnage Zone records the destruction of oceanic crust and the closing of Iapetus. Cambrian and Ordovician arc terranes and ophiolite suites were accreted to the North American continent during the Taconian Orogeny, and subsequent development of the Appalachian Orogen involved regional deformation, metamorphism, and extensive igneous activity (Chapter 2; Dunning *et al.*, 1990). The $480 \pm 4/-3$ Ma U-Pb zircon age determined for felsic tuff in the Hammer Down prospect is in agreement with the previously reported Arenig paleontological age of the Catcher's Pond Group, and is compatible with other Early to Middle Ordovician ages for volcanic activity in arc sequences and ophiolitic rocks throughout the Notre Dame Subzone (Dunning and Krogh, 1985; Swinden *et al.*, 1988). Outside of narrow highly deformed and altered zones, the host volcanic and sedimentary sequence contains low grade metamorphic minerals similar to the assemblages developed throughout the Springdale Peninsula (Kean, 1988; Kean and

Evans, 1990). The degree of metamorphism in the vicinity of the Hammer Down prospect is broadly comparable to that developed in other oceanic terranes of the region.

Felsic porphyry dykes are characteristic features of the Hammer Down prospect, and are the immediate hosts to many of the largest and richest gold-bearing veins. After an early phase of deformation that predated felsic dyke intrusion (D_1 of Dubé *et al.*, 1992), the main ore zones were formed contemporaneously with a brittle-ductile D_2 fabric related to folding (Dubé *et al.*, 1992). The igneous crystallization age of 437 ± 4 Ma for zircon from a felsic porphyry dyke that hosts gold in the Hammer Down prospect overlaps with early Silurian U-Pb ages of the Burlington Granodiorite and the Cape Brulé porphyry from the eastern Baie Verte Peninsula, and with the emplacement age of the Rainy Lake Complex 50 km to the southwest (Chapter 5). Correlation of felsic porphyry dykes in the gold prospect with the Burlington Granodiorite (Chapters 3 and 5) provides a direct geologic link across the Green Bay fault, and forms a basis for incorporation of the tectonic and geologic development of the King's Point area into that of the Baie Verte Peninsula.

Radiometric ages presented in Figure 7.1 identify a major phase of igneous activity both in the deformed and metamorphosed continental margin (Humber Zone) west of the Baie Verte-Brompton Line, and in the accreted terranes to the east (Dunnage Zone). Voluminous Silurian magmatism in the eastern Baie Verte and Springdale areas was accompanied by caldera development, cauldron subsidence, and

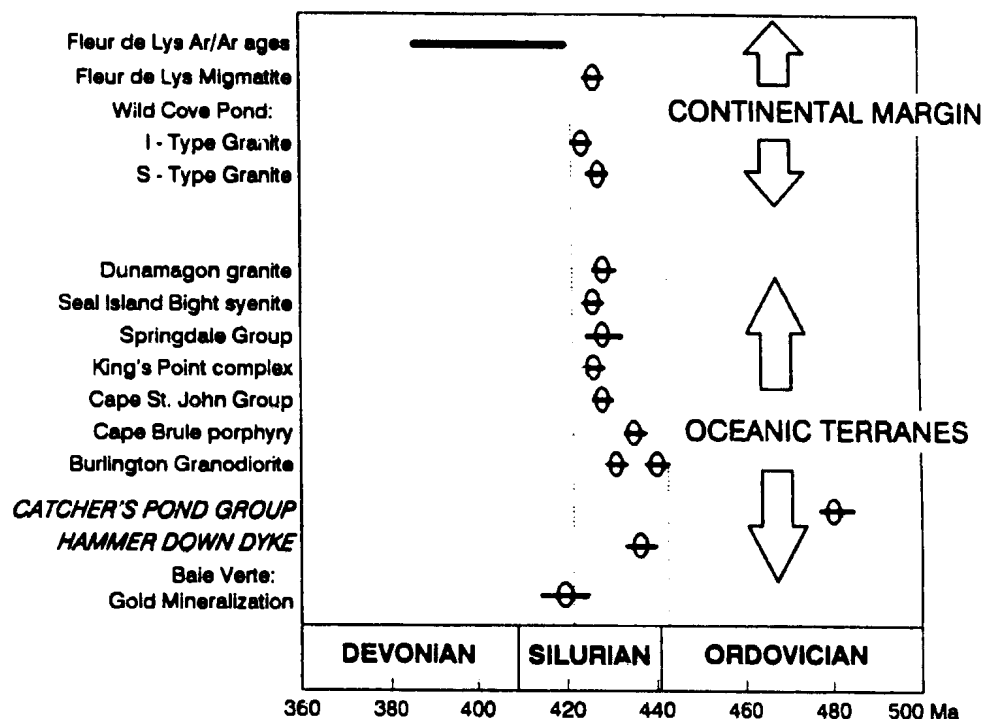


Figure 7.1 Compilation of radiometric ages from the Baie Verte-King's Point region. Catcher's Pond Group and Hammer Down dyke ages are from this study, other sources are as in Table 5.2, except Ar/Ar Fleur de Lys data (Dallmeyer, 1977); Fleur de Lys, Wild Cove Pond, Dunamagon, and Seal Island Bight ages (G.R. Dunning and P.A. Cawood, unpublished data); Cape St. John data (Coyle, 1990); and Baie Verte gold mineralization age (Ramezani, 1993). Vertical dashed lines mark limits of igneous ages.

movement along regional faults (Coyle and Strong, 1986). The age compilation of Figure 7.1 also incorporates a U-Pb monazite age of 427 ± 2 Ma (Early-Middle Silurian) for peak metamorphic conditions (formation of migmatite) in the Fleur de Lys Supergroup (G.R. Dunning and P.A. Cawood, unpublished data), and $^{40}\text{Ar}/^{39}\text{Ar}$ cooling ages from hornblende and biotite that are consistent with a late Ordovician or Silurian metamorphic peak (Dallmeyer, 1977; Hibbard, 1983; Jamieson, 1987). $^{40}\text{Ar}/^{39}\text{Ar}$ ages of biotite from some portions of the northern Baie Verte Peninsula extend to approximately 345 Ma (Hibbard, 1983). Metamorphism associated with orogenesis along the Humber-Dunnage boundary zone included the generation of eclogite under high pressure and low temperature conditions produced by thrust faulting and crustal thickening (Jamieson, 1990). Many structural and stratigraphic features of the Baie Verte Peninsula, and the preservation and exhumation of eclogite, are explained by a major episode of Silurian crustal uplift and extension after the compressional stage of orogenesis (Jamieson, 1993).

Zircon from a felsic porphyry dyke in the Hammer Down prospect has a high degree of Proterozoic inheritance, with $^{207}\text{Pb}/^{206}\text{Pb}$ ages as old as 960 Ma (Chapter 5; Table 5.1). Inheritance is interpreted to reflect the presence of a significant Proterozoic crustal component, probably of Grenvillian age, in the magma source region for the dykes. By the time of felsic dyke intrusion in the Early Silurian, the host volcanic sequences of the Hammer Down prospect (and probably other oceanic terranes as well) must have been emplaced over Grenville continental basement,

which is interpreted from seismic data to extend, at present, far to the east of the prospect area (Keen *et al.*, 1986). The overall geologic environment of gold mineralization therefore contains continental elements, in addition to the oceanic host terranes.

The total range of Silurian igneous (and migmatite) ages from the Baie Verte Peninsula extends from 442 Ma to 420 Ma, and encompasses the $^{207}\text{Pb}/^{206}\text{Pb}$ felsic porphyry dyke age (Figure 7.1). The crystallization age ($480 \pm 4\text{--}3$ Ma) of volcanic rocks in the Catchers Pond Group at Hammer Down is approximately 50 Ma older than the U-Pb zircon ages for major felsic plutonic and volcanic units on the Baie Verte Peninsula. Mesothermal gold mineralization at the Stog'er Tight prospect in the Point Rousse ophiolite complex near the town of Baie Verte is directly dated by a 420 ± 5 Ma U-Pb age from hydrothermal zircon (Ramezani, 1993), which is also included in Figure 7.1. Although uncertainty of the age for gold deposition at Stog'er Tight overlaps ages of several igneous units, it is consistent with the generalized model of mesothermal gold mineralization after peak metamorphic conditions were attained. Gold mineralization in the Hammer Down prospect postdates the intrusion of felsic porphyry dykes, and may therefore have been coeval with the widespread Silurian igneous activity.

Fluorite-bearing veins (type III) are the same age or younger than gold-bearing veins, and their age thereby constrains the time of gold deposition. If the presence of fluorite in veins is attributed to hydrothermal fluids of magmatic origin

associated with the nearby King's Point volcanic-plutonic complex, then the age of gold deposition should be close to the 427 ± 2 Ma igneous age reported by Coyle (1990) for the complex. This younger age limit is, however, speculative. Based on a tentative correlation of dykes in the Hammer Down prospect to the King's Point complex, Andrews and Huard (1991) developed a model of fluid flow and gold mineralization temporally and genetically linked to magmatism in the complex. Magmatic fluid sources older than 437 Ma are ruled out as possible contributors, because type II (gold-bearing) and type III veins postdate the intrusion of felsic porphyry dykes. Displacement along the Green Bay fault, which may have been genetically related to gold mineralization in a regional context as part of the Silurian crustal movements, extends in time into the Carboniferous or younger periods (Hibbard, 1983). Directly within the Hammer Down prospect, at least one phase of deformation (D_3 of Dubé *et al.*, 1992) postdates gold mineralization, and the main zone of gold-bearing veins is apparently truncated by the lower brittle fault.

7.1.2 Origin of hydrothermal fluids

Accretionary belts that contain mesothermal gold deposits have complex hydrologic regimes that allow the possible interaction of diverse fluids. The isotopic compositions of ore-forming solutions in many of these deposits are compatible with fluid derivation from metamorphic and igneous sources, linked ultimately to prograde

metamorphism and melt generation in thickened crust (review in Kerrich, 1989b). Contributions from meteoric water in some deposits, or a predominantly meteoric source have been proposed by various workers (e.g. Nesbitt 1988; Koons and Craw, 1991).

Vein-forming fluids in the Hammer Down prospect had $\delta^{18}\text{O}$ values between 2.2 and 5.2 ‰ (Chapter 6), and are interpreted to reflect a meteoric component in addition to water from igneous or metamorphic sources. Only a portion of the total fluid budget is likely to be of meteoric derivation, because the calculated $\delta^{18}\text{O}$ values of fluids differ from those of typical Archean mesothermal gold mineralizing solutions by only 2 or 3 ‰, and they do not extend to negative values typical of most meteoric fluids. The vein-forming system probably contained a large proportion of water from igneous or metamorphic reservoirs. The field of metamorphic fluids in Figure 6.4 is not well defined, and if extended to slightly lighter isotopic compositions, it would encompass the calculated range of the Hammer Down prospect.

Mechanisms for changing the isotopic composition of a fluid include physical and chemical processes such as water-rock interaction and phase changes (e.g. boiling), or mixing with fluids of different isotopic compositions from other sources. Low-latitude or coastal meteoric water with values of δD near -30 could attain the fluid compositions calculated for the Hammer Down prospect by enrichment in ^{18}O by about 8 ‰ during interaction with crustal rocks. Metamorphic fluids that originally had $\delta^{18}\text{O}$ values higher than 4 ‰ could become depleted in ^{18}O by CO_2 immiscibility

(Kerrick, 1987), and approach the calculated compositions for Hammer Down. Below 300° C, the fractionation of ^{18}O between CO_2 (g) and H_2O (l) exceeds 13 ‰ (Brenninkmeijer *et al.*, 1983), so that separation of 10 to 20 mole % of CO_2 could lower the $\delta^{18}\text{O}$ value of the residual liquid by at least 2 ‰. Reaction of water with graphite to produce CO_2 and CH_4 is an additional process that reduces the ^{18}O content of metamorphic water, again because of the strong ^{18}O fractionation. Under closed system conditions at 300° C, conversion of 15% of the original water mass to CO_2 decreases the $\delta^{18}\text{O}$ value of the residual water by 2 ‰ (Lynch *et al.*, 1990). Because many mesothermal gold deposits have structural styles, geologic settings, and mineral assemblages similar to those in the Hammer Down prospect, the lower $\delta^{18}\text{O}$ values of fluids are probably not related to processes such as CO_2 immiscibility or reaction with graphite that do not generally operate in mesothermal systems. The preferred mechanism to produce the lower than typical $\delta^{18}\text{O}$ values of fluids is mixing of fluids from different reservoirs, including a meteoric source. The calculated isotopic compositions of fluids in the Hammer Down prospect are consistent with those generated primarily by metamorphic processes, with a contribution from meteoric water or ^{18}O -shifted meteoric water. Some input of fluids from igneous sources is not ruled out by the isotopic data. Possible ^{18}O -shifting of a meteoric component is masked by the interpreted larger proportion of metamorphic fluids.

A collisional or transpressive geodynamic regime contains many potential reservoirs that might contribute to fluid flow (Kyser and Kerrich, 1990). Fluid

sources shown schematically in Figure 7.2 include metamorphic fluids from diverse crustal rocks [sources (2) and (3)], magmatic volatiles [(6)], and meteoric water percolating through fractured rocks [(7)]. These are the 3 principal reservoirs most likely to have contributed to vein-forming fluids in the Hammer Down prospect. Circulation of meteoric water is promoted by topographic effects in mountain ranges (*e.g.* Kyser and Kerrich, 1990; Koons and Craw, 1991; Nesbitt, 1992), and flow of meteoric water downward to the brittle-ductile transition in orogenic belts has been proposed as an ore-forming mechanism for mesothermal gold deposits in British Columbia and New Zealand (Nesbitt, 1988; 1992; Koons and Craw 1991).

In an extensional crustal regime or metamorphic core complex, illustrated schematically in Figure 7.3, meteoric water infiltrates brittle faults, and may mix with metamorphic fluids advected along detachment faults (Kyser and Kerrich, 1990). The zone of mixing between fluids of meteoric origin and metamorphic or mantle-derived fluids [types (2) and (3) or (2) and (6) in Figure 7.3] is specifically cited as an area of mineralization in detachment faults (*e.g.* Spencer and Welty, 1986; Beaudoin *et al.*, 1991). Base- and precious-metal mineral deposits associated with circulation of surface-derived water in extensional detachment faults are characterized by oxidized mineral assemblages (*e.g.* Spencer and Welty, 1986; Roddy *et al.*, 1988), unlike those in the Hammer Down prospect. High level igneous intrusions in these extensional settings also contribute to the total fluid budget, and the heat flow associated with them may promote fluid movement.

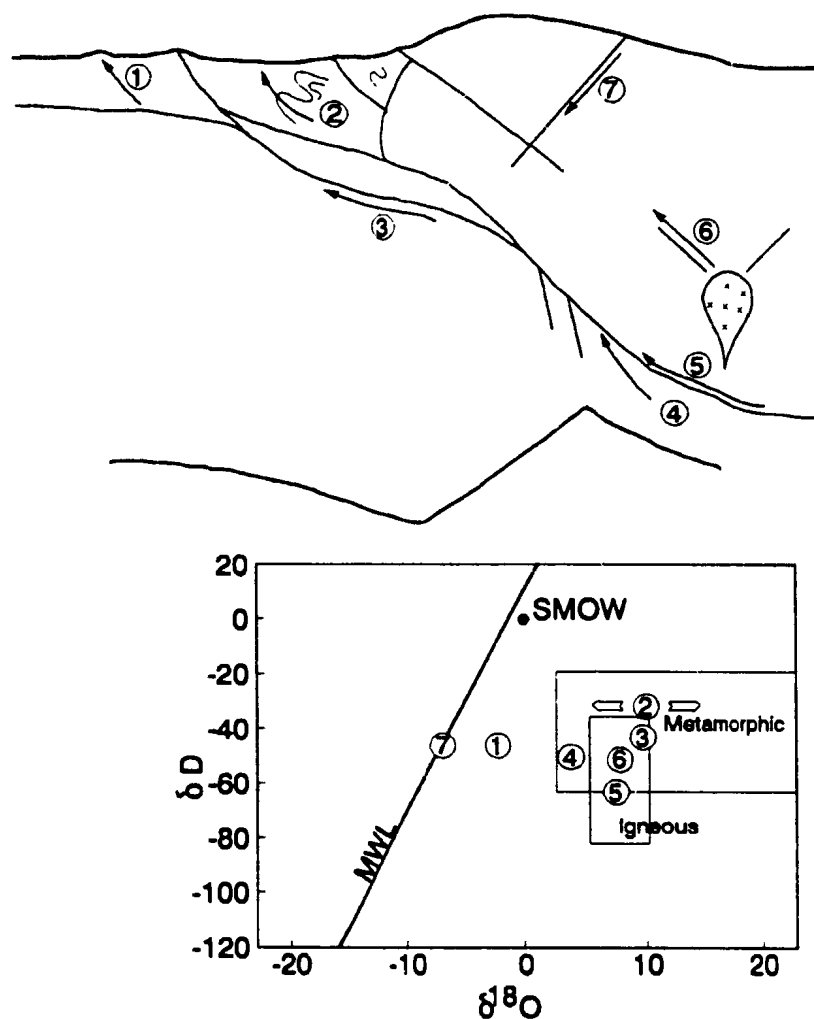


Figure 7.2 Schematic crustal section in a collisional orogen, showing possible fluid reservoirs and flow paths, modified from Kyser and Kerrich (1990), with schematic section adapted from Jamieson (1991). Fluids: (1) formation waters expelled in thrust faults; (2) syntectonic fluids buffered by regional lithologies; (3) metamorphic fluids from old crust; (4) metamorphic fluids from subcreted oceanic crust; (5) mantle volatiles advected up suture; (6) magmatic fluids from partial crustal melts; (7) meteoric water in fault zones. O and H isotopic compositions of igneous and metamorphic fluids from Taylor (1974).

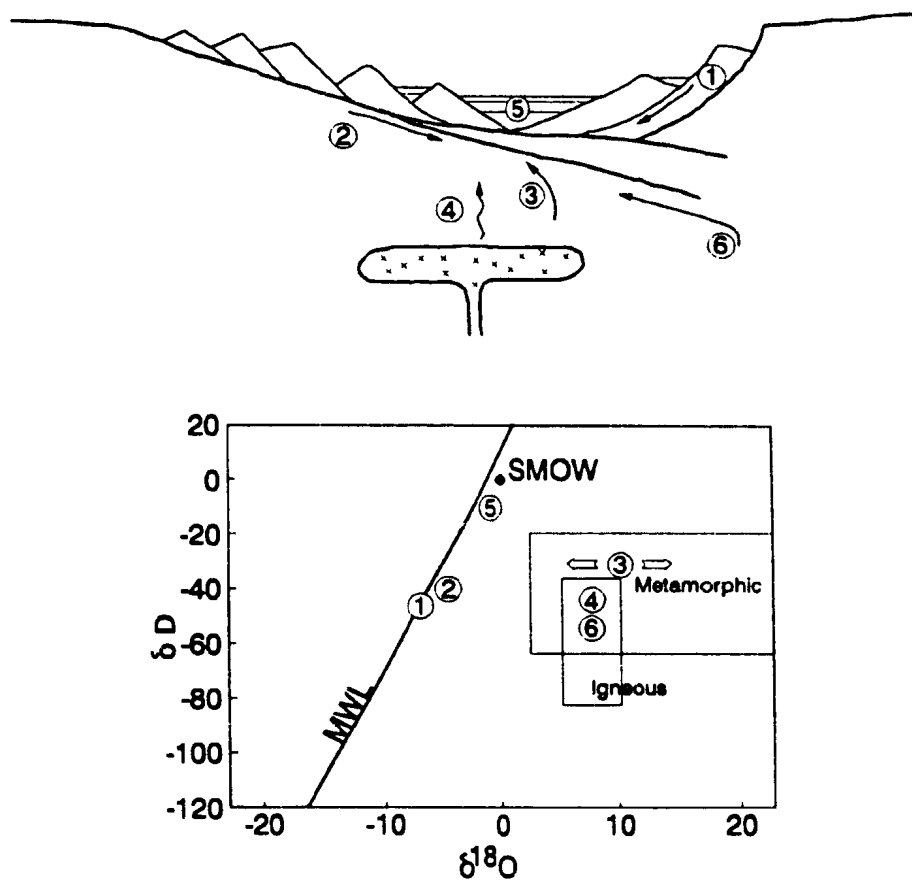


Figure 7.3 Schematic section of crust undergoing extension, showing possible fluid reservoirs, flow paths, and O and H isotopic compositions, modified from Kyser and Kerrich (1990). Fluids: (1) meteoric water in upper-level fault zones; (2) meteoric water infiltrates detachment faults; (3) metamorphic fluids generated by dehydration; (4) fluids from syn-kinematic intrusions; (5) saline basinal brines; (6) mantle-derived volatiles. O and H isotopic compositions of igneous and metamorphic fluids from Taylor (1974).

An important episode of Silurian regional extension in the Baie Verte Peninsula has been identified by Jamieson *et al.* (1993), and an extensional model for fluid flow in the King's Point area is consistent with the caldera model of Silurian magmatism (Coyle and Strong, 1986). Tensional movements would promote the circulation of meteoric water to depth, but a purely extensional model for gold deposition is incompatible with the structural development of the Hammer Down prospect, where gold mineralization is developed within compressional F_2 folds (Section 3.2.1). Extension on a regional scale in the Baie Verte and King's Point area, however, may have allowed a substantial meteoric water component to enter broadly based fluid reservoirs that contributed to gold ore deposition. Nesbitt (1992) has correlated episodes of crustal extension with periods of extensive epigenetic mineralization, including mesothermal gold, in the Canadian Cordillera. Crustal extension promotes vertical fracturing, which allows the influx of surface fluids and the ascent of fluids from devolatilization at depth, such that extensional regimes are preferentially mineralized (Nesbitt, 1992).

Aspects of both compressional and extensional tectonics can be applied to fluid flow and gold mineralization in the Baie Verte and King's Point region, because timing constraints indicate that crustal extension closely followed the collisional stage. Preservation of high-pressure mineral assemblages, such as the eclogites described by Jamieson (1990), requires rapid uplift and decompression following deep burial. Rapid cooling from the peak of metamorphism and conditions of crustal melting to

approximately 300°C is indicated by the limited mineralogical discordance of Middle and Late Silurian $^{40}\text{Ar}/^{39}\text{Ar}$ ages for biotite, hornblende, and muscovite from the Fleur de Lys Supergroup and the Burlington Granodiorite (Dallmeyer, 1977). Metamorphic fluids related to crustal thickening are reasonably expected to have remained in crustal reservoirs when the extensional phase promoted the influx of meteoric water.

Abundant Silurian magmatism and high heat flow in the area would provide a deep crustal driving mechanism for devolatilization during extension, and for the circulation of fluids. A contribution from igneous fluids is not ruled out by the calculated fluid isotopic compositions.

7.1.3 Mechanism of gold transport and deposition

Gold mineralization in the Hammer Down prospect is largely confined to brittle-ductile shear zones developed preferentially within felsic porphyry dykes and along dyke margins. Rich ore-bearing zones are present in host lithologies of very different composition, specifically, felsic porphyry dykes, and the predominantly mafic volcanic rocks they intrude. Coupled with the very limited extent of alteration and mineralization outside of veins, this mode of occurrence strongly suggests a process of gold deposition other than chemical interaction between fluids and wall-rocks. Only within narrow zones adjacent to some type II veins does gold-bearing pyrite replace chlorite or Fe-Ti oxides as the principal iron-bearing mineral (sections

4.3.1 and 4.4). The lack of evidence for widespread interaction between vein-forming fluids and wall rocks also indicates that ore and gangue components in the veins were brought into the prospect from external sources.

Gold is soluble as an aqueous chloride complex, AuCl_2^- , in acidic oxidizing solutions, or as bisulphide complexes, $\text{Au}(\text{HS})_2^{2-}$ or $\text{Au}_2\text{S}(\text{HS})_2^{2-}$, under reducing conditions (Seward, 1973; Romberger, 1988; Shenberger and Barnes, 1989). Chloride complexes are effective transporters of gold in moderately saline solutions (5.8 weight % NaCl) at oxidation states that correspond to hematite stability, and are generally above the stability fields for pyrite, chlorite, and magnetite (Romberger, 1988), which are the iron-bearing minerals found throughout the Hammer Down prospect. At temperatures near 250° C, gold is most soluble as bisulphide complexes in reduced, slightly alkaline solutions. Precipitation of gold from aqueous bisulphide complexes may be accomplished by an increase in oxygen activity, decrease in sulphur activity, or changes in pH (Shenberger and Barnes, 1989), with oxidation being the most efficient means because of steep gold solubility gradients under conditions of increasing oxygen activity (Romberger, 1988). Other than chemical reaction with host rocks, processes that lead to gold deposition include fluid mixing to change chemical composition or oxidation state, boiling or effervescence to alter fluid chemistry, and precipitation of sulphides to reduce sulphur activity. The low abundance of gold-bearing pyrite in wall rocks, and the small extent of hydrothermal alteration adjacent to veins indicate that sulphidation of wall rocks was not a

mechanism which acted extensively to reduce sulphur activity of the vein-forming fluid or to deposit gold ore in the Hammer Down prospect.

Bisulphide complexes of copper and zinc are stable and soluble at temperatures above 200° C and pH values between 5 and 7 (Lydon, 1988, and references therein). Changes in pH, which alter the relative abundances of H_2S and HS^- , and changes in total sulphur activity are effective mechanisms of sulphide precipitation (Barnes, 1979; Lydon, 1988). In many epithermal deposits, boiling is a mechanism of mineral deposition that results in oxidation of the residual liquid and a decrease in sulphur activity by partition of H_2S into the vapour (*e.g.* Kamilli and Ohmoto, 1977; Barnes, 1979; Romberger, 1988). Partial loss of CO_2 and H_2S into a vapour phase will promote carbonate mineral precipitation, and produces an increase in pH of the liquid (Kamilli and Ohmoto, 1977). There is no field or petrographic evidence for boiling in the Hammer Down prospect, although Kerrich (1989a) has outlined mechanisms for phase separation induced by pressure fluctuations during active deformation and fluid flow in mesothermal gold deposits, which result in the residual fluid becoming more oxidized and less rich in sulphur. Gold will be deposited from undersaturated solutions if the precipitation of sulphide minerals produces a sufficient reduction in the total activity of sulphur.

Mixing of the gold-bearing solutions with other fluids could result in changes of pH or oxygen activity that would lead to ore deposition. The different $\delta^{13}C$ values of carbonate minerals in type II and type III veins do provide some evidence for the

presence of multiple fluids in the mineralized zones, but type III veins may not be directly related to gold. The narrow range of quartz isotopic compositions in both vein sets, and the lack of any clear mixing trends in $\delta^{18}\text{O}$ and δD values of vein forming fluids indicate the probable role of a single fluid (although possibly of mixed origin) of nearly uniform composition. Cooling is a simple mechanism that would promote the coprecipitation of quartz, pyrite, sphalerite, and chalcopyrite as indicated by ore textures in the Hammer Down prospect, although changes in temperature have less influence on the solubility of copper and zinc bisulphide complexes than other chemical parameters (Barnes, 1979; Lydon, 1988). If copper and zinc were carried in solution as chloride complexes, cooling would be a contributing mechanism to base metal deposition (*e.g.* Barnes, 1979; Hutchinson, 1990)

Increased alkalinity and oxidation by unmixing of a CO_2 -rich fluid and destabilization of aqueous gold bisulphide complexes by precipitation of sulphide minerals (possibly influenced by cooling) are the most viable means of gold deposition in the Hammer Down prospect, and are consistent with the available geological and geochemical data.

7.2 Comparison to other mesothermal gold deposits

7.2.1 General characteristics and fluid regimes

Geological features that the Hammer Down prospect has in common with mesothermal gold deposits of all ages include proximity to a major fault zone of regional extent (the Green Bay fault) within an overall accretionary setting, and structural control on the distribution of ore at a local scale. The temperatures of vein formation, inferred fluid sources, and geologic setting are all consistent with a mesothermal style of epigenetic mineralization at the Hammer Down prospect.

Figure 7.4 provides a comparison of $\delta^{18}\text{O}$ values for quartz in the type II veins of the Hammer Down prospect to the ranges of values compiled for Archean, Paleozoic, Mesozoic, and Tertiary mesothermal gold deposits and districts. Together, the deposits define a limited range of isotopic compositions, that is distinct from that of epithermal gold deposits, which have $\delta^{18}\text{O}$ values of quartz mostly below 10 ‰, and extending to negative values. Of the examples listed in Figure 7.4, the Hammer Down prospect is most like the Archean deposits of the Abitibi greenstone belt, Yellowknife, and western Australia, in terms of quartz isotopic compositions. The average $\delta^{18}\text{O}$ value of quartz from the Hammer Down prospect is approximately 2 ‰ lower than values from gold deposits of the Meguma Group in Nova Scotia, which is a major Paleozoic mesothermal gold district within the Appalachian Orogen.

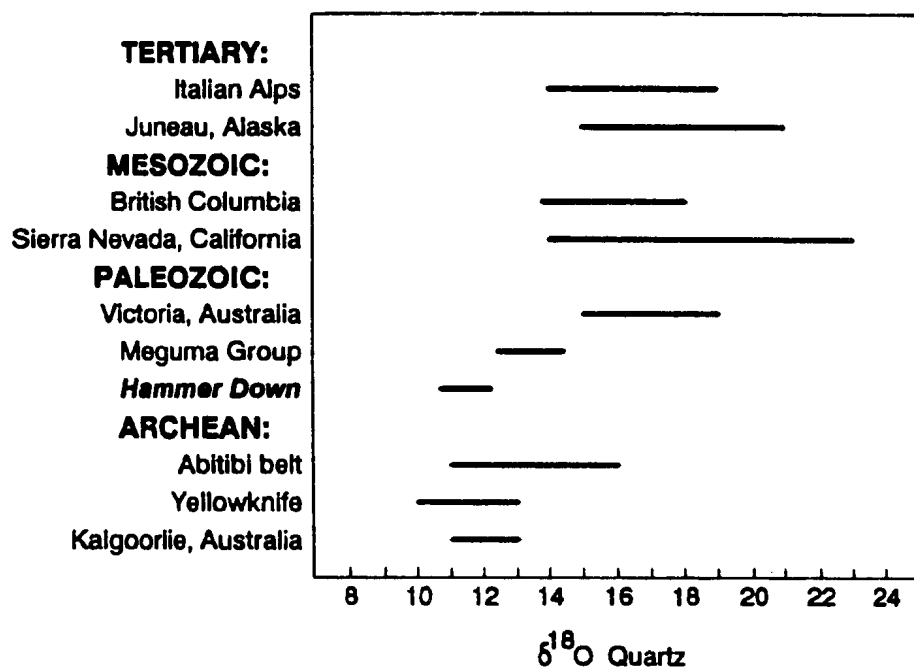


Figure 7.4 Compilation of $\delta^{18}\text{O}$ values of quartz from mesothermal gold deposits of various ages. Data sources other than Hammer Down are Curti (1987), Goldfarb *et al.* (1988), Bohlke and Kistler (1986), Leitch *et al.* (1991), Kontak *et al.* (1990), and compilation in Kerrich (1987).

Oxygen and hydrogen isotopic compositions of vein fluids in the Hammer Down prospect are somewhat different than compositional ranges for mesothermal gold deposits in Archean greenstone belts of Canada and Australia, and Mesozoic and Tertiary districts in California, British Columbia, and Alaska (Figure 7.5).

Calculated $\delta^{18}\text{O}$ and δD values from Hammer Down are most like those from the Archean belts, but they do not overlap with the fields for Juneau, California, or Canadian Cordilleran deposits. The compositions of type II and type III vein fluids in the Hammer Down prospect correspond approximately to those for post-ore oxidizing fluids in the Archean Macassa mine at Kirkland Lake, Ontario, that deposited quartz-magnetite stringers and had $\delta^{18}\text{O}$ values between 0 and 2.2 and δD values of -20 to -70 (Kerrick and Watson, 1984). These fluids were depleted in ^{18}O relative to the main-stage gold-mineralizing solutions, and were interpreted as being of evolved meteoric or marine origin, (Kerrick and Watson, 1984).

In epithermal gold deposits of the southwest United States, fluid $\delta^{18}\text{O}$ and δD values are very low (typically -10 and -100 ‰, respectively), indicating the dominance of meteoric water in those systems. The δD values of chlorite and muscovite from the Hammer Down prospect are between -64 and -80, and do not discriminate between igneous or metamorphic fluid sources.

The very low δD values for the deposits of the Canadian Cordillera (Figure 7.5) were measured from fluid inclusion waters in gold-bearing veins, whereas other fields were derived from isotopic compositions of hydrous minerals associated with

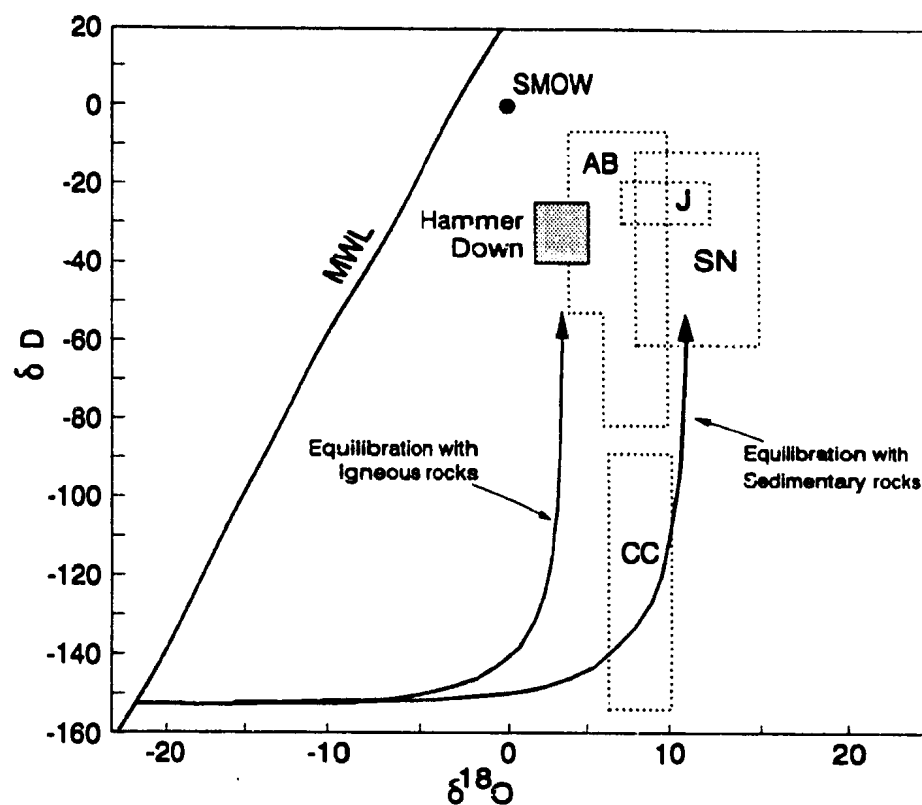


Figure 7.5 Calculated δD and $\delta^{18}O$ values of hydrothermal fluids in type II and type III veins from the Hammer Down prospect (shaded rectangle) compared to compositional fields for mesothermal deposits in specified districts: AB = Archaean greenstone belts of Canada and Australia (compiled by Kerrich, 1989b), J = Juneau Belt, Alaska (Goldfarb *et al.*, 1988), SN = Sierra Nevada districts, California (Bohlke and Kistler, 1986), CC = Canadian Cordillera (Nesbitt *et al.*, 1986). Curved arrows are evolutionary trends for meteoric water during progressive interaction with igneous or sedimentary rocks at 300°C (Nesbitt *et al.*, 1989).

gold. There is no substantial discrepancy among hydrogen isotopic compositions for the Hammer Down, Archean, Juneau, and Sierra Nevada fluids (Figure 7.5). The measurement of δD values from inclusion fluids has been questioned (*e.g.* Pickthorn *et al.*, 1987), on grounds that the sampled inclusions may be secondary, and therefore contain fluids that were not related to gold mineralization. Fluid inclusion waters from the Juneau belt have δD values between -50 and -110, and are attributed to various mixtures of ore fluids from primary inclusions ($\delta D = -15$ to -35) and meteoric waters with δD below -80 (Pickthorn *et al.*, 1987; Goldfarb *et al.*, 1988). Similarly, calculated fluid δD values for the Alleghany district of the Sierra Nevada foothills metamorphic belt are less negative than values measured from inclusion waters, which are interpreted as secondary (Bohlke and Kistler, 1986, and references therein).

Curved fluid evolutionary tracks in Figure 7.5 represent the $\delta^{18}O$ and δD values of isotopically depleted meteoric water during modification by interaction with igneous or sedimentary rocks at progressively lower water/rock ratios (Nesbitt *et al.*, 1989). Isotopic exchange of meteoric water with sedimentary rock (right-hand curve in Figure 7.5) can produce the compositions proposed for gold deposits of the Canadian Cordillera (Nesbitt *et al.*, 1989), but only at water/rock ratios substantially smaller than 0.01 would these evolutionary paths approach the 4 compositional fields at higher δD values calculated for fluids in equilibrium with hydrous minerals. At higher water/rock ratios, meteoric water with a δD value near -35 could evolve along a horizontal trajectory to acquire the O isotopic composition of gold mineralizing

fluids for the Hammer Down prospect. Such an evolutionary line would have the same form as a mixing line between meteoric and metamorphic fluids with the same δD values. The preferred model for the origin of vein fluids in the Hammer Down prospect is addition of a meteoric component to a predominantly metamorphic reservoir to account for the calculated O isotopic compositions, rather than ^{18}O shifted meteoric water. The role of meteoric water in a mixing model is distinct from the regimes of fluid evolution in epithermal gold deposits (*e.g.* Field and Fifiarek, 1985) and certain gold-bearing polymetallic vein systems (*e.g.* Kamilli and Ohmoto, 1977).

Outside the immediate mineralized zones, host rocks to the Hammer Down prospect include thick felsic volcanic sequences of the Catcher's Pond Group, mafic and minor ultramafic rocks of the Lush's Bight Group, and felsic intrusive rocks that predate mineralization, including the felsic porphyry dykes within the prospect and possible regional correlatives to them. Seismic studies (Keen *et al.*, 1986) and patterns of zircon inheritance in a felsic dyke from the Hammer Down prospect suggest that Grenvillian crystalline crust underlies these units at depth in the Baie Verte and King's Point region, so that another component, one that is not directly accessible at surface, forms part of the overall environment of gold mineralization. This geologic setting is in contrast to the dominantly mafic and ultramafic associations in typical mesothermal gold deposits of Archean greenstone belts.

Late Archean belts (approximately 2900 to 2600 Ma old) were formed during a period of rapid growth and stabilization of continental crust on a large scale, and

contain abundant mesothermal gold mineralization, whereas Proterozoic and Phanerozoic orogens, with accretionary regimes similar to those of the Archean belts, have the same style of mineralization at a smaller scale (*e.g.* Barley *et al.*, 1989; Kerrich and Wyman, 1990; Barley and Groves, 1992). In terms of tectonic style and overall geologic setting, the Hammer Down gold prospect is more like mesothermal gold deposits of Phanerozoic age, such as those in the Mother Lode and Alleghany districts, the Canadian Cordillera, and Alaska, than deposits in Archean greenstone belts, yet the quartz $\delta^{18}\text{O}$ values and calculated fluid isotopic compositions are closer to the Archean examples. Gold deposits within the Sierra Nevada foothills belt of California have geographic variations in their O and Sr isotopic compositions that are correlated in part with the nature and origin of their host rocks and surrounding lithological belts (Bohlke and Kistler, 1986). In the Alleghany district, fluid $\delta^{18}\text{O}$ values range from 8 ‰ in deposits with relatively abundant ^{18}O -depleted ultramafic rocks, to approximately 14 ‰ in veins from chert-rich parts of the district (Bohlke and Kistler, 1986, and references therein). The lower $\delta^{18}\text{O}$ fluids overlap with those of Archean belts in Figure 7.5. In the Grass Valley and Washington districts of the same belt, other low $\delta^{18}\text{O}$ values are attributed to interaction with ^{18}O -depleted volcanic and sedimentary rocks (Bohlke and Kistler, 1986). By analogy with the California examples, fluid compositions from the Hammer Down prospect may reflect, to some degree, complex and heterogeneous rock compositions in the

Dunnage Zone, although the isotopic compositions of the different volcanic, sedimentary, metamorphic, and intrusive units have not been measured at present.

7.2.2 Polymetallic mineral assemblages

Mineral assemblages in the main gold-bearing veins of the Hammer Down prospect are dominated by quartz, pyrite, sphalerite, and chalcopyrite, and the textures of ore minerals and intergrowths indicate coprecipitation of gold and base metal sulphides.

The lack of assay data for metals other than gold in the Hammer Down veins does not permit the calculation of enrichment factors for copper, lead, and zinc in veins and mineralized wall rocks relative to host rocks. In Archean lode gold deposits, Kerrich and Fryer (1981), Kerrich (1983), Kerrich and Watson (1984), and Kishida and Kerrich (1987) have reported slight elevation of copper values in ore relative to host rock contents, and depletions or very small enrichments for lead and zinc. Sphalerite and chalcopyrite are common and widespread, but often minor, constituents of most mesothermal gold systems. In contrast to the patterns of element distribution in deposits depleted in base metals, Ojala *et al.* (1992) reported abundant sphalerite and chalcopyrite in Archean mesothermal-type gold-bearing quartz-tourmaline veins in eastern Finland, and positive correlations between Cu, Zn, and Au. High gold contents coupled with low base metal abundances have been attributed

to low water/rock ratios in the fluid source region (Kerrick and Fryer, 1981; Kerrich, 1983), which is in accord with the general model of metamorphic devolatilization for the origin of gold-bearing fluids. The Hammer Down prospect is distinguished from the Archean deposits listed above by its high abundance of base metal sulphide minerals (Chapter 4).

Fluid inclusion studies of mesothermal gold deposits (e.g. Robert and Kelly, 1987; Leitch *et al.*, 1991; Goldfarb *et al.*, 1988; Nesbitt, 1988, and many others) have identified the ore-forming solutions as H₂O-CO₂ fluids of low salinity (mostly < 4 wt. % NaCl equivalent) that would not be capable of carrying abundant base metals as chloride complexes. In contrast to fluid inclusions from mesothermal gold deposits, at least some of those in volcanogenic massive sulphide and porphyry type deposits are highly saline, and may be directly related to magmatism. The association of copper, lead, and zinc with gold is characteristic of certain examples of these two deposit types. In mesothermal lode-type deposits, a gold and base metal association has been attributed to a magmatic (e.g. Wilton and Strong, 1986), or evolved seawater (e.g. Ansdell and Kyser, 1991) component in the ore-forming fluid.

The regional geology of the Hammer Down prospect and the King's Point area incorporates the Lush's Bight Group, which is a prolific host to massive sulphide occurrences (Kean, 1988). It contains the highest density of prospects and showings of any mafic terrane in Newfoundland (Dean, 1978; Evans *et al.*, 1992), including the auriferous copper and zinc prospect at Rendell - Jackman, only 4 km northeast of the

main Hammer Down zone. This metallic occurrence and others like it could contribute metals to percolating fluids of metamorphic, igneous, or mixed origin. Furthermore, the Hammer Down gold prospect is less than 400 m from the Lochinvar mineralized zone (P.A. Andrews and M. Basha, personal communication, 1990; Evans *et al.*, 1992), which contains high grades of lead, zinc, and silver. The metal content is not necessarily indicative of a unique mode or origin for the mineralization, because of variability within the broad class of mesothermal mineral deposits. Provinciality in the composition (and by inference, source) of ore forming solutions in mesothermal lode gold deposits has been demonstrated by Sr, Pb, and O isotopic tracer studies (*e.g.* Bohlke and Kistler, 1986; Curti, 1987; King and Kerrich, 1989), and by extension of this concept, it is possible that local and regional geology will exert some control on the metal content and style of epigenetic mineralization in an individual deposit. An example of the wide mineralogical variation possible in mesothermal vein systems, and of the possibility of host rock control on the metallic content of vein deposits, is the Coeur d'Alene district of Idaho and Montana, where deposits contains Ag, Pb, Zn, Cu in shear-parallel quartz veins (Leach *et al.*, 1988), that have alteration haloes with muscovite and iron carbonate in much the same structural setting as the Hammer Down prospect. Geochronology and fluid inclusion studies indicate that ore was deposited at 250 - 350°C from moderately saline (5 - 10 % NaCl equivalent) fluids derived by regional metamorphism of Ag- and base metal-rich sedimentary units (Leach *et al.*, 1988). The mineralization temperatures and

fluid sources in the Coeur d'Alene district are similar to those of mesothermal lode gold deposits.

In terms of ore mineralogy, the Hammer Down prospect has certain similarities to other structurally controlled gold-polymetallic occurrences in Newfoundland. Base metal sulphide- and gold-bearing quartz veins are developed in granite and schist within the Cape Ray fault zone near the southwestern tip of Newfoundland, where ore minerals consist mainly of galena, sphalerite, chalcopyrite, pyrite, and electrum (Wilton, 1984; Wilton and Strong, 1986). Mineralized zones in the Cape Ray deposit are highly to moderately enriched in Au, Ag, Pb, Zn, Cu, and As, relative to host rocks (Wilton and Strong, 1986). The small Handcamp prospect occupies a shear zone developed within Ordovician volcanic and sedimentary rocks of the Roberts Arm Group 45 km south of King's Point, and contains pyrite, chalcopyrite, sphalerite, and minor galena, with sporadic gold and silver (Hudson and Swinden, 1989). Single samples from the Handcamp prospect contain 587 ppm Ag and 74 ppm Au (Hudson and Swinden, 1989), whereas average grades of various showings at Cape Ray are up to 60 ppm Ag and 20 ppm Au (Wilton and strong, 1986). With the limited evidence available, mineralized zones in the Hammer Down prospect appear to contain less silver than at Handcamp or Cape Ray, but silver-bearing minerals have been discovered as a vein constituent at Hammer Down (Chapter 4), and the coexistence of gold with abundant base metal sulphides is consistent in all three occurrences. Gold, silver, and base metal mineralization in the

Proterozoic Laurel Lake deposit of northern Saskatchewan was developed from saline hydrothermal fluids derived from modified seawater (Ansdell and Kyser, 1990). A component of igneous fluid, which is compatible with the available stable isotope data from the Hammer Down prospect, could provide the relatively higher salinities if they are necessary for the coenrichment of gold and base metals.

The mineralogic, geochemical, and isotopic features of gold mineralization in the Hammer Down prospect are not all shared by other mesothermal gold occurrences in western and central Newfoundland. The Stog'er Tight prospect near the town of Baie Verte and several other gold occurrences have many structural, mineralogical, and chemical characteristics of typical mesothermal gold deposits (Ramezani, 1993), and the H and O isotopic compositions of fluids correspond to those compiled by Kerrich (1987) for Archean lode gold deposits (J. Ramezani and M. Wilson, unpublished data).

7.3 Outstanding problems

The characterization of ore-forming solutions in the Hammer Down prospect might be substantially augmented by fluid inclusion studies. Fluid inclusion homogenization temperatures could be compared to those calculated from quartz-chlorite and quartz-muscovite ^{18}O thermometry. Particularly in consideration that Cu and Zn might have been carried as chloride complexes in solution, salinity data from

fluid inclusions would provide information on fluid compositions that might contribute significantly to a model for fluid origins, metal transport, and ore deposition. Fluid inclusion measurements were excluded from this project principally because preservation of useful primary inclusions in quartz from the highly strained type II gold-bearing veins was considered unlikely. Undeformed ore-stage minerals such as sphalerite (illustrated in Plates 4.5, 4.6, and 4.8) have, however, been identified by subsequent petrographic studies, and are suitable hosts for primary fluid inclusions. Measurements from inclusions in these minerals could be compared to those from undeformed quartz, calcite, and fluorite in type III veins to produce a further comparison of the two main vein sets in the Hammer Down prospect.

Further investigation of the extent of felsic porphyry dyke distribution on the Springdale Peninsula could be approached as a petrological problem coupled with systematic study of the correlative Burlington Granodiorite, or as a primarily economic endeavour, because felsic dykes are closely associated with gold in the Hammer Down prospect.

7.4 Conclusions

The Hammer Down prospect is a structurally controlled mesothermal vein-type lode gold occurrence. Sheared, laminated gold-bearing quartz veins, containing abundant co-precipitated chalcopyrite and sphalerite, were emplaced within

contemporaneous brittle-ductile high strain zones (D_2 deformation) that postdate regional metamorphism and an early phase of deformation (D_1). The structurally preferred sites for gold mineralization were fold hinges related to D_2 , and dilational zones within and adjacent to a series of felsic porphyry dykes that intruded the host volcanic and sedimentary units after the development of D_1 (Dubé *et al.*, 1992). Quartz, pyrite, sphalerite, chalcopyrite, and calcite are the principal vein constituents. Less abundant vein minerals include chlorite, ferroan dolomite, scheelite, galena, magnetite, and Au/Ag- and Pb- tellurides. Hydrothermal alteration associated with gold mineralization is absent or developed over a range of less than 1 m in wall rocks adjacent to the main gold-bearing veins. Muscovite (sericite), pyrite, calcite, chlorite, and rutile are the prominent hydrothermal minerals in altered mafic and felsic host rocks and wall rock inclusions within veins. Sericitic and pyritic alteration in mafic rocks was accompanied by minor and rare deposition of gold and chalcopyrite, and by enrichments in K, Rb, Ba, S, Cu, and Zn, and possible depletion of Na. Elsewhere, host rocks have largely retained their igneous or metamorphic chemical compositions.

Paragenetically younger quartz-carbonate veins (type III) are spatially associated with the main gold-bearing zones (type II veins), and commonly contain fluorite, with or without muscovite. Mineralized structures and type II and type III veins do not extend below a late brittle fault that dips beneath the prospect. This fault postdates gold mineralization and is characterized by breccia and chloritic fault gouge

with calcite veinlets (type IV veins) and cement.

Oxygen isotope thermometry for type II and type III veins indicates temperatures of mineralization between 240 and 320° C. Vein-forming solutions had calculated O and H isotopic compositions generally compatible with those of many other mesothermal gold districts, but they are somewhat depleted in ^{18}O relative to most major deposits of this type. The gold-mineralizing fluids had $\delta^{18}\text{O}$ values between 2.2 and 5.2 ‰ and δD values between -27 and -22 ‰. These fluids are interpreted to have been derived primarily by metamorphic devolatilization, with a component of meteoric water. This mixed fluid regime is attributed to the regional tectonic environment at the time of gold deposition, which included crustal thickening, prograde metamorphism, and crustal melting, followed by extension that promoted the circulation of surface-derived water. Carbon isotopic compositions of calcite and ferroan dolomite from type II and type III veins are close to average crustal values, but the average $\delta^{13}\text{C}$ value of calcite from type II veins is 0.8 ‰ lighter than for type III veins. The $\delta^{18}\text{O}$ and δD values of silicate minerals from type II and type III veins are similar, and the calculated oxygen and hydrogen isotopic compositions do not indicate distinct fluid sources for the two vein sets.

The rock units that host gold in the Hammer Down prospect have igneous crystallization ages of 480 ± 4 -3 Ma (felsic tuff of Catchers Pond Group), and 437 ± 4 Ma (felsic porphyry dyke). Both major host lithologies experienced sub-greenschist to greenschist facies regional metamorphism prior to the deposition of

gold. Arc-related mafic and felsic volcanic rocks are chemically similar to other units in the King's Point area and Springdale Peninsula. Felsic dykes that host gold in the Hammer Down prospect are distinct from intrusive and extrusive units of the nearby King's Point volcanic-plutonic complex in terms of mineralogy, chemical composition, and age. Correlations of the King's Point complex to the Springdale Group and its associated intrusive rocks (Coyle and strong, 1987; Coyle, 1990), and of the felsic porphyry dykes to the Burlington Granodiorite (Chapters 3 and 5), indicate contemporaneous Early and Middle Silurian magmatic activity on opposite sides of the Green Bay fault.

Gold mineralization in the Hammer Down prospect has a maximum age of 437 +/- 4 Ma, and regional geological considerations and geochronological constraints link the event of ore formation to Silurian orogenic activity in the Baie Verte area. The Hammer Down gold prospect is interpreted to have formed during a period of deformation and fluid movement that probably accompanied, but was not necessarily generated by, Silurian magmatic activity. A mixed hydrothermal solution is interpreted to have been focused into structurally favourable sites during active deformation of the host rocks, where physical conditions of cooling, CO_2 immiscibility, or both led to deposition of quartz, pyrite, chalcopyrite, and sphalerite, along with gold and other less abundant minerals in veins and altered host rocks. Chemical reaction between vein fluids and wall rocks was a minor mineralizing process.

References Cited:

- Andrews, P.W., 1990a. A summary of the geology and exploration history of the Hammer Down gold deposit, Springdale area, central Newfoundland. In Swinden, H.S., Evans, D.T.W., and Kean, B.F., (eds.), Metallogenic framework of base and precious metal deposits, central and western Newfoundland, Field trip guidebook 8th IAGOD Symposium, Geological Survey of Canada, Open File 2156.
- Andrews P.W., 1990b. Rendell-Jackman grid compilation. Unpublished map, Noranda Exploration Co. Ltd.
- Andrews, P.W. and Huard, A.A., 1991. Geology of the Hammer Down deposit, Green Bay, north-central Newfoundland. Ore Horizons (Geological Survey Branch, Department of Mines and Energy, Government of Newfoundland and Labrador) v.1, 63-74.
- Ansdell, K.M. and Kyser, T.K., 1991. The geochemistry and fluid history of the Proterozoic Laurel Lake Au-Ag deposit, Flin Flon greenstone belt. Canadian Journal of Earth Sciences, v.28, p.155-171.
- Barley, M.E. and Groves, D.I., 1992. Supercontinent cycles and the distribution of metal deposits through time. Geology, v. 20, p.291-294.
- Barley, M.E., Eisenlohr, B.N., Groves, D.I., Perring, C.S., and Vearncombe, J.R., 1989. Late Archean convergent margin tectonics and gold mineralization: A new look at the Norseman-Wiluna Belt, Western Australia. Geology v.17, p.826-829.
- Barnes, H.L., 1979. Solubilities of ore minerals. In Barnes, H.L. (ed.), The geochemistry of hydrothermal ore deposits. Second edition. John Wiley and Sons, New York, 798 pp, p.404-460.
- Barr, S.M. and Raeside, R.P., 1989. Tectono-stratigraphic terranes in Cape Breton Island, Nova Scotia: Implications for the configuration of the northern Appalachian orogen. Geology v.17, p.822-825.
- Barton., P.B. Jr., and Bethke, P.M., 1987. Chalcopyrite disease in sphalerite: Pathology and epidemiology. American Mineralogist, v.72, p.451-467.

- Beaudoin, G., Taylor, B.E., and Sangster, D.F., 1991. Silver-lead-zinc veins, metamorphic core complexes, and hydrologic regimes during crustal extension. *Geology* v.19, p.1217-1220.
- Berry, L.G., and Mason, B., 1959. *Mineralogy*. W.H. Freeman and Company, San Francisco. 630 pp.
- Böhlke, J.K. and Kistler, R.W., 1986. Rb-Sr, K-Ar and stable isotope evidence for the ages and sources of fluid components of gold bearing quartz veins in the northern Sierra Nevada Foothills Metamorphic Belt, California. *Economic Geology* v.81, p.296-322.
- Bortnikov, N.S., Genkin, A.D., Dobrovol'skaya, M.G., Muravitskaya, G.N., and Filimonova, A.A., 1991. The nature of chalcopyrite inclusions in sphalerite: Exsolution, coprecipitation, or "disease"? *Economic Geology*, v.86, p.1070-1082.
- Borodaevskaya, M.B., and Rozhkov, I.S., 1977. Deposits of Gold. In Smirnov, V.I. (ed.), *Ore deposits of the U.S.S.R.* Pitman, London, 492 pp.
- Boyle, R.W., 1979. The geochemistry of gold and its deposits. Geological Survey of Canada, Bulletin 280. Ottawa, Ontario, Canada, 584 pp.
- Brenninkmeijer, C.A.M., Kraft, P., and Mook, W.G., 1983. Oxygen isotope fractionation between CO₂ and H₂O. *Isotope Geoscience* v.1, (Chemical Geology v.41) p.181-190
- Briqueau, L., Bougault, H., and Joron, J.-L., 1984. Quantification of Nb, Ta, Ti and V anomalies in magmas associated with subduction zones: petrogenetic implications. *Earth and Planetary Science Letters*, v.68, p.297-308.
- Burrows, D.R., and Spooner, E.T.C., 1987. Generation of a magmatic H₂O-CO₂ fluid enriched in Mo, Au, and W within an Archean sodic granodiorite stock, Mink Lake, northwestern Ontario. *Economic Geology*, v.82, p.1931-1937.
- Cameron, E.M., and Hattori, K., 1987. Archean gold mineralization and oxidized hydrothermal fluids. *Economic Geology*, v.82, p.1177-1191.
- Clayton, R.N., and Mayeda, T.K., 1963. The use of bromine pentafluoride in the extraction of oxygen from oxides and silicates for isotopic analysis. *Geochimica et Cosmochimica Acta*, v.27, p.43-52.

- Clayton, , R.N., O'Neil, J.R., and Mayeda, T.K., 1972. Oxygen isotope exchange between quartz and water. *Journal of Geophysical Research*, v.77, p.1197-1201.
- Colman-Sadd, S.P., 1980. Geology of south-central Newfoundland and the evolution of the eastern margin of Iapetus. *American Journal of Science*, v.280., p.991-1017.
- Colman-Sadd, S.P., Dunning, G.R., and Dec, T., 1992. Dunnage-Gander relationships and Ordovician orogeny in central Newfoundland: A sediment provenance and U/Pb age study. *American Journal of Science*, v.292, p.317-355.
- Colman-Sadd, S.P. and Swinden, H.S., 1984. A tectonic window in Central Newfoundland? Geological evidence that the Appalachian Dunnage Zone may be allocthonous. *Canadian Journal of Earth Sciences*, v.21, p.1349-1367.
- Colvine, A.C., 1989. An empirical model for the formation of Archean gold deposits: products of final cratonization of the Superior Province, Canada. In R.R. Keays, W.R.H. Ramsay, D.I. Groves (eds.); *The Geology of Gold Deposits: the Perspective in 1988*. *Economic Geology Monograph* 6, p. 19-36.
- Cox, K.G., Bell, J.D., and Pankhurst, R.J., 1983. The interpretation of igneous rocks. George Allwn and Unwin, London, 450 pp.
- Cox, S.F., Etheridge, M.A., and Wall, V.J., 1987. The role of fluids in syntectonic mass transport, and the localization of metamorphic vein-type ore deposits. *Ore Geology Reviews*, v.2. p.65-86.
- Coyle, M., 1990. Geology, geochemistry, and geochronology of the Springdale Group, an early Silurian caldera in central Newfoundland. Unpublished Ph.D. thesis, Memorial University of Newfoundland, St. John's, Newfoundland, 310 pp.
- Coyle, M., and Strong, D.F., 1987. Geology of the Springdale Group: a newly recognized Silurian epicontinental-type caldera in Newfoundland. *Canadian Journal of Earth Sciences*, v.24, p.1135-1148.
- Craw, D., 1992. Fluid evolution, fluid immiscibility and gold deposition during Cretaceous-Recent tectonics and uplift of the Otago and Alpine Schist, New Zealand. *Chemical Geology*, v.98, p.221-236.

- Curti, E., 1987. Lead and oxygen isotope evidence for the origin of the Monte Rosa Gold lode deposits (Western Alps, Italy): A comparison with Archean lode deposits. *Economic Geology*, v.82, p.2115-2140.
- Dallmeyer, R.D., 1977. $^{40}\text{Ar}/^{39}\text{Ar}$ age spectra of minerals from the Fleur de Lys terrane in northwest Newfoundland: their bearing on chronology of metamorphism within the Appalachian orotectonic zone. *Journal of Geology*, v.85, p.89-103.
- Dallmeyer, R.D., and Hibbard, J., 1984. Geochronology of the Baie Verte Peninsula, Newfoundland: implications for the tectonic evolution of the Humber and Dunnage zones of the Appalachian orogen. *Journal of Geology*, v.92, p.489-512.
- Dean, W.T., 1970. Lower Ordovician trilobites from the vicinity of South Catcher Pond, northeastern Newfoundland. *Geological Survey of Canada, Paper 70-44*, 15 pp.
- Dean, P.L., 1978. The volcanic stratigraphy and metallogeny of Notre Dame Bay, Newfoundland. *Memorial University of Newfoundland Geology Report 7*, 205 pp.
- Dec, T., and Colman-Sadd, S., 1990. Timing of ophiolite emplacement onto the Gander Zone: evidence from provenance studies in the Mount Cormack Subzone. *Current Research, Newfoundland Department of Mines and Energy, Geological Survey Branch, Report 90-01*, p.289-304.
- Deer, W.A., Howie, R.A., and Zussman, J., 1962. Rock forming minerals, volume 1: Ortho- and ring silicates. Longmans, Green, and Company, London 333 pp.
- Deer, W.A., Howie, R.A., and Zussman, J., 1966. Rock forming minerals, volume 5: Non-silicates. Longmans, Green, and Company, London 371 pp.
- Dubé, B., 1990. A preliminary report on contrasting structural styles of gold-only deposits in western Newfoundland. *Current Research, Part B, Geological Survey of Canada, Paper 90-1B*, p.77-90.
- Dubé, B., Lauziere, K., Gaboury, D., 1992. Preliminary report on the structural control of the Rendell-Jackman gold deposit, Springdale Peninsula, Newfoundland. *Current Research, Part D, Geological Survey of Canada, Paper 92-1D*, p. i-10.

- Dunning, G.R., Kean, B.F., Thurlow, J.G., and Swinden, H.S., 1987. Geochronology of the Buchans, Roberts Arm and Victoria Lake Groups and Mansfield Cove Complex, Newfoundland. *Canadian Journal of Earth Sciences*, v.24, p.1175-1184.
- Dunning, G.R. and Krogh, T.E., 1985. Geochronology of ophiolites of the Newfoundland Appalachians. *Canadian Journal of Earth Sciences*, v.22, p.1659-1670.
- Dunning, G.R. and Krogh, T.E., 1991. Stratigraphic correlation of the Appalachian Ordovician using advanced U-Pb zircon geochronology techniques. In C.R. Barnes and S.H. Williams (eds.); *Advances in Ordovician Geology*. Geological Survey of Canada, Paper 90-09, p.85-92.
- Dunning, G.R., O'Brien, S.J., Colman-Sadd, S.P., Blackwood, R.F., Dickson, W.L., O'Neill, P.P., and Krogh, T.E., 1990. Silurian orogeny in the Newfoundland Appalachians. *Journal of Geology*, v. 98, p. 895-913.
- Dunning, G.R., Swinden, H.S., Kean, B.F., Evans, D.T.W., and Jenner, G.A., 1991. A Cambrian island arc in Iapetus: geochronology and geochemistry of the Lake Ambrose volcanic belt, Newfoundland Appalachians. *Geological Magazine*, v.128, p.1-17.
- Eisenlohr, B.N., Groves, D.I., and Partington, G.A., 1989. Crustal-scale shear zones and their significance to Archaean gold mineralization in Western Australia. *Mineralium Deposita*, v.24, 1-8.
- Epstein, R.S., 1983. The eastern margin of the Burlington Granodiorite, Newfoundland. Unpublished M.Sc.thesis, University of Western Ontario, London, Ontario, 188 pp.
- Espenshade, G.H., 1937. Geology and mineral deposits of the Pilley's Island area. Newfoundland Department of Natural Resources, Geological Section, Bulletin No. 6, 56 pp.
- Evans, D.T.W., 1991. Gold Metallogeny, Eastern Dunnage Zone, central Newfoundland. Current Research, Newfoundland Department of Mines and Energy, Geological Survey Branch, Report 91-01, p.310-318.

- Evans, D.T.W., 1992. Gold Metallogeny of the eastern Dunnage Zone, central Newfoundland. Current Research, Newfoundland Department of Mines and Energy, Geological Survey Branch, Report 92-01, p. 231-244.
- Evans, D.T.W., Kean, B.F., and Dunning, G.R., 1990. Geological studies, Victoria Lake Group, central Newfoundland. Current Research, Newfoundland Department of Mines and Energy, Geological Survey Branch, Report 90-01, p.131-144.
- Evans, D.T.W., Swinden, H.S., Kean, B.F., and Hogan, A. 1992. Metallogeny of the vestiges of Iapetus, Island of Newfoundland. Department of Mines and Energy, Government of Newfoundland and Labrador, Map 92-19.
- Faure, G., 1986. Principles of isotope Geology Second Edition. J. Wiley and Sons, New York, 589pp.
- Field, C.W., and Ficarek, R.H., 1985. Light stable-isotope sytematics in the epithermal environment. In Berger, B.R., and Bethke, P.M. (eds.), Geology and geochemistry of epithermal systems. Society of Economic Geology, Reviews in Economic Geology, volume 2, p.99-128.
- Fyfe, W.S., Price, N.J., and Thompson, A.B., 1978. Fluids in the Earth's Crust. Elsevier, Amsterdam, 383 pp.
- Goldfarb, R.J., Leach, D.L., Pickthorn, W.J., and Paterson, C.J., 1988. Origin of lode-gold deposits of the Juneau gold belt, southeastern Alaska. Geology v.16, p.440-443.
- Goldfarb, R.J., Newberry, R.J., Pickthorn, W.J., and Gent, C.A., 1991a. Oxygen, hydrogen, and sulfur isotope studies in the Juneau gold Belt, southeastern Alaska: Constraints on the origin of hydrothermal fluids. Economic Geology, v.86, p.66-80.
- Goldfarb, R.J., Snee, L.W., Miller, L.B., and Newberry, R.J., 1991b. Rapid dewatering of the crust deduced from ages of mesothermal gold deposits. Nature, v.354, p.296-298.
- Groves, D.I., and Phillips, G.N., 1987. The genesis and tectonic control on Archean gold deposits of the Western Australian Shield - metamorphic replacement model. Ore Geology Reviews, v.2, p.287-322.

- Harland, W.B., and Gayer, R.A., 1972. The Arctic Caledonides and earlier oceans. *Geological Magazine*, v.109, p.289-314.
- Hibbard, J., 1983. Geology of the Baie Verte Peninsula, Newfoundland. Mineral Development Division, Department of Mines and Energy, Memoir 2. Government of Newfoundland and Labrador, St. John's, Newfoundland, 279 pp.
- Hudson, K.A., and Swinden, H.S., 1989. Geology and petrology of the Handcamp gold prospect, Robert's Arm Group, Newfoundland. Current Research, part B, geological Survey of Canada, Paper 89-1B, p.93-105.
- Irvine, T.N., and Baragar, W.R.A., 1971. A guide to the chemical classification of the common volcanic rocks. *Canadian Journal of Earth Sciences*, v.8, p.523-548.
- Jaffey, A.H., Flynn, K.F., Glendenin, L.E., Bentley, W.C., and Essling, A.M., 1971. Precision measurement of half-lives and specific activities of ^{235}U and ^{238}U . *Physical Review* v.4, p.1889-1906.
- Jamieson, R.A. 1990. Metamorphism of an Early Palaeozoic continental margin, western Baie Verte Peninsula, Newfoundland. *Journal of Metamorphic Geology*, v.8, p.269-288.
- Jamieson, R.A. 1991. P-T-t paths of collisional orogens. *Geologische Rundschau*, v.80, p.321-332.
- Jamieson, R.A., Anderson, S., and McDonald, L., 1993. Slip on the scrape-an extensional allochthon east of the Baie Verte Line, Newfoundland. *Geological Society of America Northeastern Section Abstracts with programs*, v.25, p.26.
- Jemielita, R.A., Davis, D.W., and Krogh, T.E., 1990. U-Pb evidence for Abitibi gold mineralization postdating greenstone metamorphism. *Nature*, v.346, p.831-833.
- Jenner, G.A. and Szybinski, Z.A., 1987. Geology, geochemistry and metallogeny of the Catchers Pond Group and geochemistry of the Western Arm Group, Newfoundland. Final report for D.S.S. contract no. 23233-6-0285/01-ST, Geological Survey of Canada open file, 116 pp.

- Kamilli, R.J., and Ohmoto, H., 1977. Paragenesis, zoning, fluid inclusion, and isotopic studies of the Finlandia vein, Colqui district, central Peru. *Economic Geology*, v.72, p.950-982.
- Kean, B.F., 1988. Regional Geology of the Springdale Peninsula. In Swinden, H.S., and Kean, B.F. (eds.), *The Volcanogenic Sulphide Districts of Central Newfoundland*. Mineral Deposits Division, Geological Association of Canada, p.74-79.
- Kean, B.F. and Evans, D.T.W., 1987. King's Point, Newfoundland (12H/9). Department of Mines and Energy, Government of Newfoundland and Labrador, Map 87-06.
- Kean, B.F. and Evans, D.T.W., 1990. Geology and mineralization of the Lushs Bight Group Springdale Peninsula; In Swinden, H.S., Evans, D.T.W., and Kean, B.F., (eds.), *Metallogenic Framework of Base and Precious Metal Deposits, Central and Western Newfoundland*, Field trip guidebook 8th IAGOD Symposium, Geological Survey of Canada, Open File 2156, p.130-133.
- Kean, B.F. and Strong, D.F., 1975. Geochemical evolution of an Ordovician island arc of the central Newfoundland Appalachians. *American Journal of Science*, v.275, p.97-118.
- Keen, C.E., Keen, M.J., Nichols, B., Reid, I., Stockmal, G.S., Colman-Sadd, S.P., O'Brien, S.J., Miller, H., Quinlan, G., Williams, H., and Wright, J., 1986. Deep seismic reflection profile across the northern Appalachians. *Geology* v.14, p.141-145.
- Kennedy, L.P., and Kerrich, R., 1982. Transition from marine to meteoric water hydrothermal regimes in an emerging Archean intrusive complex: ^{18}O evidence from the Flavrian Pluton. Abstracts, American Geophysical Union, San Francisco, December, 1992.
- Kerrich, R., Fryer, B.J., King, R.W., Willmore, L.M., and van Hees, E., 1987. Crustal outgassing and LILE enrichment in major lithospheric structures, Archean Abitibi greenstone belt: evidence on the source reservoir from strontium and carbon isotope tracers. *Contributions to Mineralogy and Petrology*, v.97, p.156-168.

- Kerrick, R., 1987. The stable isotope geochemistry of Au-Ag vein deposits in metamorphic rocks. In Kyser, T.K. (ed.), *Stable Isotope Geochemistry of Low Temperature Fluids*. Mineralogical Association of Canada Short Course Notes Volume 13, p.287-336.
- Kerrick, R., 1989a. Geodynamic setting and hydraulic regimes: Shear zone hosted mesothermal gold deposits. In J.T. Bursnall (ed.); *Mineralization and Shear Zones*. Geological Association of Canada Short Course Notes Volume 6, p.89-128.
- Kerrick, R., 1989b. Geochemical evidence on the sources of fluids and solutes for shear zone hosted mesothermal Au deposits. In J.T. Bursnall (ed.); *Mineralization and Shear Zones*. Geological Association of Canada Short Course Notes Volume 6, p.129-198.
- Kerrick, R., 1990. Carbon-isotope systematics of Archean Au-Ag vein deposits in the Superior Province. *Canadian Journal of Earth Sciences*, v.27, p.40-56.
- Kerrick, R., and Watson, G.P., 1984. The Macassa Mine Archean lode gold deposit, Kirkland Lake, Ontario: Geology, patterns of alteration, and hydrothermal regimes. *Economic Geology* v.79, p.1104-1130.
- Kerrick, R. and Wyman, D., 1990. Geodynamic setting of mesothermal gold deposits: an association with accretionary tectonic regimes. *Geology* v.18, p.882-885.
- King, A.F., 1988. Geology of the Avalon Peninsula, Newfoundland (parts of 1K, 1L, 1M, 1N, and 2C). Newfoundland Department of Mines, Mineral Development Division, Map 88-01.
- King, R.W. and Kerrich, R., 1989. Strontium isotope compositions of tourmaline from lode gold deposits of the Archean Abitibi greenstone belt (Ontario-Quebec, Canada): Implications for source reservoirs. *Chemical Geology (Isotope Geoscience Section)*, v.79, 225-240.
- Kirkwood, D., and Dubé, B., 1992. Structural control of sill-hosted gold mineralization: the Stog'er Tight gold deposit, Baie Verte Peninsula, northwestern Newfoundland. *Current Research, Part D, Geological Survey of Canada, Paper 92-1D*, p.211-222.

- Kishida, A., and Kerrich, R., 1987. Hydrothermal alteration zoning and gold concentration at the Kerr-Addison Archean lode gold deposit, Kirkland Lake, Ontario. *Economic Geology*, v.82, p.649-690.
- Knight, I., 1983. Geology of the Carboniferous Bay St. George Sub-basin, western Newfoundland. Mineral Development Division, Newfoundland Department of Mines and Energy, Memoir 1. Government of Newfoundland and Labrador, St. John's, Newfoundland, 358 pp.
- Kontak, D.J., Smith, P.K., Kerrich, R., and Williams, P.F., 1990. Integrated model for Meguma Group lode gold deposits, Nova Scotia, Canada. *Geology*, v.18, p.238-242.
- Kontak, D.J., Smith, P.K., and Reynolds, P.H., 1993. Geology and $^{40}\text{Ar}/^{39}\text{Ar}$ geochronology of the Beaver Dam gold deposit, Meguma Terrane, Nova Scotia, Canada: Evidence for mineralization at 370 Ma. *Economic Geology*, v.88, p.139-170.
- Kontak, D.J., and Strong, D.F., 1986. The volcano-plutonic King's Point complex, Newfoundland. *Current Research, Part A, Geological Survey of Canada, Paper 86-1A*, p.465-470.
- Koons, P.O., and Craw, D., 1991. Gold mineralization as a consequence of continental collision: an example from the Southern Alps, New Zealand. *Earth and Planetary Science Letters*, v.103, p.1-9.
- Krogh, T.E., 1973. A low contamination method for hydrothermal decomposition of zircon and extraction of U and Pb for isotopic age determinations. *Geochimica et Cosmochimica Acta*, v.37, p.485-494.
- Krogh, T.E., 1982. Improved accuracy of U-Pb ages by the creation of more concordant systems using an air abrasion technique. *Geochimica et Cosmochimica Acta*, v.46, p.637-649.
- Kyser, T.K., 1987. Equilibrium fractionation factors for stable isotopes. In Kyser, T.K. (ed.), *Stable Isotope Geochemistry of Low Temperature Fluids*. Mineralogical Association of Canada Short Course Notes Volume 13, p.1-84.

- Kyser, T.K. and Kerrich, R., 1990. Geochemistry of fluids in tectonically active crustal regions. In B.E. Nesbitt (ed.); *Fluids in Tectonically Active Regimes of the Continental Crust*. Mineralogical Association of Canada Short Course Notes Volume 18, p.133-230.
- Leach, D.L., Landis, G.P., and Hofstra, A.H., 1988. Metamorphic origin of the Coeur d'Alene base- and precious metal veins in the Belt basin, Idaho and Montana. *Geology* v.16, p.122-125.
- Leitch, C.H.B., Godwin, C.I., Brown, T.H., and Taylor, B.E., 1991. Geochemistry of mineralizing fluids in the Bralorne-Pioneer mesothermal gold vein deposit, British Columbia, Canada. *Economic Geology*, v.86, p.318-353.
- Liou, J.G., Maruyama, S., and Cho, M., 1985. Phase equilibria and mineral parageneses of metabasites in low-grade metamorphism. *Mineralogical Magazine*, v.49, p.321-333.
- Lydon, J.W., 1988. Volcanogenic massive sulphide deposits, part 2: Genetic models. *Geoscience Canada* v.15 p.115-182.
- Lynch, V.G., Longstaffe, F.J., and Nesbitt, B.E., 1990. Stable isotopic and fluid inclusion indications of large-scale hydrothermal paleoflow, boiling, and fluid mixing in the Keno Hill Ag-Pb-Zn district, Yukon Territory, Canada. *Geochimica et Cosmochimica Acta*, v.54, p.1045-1059.
- MacLean, H.J., 1947. Geology and mineral deposits of the Little Bay area. Geological Survey of Newfoundland, Bulletin 22, 36 pp.
- Markham, N.L., 1960. Synthetic and natural phases in the system Au-Ag-Te. *Economic Geology*, v.55, p.1148-1178 & 1460-1477.
- Matsuhisa, Y., Goldsmith, J.R., and Clayton, R.N., 1979. Oxygen isotopic fractionation in the system quartz-albite-anorthite-water. *Geochimica et Cosmochimica Acta*, v.43, 1131-1140.
- Matthews, A., and Katz, A., 1977. Oxygen isotope fractionation during dolomitization of calcium carbonate. *Geochimica et Cosmochimica Acta*, v.41, 1431-1438.

- Marmont, S. and Corfu, F., 1989. Timing of gold introduction in the Late Archean tectonic framework of the Canadian Shield: Evidence from U-Pb zircon geochronology of the Abitibi Subprovince. In R.R. Keays, W.R.H. Ramsay, D.I. Groves (eds.); *The Geology of Gold Deposits: the Perspective in 1988*. Economic Geology Monograph 6, p. 101-111.
- Mason, R., 1978. *Petrology of the Metamorphic Rocks*. George Allen and Unwin, London, 254 pp.
- McBride, D.E., 1989. The Nugget Pond deposit. Oral presentation given at the Baie Verte mining meeting, June 24, 1989.
- McCrea, J.M., 1950. On the isotope chemistry of carbonates and a paleotemperature scale. *Journal of Chemical Physics*, v.18, p.849-857.
- Mercer, B., Strong, D.F., Wilton, D.H.C., and Gibbons, D., 1985. The King's Point Complex, western Newfoundland; in *Current Research, Part A*, Geological Survey of Canada, Paper 85-1A, p.737-741.
- Meschede, M., 1986. A method of discriminating between different types of mid-ocean ridge basalts and continental tholeiites with the Nb-Zr-Y diagram. *Chemical Geology*, v.56, p.207-218.
- Meyer, J.R., Dean, P.L., and Barnes, C.R., 1988. Conodont ages for three carbonate samples from Middle Ordovician cherts and shales in central Newfoundland. *Current Research, Newfoundland Department of Mines, Mineral Development Division, Report 88-1*, p.198-192.
- Miyashiro, A., 1973. *Metamorphism and Metamorphic Belts*. J. Wiley and Sons, New York, 492 pp.
- Muehlenbachs, K., 1986. Alteration of the ocean crust and the ^{18}O history of seawater. In Valley, J.W., Taylor, H.P., and O'Neil, J.R. (eds.), *Stable isotopes in high temperature geological processes*. Mineralogical Society of America Reviews in Mineralogy Volume 16, p.425-444.
- Muehlenbachs, K., 1987. Oxygen isotope exchange during weathering and low temperature alteration. In Kyser, T.K. (ed.), *Stable Isotope Geochemistry of Low Temperature Fluids*. Mineralogical Association of Canada Short Course Notes Volume 13 p.162-186.

- Mueller, A.G., de Laeter, J.R., and Groves, D.I., 1991. Strontium isotope systematics of hydrothermal minerals from epigenetic Archean gold deposits in the Yilgarn Block, western Australia. *Economic Geology*, v.86, p.780-809.
- Mumme, W.G., Welin, E., and Wuensch, B.J., 1976. Crystal chemistry and proposed nomenclature for sulfosalts intermediate in the system bismuthinite-aikinite (Bi_2S_3 - CuPbBiS_3). *American Mineralogist*, v.61, p. 15-20.
- Neale, E.R.W. and Nash, W.A., 1963. Sandy Lake (East half) Newfoundland 12H E1/2; Geological Survey of Canada, Paper 62-28, 40 pp.
- Neale, E.R.W., Nash, W.A., and Innes, G.M., 1960. King's Point, Newfoundland; Geological Survey of Canada, Map 35-1960.
- Nesbitt, B.E., 1988. Gold deposit continuum: a genetic model for lode Au mineralization in the continental crust. *Geology* v.16, p.1044-1048.
- Nesbitt, B.E., 1992. Orogeny, crustal hydrogeology and the generation of epigenetic ore deposits in the Canadian Cordillera. *Mineralogy and Petrology*, v.45, p.153-179.
- Nesbitt, B.E., Muehlenbachs, K., and Murowchick, J.B., 1989. Genetic implications of stable isotope characteristics of mesothermal Au deposits and related Sb and Hg deposits in the Canadian Cordillera. *Economic Geology* v.84, p.1489-1506.
- Nesbitt, B.E., Murowchick, J.B., and Muehlenbachs, K., 1986. Dual origins of gold deposits in the Canadian Cordillera. *Geology*, v.14, p.506-509.
- Nowlan, G.S. and Thurlow, J.G., 1984. Middle Ordovician conodonts from the Buchans Group, central Newfoundland, and their significance for regional stratigraphy of the Central Volcanic Belt. *Canadian Journal of Earth Sciences*, v.21, p.284-296.
- O'Brien, F.H.C., and Szybinski, Z.A., 1989. Implications of the conodont fauna on the stratigraphy and structure of the Cutwell Group, central Newfoundland. Geological Association of Canada Mineralogical Association of Canada, Program with Abstracts, v.14, p.A15.

- O'Brien, S.J., O'Brien, B.H., and Dunning, G.R., 1989. Silurian and Precambrian events along the southeast margin of the Newfoundland Central Mobile Belt. Geological Association of Canada Mineralogical Association of Canada, Program with Abstracts v.14,p.A10.
- O'Brien, S.J., O'Driscoll, C.F., Tucker, R.D., and Dunning, G.R., 1992. Four-fold subdivision of the late Precambrian magmatic record of the Avalon Zone type area (east Newfoundland): Nature and significance (Abstract). Geological Association of Canada Mineralogical Association of Canada, Abstracts v.17, p.A85.
- O'Neil, J.R., and Taylor, H.P. Jr., 1969. Oxygen isotope equilibrium between muscovite and water. *Journal of Geophysical Research*, v.74, p.6012-6022.
- O'Neil, J.R., Clayton, R.N., and Mayeda, T.K., 1969. Oxygen isotope fractionation in divalent metal carbonates. *Journal of Chemical Physics*, v.51, 5547-5558.
- Ohmoto, H., 1986. Stable isotope geochemistry of ore deposits. In Valley, J.W., Taylor, H.P., and O'Neil, J.R. (eds.), *Stable isotopes in high temperature geological processes*. Mineralogical Society of America Reviews in Mineralogy Volume 16, p.491-560.
- Ohmoto, H., and Rye, R.O., 1979. Isotopes of sulphur and carbon. In Barnes, H.L. (ed.), *The geochemistry of hydrothermal ore deposits*. Second edition. John Wiley and Sons, New York, 798 pp, p.509-567.
- Ojala, V.J., Pekkarinen, L.J., Piirainen, T., and Tuukki, P.A., 1992. The Archaean gold mineralization in Rämepuro, Ilomantsi greenstone belt, Eastern Finland. *Terra Nova*, v.2, p.238-242.
- Palmer, A.R., 1983. The Decade of North American Geology, 1983 geologic time scale. *Geology* 10, 503-504.
- Pearce, J.A., 1982. Trace element characteristics of lavas from destructive plate boundaries. In Thorpe, R.S. (ed.), *Andesites: Orogenic andesites and related rocks*. Wiley-Interscience, Chichester, 724 pp, p.525-548.
- Pearce, J.A., and Cann, J.R., 1973. Tectonic setting of basic volcanic rocks determined using trace element analysis. *Earth and Planetary Science Letters*, v.19, p.290-300.

- Pearce, J.A., Harris, N.B.W., and Tindle, A.G., 1984. Trace element discrimination diagrams for the interpretation of granitic rocks. *Journal of Petrology*, v.25, 956-983.
- Pickthorn, W.J., Goldfarb, R.J., and Leach, D.L., 1987. Comment on "Dual origins of gold lode deposits in the Canadian Cordillera". *Geology*, v.15, p.471-472.
- Ramezani, J., 1993. M.Sc. thesis in preparation, Memorial University of Newfoundland, St. John's Newfoundland.
- Robert, F., and Brown, A.C., 1986. Archean gold-bearing quartz veins at the Sigma Mine, Abitibi Greenstone Belt, Quebec: Part II Vein paragenesis and hydrothermal alteration. *Economic Geology*, v.81, p.593-616.
- Robert, F. and Kelly, W.C., 1987. Ore-forming fluids in Archean gold-bearing quartz veins at the Sigma mine, Val d'Or, Quebec, Canada. *Economic Geology*, v.82, p.1464-1482.
- Roddy, M.S., Reynolds, S.J., Smith., B.M., and Ruiz, J. 1988. K-metasomatism and detachment -related mineralization, Harcuvar Mountains, Arizona. *Geological Society of America Bulletin*, v.100, p.1627-1639.
- Romberger, S.B., 1986. Disseminated gold deposits. *Geoscience Canada* v.13 p.21-30.
- Romberger, S.B., 1988. Geochemistry of gold in hydrothermal deposits. In Shawe, D.R., and Ashley, R.P. (eds.), *Introduction to geology and resources of gold, and geochemistry of gold*. United States Geological Survey Bulletin 1857-A, p.A9-A25.
- Sandiford, M., and Keays, R.R., 1986. Structural and tectonic constraints on the origin of gold deposits in the Ballarat Slate Belt, Victoria. In Keppie, J.D., Boyle, R.W., and Haynes, S.J. (eds.), *Turbidite-Hosted Gold Deposits*, Geological Association of Canada Special Paper 32, p.15-26.
- Seward, T.M., 1973. Thiocomplexes of gold and the transport of gold in hydrothermal ore solutions. *Geochimica et Cosmochimica Acta*, v.37, p.379-399.

- Shenberger, D.M., and Barnes, H.L., 1989. Solubility of gold in aqueous sulfide solutions from 150 to 350°C. *Geochimica et Cosmochimica Acta*, v.53, p.269-278.
- Sheppard, S.M.F., and Schwartz, H.P., 1970. Fractionation of carbon and oxygen isotopes and magnesium between co-existing metamorphic calcite and dolomite. *Contributions to Mineralogy and Petrology*, v.26, p.161-198.
- Sibson, R.H., Robert, F., and Poulsen, K.H., 1988. High-angle reverse faults, fluid-pressure cycling, and mesothermal gold-quartz deposits. *Geology* v.16, p.551-555.
- Smith, B.M., Reynolds, S.J., Day, H.W., and Bodnar, R.J., 1991., Deep-seated fluid involvement in ductile-brittle deformation and mineralization, South Mountains metamorphic core complex, Arizona. *Geological Society of America Bulletin*, v.103, p.559-569.
- Snelgrove, A.K., 1935. Geology of gold deposits of Newfoundland. Newfoundland Department of Natural Resources Geological Section, Bulletin 2, 46 pp.
- Spencer, J.E., and Welty, J.W., 1986. Possible controls on base- and precious-metal mineralization associated with Tertiary detachment faults in the lower Colorado River trough, Arizona and California. *Geology*, v.14, p.195-198.
- Stacey, J.S., and Kramers, J.D., 1975. Approximation of terrestrial lead isotope evolution by a two-stage model. *Earth and Planetary Science Letters*, v.26, p.207-221.
- Steiger, R.H and Jäger, E., 1977. Subcommittee on geochronology: convention on the use of decay constants in geo- and cosmochemistry. *Earth and Planetary Science Letters*, v.36, p.359-362.
- Stern, R.J., and Ito, E., 1983. Trace element and isotopic constraints on the source of magmas in the active Volcano and Mariana Island Arcs, Western Pacific. *Journal of Volcanology and Geothermal Research*, v.18, p.461-482.
- Stevens, R.K., 1970. Cambro-Ordovician flysch sedimentation and tectonics in west Newfoundland and their possible bearing on a Proto-Atlantic Ocean. *Geological Association of Canada, Special Paper 7*, p.165-177.

- Stukas, V. and Reynolds, P.H., 1975. $^{40}\text{Ar}/^{39}\text{Ar}$ dating of the Brighton gabbro complex, Lushs Bight Terrane, Newfoundland. *Canadian Journal of Earth Sciences*, v. 11, p.1485-1488.
- Suzouki, T., and Epstein, S., 1976. Hydrogen isotope fractionation between OH-bearing minerals and water. *Geochimica et Cosmochimica Acta*, v. 40, p.1229-1240.
- Swinden, H.S., Kean, B.F., and Dunning, G.R., 1988. Geological and paleotectonic settings of volcanogenic sulphide mineralization in central Newfoundland. In Swinden, H.S., and Kean, B.F. (eds.), *The Volcanogenic Sulphide Districts of Central Newfoundland*. Mineral Deposits Division, Geological Association of Canada, p.5-26.
- Swinden, H.S., 1991. Paleotectonic setting of volcanogenic massive sulphide deposits in the Dunnage Zone, Newfoundland Appalachians. *Canadian Institute of Mining and Metallurgy Bulletin*, v. 84, p.59-69.
- Szybinski, Z.A. and Jenner, G.A., 1989. Paleotectonic setting of the Ordovician volcanic rocks in the northwestern Dunnage Zone, Newfoundland. *GAC - MAC Program with Abstracts* v. 13, p.A40.
- Szybinski, Z.A., Swinden, H.S., O'Brien, F.H.C., Jenner, G.A., and Dunning, G.R., 1990. Correlation of Ordovician volcanic terranes in the Newfoundland Appalachians: Lithological, geochemical and age constraints. *GAC - MAC Program with Abstracts* v. 15, p.A128.
- Taylor, B.E., 1987. Stable isotope geochemistry of ore-forming fluids. In Kyser, T.K. (ed.), *Stable Isotope Geochemistry of Low Temperature Fluids*. Mineralogical Association of Canada Short Course Notes Volume 13, p.337-445.
- Taylor, H.P. Jr., 1968. The oxygen isotope geochemistry of igneous rocks. *Contributions to Mineralogy and Petrology*, v. 19, p.1-71.
- Taylor, H.P. Jr., 1974. The application of oxygen and hydrogen isotope studies to problems of hydrothermal alteration and ore deposition. *Economic Geology*, v. 69, p.843-883.
- Taylor, H.P. Jr., 1980. The effects of assimilation of country rocks by magmas on $^{18}\text{O}/^{16}\text{O}$ and $^{87}\text{Sr}/^{86}\text{Sr}$ systematics in igneous rocks. *Earth and Planetary Science Letters*, v. 47, p.243-254.

- Taylor, H.P. Jr., 1986. Igneous rocks: II isotopic case studies of circumpacific magmatism. In Valley, J.W., Taylor, H.P., and O'Neil, J.R. (eds.) Stable isotopes in high temperature geological processes. Mineralogical Society of America Reviews in Mineralogy v.16, p. 273-318.
- Taylor, H.P. Jr., and Sheppard, S.M.F., 1986. Igneous rocks: I processes of isotopic fractionation and isotope systematics. In Valley, J.W., Taylor, H.P., and O'Neil, J.R. (eds.) Stable isotopes in high temperature geological processes. Mineralogical Society of America Reviews in Mineralogy v.16, p. 227-272.
- Taylor, S.R. and McLennan, S.M., 1981. The composition and evolution of the continental crust: rare earth element evidence from sedimentary rocks. Philosophical Transactions, Royal Society of London. v.A310, 381-399.
- Tuach, J., 1987. Mineralized environments, metallogenesis, and the Doucens Valley fault complex, western White Bay: A philosophy for gold exploration in Newfoundland. Current Research, Newfoundland Department of Mines, Mineral Development Division, Report 87-1, p.129-144.
- Tuach, J., Dean, P.L., Swinden, H.S., O'Driscoll, C.F., Kean, B.F., and Evans, D.T.W., 1988. Gold mineralization in Newfoundland: A 1988 Review. Current Research, Newfoundland Department of Mines, Mineral Development Division, Report 88-1, p. 279-306.
- Tucker, R.D., Krogh, T.E., Ross, R.J., and Williams, S.H., 1990. Time-scale calibration by high-precision U-Pb zircon dating of interstratified volcanic ashes in the Ordovician and Lower Silurian stratotypes of Britain. Earth and Planetary Sciences v.100, p.51-58.
- Weir, R.H. and Kerrick, D.M., 1987. Mineralogic, fluid inclusion, and stable isotope studies of several gold mines in the Mother Lode, Tuolumne and Mariposa Counties, California. Economic Geology, v.82, p.328-344.
- Wenner, D.B., and Taylor, H.P. Jr., 1971. Temperatures of serpentinization of ultramafic rocks based on $^{18}\text{O}/^{16}\text{O}$ fractionation between coexisting serpentine and magnetite. Contributions to Mineralogy and Petrology, v.32, p.165-185.
- Whalen, J.B. and Currie, K.L., 1982. Volcanic and plutonic rocks in the Rainy Lake area, Newfoundland. Current Research, Part A. Geological Survey of Canada, Paper 82-1A. p.17-22.

- Whalen, J.B. and Currie, K.L., 1983. The Topsails igneous terrane of western Newfoundland. Current Research, Part A. Geological Survey of Canada, Paper 83-1A, p.15-23.
- Whalen, J.B., Currie, K.L., and van Breeman, O. 1987. Episodic Ordovician-Silurian plutonism in the Topsails igneous terrane of western Newfoundland. Transactions of the Royal Society of Edinburgh. Earth Sciences, v.78, p.17-28.
- Williams, H., 1964. The Appalachians in Newfoundland - a two-sided symmetrical system. American Journal of Science, v.262, p.1137-1158.
- Williams, H. 1979. Appalachian Orogen in Canada. Canadian Journal of Earth Sciences Tuzo Wilson Volume, v. 16, p. 792-807.
- Williams, H., Colman-Sadd, S.P., and Swinden, H.S., 1988. Tectonic-stratigraphic subdivisions of central Newfoundland. Current Research, Part B, Geological Survey of Canada, Paper 88-1B, p. 91-98.
- Williams, H., Gillespie, R.T., and van Breeman, O., 1985. A Late Precambrian rift-related igneous suite in western Newfoundland. Canadian Journal of Earth Sciences v.22, p.1727-1735.
- Williams, H. and Hatcher, R.D. Jr., 1982. Suspect terranes and accretionary history of the Appalachian orogen. Geology, v.10, p. 530-536.
- Williams, H. and Hiscott, R.N., 1987. Definition of the Iapetus rift-drift transition in western Newfoundland. Geology, v.15, p.1044-1047.
- Williams, H. and St. Julien, P., 1982. The Baie Verte - Brompton Line: Continent-ocean interface in the northern Appalachians. In Major Structural Zones and Faults of the Northern Appalachians, P. St. Julien and J. Beland (eds.); Geological Association of Canada, Special Paper No. 11, p. 181-261.
- Williams, S.H., 1988. Middle Ordovician Graptolites from Central Newfoundland. Current Research, Newfoundland Department of Mines, Mineral Development Division, Report 88-1, p.183-188.
- Wilson, J.T., 1966. Did the Atlantic close and then reopen? Nature, v.211, p.31-36.

- Wilton, D.H.C., 1984. Metallogenic, tectonic, and geochemical evolution of the Cape Ray Fault Zone with emphasis on electrum mineralization. Unpublished Ph.D. thesis, Memorial University of Newfoundland, St. John's, Newfoundland, 618 pp.
- Wilton, D.H.C. and Strong, D.F., 1986. Granite-related gold mineralization in the Cape Ray Fault Zone of southwestern Newfoundland. *Economic Geology*, v.81, p.281-295.
- Winchester, J.A., and Floyd, P.A., 1977. Geochemical discrimination of different magma series and their differentiation products using immobile elements. *Chemical Geology*, v.20, p.325-343.
- Winkler, H.G.F., 1976. *Petrogenesis of Metamorphic Rocks*, Fourth edition. Springer Verlag, New York 334 pp.
- Wong, L., Davis, D.W., Krogh, T.E., and Robert, F., 1991. U-Pb zircon and rutile chronology of Archean greenstone formation and gold mineralization in the Val d'Or region, Quebec. *Earth and Planetary Science Letters*, v.104, p.325-336.
- Yardley, B.W.D., 1983. Quartz veins and devolatilization during metamorphism. *Geological Society of London Journal*, v.140, p.657-663.
- Yule, A., 1988. The Hope Brook gold deposit, Newfoundland, Canada: surface geology, representative lithochemistry and styles of hydrothermal alteration. Unpublished M.Sc. thesis, Dalhousie University, Halifax, Nova Scotia, 249 pp.

APPENDIX A

Sample locations

Grid references for outcrop sample locations listed in Table A-1 are:

(1) Metre grid of Noranda Exploration Co. Ltd. Rendell - Jackman grid
(Andrews, 1990; Figure 3.1)

(2) Universal transverse mercator coordinates on NTS map 12H/9, northings prefixed by 54(00000m), and eastings prefixed by 5(00000m).

Location of diamond drill holes for drill core samples listed in Table A-2 are as follows, with grid references as in (1) above:

DDH MS-88-5	9985 N	9949 E
DDH MS-88-6	10010 N	9949 E
DDH MS-88-7	10012 N	9950 E
DDH MS-88-14	10050 N	9950 E
DDH MS-89-16	10085 N	9948 E
DDH MS-89-17	10080 N	10000 E
DDH MS-89-27	10125 N	9948 E
DDH MS-90-49	10175 N	9948 E

All diamond drill cores logged and sampled were drilled at an azimuth of 180°, with dips of 45°.

Table A-1
Outcrop Sample Locations

Sample	East	North	Grid
D-1	9943	9957	1
D-2	9963	9960	1
SV-1	9951	9956	1
SV-2	10010	9912	1
MV-1	9914	9955	1
MV-2	9912	9959	1
V-1	9933	9957	1
MV-3	9945	9957	1
D-3	9970	10170	1
DR-91-220	9568	9995	1
KP-1	59400	95100	2
KP-2	59400	95100	2
KP-3	59400	95200	2
KP-4	59400	94100	2
KP-5	59400	95800	2
KP-6	52800	89600	2
KP-7	53000	89800	2
KP-8	53300	89900	2
KP-9	59200	96800	2
KP-10	59300	96800	2
KP-11	63700	99500	2

Table A-1 (continued)

Sample	East	North	Grid
V-3	9979	9964	1
V-4	9979	9965	1
V-5	9977	9967	1
V-6	9935	9957	1
V-7	9967	9964	1
V-8	9947	9962	1
V-9	9956	9957	1
V-10	9940	9959	1
V-11	9770	9921	1
MV-4	9780	9918	1

Table A-2

Drill Core Sample Locations

Sample	DDH MS-	Depth (m)	Sample	DDH MS-	Depth (m)
DR-90-01	88-15	214.2-214.4	DR-90-23	89-27	200.0
DR-90-02	88-15	208.1-208.3	DR-90-24	89-27	39.0 - 39.3
DR-90-03	88-15	205.1-205.2	DR-90-25	89-27	61.4 - 61.5
DR-90-04	88-15	186.5-186.6	DR-90-26	89-27	72.0 - 72.1
DR-90-05	88-15	185.3	DR-90-27	89-16	81.5 - 81.6
DR-90-06	88-15	175.8	DR-90-28	89-16	88.7 - 89.0
DR-90-07	88-15	110.4	DR-90-29	89-16	101.3-101.4
DR-90-08	88-15	24.6	DR-90-30	89-16	126.5-126.6
DR-90-09	88-15	119.3	DR-90-31	89-16	93.9 - 94.0
DR-90-10	88-15	76.5	DR-90-32	89-27	21.5 - 21.6
DR-90-11	88-15	50.9	DR-90-33	89-16	133.7-134.0
DR-90-12	88-07	61.5	DR-90-34	89-16	146.5-146.7
DR-90-13	88-15	118.2	DR-90-35	89-16	148.2-148.4
DR-90-14	88-15	82.4	DR-90-36	89-16	151.0-151.1
DR-90-15	88-15	75	DR-90-37	89-16	152.1-152.2
DR-90-16	88-15	55.7	DR-90-38	89-16	152.8-153.1
DR-90-17	88-05	17.9	DR-90-39	89-16	153.4-153.5
DR-90-18	88-05	29.6	DR-90-40	89-16	153.9-154.0
DR-90-19	88-05	40.0	DR-90-41	89-16	155.6-155.8
DR-90-20	88-05	20.6	DR-90-42	89-16	156.7-157.0
DR-90-21	89-27	11.0 - 11.2	DR-90-43	89-16	158.4-158.5
DR-90-22	89-27	53.4 - 53.5	DR-90-44	89-16	159.1-159.4

Table A-2 (continued)

Sample	DDH MS-	Depth (m)	Sample	DDH MS-	Depth (m)
DR-90-45	89-16	173.9-174.0	DR-90-69	88-15	9.8 - 10.0
DR-90-46	89-16	180.8-181.1	DR-90-70	88-05	15.1 - 15.3
DR-90-47	89-16	188.1-188.4	DR-90-71	88-05	16.3 - 16.7
DR-90-48	88-15	83.4 - 83.6	DR-90-72	88-05	17.3 - 17.6
DR-90-49	88-15	119.4-119.5	DR-90-73	88-05	23.8 - 23.9
DR-90-50	88-15	132.0-132.3	DR-90-74	88-05	29.2
DR-90-51	88-15	106.0-106.3	DR-90-75	88-05	29.8 - 30.0
DR-90-52	88-15	125.5-125.8	DR-90-76	88-05	35.1
DR-90-53	88-15	109.0	DR-90-77	88-05	36.3
DR-90-54	88-15	109.3	DR-90-78	88-05	44.2
DR-90-55	88-15	104.9	DR-90-79	88-05	47.9
DR-90-56	88-15	77.6 - 77.7	DR-90-80	88-05	49.4 - 49.6
DR-90-57	88-15	126.3-126.5	DR-90-81	88-05	61.4 - 61.5
DR-90-58	89-16	154.3-154.5	DR-90-82	88-05	61.5 - 61.6
DR-90-59	89-16	156.2-156.4	DR-90-83	88-05	61.6 - 61.8
DR-90-60	89-16	7.5 - 7.7	DR-91-84	89-27	80.1 - 80.2
DR-90-61	89-16	193.5-193.8	DR-91-85	88-15	16.0 - 16.1
DR-90-62	89-16	218.0-218.2	DR-91-86	88-15	32.5 - 32.6
DR-90-63	89-27	239.0-239.3	DR-91-87	88-15	43.3 - 43.5
DR-90-64	89-27	241.8-242.1	DR-91-88	88-15	56.4 - 56.5
DR-90-65	88-15	50.7	DR-91-89	88-15	81.4 - 81.6
DR-90-66	88-15	5.4 - 5.6	DR-91-90	88-15	104.5-104.6
DR-90-67	88-15	6.5 - 6.7	DR-91-91	89-17	46.6-46.8
DR-90-68	88-15	15.7 - 15.9	DR-91-92	90-49	48.4-48.6

Table A-2 (continued)

Sample	DDH MS-	Depth (m)	Sample	DDH MS-	Depth (m)
DR-91-93	90-49	167.6-167.8	DR-91-114	88-05	95.1-95.2
DR-91-94	90-49	249.0-249.2	DR-91-115	89-17	32.1-32.3
DR-91-95	90-49	247.7-247.8	DR-91-116	89-17	32.7-32.8
DR-91-96	90-49	281.9-282.1	DR-91-117	89-27	237.0-237.2
DR-91-97	88-13	144.9-144.95	DR-91-118	89-27	240.0-240.2
DR-91-98	88-13	110.8-110.9	DR-91-119	89-27	243.0-243.1
DR-91-99	88-13	110.5-110.7	DR-91-120	88-06	15.9-16.0
DR-91-100	88-15	50.6-50.7	DR-91-121	88-15	202.6-202.9
DR-91-101	88-05	60.7-60.9	DR-91-122	88-15	48.6-48.8
DR-91-102	88-13	105.8-105.9	DR-91-123	88-15	33.2-33.3
DR-91-103	88-13	115.8-115.9	DR-91-124	89-16	137.4-137.6
DR-91-104	88-13	112.2-112.3	DR-91-125	89-16	205.2-205.5
DR-91-105	88-13	147.3	DR-91-126	88-15	143.2-143.3
DR-91-106	88-13	126.7-126.8	DR-91-127	88-15	50.2-50.7
DR-91-107	89-17	124.4-124.7	DR-91-128	88-15	51.7-53.2
DR-91-108	89-17	128.8-128.9	DR-91-129	89-16	158.8-159.8
DR-91-109	89-17	127.2-127.3	DR-91-130	89-16	160.0-160.4
DR-91-110	89-17	128.9-129.0	DR-91-131	88-15	51.2-51.6
DR-91-111	89-27	49.5-49.6	DR-91-132	89-16	153.4-153.8
DR-91-112	89-27	56.8-56.9	DR-91-133	89-16	84.5-84.6
DR-91-113	88-05	83.9-84.0			

Reference cited in Appendix A:

Andrews P.W., 1990. Rendell-Jackman grid compilation. Unpublished map, Noranda Exploration Co. Ltd.

APPENDIX B

Whole rock chemistry

For whole rock chemical analyses reported in this section, 100 to 300 g of unweathered rock was crushed to less than 1 cm pieces in a steel jaw crusher. Approximately 100 g of the resulting rock chips were powdered in a tungsten carbide mill to a grain size smaller than 100 mesh.

Major element contents are listed in Table B-1 as weight percent oxides; . Loss on ignition was determined at 1050°C. Atomic Absorption (AA) measurements of major element oxides were determined in the Department of Earth Sciences at Memorial University on a Perkin Elmer™ spectrophotometer, following HF-HNO₃ dissolution. Preparation of samples for major element oxide analyses by inductively coupled plasma-optical emission spectroscopy (ICP-OES) at the Newfoundland and Labrador Department of Mines and Energy geochemical laboratory in St. John's was based on procedures described by Wagenbauer *et al.* (1983), and includes lithium metaborate fusion and HCl-HF digestion. Each analysis reported in Table B-1 is the mean of two determinations.

A suite of trace elements was determined on the ARL 8420 X-ray fluorescence (XRF) analyser in the Department of Earth Sciences at Memorial University using pressed pellets prepared from approximately 5 g of rock powder with a phenolic resin binder.

Samples for trace element analysis by inductively coupled plasma-mass spectrometry (ICP-MS) at the Department of Earth Sciences at Memorial University were prepared by HF-HNO₃ dissolution or a Na₂O₂ sinter (Jenner *et al.*, 1990; Longerich *et al.*, 1990). Trace element analyses for XRF and ICP-MS are reported in Table B-1 in parts per million.

References cited in Appendix B:

- Jenner, G.A., Longerich, H.P., Jackson, S.E., and Fryer, B.J., 1990. ICP-MS - a powerful tool for high-precision trace-element analysis in Earth-sciences; Evidence from analysis of selected U.S.G.S. reference samples. *Chemical Geology*, v.83, 133-148.
- Longerich, H.P., Jenner, G.A., Fryer, B.J., and Jackson, S.E., 1990. Inductively coupled plasma-mass spectrometric analysis of geological samples: A critical evaluation based on case studies. *Chemical Geology*, v.83, 105-118.
- Wagenbauer, H.A., Riley, C.A., and Dawe, G., 1983. Geochemical Laboratory. Current Research, Newfoundland and Labrador Department of Mines and Energy, Mineral Development Division, Report 83-1, p. 133-137.

Table B-1 Whole Rock Chemistry

Sample Name	DR-90-01 ¹	DR-90-03 ¹	DR-90-21 ²	DR-90-28 ²	DR-90-33 ²	DR-90-34 ²
Rock Type	Basalt	Basalt	Mafic tuff	Basalt	Basalt	Basalt
SiO ₂	44.05	44.18	43.80	48.40	43.60	45.50
TiO ₂	2.92	3.45	0.78	1.76	1.27	1.72
Al ₂ O ₃	13.52	13.74	14.60	13.80	13.20	12.20
Fe ₂ O ₃ *			10.19	12.31	10.24	10.19
Fe ₂ O ₃	4.39	6.60				
FeO	8.84	8.62				
MnO	0.22	0.20	0.17	0.20	0.17	0.18
MgO	5.48	4.61	7.81	6.18	6.81	5.86
CaO	9.59	8.36	11.54	7.78	9.57	9.43
Na ₂ O	2.90	3.99	0.74	2.66	3.33	3.15
K ₂ O	0.17	0.23	0.03	0.13	0.04	0.03
P ₂ O ₅	0.38	0.45	0.01	0.19	0.12	0.11
L.O.I.	7.00	4.62	7.90	3.04	9.88	9.53
TOTAL	99.46	99.05	97.57	96.45	98.23	97.89
S	788	1752	389	536	191	582
Cl	32	36	19	24	19	21
Sc	36	42	33	51	54	57
V	441	514	285	333	343	349
Cr	87	45	512	96	376	260
Ni	33.0	17.9	202.0	36.2	49.5	44.0
Cu	33.1	32.7	33.4	60.6	64.1	69.9
Zn	134.4	147.1	101.6	107.4	94.0	112.7
Ga	17.2	25.0	13.6	19.5	16.4	17.8
As	3	-10	32	4	-1	2
Rb	2.6	3.3	0.3	2.5	0.4	0.8
Y	53.0	62.1	21.0	42.0	27.5	31.8
Zr	250.2	290.3	17.7	156.6	102.1	107.5
Nb	11.5	14.4	0.6	4.9	2.7	2.3

Sample Name	DR-90-01 ¹	DR-90-03 ¹	DR-90-21 ²	DR-90-28 ²	DR-90-33 ²	DR-90-34 ²
Rock Type	Basalt	Basalt	Basalt	Basalt	Basalt	Basalt
Li			16.95	5.53	13.31	14.76
Be			0.27	1.17	0.69	1.20
Sr	273.21	227.48	103.21	303.77	101.81	160.53
Mo			0.14	0.65	0.44	0.49
Cs			0.10	0.05	0.09	0.05
Ba	30.67	36.57	7.49	34.52	12.61	10.39
La	12.99	15.82	0.39	6.77	4.58	4.47
Ce	36.10	43.09	1.58	20.70	13.86	13.66
Pr	5.30	6.32	0.33	3.28	2.21	2.24
Nd	25.31	29.24	2.38	16.42	11.59	11.36
Sm	7.02	7.89	1.31	5.33	3.68	3.74
Eu	2.28	2.67	0.48	1.85	1.42	1.46
Gd	8.39	9.31	2.43	6.78	4.88	5.10
Tb	1.38	1.56	0.48	1.11	0.74	0.83
Dy	8.72	9.76	3.52	7.09	4.92	5.52
Ho	1.87	2.09	0.76	1.46	1.00	1.14
Er	5.54	6.01	2.42	4.00	2.81	3.44
Tm	0.77	0.88	0.35	0.56	0.37	0.49
Yb	5.10	5.09	2.35	3.31	2.49	2.99
Lu	0.74	0.84	0.33	0.45	0.31	0.41
Hf	6.01	6.67	0.45	2.06	1.38	1.75
Ta	1.05	1.31	0.18	0.77	0.26	0.31
Tl			0.00	0.02	0.01	0.00
Pb	5.00	12.00	7.44	3.65	2.47	4.60
Bi			0.04	0.03	0.02	0.02
Th	0.82	1.13	0.04	0.29	0.20	0.19
U			0.01	0.13	0.08	0.08

Sample Name	DR-90-35 ²	DR-90-40 ¹	DR-90-41 ¹	DR-90-44 ²	DR-90-46 ²	DR-90-47 ²
Rock Type	Basalt	Basalt	Basalt	Basalt	Basalt	Basaltic dyke
SiO ₂	45.00	43.45	43.90	44.00	43.60	44.40
TiO ₂	2.02	1.88	2.00	2.26	1.10	1.70
Al ₂ O ₃	12.80	12.56	13.32	12.30	17.30	13.30
Fe ₂ O ₃ *	10.58			10.99	6.24	10.37
Fe ₂ O ₃		0.59	0.88			
FeO		10.88	10.63			
MnO	0.17	0.28	0.28	0.22	0.08	0.17
MgO	5.40	5.72	5.70	5.13	1.79	6.06
CaO	9.24	8.89	8.30	9.48	10.56	8.88
Na ₂ O	3.63	2.15	2.60	2.96	4.88	3.16
K ₂ O	0.06	0.46	0.32	0.05	2.33	0.04
P ₂ O ₅	0.16	0.18	0.20	0.19	0.10	0.14
L.O.I.	9.56	11.05	10.82	10.29	10.19	11.53
TOTAL	98.62	98.09	98.95	97.87	98.17	99.76
S	1092	3195	957	1144	519	660
Cl	20	33	42	29	34	27
Sc	55	56	62	55	38	55
V	337	397	429	371	197	383
Cr	173	166	164	173	232	235
Ni	34.9	29.8	28.5	39.1	36.6	48.2
Cu	78.3	384.5	60.0	30.9	50.0	51.2
Zn	126.9	401.0	608.6	189.1	46.6	108.9
Ga	19.7	11.2	12.2	20.0	17.5	17.0
As	-3	-3	0	-4	-5	-3
Rb	1.9	18.8	12.1	1.3	56.0	0.6
Y	34.5	30.8	36.4	36.4	18.1	32.6
Zr	142.0	129.5	140.7	153.9	89.8	116.9
Nb	4.4	4.5	5.0	5.9	3.0	2.8

Sample Name	DR-90-35 ²	DR-90-40 ¹	DR-90-41 ¹	DR-90-44 ²	DR-90-46 ²	DR-90-47 ²
Rock Type	Basalt	Basalt	Basalt	Basalt	Basalt	Basaltic dyke
Li	14.16			18.46	8.60	19.81
Be	2.50			5.08	2.00	1.41
Sr	185.82	218.30	162.12	184.50	209.52	153.16
Mo	0.72			0.59	0.28	0.66
Cs	0.05			0.07	1.66	0.03
Ba	14.44	54.20	35.22	11.64	159.52	10.25
La	6.85	6.46	6.85	8.86	5.42	5.18
Ce	19.42	17.31	17.30	24.54	14.61	15.40
Pr	2.98	2.60	2.49	3.64	2.11	2.42
Nd	15.06	12.73	11.99	17.96	9.84	12.22
Sm	4.37	3.83	3.86	5.38	2.59	3.76
Eu	1.46	1.29	1.33	1.99	1.03	1.13
Gd	5.28	4.66	4.75	6.61	2.98	3.72
Tb	0.83	0.82	0.82	1.09	0.41	0.52
Dy	4.91	5.50	5.28	6.86	2.46	2.88
Ho	0.96	1.13	1.15	1.37	0.47	0.49
Er	2.54	3.17	3.24	3.86	1.32	1.35
Tm	0.38	0.47	0.48	0.53	0.18	0.20
Yb	2.59	2.97	3.14	3.26	1.39	1.53
Lu	0.34	0.43	0.44	0.42	0.18	0.20
Hf	2.63	3.08	3.47	2.46	1.17	1.28
Ta	0.46	0.60	0.56	0.52	0.37	0.34
Tl	0.01			0.01	0.33	0.00
Pb	8.46	7.00	8.00	15.27	6.23	6.72
Bi	0.05			0.11	0.05	0.07
Th	0.55	0.38	0.37	0.49	0.57	0.20
U	0.30			0.22	0.34	0.10

Sample Name	DR-91-124 ¹	DR-91-125 ¹	DR-91-220 ¹	SV-1 ²	SV-2 ²
Rock Type	Mafic tuff	Mafic tuff	Basalt	Felsic tuff	Felsic tuff
SiO ₂	44.92	41.42	49.28	70.40	68.30
TiO ₂	2.72	1.54	1.60	0.84	0.87
Al ₂ O ₃	13.12	11.74	15.42	12.40	13.10
Fe ₂ O ₃ *				3.51	4.04
Fe ₂ O ₃	5.69	0.43	2.36		
FeO	8.05	9.42	6.98		
MnO	0.23	0.20	0.14	0.06	0.11
MgO	4.94	5.16	3.80	0.78	0.51
CaO	7.94	12.32	6.76	2.44	2.72
Na ₂ O	4.04	2.62	5.96	6.00	4.72
K ₂ O	0.04	0.08	0.13	0.45	1.02
P ₂ O ₅	0.32	0.16	0.23	0.15	0.16
L.O.I.	6.88	13.30	6.87	2.22	2.91
TOTAL	98.89	98.39	99.53	99.25	98.46
S	510	2230	716	527	42
Cl	28	27	21	18	14
Sc	45	59	43	31	39
V	440	364	273	62	65
Cr	23	196	21	0	4
Ni	10.3	37.7	5.2	-1.5	-0.1
Cu	85.8	44.0	10.0	74.5	-0.4
Zn	247.8	83.0	70.3	39.0	81.6
Ga	14.9	4.3	9.2	10.4	16.4
As	-5	-9	1	8	0
Rb	0.7	2.0	1.9	13.7	16.1
Y	35.7	30.9	31.1	31.4	29.5
Zr	209.7	114.8	162.4	119.9	119.8
Nb	9.9	3.9	6.1	4.5	4.6

Sample Name	DR-91-124 ¹	DR-91-125 ¹	DR-91-220 ¹	SV-1 ²	SV-2 ²
Rock Type	Mafic tuff	Mafic tuff	Basalt	Felsic tuff	Felsic tuff
Li				3.83	4.00
Be				1.31	1.18
Sr	216.27	166.87	156.76	150.30	132.03
Mo				1.70	0.40
Cs				0.31	0.27
Ba	34.05	14.78	47.39	34.73	282.22
La	11.55	4.76	10.52	10.18	9.62
Ce	31.56	14.19	26.23	24.42	24.67
Pr	4.51	2.18	3.61	3.16	3.06
Nd	20.81	10.60	15.59	13.84	13.94
Sm	5.32	3.59	4.01	3.77	3.83
Eu	1.94	1.19	1.45	0.91	1.11
Gd	5.86	4.32	4.63	4.10	4.71
Tb	0.93	0.70	0.77	0.60	0.74
Dy	5.89	4.45	4.78	3.90	4.70
Ho	1.17	1.02	1.02	0.81	0.99
Er	3.30	2.87	2.95	2.54	2.96
Tm	0.49	0.41	0.43	0.37	0.44
Yb	3.07	2.72	2.60	2.63	3.17
Lu	0.46	0.42	0.40	0.42	0.45
Hf	4.57	3.12	3.60	3.07	3.43
Ta	0.96	0.49	0.55	2.05	1.53
Tl				0.11	0.23
Pb	6.00	8.00	0.00	4.49	7.34
Bi				0.05	0.02
Th	0.75	0.21	1.62	2.19	2.57
U				0.77	0.80

Sample Name	DR-90-14 ²	DR-90-17 ²	DR-90-38 ²	DR-90-48 ²	D-1 ²	D-3 ¹
Rock Type	Felsic dyke	Felsic dyke	Felsic dyke	Felsic dyke	Felsic dyke	Felsic dyke
SiO ₂	67.90	67.00	69.70	68.60	66.20	67.22
TiO ₂	0.30	0.35	0.22	0.27	0.37	0.28
Al ₂ O ₃	14.80	15.30	14.00	14.80	15.20	15.56
Fe ₂ O ₃ *	1.57	2.27	1.39	1.82	2.21	
Fe ₂ O ₃						0.74
FeO	0.00	0.00	0.00	0.00	0.00	1.31
MnO	0.07	0.05	0.08	0.08	0.06	0.04
MgO	0.94	1.24	0.96	0.89	1.23	1.01
CaO	3.15	3.15	3.20	2.74	3.92	2.78
Na ₂ O	4.68	5.25	4.59	5.01	4.60	4.61
K ₂ O	2.40	2.06	2.11	2.38	2.23	2.27
P ₂ O ₅	0.06	0.08	0.06	0.07	0.08	0.08
L.O.I.	3.33	3.32	3.53	3.03	3.98	3.36
TOTAL	99.19	100.06	99.85	99.69	100.08	99.26
S	1161	207	1368	1433	194	243
Cl	18	29	30	26	16	22
Sc	9	9	11	9	8	11
V	46	67	43	47	69	44
Cr	16	23	25	13	20	26
Ni	6.5	9.8	4.4	5.4	7.7	3.3
Cu	4.5	5.7	20.9	9.2	9.3	5.4
Zn	45.3	38.7	36.4	57.8	100.9	20.2
Ga	17.4	16.8	16.1	16.5	17.1	9.8
As	2	3	-2	4	-1	-5
Rb	78.8	68.6	73.3	84.4	75.3	57.6
Y	4.4	6.3	4.4	5.2	5.9	6.0
Zr	87.5	85.6	68.5	89.6	84.6	87.7
Nb	2.7	2.2	2.6	2.7	2.3	2.6

Sample Name	DR-90-14 ²	DR-90-17 ²	DR-90-38 ²	DR-90-48 ²	D-1 ²	D-3 ¹
Rock Type	Felsic dyke	Felsic dyke	Felsic dyke	Felsic dyke	Felsic dyke	Felsic dyke
Li	3.44	3.68	4.27	2.97	6.46	
Be	1.54	1.15	2.96	1.33	2.10	
Sr	314.43	313.78	269.41	289.71	404.27	275.73
Mo	0.24	0.19	0.19	0.14	0.13	
Cs	1.57	1.39	1.13	1.71	1.41	
Ba	569.76	603.27	339.60	513.75	570.13	438.20
La	7.67	8.18	4.93	8.23	9.48	8.46
Ce	19.59	19.97	12.44	19.71	21.95	18.00
Pr	2.03	2.18	1.32	2.09	2.44	2.06
Nd	7.93	8.91	5.39	8.55	9.88	7.93
Sm	1.68	1.74	1.21	1.75	1.89	1.65
Eu	0.46	0.57	0.38	0.55	0.58	0.43
Gd	0.00	0.00	0.00	0.00	0.00	1.38
Tb	0.17	0.22	0.15	0.18	0.23	0.17
Dy	0.96	1.20	0.90	1.04	1.22	1.11
Ho	0.19	0.23	0.17	0.21	0.23	0.21
Er	0.52	0.70	0.51	0.59	0.68	0.57
Tm	0.07	0.11	0.07	0.08	0.09	0.08
Yb	0.45	0.61	0.45	0.51	0.66	0.43
Lu	0.08	0.10	0.07	0.08	0.11	0.08
Hf	2.25	2.25	1.86	2.42	2.40	2.15
Ta	1.07	0.82	1.80	1.47	1.19	0.96
Tl	0.48	0.45	0.44	0.48	0.43	
Pb	10.84	10.62	8.40	8.61	9.49	4.00
Bi	0.09	0.04	0.31	0.19	0.07	
Th	3.27	2.73	1.99	3.19	2.94	2.82
U	1.38	1.18	0.98	1.36	1.22	

Sample Name	KP-8 ¹	KP-9 ¹	KP-10 ¹	KP-11
Rock Type	King's Point	King's Point	King's Point	King's Point
SiO ₂	76.08	77.15	73.38	73.70
TiO ₂	0.26	0.16	0.25	0.26
Al ₂ O ₃	10.92	11.35	12.12	12.93
Fe ₂ O ₃ *				
Fe ₂ O ₃	2.69	1.54	3.00	0.98
FeO	0.62	0.00	0.00	0.66
MnO	0.02	0.02	0.07	0.03
MgO	0.12	0.06	0.12	0.32
CaO	0.23	0.32	0.46	0.64
Na ₂ O	2.98	2.24	4.24	4.24
K ₂ O	4.22	5.05	4.74	4.34
P ₂ O ₅	0.04	0.02	0.02	0.04
L.O.I.	0.74	1.12	0.86	0.70
TOTAL	99.92	99.03	99.26	98.84
S	28	1706	4021	38
Cl	74	43	64	306
Sc	7	6	5	2
V	-2	-3	-2	10
Cr	11	34	23	26
Ni	-2.2	8.7	2.7	4.1
Cu	-1.0	2.8	0.2	-1.2
Zn	65.2	58.0	276.8	7.2
Ga	7.2	6.3	29.6	9.8
As	-1	7	1	4
Rb	133.3	112.9	101.8	150.9
Y	78.7	54.1	73.1	27.9
Zr	564.6	326.9	620.2	183.1
Nb	22.8	13.8	31.4	10.8

Sample Name	KP-8 ¹	KP-9 ¹	KP-10 ¹	KP-11 ¹
Rock Type	King's Point	King's Point	King's Point	King's Point
Li				
Be				
Sr	62.49	58.74	51.74	86.67
Mo				
Cs				
Ba	762.22	328.26	137.47	376.98
La	47.62	59.39	61.63	26.50
Ce	101.54	123.43	136.64	56.08
Pr	13.04	14.56	16.67	6.21
Nd	51.92	54.20	65.10	21.16
Sm	11.56	9.52	12.45	4.13
Eu	2.31	0.78	1.39	0.56
Gd	11.21	8.11	11.75	3.65
Tb	1.88	1.21	1.84	0.58
Dy	11.31	7.48	11.26	3.76
Ho	2.35	1.63	2.26	0.80
Er	6.99	5.08	6.71	2.52
Tm	0.99	0.74	0.97	0.39
Yb	6.33	4.98	6.13	2.56
Lu	1.03	0.80	0.97	0.39
Hf	6.28	4.87	7.07	4.17
Ta	3.65	3.02	3.71	3.32
Tl				
Pb	13.00	23.00	61.00	15.00
Bi				
Th	12.36	12.01	9.51	16.50
U				

Notes on Table B-1:

¹ Major element oxides by ICP-OES, trace elements listed S - Nb by XRF, trace elements Li - U by ICP-MS (Na₂O₂)

² Major element oxides by AA, trace elements listed S - Nb by XRF, trace elements Li - U by ICP-MS (HF/HNO₃)

